Epidemiological and Immunological Perspectives on SARS-CoV-2

DISSERTATION ZUR ERLANGUNG DES DOKTORGRADES DER NATURWISSENSCHAFTEN (DR. RER. NAT.)

DER FAKULTÄT FÜR BIOLOGIE UND VORKLINISCHE MEDIZIN DER UNIVERSITÄT REGENSBURG

vorgelegt von

Sebastian Einhauser

aus

Regensburg

im Jahr

2025

Das Promotionsgesuch wurde eingereicht am:

_____

Diese Arbeit wurde angeleitet von:

Prof. Dr. Ralf Wagner

Unterschrift:

Sebastian Einhauser

Table of Contents

Content Declaration

This thesis focuses the results section on five selected manuscripts, all of which are published in open-access, peer-reviewed journals. On top of the 5 main publications, additional contributions connected to SARS-CoV-2 and the PhD project, were co-authored and published in peer-reviewed, open-access journals. Due to limited space, only the title, authors and abstract are shown in this thesis. Furthermore, critical contributions to all manuscripts listed in this thesis were highlighted. All results (both main and appendix publications) are covered in the summary of results and discussion section.
A link/DOI to the full publication is provided for each publication. Appendix publications are listed chronologically with reference to the date of publication. Within the thesis and the manuscripts, Large Language Models and Grammarly were used for proofreading and text improvement, all changes and generations made by those tools were proofread and the author takes full responsibility for the contents.

A) Main Manuscripts

Manuscript 1: "Symptoms, SARS-CoV-2 antibodies and neutralization capacity in a cross sectional-population of German children"

This manuscript was published online under the above-named title in the peer-reviewed journal Frontiers in Pediatrics on 4th of October 2021. DOI: 10.3389/fped.2021.678937

Authors: Otto Laub*, Georg Leipold*, Antoaneta A. Toncheva*, David Peterhoff*, **Sebastian Einhauser***, Patrick Neckermann, Natascha Borchers, Elisangela Santos-Valente, Parastoo Kheiroddin, Heike Buntrock-Döpke, Sarah Laub, Patricia Schöberl, Andrea Schweiger-Kabesch, Dominik Ewald, Michael Horn, Jakob Niggel, Andreas Ambrosch, Klaus Überla, Stephan Gerling, Susanne Brandstetter, Ralf Wagner*, Michael Kabesch* on behalf of the Corona Virus Antibodies in Children from Bavaria (CoKiBa) Study group

* Authors contributed equally and share first or last authorship

Author contributions:

OL, GL, SG, KÜ, RW, and MK were responsible for the study design. OL, GL, HB-D, SL, AS-K, DE, MH, JN, and MK performed the data collection. AT, DP, **SE**, PN, NB, ES-V, PK, PS, RW, and AA carried out the laboratory analysis and the data interpretation. Data Analysis was performed by DP, **SE**, PN, SB, RW, and MK. OL, GL, DP, **SE**, SB, RW, and MK wrote this manuscript.

Detailed personal contribution: Sebastian Einhauser (SE) developed and performed the neutralization assays and did the comparative analysis of the ELISA, N-antibody and neutralization. He wrote the algorithm to perform a random but sex and age-stratified drawing of the negative control and measured the negative control. He performed the analysis of interconnection between age, sex and antibody response. SE also contributed to analysis of the connection of N-antibody to neutralization ratio with COVID-19 symptoms. Furthermore, SE contributed to data and sera curation as well as writing and revising the manuscript.

Manuscript 2: "Spectrum Bias and Individual Strengths of SARS-CoV-2 Serological Tests-A Population-Based Evaluation"

This manuscript was published online under the above-named title in the peer-reviewed journal diagnostics on 6th of October 2021. DOI: 10.3390/diagnostics11101843

Authors: Sebastian Einhauser*, David Peterhoff*, Hans Helmut Niller, Stephanie Beileke, Felix Günther,, Philipp Steininger, Ralph Burkhardt, Iris M Heid, Annette B Pfahlberg, Klaus Überla, Olaf Gefeller*, Ralf Wagner*

* Authors contributed equally and share first or last authorship

Author contributions:

Conceptualization, R.W., O.G., D.P., **S.E**., K.Ü.; Data curation, **S.E.**, D.P., S.B., R.W., O.G.; Formal analysis, **S.E.**, D.P., A.B.P. and O.G.; Funding acquisition, R.W. and K.Ü.; Investigation, **S.E.**, D.P., S.B., H.H.N., P.S., R.B.; Methodology, **S.E.**, D.P., A.B.P., O.G., R.W.; Project administration, R.W. and K.Ü.; Resources, R.W., R.B., I.M.H., O.G. and K.Ü.; Software, O.G., A.B.P., F.G., **S.E.**; Supervision, R.W., D.P., O.G. and K.Ü.; Validation, R.W., D.P., O.G.; Visualization, **S.E.**, O.G.; Writing—original draft, O.G. and **S.E**.; Writing—review & editing, R.W., D.P., **S.E.**, O.G., K.Ü.

Detailed personal contribution: Sebastian Einhauser (SE) contributed to developing the concept of the manuscript. He performed the neutralization assays, the selection of the cohort subgroup, the spectrum-bias subgroup, and curated the data as well as the samples. Together with OG, SE performed all the statistical and comparative analyses and illustrated the spectrum bias on earlier tests as well as the quantitative connection between tests. Furthermore, SE together with OG wrote the original manuscript and contributed to the revision of the manuscript.

Manuscript 3: "Time Trend in SARS-CoV-2 Seropositivity, Surveillance Detection- and Infection Fatality Ratio until Spring 2021 in the Tirschenreuth County-Results from a Population-Based Longitudinal Study in Germany"

This manuscript was published online under the above-named title in the peer-reviewed journal Viruses on 6th of May 2022. DOI: doi: 10.3390/v14061168

Authors: Sebastian Einhauser, David Peterhoff, Stephanie Beileke, Felix Günther, Hans-Helmut Niller, Philipp Steininger, Antje Knöll, Klaus Korn, Melanie Berr, Anja Schütz, Simon Wiegrebe, Klaus J Stark, André Gessner, Ralph Burkhardt, Michael Kabesch, Holger Schedl, Helmut Küchenhoff, Annette B Pfahlberg, Iris M Heid, Olaf Gefeller, Klaus Überla*, Ralf Wagner*

* Authors contributed equally and share first or last authorship

Author contributions:

Conceptualization, K.Ü. and R.W.; methodology, **S.E.**, D.P., F.G. and A.B.P.; validation, **S.E.**, D.P. and S.W.; formal analysis, F.G., S.W., A.B.P., I.M.H. and O.G.; investigation D.P., **S.E.**, R.B., S.B., P.S., A.K., K.K., A.S., K.J.S. and H.-H.N.; resources, A.G., H.S., I.M.H., O.G.,K.Ü. and R.W.; data curation, **S.E.**, S.B., F.G., M.B., M.K., K.Ü. and R.W.; writing—original draft preparation, **S.E.** and R.W.; writing—review and editing, K.Ü., O.G., F.G. and I.M.H.; visualization, **S.E.** and R.W.; supervision, K.Ü., O.G., H.K., I.M.H. and R.W.; project administration and funding acquisition R.W. and K.Ü.

Detailed personal contribution: Sebastian Einhauser (SE) analyzed the questionnaire results and curated the data. SE performed the weight-based standardization to age, sex and municipality. SE analyzed patient characteristics and performed the dropout analysis. SE computed the crude seropositivity over time, as well as the serology and PCR concordance. Furthermore, he analyzed the dynamics of standardized N-antibody seropositivity, surveillance detection and infection fatality, accounting for test misclassification and unobservable deaths, together with a subgroup analysis for senior care homes. All Wilson-Confidence intervals were computed by SE, Bayesian-credibility intervalls by FG. Vaccination analysis was performed by SE. SE wrote the original manuscript.

Manuscript 4: "Comparative Immunogenicity of COVID-19 Vaccines in a Population-Based Cohort Study with SARS-CoV-2-Infected and Uninfected Participants"

This manuscript was published online under the above-named title in the peer-reviewed journal Vaccines on 22th of February 2022. DOI: 10.3390/vaccines10020324

Authors: David Peterhoff*, **Sebastian Einhauser***, Stephanie Beileke*, Hans-Helmut Niller, Felix Günther, Michael Schachtner, Benedikt Asbach, Philipp Steininger, Matthias Tenbusch, Antonia S Peter, Andre Gessner, Ralph Burkhardt, Iris M Heid, Ralf Wagner*, Klaus Überla*

* Authors contributed equally and share first or last authorship

Author contributions:

Conceptualization, K.Ü. and R.W.; methodology, D.P., **S.E.**, R.B. and M.T.; validation, D.P., **S.E.**, S.B., K.Ü. and R.W.; formal analysis, S.B., K.Ü., B.A., F.G. and I.M.H.; investigation, D.P., **S.E.**, M.S., R.B., A.S.P., S.B. and H.-H.N.; resources, R.W., A.G., I.M.H. and K.Ü.; data curation, **S.E.**, S.B., R.W. and K.Ü.; writing—original draft preparation, K.Ü. and R.W.; writing—review and editing, **S.E.**, D.P., F.G., I.M.H., M.T. and P.S.; visualization, K.Ü. and S.B.; supervision, R.W. and K.Ü.; project administration and funding acquisition R.W. and K.Ü.

Detailed personal contribution: Sebastian Einhauser (SE) curated the data and measured neutralization. SE contributed to Model-based binding levels related to age and time since vaccination with preparatory analysis. SE provided key reagents and protocols for variant-specific neutralization. Finally, SE contributed to methodological decisions and the revision of the manuscript.

Manuscript 5: "Longitudinal effects of SARS-CoV-2 breakthrough infection on imprinting of neutralizing antibody responses"

This manuscript was published online under the above-mentioned title in the peer-reviewed journal *eBiomedicine* in November 2024. DOI 10.1016/j.ebiom.2024.105438

Authors: **Sebastian Einhauser,** Claudia Asam, Manuela Weps, Antonia Senninger, David Peterhoff, Stilla Bauernfeind, Benedikt Asbach, George William Carnell, Jonathan Luke Heeney, Monika Wytopil, André Fuchs, Helmut Messmann, Martina Prelog, Johannes Liese, Samuel D. Jeske, Ulrike Protzer, Michael Hoelscher, Christof Geldmacher, Klaus Überla, Philipp Steininger* and Ralf Wagner*
on behalf of the CoVaKo Study group
* Authors contributed equally and share first or last authorship

Author contributions:

Conceptualization: R.W., K.Ü., P.S.; Methodology: **S.E.**, C.A., R.W., Participant recruitment and study visits: S.D.J., C.A., A.F., M.W., S.B., C.J., C.C., A.Wil., M.V., M.We., B.M.J.L., V.S., B.L., P.S.; Laboratory investigations: **S.E.**, A.S., D.P.; Statistical analysis: **S.E.**, B.A., R.W. Visualization: **S.E.**, C.A., P.S.; Resources: M.P., H.M., U.P., J.L., M.H., R.W., K.Ü.; Writing (original draft): **S.E.**, C.A., R.W.; Writing (review and editing): all authors Supervision: M.P., H.M., U.P., J.L., M.H., R.W., K.Ü., P.S.; Project administration: K.Ü., P.S.; Funding acquisition: H.M., U.P., J.L., M.H., R.W., K.Ü.

Detailed personal contribution: Sebastian Einhauser (SE) developed the methodology of the manuscript and curated the data. He performed and established the variant-specific neutralization assays and did the subgroup analytics and statistics. SE developed scripts for non-linear generalized additive modeling approaches to simultaneously analyze the influence of time between vaccination, infection variant and breadth of the neutralizing antibody response. Furthermore, SE implemented the magnitude-breadth analysis method to SARS-CoV-2 for simultaneous analysis of the neutralizing antibody response against multiple virus variants. SE wrote scripts for antigenic mapping and antibody landscaping. SE established and wrote the scripts for random forest and neural network machine learning models and developed the algorithm cushioning bias from smaller group sizes for the prediction of infecting VOCs from neutralizing antibody profiles. SE performed all the statistical and bioinformatic analysis. SE wrote the original manuscript together with CA and RW.

B) Appendix publications

Appendix publication 1: "SARS-CoV-2 Spike Protein Stabilized in the Closed State Induces Potent Neutralizing Responses."

Authors: Carnell GW, Ciazynska KA, Wells DA, Xiong X, Aguinam ET, McLaughlin SH, Mallery D, Ebrahimi S, Ceron-Gutierrez L, Asbach B, **Einhauser S**, Wagner R, James LC, Doffinger R, Heeney JL, Briggs JAG

Published on 12th of **July 2021 in Journal of Virology**

DOI: 10.1128/JVI.00203-21

Author contributions: Conceptualization: G.W.C., X.X., L.C.J., J.L.H., J.A.G.B. Data curation: G.W.C., K.A.C., D.A.W., S.H.M., D.M., R.D., J.A.G.B. Formal Analysis: D.A.W., S.H.M. Funding acquisition: R.W., L.C.J., J.L.H., J.A.G.B. Investigation: G.W.C., K.A.C., X.X., E.T.A., S.H.M., D.M., **S.E.**, L.C.G. Methodology: G.W.C., R.D. Project administration: J.L.H., J.A.G.B. Resources: B.A., **S.E.**, R.W. Supervision: L.C.J., R.D., J.L.H., J.A.G.B. Visualization: G.W.C., K.A.C., D.A.W., S.H.M., D.M., J.A.G.B. Writing – original draft: G.W.C., J.A.G.B. Writing – review and editing: G.W.C., K.A.C., D.A.W., X.X., E.T.A., S.H.M., D.M., R.W., L.C.J., R.D., J.L.H., J.A.G.B.

Personal contribution: Sebastian Einhauser contributed key reagents and protocols for neutralization assays.

Appendix publication 2: "Estimates and Determinants of SARS-Cov-2 Seroprevalence and Infection Fatality Ratio Using Latent Class Analysis: The Population-Based Tirschenreuth Study in the Hardest-Hit German County in Spring 2020"

Authors: Ralf Wagner*, David Peterhoff†, Stephanie Beileke†, Felix Günther†, Melanie Berr, **Sebastian Einhauser**, Anja Schütz, Hans Helmut Niller, Philipp Steininger, Antje Knöll, Matthias Tenbusch, Clara Maier, Klaus Korn, Klaus J. Stark, André Gessner, Ralph Burkhardt, Michael Kabesch, Holger Schedl, Helmut Küchenhoff, Annette B. Pfahlberg, Iris M. Heid†, Olaf Gefeller†, and Klaus Überla*

Published on 10th **June 2021 in Viruses**.

DOI: 10.3390/v13061118

Author contributions: Conceptualization, R.W., I.M.H., O.G. and K.Ü.; Data curation, R.W., S.B., F.G., M.B., I.M.H., O.G. and K.Ü.; Formal analysis, D.P., F.G., **S.E.**, M.T., K.J.S., A.B.P., I.M.H. and O.G.; Funding acquisition, R.W. and K.Ü.; Investigation, D.P., S.B., **S.E.**, A.S., H.H.N., P.S., A.K., M.T., C.M., K.K. and R.B.; Methodology, D.P., F.G., K.J.S. and O.G.; Project administration, R.W., S.B., M.B., H.H.N., A.K., H.S. and K.Ü.; Resources, R.W., A.G., R.B., M.K., H.S., H.K., I.M.H., O.G. and K.Ü.; Software, F.G., A.B.P. and O.G.; Supervision, R.W., D.P., M.T., R.B., H.K., I.M.H., O.G. and K.Ü.; Validation, R.W., D.P., F.G., M.B., I.M.H., O.G. and K.Ü.; Visualization, R.W., S.B., F.G., **S.E.** and K.Ü.; Writing—original draft, R.W., D.P.,

F.G., I.M.H., O.G. and K.Ü.; Writing—review & editing, R.W., H.K., A.B.P., I.M.H., O.G. and K.Ü. All authors have read and agreed to the published version of the manuscript.

Personal contribution: Sebastian Einhauser performed statistical analysis, data curation and visualized figures/tables.

Appendix publication 3: "Paucity and discordance of neutralising antibody responses to SARS-CoV-2 VOCs in vaccinated immunodeficient patients and health-care workers in the UK."

Authors: Nadesalingam A, Cantoni D, Wells DA, Aguinam ET, Ferrari M, Smith P, Chan A, Carnell G, Ohlendorf L, **Einhauser S**, George C, Wagner R, Temperton N, Castillo-Olivares J, Baxendale H, Heeney JL; HICC consortium.

Published in **September 2021 in The Lancet Microbe**.

Doi: 10.1016/S2666-5247(21)00157-9

Author contributions: .not published in the manuscript.

Personal contribution: Sebastian Einhauser provided protocols and material for SARS-CoV-2 VOC neutralization assays.

Appendix publication 4: "Coronavirus Pseudotypes for All Circulating Human Coronaviruses for Quantification of Cross-Neutralizing Antibody Responses."

Authors: Sampson AT, Heeney J, Cantoni D, Ferrari M, Sans MS, George C, Di Genova C, Mayora Neto M, **Einhauser S**, Asbach B, Wagner R, Baxendale H, Temperton N, Carnell G

Published on 10th of **August 2021 in Viruses**

DOI: 10.3390/v13081579

Author contributions: Conceptualization, A.T.S., J.H., N.T. and G.C.; Funding acquisition, J.H. and N.T.; Investigation, A.T.S., M.F., C.G., M.S.S., R.W., C.D.G., D.C., M.M.N., **S.E.**, B.A., N.T. and G.C.; Methodology A.T.S., M.F., C.G., M.S.S., C.D.G., D.C., M.M.N., N.T. and G.C.; Resources, R.W., **S.E.**, B.A., H.B. and N.T.; Writing—original draft, A.T.S.; Writing—review and editing, J.H., M.F., M.S.S., C.G., R.W., C.D.G., D.C., M.M.N., **S.E.**, B.A., H.B., N.T. and G.C.

Personal contribution: Sebastian Einhauser helped develop protocols and provided critical reagents for variant specific neutralization assays.

Appendix publication 5: "Association between Reactogenicity and Immunogenicity after Vaccination with BNT162b2."

Authors: Bauernfeind S, Salzberger B, Hitzenbichler F, Scigala K, **Einhauser S**, Wagner R, Gessner A, Koestler J, Peterhoff D.

Published on 27th of **September 2021 in Vaccines**

DOI: 10.3390/vaccines9101089

Author contributions: S.B., B.S. and A.G. conceived the study. S.B. and K.S. collected samples. J.K., D.P. and **S.E.** performed experiments. S.B., B.S., J.K., D.P., **S.E.** and R.W. analyzed the data. S.B. and F.H. drafted the manuscript.

Personal contribution: Sebastian Einhauser performed neutralization assays and did the statistical analysis to find the association between reactogenicity and immunogenicity after vaccination.

Appendix publication 6: "Neutralisation Hierarchy of SARS-CoV-2 Variants of Concern Using Standardised, Quantitative Neutralisation Assays Reveals a Correlation With Disease Severity; Towards Deciphering Protective Antibody Thresholds."

Authors: Cantoni D, Mayora-Neto M, Nadesalingam A, Wells DA, Carnell GW, Ohlendorf L, Ferrari M, Palmer P, Chan ACY, Smith P, Bentley EM, **Einhauser S**, Wagner R, Page M, Raddi G, Baxendale H, Castillo-Olivares J, Heeney J, Temperton N.

Published on 7th of **March 2022 in Frontiers of Immunology**

DOI: 10.3389/fimmu.2022.773982

Author contributions: DC, HB, JC-O, JH, MP, RW, and NT designed the study. DC and MM-N carried out the experiments. GR and HB co-ordinated patient and HCW selection, for blood sample collection from RPH. AN, AC, and PS contributed by processing blood sample into sera, cataloguing and providing reagents. EB, RW, and **SE** contributed by generating plasmids of VOCs. DW and PP contributed by processing data and performing statistical analysis of the results. GC, LO, MF, and **SE** contributed to sample preparation, optimisation of pseudotype virus production, protocol design and interpretation of results. DC wrote the original draft of the manuscript. MM-N, AN, DW, GC, LO, MF, PP, AC, PS, EB, **SE**, RW, MP, GR, HB, JC-O, JH, and NT provided critical feedback on the data presentation, data analysis and manuscript.

Personal contribution: Sebastian Einhauser helped develop protocols and provided critical reagents for variant specific neutralization assays.

Appendix publication 7: "Association between Adverse Reactions and Humoral Immune Response No Longer Detectable after BNT162b2 Booster Vaccination."

Authors: Bauernfeind S, **Einhauser S**, Tydykov L, Mader AL, Salzberger B, Hitzenbichler F, Mohr A, Burkhardt R, Wagner R, Peterhoff D

Published on 25th of **September 2022 in Vaccines**

DOI: 10.3390/vaccines10101608

Author contributions: S.B. conceived the study. S.B. collected samples. D.P., L.T., A.-L.M., **S.E**. and R.B. performed experiments. S.B., B.S., D.P., **S.E.** and R.W. analyzed the data. S.B., F.H. and A.M. drafted the manuscript.

Personal contribution: Sebastian Einhauser performed neutralization assays and contributed to data/statistical analysis.

Appendix publication 8: "Higher Infection Risk among Health Care Workers and Lower Risk among Smokers Persistent across SARS-CoV-2 Waves-Longitudinal Results from the Population-Based TiKoCo Seroprevalence Study."

Authors: Günther F, **Einhauser S**, Peterhoff D, Wiegrebe S, Niller HH, Beileke S, Steininger P, Burkhardt R, Küchenhoff H, Gefeller O, Überla K, Heid IM, Wagner R.

Published on 17th of **December 2022 in International Journal of Environmental Research and Public Health**

DOI: 10.3390/ijerph192416996

Author contributions: Conceptualization, K.Ü. and R.W.; methodology, F.G., D.P. and **S.E.**; sample access and investigation, D.P., **S.E.**, R.B., S.B., P.S., H.H.N., K.Ü. and R.W.; validation, F.G., **S.E**., D.P. and S.W.; formal analysis, F.G., S.W., I.M.H. and O.G.; data curation, F.G., **S.E.**, S.B., K.Ü. and R.W.; resources, I.M.H., K.Ü. and R.W.; writing—original draft preparation, F.G., I.M.H. and R.W.; writing—review and editing, K.Ü., O.G. and **S.E.**; visualization, F.G.; supervision, I.M.H., H.K., K.Ü. and R.W.; project administration and funding acquisition, R.W. and K.Ü.

Personal contribution: Sebastian Einhauser curated the samples and data, measured neutralizing antibodies, helped to decide on appropriate methodology and reviewed and edited the manuscript.

Appendix publication 9: "Liposome-based high-throughput and point-of-care assays toward the quick, simple, and sensitive detection of neutralizing antibodies against SARS-CoV-2 in patient sera"

Authors: Streif S, Neckermann P, Spitzenberg C, Weiss K, Hoecherl K, Kulikowski K, Hahner S, Noelting C, **Einhauser S**, Peterhoff D, Asam C, Wagner R, Baeumner AJ.

Published in **March 2023 in Analytical and Bioanalytical Chemistry**

DOI: 10.1007/s00216-023-04548-3

Author contributions: Conceptualization, AJB, RW, and SS; performed HTS experiments, SS; performed POC experiments, SS and KW; liposome synthesis and optimization, SS, KH, CS, KK; cloning of recombinant protein expression plasmids, PN and CA; expression, purification, and quality control of recombinant ACE2 and RBD, PN, CA, DP, SH; pseudovirus neutralization assays, **SE**; RBD binding antibody test, CN; writing — original draft, SS; writing — review and editing, **SE**, PN, RW, AJB

Personal contribution: Sebastian Einhauser provided serum samples, measured neutralizing antibodies and reviewed and edited the manuscript thoroughly.

Appendix publication 10: "Glycan masking of a non-neutralising epitope enhances neutralising antibodies targeting the RBD of SARS-CoV-2 and its variants."

Authors: Carnell GW, Billmeier M, Vishwanath S, Suau Sans M, Wein H, George CL, Neckermann P, Del Rosario JMM, Sampson AT, **Einhauser S**, Aguinam ET, Ferrari M, Tonks P, Nadesalingam A, Schütz A, Huang CQ, Wells DA, Paloniemi M, Jordan I, Cantoni D, Peterhoff D, Asbach B, Sandig V, Temperton N, Kinsley R, Wagner R, Heeney JL

Published on 23rd of **February 2023 in Frontiers of Immunology**

DOI: 10.3389/fimmu.2023.1118523

Author contributions: Conceptualization, JH, RW, RK. Data curation: GC, MB, SV. Investigation: GC, MB, SV, BA, JH, RK, RW. Methodology: GC, MB, SV, HW, AS, MSS, CG, JDR, ATS, AN, CH, DW, MF, MP, PT, DP. Critical reagents: **SE**, PN, DC, NT, IJ, VS. Project administration: JH, RW. Resources: JH, RW. Supervision: JH, RW, RK. Visualization: GC, MB, SV. Writing—original draft: GC, MB, SV. Writing—review and editing: GC, MB, SV, JH, RW, IJ.

Personal contribution: Sebastian Einhauser provided critical reagents, namely protocols and DNA constructs for variant specific neutralization assays.

Appendix publication 11: "A second update on mapping the human genetic architecture of COVID-19."

Authors: COVID-19 Host Genetics Initiative

Published on 6th of **September 2023 in Nature**

DOI: 10.1038/s41586-023-06355-3

Author contributions: Initiative consists of too many authors to type out here.

Personal contribution: Sebastian Einhauser together with others contributed data from the TiKoCo19 study.

Appendix publication 12: "A computationally designed antigen eliciting broad humoral responses against SARS-CoV-2 and related sarbecoviruses."

Authors: Vishwanath S, Carnell GW, Ferrari M, Asbach B, Billmeier M, George C, Sans MS, Nadesalingam A, Huang CQ, Paloniemi M, Stewart H, Chan A, Wells DA, Neckermann P, Peterhoff D, **Einhauser S**, Cantoni D, Neto MM, Jordan I, Sandig V, Tonks P, Temperton N, Frost S, Sohr K, Ballesteros MTL, Arbabi F, Geiger J, Dohmen C, Plank C, Kinsley R, Wagner R, Heeney JL

Published on 25th of **September 2023 in Nature Biomedical Engineering**

DOI: 10.1038/s41551-023-01094-2

Author contributions: S.V., D.A.W. and S.F. developed the computational pipeline. G.W.C., M.F., C.G., M.S.S., A.N., C.Q.H., M.P., H.S. and A.C. performed the in vitro assays. G.W.C. and P.T. performed the animal experiments. B.A., M.B., P.N., D.P. and **S.E.** performed DNA purification and preparation. M.B., I.J. and V.S. performed MVA production and purification. K.S., M.T.L.B., F.A., J.G., C.D. and C.P. performed mRNA production and purification. D.C., M.M.N. and N.T. provided key reagents. S.V. and G.W.C. analysed and visualized the data. R.K., R.W. and J.L.H. acquired funding, conceptualized the investigation, reviewed data and administered the project. R.W. and J.L.H. supervised the project. S.V. wrote the original draft. S.V., G.W.C. and J.L.H. reviewed and edited the manuscript.

Personal contribution: Sebastian Einhauser contributed key reagents/DNA constructs.

Appendix publication 13: "Population-based study of the durability of humoral immunity after SARS-CoV-2 infection."

Authors: Peterhoff D, Wiegrebe S, **Einhauser S**, Patt AJ, Beileke S, Günther F, Steininger P, Niller HH, Burkhardt R, Küchenhoff H, Gefeller O, Überla K, Heid IM, Wagner R.

Published on 5th of **October 2023 in Frontiers of Immunology**

DOI: 10.3389/fimmu.2023.1242536

Author contributions: RW and KÜ conceived the study. RW, KÜ, IH, OG, and DP conceptualized the study. RW, IH, RB, and DP supervised the research activities. HN, SB, PS collected the blood samples. DP developed the serological methodology. DP, **SE**, and AP collected the data. Data curation was done by SW, DP, FG, and **SE**. DP, SW and IH performed the statistical analysis. Visualization of the data was done by DP and SW. DP drafted the manuscript. SW, IH and RW contributed to the revision of the manuscript.

Personal contribution: Sebastian Einhauser performed all neutralization assays for the three time points (633 samples) and contributed to data analysis and sample curation.

Appendix publication 14: "Clinical and immunological benefits of full primary COVID-19 vaccination in individuals with SARS-CoV-2 breakthrough infections: A prospective cohort study in non-hospitalized adults."

Authors: Prelog M, Jeske SD, Asam C, Fuchs A, Wieser A, Gall C, Wytopil M, Mueller-Schmucker SM, Beileke S, Goekkaya M, Kling E, Geldmacher C, Rubio-Acero R, Plank M, Christa C, Willmann A, Vu M, **Einhauser S**, Weps M, Lampl BMJ, Almanzar G, Kousha K, Schwägerl V, Liebl B, Weber B, Drescher J, Scheidt J, Gefeller O, Messmann H, Protzer U, Liese J, Hoelscher M, Wagner R, Überla K, Steininger P; CoVaKo Study Group.

Published in **November 2023 in Journal of Clinical Virology**
DOI: 10.1016/j.jcv.2023.105622

Author contributions: Martina Prelog: Conceptualization, Formal analysis, Investigation, Methodology, Resources, Supervision, Visualization, Writing – original draft, Writing – review & editing. Samuel D. Jeske: Investigation, Methodology. Claudia Asam: Investigation, Visualization, Writing – review & editing. Andre Fuchs: Investigation, Methodology, Writing – original draft, Writing – review & editing. Andreas Wieser: Investigation, Methodology. Christine Gall: Formal analysis, Visualization, Writing – review & editing. Monika Wytopil: Investigation, Writing – review & editing. Sandra M. Mueller-Schmucker: Investigation, Writing – review & editing. Stephanie Beileke: Investigation, Writing – review & editing. Mehmet Goekkaya: Investigation, Writing – review & editing. Elisabeth Kling: Investigation. Christof Geldmacher: Investigation. Raquel Rubio-Acero: Investigation. Michael Plank: Investigation. Catharina Christa: Investigation. Annika Willmann: Investigation. Martin

Vu: Investigation. **Sebastian Einhauser**: Investigation, Writing – review & editing. Manuela Weps: Investigation. Benedikt M.J. Lampl: Investigation. Giovanni Almanzar: Investigation. Kimia Kousha: Investigation. Valeria Schwägerl: Investigation. Bernhard Liebl: Investigation. Beatrix Weber: Data curation. Johannes Drescher: Data curation. Jörg Scheidt: Data curation. Olaf Gefeller: Formal analysis, Writing – review & editing. Helmut Messmann: Funding acquisition, Resources, Supervision. Ulrike Protzer: Funding acquisition, Resources, Supervision, Conceptualization. Johannes Liese: Conceptualization, Funding acquisition, Resources, Supervision. Michael Hoelscher: Funding acquisition, Resources, Supervision. Ralf Wagner: Conceptualization, Funding acquisition, Methodology, Resources, Supervision, Writing – review & editing. Klaus Überla: Conceptualization, Funding acquisition, Methodology, Project administration, Resources, Supervision, Writing – review & editing. Philipp Steininger: Conceptualization, Data curation, Formal analysis, Investigation, Methodology, Project administration, Supervision, Visualization, Writing – original draft, Writing – review & editing

Personal contribution: Sebastian Einhauser performed VOC specific neutralization assays, contributed to data analysis and review and writing of the manuscript.

Appendix publication 15: "Evolution of protective SARS-CoV-2-specific B and T cell responses upon vaccination and Omicron breakthrough infection"

Authors: Ahmed MIM, **Einhauser S**, Peiter C, Senninger A, Baranov O, Eser TM, Huth M, Olbrich L, Castelletti N, Rubio-Acero R, Carnell G, Heeney J, Kroidl I, Held K, Wieser A, Janke C, Hoelscher M, Hasenauer J, Wagner R, Geldmacher C; KoCo19/ORCHESTRA working group.

Published on 21st of **June 2024 in iScience**

DOI: 10.1016/j.isci.2024.110138

Author contributions: R.W., **S.E.**, A.S., J. Heeney, and G.C. contributed to the experimental work and analyzed neutralizing antibody responses. M.I.M.A., T.M.E., and K.H. contributed to the experimental work and analyzed T cell responses. R.R.-A. and A.W. analyzed binding antibody responses. C.P., M. Huth, and J. Hasenauer developed the mathematical models. M.I.M.A., **S.E**., J. Hasenauer, C.P., N.C., C.G., and O.B. performed the statistical analysis and prepared figures. The human cohort study was planned by C.G., I.K., A.W., L.O., and M. Hoelscher (KoCo19-sub-study). C.G., J. Hasenauer, and M.I.M.A. conceived the study. M.I.M.A., C.J., and I.K. contributed to the clinical work.

Personal contribution: Sebastian Einhauser performed VOC specific neutralization assays and contributed to statistical analysis, figure design and writing.

Appendix publication 16: "Impedance-based monitoring of titration and neutralization assays with VSV-G and SARS-CoV-2-spike pseudoviruses"

Authors: Anne-Kathrin Mildner, Sebastian Einhauser, Stefanie Michaelis, Klara Rogalla v. Bieberstein, Ralf Wagner, Joachim Wegener.

Published on 27th **August 2024 in Applied Research**.

DOI: 10.1002/appl.202400097.

Author contributions not published.

Personal contribution: Sebastian Einhauser provided key reagents, including custom rescued pseudoviruses, human sera and antibodies.

Appendix publication 17: "Computationally designed Spike antigens induce neutralising responses against the breadth of SARS-COV-2 variants"

Authors: Vishwanath S, Carnell GW, Billmeier M, Ohlendorf L, Neckermann P, Asbach B, George C, Sans MS, Chan A, Olivier J, Nadesalingam A, **Einhauser S**, Temperton N, Cantoni D, Grove J, Jordan I, Sandig V, Tonks P, Geiger J, Dohmen C, Mummert V, Samuel AR, Plank C, Kinsley R, Wagner R, Heeney JL.

Published on 9th **September 2024 in NPJ Vaccines**.

DOI: 10.1038/s41541-024-00950-9.

Author contributions S.V. developed the computational pipeline. G.W.C., L.O., C.G., M.S.S., A.C., J.O., and A.N., performed the in vitro assays. G.W.C. and P.T. performed the animal experiments. M.B., P.N., B.A., and **S.E**. performed DNA cloning, purification, and preparation. M.B., I.J. and V.S. performed MVA production and purification. J.G., C.D.,V.M., A.R.S., and C.P. performed mRNA production and purification. D.C., J.G., and N.T. provided key reagents. S.V. and G.W.C. analysed and visualised the data. R.K., R.W. and J.L.H. acquired funding, conceptualised the investigation, reviewed data, and administered the project. R.W. and J.L.H. supervised the project. S.V. wrote the original draft. S.V., G.W.C. and J.L.H. reviewed and edited the manuscript

Personal contribution: Sebastian Einhauser provided critical plasmids.

1 Abstract

With the start of the SARS-CoV-2 pandemic in late 2019, understanding the immune responses to SARS-CoV-2 in various populations became critical for guiding public health strategies and vaccination campaigns. The variability in how e.g. different age groups, populations and individuals with prior infections as well as individuals with vaccine breakthrough infections responded to the virus and vaccines offered valuable insights in understanding the pandemic's dynamics. This thesis synthesized data and publications from multiple cohorts to shed light on the immune dynamics of children and the general population and investigated the impact of emerging variants.

Children and adolescents often experience mild symptoms during the acute phase of COVID-19, making SARS-CoV-2 infections easily overlooked in this population. The first manuscript sought to better understand the immune responses in children following infection as well as the role of children in transmission dynamics of the early SARS-CoV-2 pandemic. In a cross-sectional design, children aged 1-17 were recruited, symptoms were recorded, and antibody responses were analyzed. Of the 2,832 children tested between May and July 2020, antibodies were identified in 162 children (5.7%). Notably, only 86% of antibody-positive children exhibited sufficient neutralizing activity, irrespective of age and sex, whereas 30% of PCR positive children showed no seroconversion at all. In contrast to grown-ups, neither specific COVID-19 symptoms except for loss of smell and taste, nor any relationship between antibody response and symptoms could be found.

SARS-CoV-2 antibody testing was rapidly introduced in early 2020 and played a crucial role in determining serostatus and potential correlates of protection. Yet, the transition from initial test development to exhaustive population-based testing harbors the risk of introducing spectrum bias. The second study of this thesis aimed to explore the presence and extent of spectrum bias and to estimate the performance measures of antibody tests in a population-based setting, using data from 856 participants within the TiKoCo-19 cohort. Notable differences in test sensitivities and specificities were observed when transitioning from simulated test-development to population-based application, with greater bias in earlier tests. The Roche ELECSYS N and S tests outperformed others in sensitivity and specificity for dichotomous outcomes but did not correlate well with neutralization capacity. In contrast, the in-house ELISA, though inferior in dichotomous testing, showed solid quantitative correlation with neutralization capacity, indicating it might better reflect protective immunity.

In the face of hotspot outbreaks, contradicting reports on infection fatality and quickly introduced vaccination, understanding the dynamics of SARS-CoV-2 spread and the impact of public health interventions required detailed population-level data over time. Thus, in the third manuscript, a

longitudinal serosurveillance study with 4203 participants in Tirschenreuth, the hardest-hit county in Germany, provided insights into seroprevalence, surveillance detection ratios (SDR), infection fatality ratios (IFR), and vaccination success. From June 2020 to April 2021, the seroprevalence increased from 9.2% to 15.4%. The SDR decreased significantly from 5 to 1, reflecting enhanced testing efforts. The general IFR of 2.3% increased slightly to 3.3% and remained highest among individuals aged 70 and above (>10%). By April 2021, vaccination rates among the elderly were high, exceeding 77.4%.

The fourth manuscript aimed to broaden the knowledge on the vaccine immunogenicity. Thus, SARS-CoV-2 antibody responses were measured in the Tirschenreuth cohort during April 2021. Single-dose vaccinated participants showed median neutralizing antibody titers of ID50 = 25 to 75, whereas two-dose vaccinated individuals had significantly higher titers. Regression analysis indicated that older age and longer time since vaccination reduced antibody levels. Previously infected participants with one vaccine dose exhibited high median ID50 levels, suggesting robust immune priming. Prior infection also led to higher IgA levels in response to vaccination compared to uninfected individuals.

The emergence of VOCs with reports of immune escape and immune imprinting as well as a co-occurring change in infection dynamics and spiking reports of vaccine breakthrough infections, further expanded the landscape of SARS-CoV-2 immune responses. The final manuscript examined the impact of SARS-CoV-2 variants of concern (VOCs) and vaccination on the neutralizing antibody profile in a longitudinal multicenter cohort study. Analysis of vaccinated and non-vaccinated individuals post-infection with Alpha, Delta, or Omicron variants showed enhanced neutralization capacity and breadth in vaccinated individuals against multiple VOCs. Sustained neutralization was observed after breakthrough infections, particularly in triple-vaccinated individuals. Antigenic mapping revealed a shift towards VOC-specific responses post-infection, yet long term responses revealed an imprinted bias towards the initially immunized antigen. Nonetheless, machine-learning models could confirm a sustained change in immune profiles following breakthrough infections.

In conclusion, this collection of studies shed light on the infection and antibody dynamics in children and hotspot regions during the early pandemic. We identified senior care homes and the elderly as drivers of infection fatality, underscored the variability in immune responses among different populations and highlighted the importance of vaccination. Additionally, multiple widely used tests were benchmarked, identifying apparent spectrum bias in early tests. Finally, variant based immune imprinting effects were illustrated, though bioinformatical methods could identify enhanced breadth and sustained shifts in immunity after antigenically distant immunization events.

2 Zusammenfassung

Mit dem Ausbruch der SARS-CoV-2-Pandemie Ende 2019 wurde rasch deutlich, dass eine detaillierte Analyse der spezifischen Immunantworten auf SARS-CoV-2 in verschiedenen Bevölkerungsgruppen nicht nur für das grundlegende Verständnis der Virus-Wirt-Interaktion von zentraler Bedeutung ist, sondern auch wichtige Impulse für Strategien im öffentlichen Gesundheitswesen und für Impfkampagnen liefern wird. Die teils deutlichen Unterschiede in den Immunantworten zwischen Altersgruppen, Bevölkerungsgruppen sowie bei Personen mit vorangegangener Infektion oder Impfdurchbruchsinfektion lieferten dabei zentrale Erkenntnisse über die Heterogenität der Immunabwehr gegen SARS-CoV-2. Diese Dissertation fasst Daten und Publikationen aus mehreren Kohorten zusammen, um die Infektionsdynamik bei Kindern und in der Allgemeinbevölkerung zu beleuchten sowie den Einfluss neu auftretender Virusvarianten zu untersuchen.

Kinder und Jugendliche zeigen während der akuten Phase von COVID-19 oft nur milde Symptome, wodurch SARS-CoV-2-Infektionen in dieser Bevölkerungsgruppe häufig unentdeckt bleiben. Das erste Manuskript hatte zum Ziel, die Immunantworten bei Kindern nach einer Infektion sowie deren Rolle in der Übertragungsdynamik der frühen SARS-CoV-2-Pandemie besser zu verstehen. In einem Querschnittsdesign wurden Kinder im Alter von 1 bis 17 Jahren rekrutiert, Symptome erfasst und Antikörperantworten analysiert. Von den 2.832 zwischen Mai und Juli 2020 getesteten Kindern, wurden bei 162 (5,7 %) Antikörper nachgewiesen. Bemerkenswerterweise wiesen nur 86 % der Antikörper-positiven Kinder eine ausreichende neutralisierende Aktivität auf, unabhängig von Alter und Geschlecht, während 30 % der PCR-positiven Kinder überhaupt keine Serokonversion zeigten. Im Gegensatz zu Erwachsenen ließen sich weder spezifische COVID-19-Symptome (mit Ausnahme von Geruchs- und Geschmacksverlust), noch ein Zusammenhang zwischen Symptomen und Antikörperantwort feststellen.

SARS-CoV-2-Antikörpertests wurden Anfang 2020 schnell eingeführt und spielten eine zentrale Rolle bei der Bestimmung von Serostatus sowie der Untersuchung potenzieller Korrelate des Schutzes. Der Übergang von initialer Testentwicklung zu flächendeckenden bevölkerungsbasierten Testungen birgt jedoch das Risiko eines Spektrum Bias. Die zweite Studie dieser Arbeit zielte darauf ab, das Vorhandensein und Ausmaß dieses Bias zu untersuchen und die Leistungsmerkmale von Antikörpertests in einem bevölkerungsbasierten Umfeld, basierend auf Daten von 856 Teilnehmenden der TiKoCo-19-Kohorte, zu bewerten. Beim Übergang von der simulierten Testentwicklung zur Anwendung in der Allgemeinbevölkerung zeigten sich deutliche Unterschiede in Sensitivität und Spezifität, mit stärkerem Bias bei früheren Tests. Die Roche ELECSYS N- und S-Tests schnitten in Bezug auf Sensitivität und Spezifität bei dichotomen Ergebnissen am besten ab, korrelierten jedoch nur

schwach mit der Neutralisationskapazität. Im Gegensatz dazu zeigte ein hausinterner ELISA, trotz schwächerer Leistung bei dichotomen Ergebnissen, eine zufriedenstellende quantitative Korrelation mit der Neutralisation.

Angesichts lokaler Ausbrüche, widersprüchlicher Berichte zur Infektionssterblichkeit und einer rasch eingeführten Impfkampagne war ein detailliertes Verständnis der Ausbreitungsdynamik von SARS-CoV-2, sowie der Auswirkungen von Maßnahmen auf Bevölkerungsebene und über die Zeit hinweg essenziell. Im dritten Manuskript wurde daher eine longitudinale Serosurveillance-Studie mit 4.203 Teilnehmenden in Tirschenreuth, dem am stärksten betroffenen Landkreis Deutschlands, durchgeführt. Die Studie ermöglichte Einblicke in Seroprävalenz, Surveillance Detection Ratios (SDR), Infektionssterblichkeitsraten (IFR) und Impferfolg. Zwischen Juni 2020 und April 2021 stieg die Seroprävalenz von 9,2 % auf 15,4 %. Die SDR sank signifikant von 5 auf 1, was auf verbesserte Teststrategien hindeutete. Die allgemeine IFR stieg leicht von 2,3 % auf 3,3 % und blieb bei Personen ab 70 Jahren am höchsten (> 10 %). Bis April 2021 war die Impfquote in der älteren Bevölkerung hoch und lag bei über 77,4 %.

Das vierte Manuskript zielte darauf ab, das Wissen zur Immunogenität der neu eingeführten Impfstoffe zu erweitern. Dazu wurden im April 2021 SARS-CoV-2-Antikörperantworten in der Tirschenreuth-Kohorte gemessen. Einfach geimpfte, seronegative Teilnehmende zeigten im Median neutralisierende Antikörpertiter (ID50) von 25 bis 75, während zweifach Geimpfte signifikant höhere Titer aufwiesen. Regressionsanalysen ergaben, dass höheres Alter und eine längere Zeit seit der Impfung mit niedrigeren Antikörperspiegeln assoziiert waren. Zuvor infizierte Teilnehmende mit nur einer Impfdosis wiesen deutlich höhere ID50-Werte auf, was auf eine verbesserte hybride Immunität hinweist. Eine vorherige Infektion führte zudem zu höheren IgA-Spiegeln nach Impfung im Vergleich zu nicht infizierten Personen.

Das Auftreten von besorgniserregenden Virusvarianten (Variants of Concern, VOCs), Berichte über Immunflucht und Immunprägung (imprinting), einhergehend mit veränderten Infektionsdynamiken und einer Zunahme von Impfdurchbrüchen, erweiterten die Variabilität und die Wichtigkeit des Verständnisses der SARS-CoV-2-Immunantworten erheblich. Das abschließende Manuskript untersuchte den Einfluss von VOCs und Impfungen auf das Profil neutralisierender Antikörper in einer longitudinalen, multizentrischen Kohortenstudie. Die Analyse geimpfter und ungeimpfter Personen nach Infektionen mit Alpha-, Delta- oder Omikron-Varianten zeigte bei Geimpften eine gesteigerte Neutralisationskapazität und -breite gegenüber mehreren VOCs. Nach Impfdurchbrüchen, insbesondere bei dreifach Geimpften, konnte eine länger anhaltende Neutralisation beobachtet

werden. Antigen Karten zeigten eine Verschiebung hin zu VOC-spezifischen Antworten nach Infektion, langfristig zeigte sich jedoch eine Prägung in Richtung des ursprünglich immunisierenden Antigens. Dennoch identifizierten Maschine-Learning-Modelle eine anhaltende Veränderung der Immunprofile nach Impfdurchbrüchen.

Zusammenfassend beleuchtet diese Sammlung von Studien die Infektions- und Antikörperdynamik bei Kindern und in Hotspot-Regionen während der frühen Pandemie. Weiterhin wurden Altenheime und ältere Menschen als Treiber der Infektionssterblichkeit identifiziert, die Variabilität der Immunantworten in verschiedenen Bevölkerungsgruppen unterstrichen und die Bedeutung der Impfung betont. Darüber hinaus wurden mehrere weit verbreitete Tests evaluiert, wobei ein deutlicher Spektrum Bias in frühen Tests festgestellt wurde. Abschließend wurden variantenabhängige Effekte der Immunprägung aufgezeigt, wenngleich bioinformatische Methoden eine verbesserte Breite und anhaltende Verschiebung der Immunantwort nach antigenisch entfernten Immunisierungsereignissen identifizieren konnten.

3 General introduction

3.1 Coronaviruses

Human coronaviruses were **first discovered** in 1965 for causing the "common cold"[1,2] and named after their characteristic solar-eclipse like appearance (lat. Corona for halo or crown) in an electron microscope[3,4] . Coronaviruses form the family Coronaviridae within the order of Nidovirales. They can be further divided in the subfamilies of Letovirinae and Orthocoronavirinae, while the latter is subdivided into the genera Alpha-, Beta-, Gamma- and Deltacoronavirus[5,6] .

Apart from a variety of animal coronaviruses mainly found in birds (Gamma, Delta), rodents and bats (Alpha, Beta)[5], there are two human **"common cold" coronaviruses** found within the Alphacoronaviruses, namely NL63 and 229E[7,8]. However, clinical interest is mainly focused on the Betacoronaviruses, containing, with OC43 an HKU1 two more common cold causing viruses[8] as well as more dangerous severe acute respiratory syndrome (SARS) coronavirus 1 and 2 and middle eastern respiratory syndrome (MERS) coronavirus[9–11]. Of note, though OC43 is nowadays known as a less dangerous common cold virus, it has been hypothesized as possible causative pathogen of the "Russian Flu" in the1890s, causing over 1 million deaths worldwide[12].

SARS-CoV-1 gained worldwide attention during an outbreak in China in 2002, resulting in an epidemic with over 8000 infections in 30 countries which lasted until 2004. The virus was cause for a most of the times severe illness with systemic and respiratory symptoms, resulting in a 9% mortality rate with even higher severity in the elderly, finally causing 774 deaths worldwide[9,11,13]. Epidemiological research suggested a zoonotic origin with links to food markets and animal handling[14,15]. Indeed, the virus was successfully isolated from civets and genetically linked to the human virus[16], but was later also found in other animals like raccoons, badgers and cats[7,17]. Thus, the definite origin of SARS-CoV-1 still remains uncertain.

The first human case of **MERS** was reported in 2012 in Egypt, with similar respiratory and systemic symptoms as SARS-CoV-1. Until today over 2500 cases have been observed with a high fatility rate of 35 % [18,19] and ongoing small outbreaks are occurring regularly. In contrast to SARS-CoV-1 with it's unknown origin, it is known that MERS is a zoonotic virus which is transmitted to humans by camels, though the actual origin is believed to be in bats[18,20].

As of today, neither dedicated vaccines, nor dedicated antiviral treatment are approved for MERS and SARS-CoV-1, though a variety of promising treatment options are researched[21].

3.2 The SARS-CoV-2 Pandemic

In December 2019 a pneumonia outbreak of unknown cause in Wuhan, China was quickly linked to a novel betacoronavirus (formerly 2019-nCoV, now **SARS-CoV-2**)[22]. Despite initial links to an animal market and possible zoonotic spread, human to human transmission was confirmed in January 2020. Regardless of drastic counter measures by the Chinese government and the WHO, the disease quickly spread in China, followed by cases in southeast Asia, Europe and the U.S[23]. In February 2020, over 1000 deaths have been recorded in connection with the "novel coronavirus disease 2019" (now named COVID-19), exceeding death counts of its predecessor SARS, and the virus was named SARS-CoV-2[24]. On 11th March 2020, the WHO officially declared a pandemic[23,25]. Despite severe countermeasures, like curfews, halting of flights, quarantine for infected, mandatory testing and more[23,26], the virus continued spreading globally in the following months, reaching around 75 million registered infections and appx. 1.8 million reported deaths by the end of the 2020.[23,27] An overview of Cases and Deaths over time in Germany is provided in **Figure 1**.

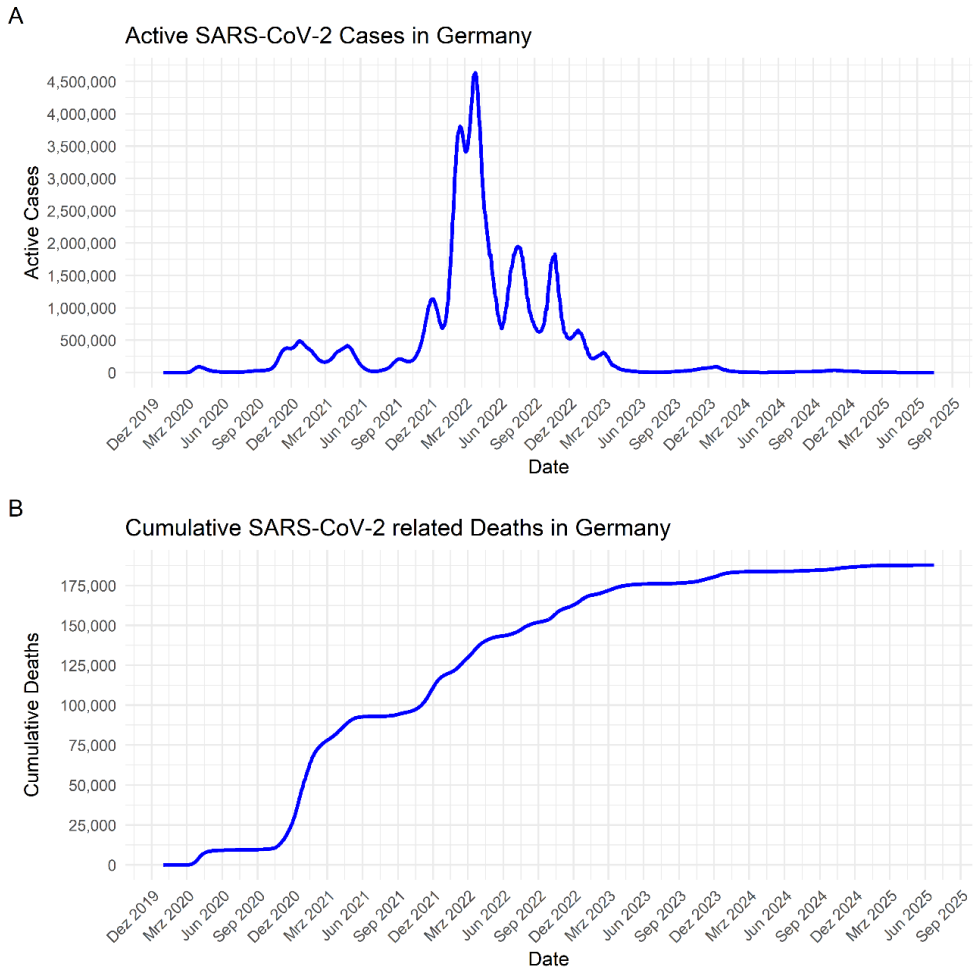

Figure 1 A Active SARS-CoV-2 cases in Germany between February 2020 and March 2024, based on PCR and LFA surveillance data. B Cumulative deaths in Germany in connection with a SARS-CoV-2 infection between February 2020 and March 2024. Figure generated from RKI data [28]

During that time, a variety of (sero-)**epidemiological studies** were initiated to investigate the incidence of the virus in certain areas, efficacy of testing, risk-factors, possible correlates of protection and more[29–33], including some of the studies comprising this manuscript. Additionally, the pandemic sparked the development and testing of a variety of novel antiviral compounds like e.g. Remdesivir[34,35], therapeutic antibodies like e.g. Regeneron[36] and several novel vaccines.

The end of 2020 marked a major change in the pandemic's dynamics. First, with Comirnaty[37,38] /BNT162b2, Vaxzevria[39–41] and Spikevax[42,43]/mRna-1273 the **first vaccines** were approved for emergency use in multiple countries[44] and initial studies reported high efficacies of over 95 % against severe disease[37,39,41,43,45] . Second, with the emergence of the Alpha variant, the so far genetically quite stable SARS-CoV-2 virus mutated notably, introducing the first Variant of Concern (VOC)[46–48]. Alpha was followed by more VOCs, e.g. Beta, Gamma, Delta, Omicron, each of which revealed different properties regarding infectivity, transmissibility, symptoms, disease severity and immune evasion[49] (as further elleborated in 0) and a multitude of Variants of Interest (VOI),describing emerging variants which in theory revealed concerning properties, but never prevailed.[46]

Over the next years the **worldwide vaccination campaign** resulted in over 13.6 billion administered vaccine doses meaning that 67% of the total human population received at least a basic immunization.[50] Despite the solid efficacy against severe disease, no sterile immunity could be achieved by vaccination, resulting in a total 777 billion registered cases and 7 million deaths worldwide, until the WHO declared the pandemic health threat over in May 2023. Following this, the majority of surveillance programs and other public health measures were stopped[51].

However, this did not mean abating numbers of **SARS-CoV-2 infections**[52], but rather a transition from an outbreak virus towards an endemic virus. Wastewater surveillance still showed high numbers of infections in 2024[53] and new VOCs emerge regularly[54]. Furthermore, a condition named long- or post-COVID has increasingly been gaining attention over the last years, with a variety of persisting symptoms impacting multiple organ systems, even after initial viral clearance[55,56]. Occurring in various strengths after appx. 7-9 % of SARS-CoV-2 infections and at even higher rates in non-vaccinated individuals, the condition affects a large number of individuals worldwide[55]. For additional information on Long COVID, readers are encouraged to consult the comprehensive reviews by Davis *et al.* [55] or Ely *et al*.[56], as this lies beyond the scope of this thesis.

3.2.1 Structure and Molecular Biology of SARS-CoV-2

SARS-CoV-2 is an **enveloped virus** forming virions of 60 to 140 nm diameter. The positive single stranded 29.9 kb RNA genome is complexed with the Nucleocapsid Protein, forming a helical structure anchored to the inside of the membrane via the M/Membrane Protein.[57] The outer membrane is additionally decorated with E/Envelope protein and the S/Spike protein, which forms the characteristical corona in the EM[58] .

The the 5' capped and 3' poly adenylated **RNA genome** can be divided in two large overlapping open reading frames, 1a and 1b, located at the 5' end, followed by multiple reading frames at the 3' end that encode the structural proteins and some accessory proteins.[57,59]

The 1a and 1b **reading frames** make up two thirds of the genome and produce the polyproteins pp1a and pp1ab, with the latter generated through a ribosomal frameshift[59–61]. These polyproteins are further processed autocatalytically into the **non-structural proteins** (NSPs 1–16). Those include essential proteins for viral replication, like a RNA-dependent RNA polymerase, RNA helicase and proteases, but also accessory proteins interacting with or modulating the host cell.[62] Of note, with Nsp14, SARS-CoV-2 possess an exonuclease with proofreading capabilities[63], resulting in a lower mutation rate compared to other RNA viruses[64]. The multiple reading frames in the 3' end of the genome encode for the **structural proteins** M, N, E and S as well as for additional accessory proteins (ORF 3a – ORF 10) as briefly summarized in Table 1.

Table 1 Overview of SARS-CoV-2 proteins by name, a short description of the proteins functions, size in Aminoacids(a.a.) and the encoding ORF, table adapted from Bai *et al.*[65]

Protein	Description	Protein size (a.a.)	ORF
Non-structural proteins (n=16)			
nsp1	Promotes degradation of cellular mRNA and suppresses innate immune responses	180	ORF1a
nsp2	Subject to positive selection pressure	638	ORF1a
nsp3	Associates with host proteins to facilitate viral replication	1,945	ORF1a
nsp4	Mediates interaction with host cell membranes	500	ORF1a
nsp5	Primary protease responsible for processing the coronavirus polyprotein	306	ORF1a
nsp6	Inhibits host antiviral responses and limits autophagosome expansion	290	ORF1a
nsp7	Forms a complex with nsp8, enhancing its stability	83	ORF1a
nsp8	Forms a complex with nsp7 to catalyze RNA primer synthesis	198	ORF1a
nsp9	Binds to nucleic acids	113	ORF1a
nsp10	Interacts with nsp14 and nsp16 to modulate viral replicase activity	139	ORF1a
nsp11	Function not yet determined	13	ORF1a
nsp12	Catalyzes viral RNA synthesis	932	ORF1b
nsp13	Regulates helicase activity through interaction with nsp8 and nsp12	601	ORF1b
nsp14	Functions as an exonuclease, reducing nucleotide mismatches	527	ORF1b
nsp15	Exhibits NendoU activity, involved in degradation of viral RNA	346	ORF1b
nsp16	Displays 2’-O-methyltransferase activity to help evade innate immune detection	298	ORF1b
Structural proteins (n=4)			
Envelope	Interacts with the M protein, contributes to viral membrane/particle formation	75	ORF4
Membrane	Defines the viral particle shape/ morphology and serves as a key mediator of coronavirus assembly	222	ORF5
Spike	Binds to host cell receptors (ACE2) to mediate attachment and fusion of viral and host membranes	1,282	ORF2
Nucleocapsid	Forms the nucleocapsid through binding of viral (genomic) RNA	419	ORF9a
Accessory proteins (n=9)			
Orf3a	Induces apoptosis, contributes to pathogenicity and viral release, and activates the inflammasome	275	ORF3a
Orf3b	Associated with AP-1 activation through the ERK and JNK signaling pathways	22	ORF3b
Orf6	Suppresses host cellular translation	61	ORF6 (27,202–27,387)
Orf7a	Involved in virus–host interactions	121	ORF7a (27,394–27,759)

Orf7b	Unknown function	43	ORF7b (27,756–27,887)
Orf8b	Involved in immune suppression and viral immune evasion	121	ORF8b (27,894–28,259)
Orf9b	Modulates the host immune response	97	ORF9b (28,284–28,942)
Orf9c	Alters mitochondrial function in host cells	70	ORF9c (28,733–28,577)
Orf10	unknown	38	ORF10 (29,558–29,674)

3.2.1.1 SARS-CoV-2 Spike

The SARS-CoV-2 spike (S) protein is a critical component of the virus's **structure and function**, playing a pivotal role in viral entry into host cells[66] . The protein is a trimeric glycoprotein, with each monomer weighing approximately 180 kDa[67]. Like other glycoproteins, the spike protein is expressed in the endoplasmic reticulum (ER) and Golgi apparatus, where it undergoes heavy glycosylation, helping it evade the host immune response while maintaining functionality[68–71]. It bears an 18-amino acid-long ER-retention signal on its C-terminus, ensuring that it remains in the ER/ERGIC/Golgi during the assembly of progeny virions[67,71]. The spike protein monomers are cleaved into two subunits, S1 and S2, by a cellular furin-like protease (S1/S2: …RRAR|SVA…), a process that represents the first step of activation and occurs within infected cells[72,73].

The **S1 subunit**, located at the N-terminus, is primarily responsible for attachment to the host cell. Its receptor-binding domain (RBD), found at the C-terminus of S1, binds specifically to the angiotensin-converting enzyme 2 (ACE2) receptor, facilitating viral entry[72]. Notably, the S1 subunit's N- and C-terminal regions fold into independent domains, a characteristic shared among coronaviruses[74,75].

The **S2 subunit**, located at the C-terminus, drives membrane fusion following receptor engagement, endocytosis and acidification[73,76,77]**.** It contains several key functional domains, including the fusion peptide, two heptad repeats (HR1 and HR2), a transmembrane region, a cytoplasmic domain for trimer formation and the aforementioned ER-retention signal. The heptad repeats are crucial for forming a six-helix bundle that, together with the fusion peptide[78], mediates the merging of viral and host membranes, a mechanism similar to the envelope proteins of other viruses e.g. HIV[79]. A second cleavage site, S2', is activated by TMPRSS2 upon receptor binding, triggering a conformational shift from a metastable closed trimer state to an open state[72,75,80,81]. This change facilitates the six-helix bundle formation and completes the membrane fusion process, enabling viral entry.

Due to the Spike protein's **exposure on the outer surface** of the virus, it serves as the primary target of neutralizing antibodies[82]. Consequently, it is subjected to high selective pressure[83] and most characteristic mutations of the VOCs are occurring in the Spike protein[84] (see 3.2.2).

3.2.1.2 SARS-CoV-2 Host Receptor(s) and Proteases

SARS-CoV-2's main **host receptor** is the Angiotensin Converting Enzyme 2 (ACE2). Off note, this receptor is also used by NL-63 [85] and SARS-CoV-1[86]. SARS-CoV-1 and SARS-CoV-2 exhibit high sequence similarity in their receptor-binding domains, however, mutations in the SARS-CoV-2 RBD enhance its receptor-binding affinity[87]. After direct binding of furin activated RBD to the peptidase domain of ACE2 through polar residues and **endosomal uptake** of the virus receptor complex, acid dependant host proteases, like cathepsins or transmembrane protease sereine protease 2/4 (TMPRSS2/4) cleave the Spike a second time and enable membrane fusion[72,73,87]. On the host cell, Spike binding ACE2 triggers cleavage by disintegrin, metallopeptidase domain 17 (ADAM17) or tumor necrosis factor converting enzyme(TACE) at the ectodomain[88–90] and TMPRSS2 at the intracellular domain[73,89]. These clevages improve viral cellular entry but also lead to shedding of ACE2(/S1-complex), possibly impairing host ACE2 function and other effects[72,89,90].

ACE2 is a type I membrane bound glycoprotein, functionally composed of a transmembrane anchor domain, a signal peptide region and a HEXXH zinc binding metalloprotease motif as a catalytic domain[90,91]. In contrast to ACE, which is ubiquitinously expressed, ACE2 is especially expressed in alveolar and capillary epithelial cells. Thus, ACE2 is especially abundant in capillary rich tissue like lung, kidney, guts and brain. Though ACE and ACE2 share structural and sequence similarities, their functionality is quite different[91]**.** While ACE activates effects of the **Renin Angiotensin Aldosterone System (RAS)** by conversion of inactive Angiotensin I to Angiotensin II, ACE2 counteracts those effects by conversion of Angiotensin I & II to Angiotensin (1-7) & Angiotensin (1-9), respectively[90,92]. Apart from ACE generated Angiotensin II, there are several alternative pathways resulting in Angiotensin II generation[91].

On a **systemic level**, activation of the RAS/ Angiotension II triggers sodium and water retention as well as a variety of signalling, possibly resulting in vasoconstriction, hypertension, endothelial damage, cell death and thrombosis. Angiotensin II induces several cellular **signalling pathways**, like Erk, JNK/MAPK, Kinases, IL-6 and TNF- α. Finally, Angiotensin II activates neutrophils and Macrophages flux to the according tissue and promotes formation of reactive oxygen species through inhibition of NADPH

Oxygenase. [90,91,93] In contrast, Angiotensin(1-7) & Angiotensin(1-9) exhibit vasodilatory and protective functions by activating MAS/G, providing a counterregulation of the RAS/ACE axis[90].

Apart from ACE-2, autopsy reports about **SARS-CoV-2 tropism** from the olfactory bulb towards the nervous system suggested additional receptors or host-factors[94]. Here **Neuropilin-1 (CD304/Nrp 1)** has been suggested as a potential receptor, since it is known to bind Furin-cleaved substrates, significantly potentiated SARS-CoV-2 infectivity and the effect could be reverted by monoclonal antibodies[95,96]. Nrp1 itself is abundantly expressed in the respiratory and olfactory epithelium as well as in blood endothelial cells and a variety of other tissue[97]. Functionally it has been associated with angiogenesis, neural development and tumor metastasis[97,98]. Though enhanced Nrp-1 expression was observed in SARS-CoV-2 infected cells, it is yet unclear whether this might translate into disease outcome or other long-term consequences[97]. As of today, it is unclear if Nrp-1 is itself a complete alternative receptor used in viral infection or if it is mainly a host-factor merely enhancing SARS-CoV-2 infectivity with a yet unknown receptor or trace amounts of ACE2[99,100].

3.2.2 VOCs and Mutations

SARS-CoV-2 **variants of concern** (VOCs) are viral strains that carry genetic mutations associated with enhanced transmissibility, altered disease severity, or reduced effectiveness of diagnostics, treatments, vaccines, and other public health measures[49]. The term Variant of High Consequence (VOHC) was used synonymously to VOC. Additionally, the term Variants of Interest (VOI) was introduced to describe variants with concerning mutations regarding diagnostics, immune escape similar to VOCs , but without a global significance[101]. An overview of variants circulating in Germany over time is provided in **Figure 2**.

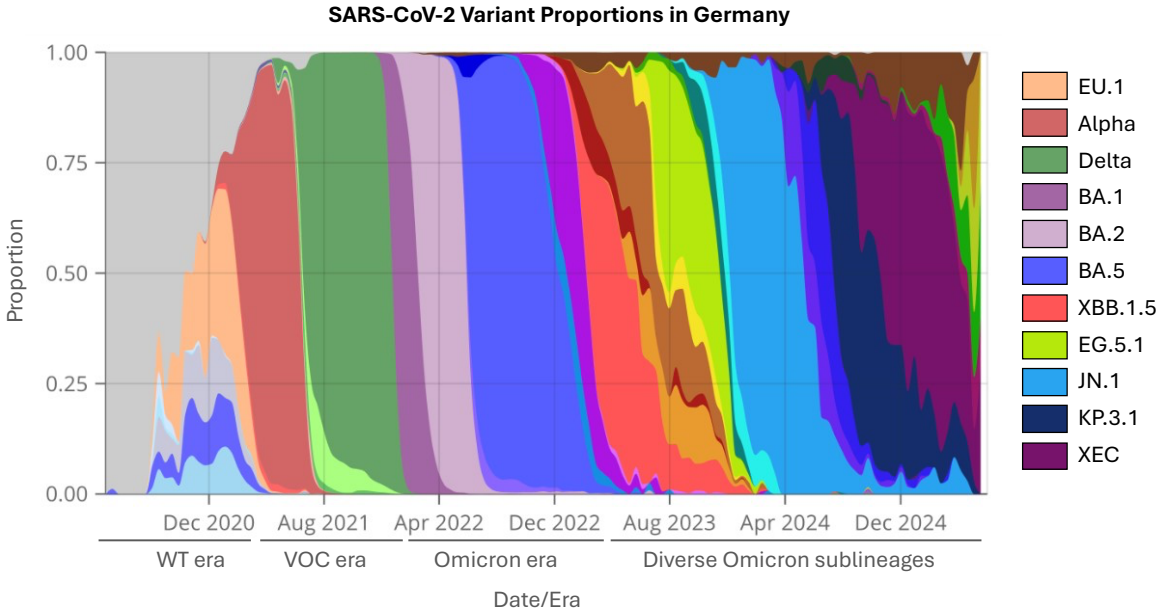

Figure 2 Proportions of SARS-CoV-2 variants circulating in Germany, over time. Color codes denote the different variants, with the most abundant/important variants shown in the legend, the full legend can be accessed on covariants.org. For better overview, time is further split into generic "Eras" with their characteristic circulating variants (WT = wildtype-like, VOC = early Variants of Concern). Proportions are based on sequencing data. Figure adapted from covariants.org[102]

The first (important) emerging SARS-CoV-2 variant was the Spike mutation **D614G**. The variant showed increased fitness in hamster upper airways and enhanced replication in humans but no significant immune escape or pathogenicity changes. This was achieved through a change in the Spike protein conformation towards an ACE-2 binding open state[103–105]. Similar to coinfection experiments in ferrets and hamsters where D614G overgrew the wildtype within a day post infection, D614G completely replaced the wildtype/original Wuhan strain in the human population within a few months. Off note, tracking of variant frequencies revealed that the mutation occurred independently in multiple geographic areas and was a feature of all the following VOCs, emphasizing the mutation as a logical step in viral evolution[106].

The second emerging VOC was the **B1.1.7 or Alpha** variant, first discovered in the UK in late 2020 quickly spreading around the whole world[47,107–109]. The variant was connected with a higher viral load in humans leading to a higher infectivity[107]. The alpha variant was further connected to an increased resistance against neutralizing antibodies and an increased disease severity[110,111]. It was mainly characterized by multiple Spike mutations mainly N501Y in the RBD, enhancing ACE2 binding[112], P681H enhancing the furin cleavage site[113] and conferring Interferon resistance[114] and finally the H69/V70 deletion conferring increased infectivity by better spike packaging[115,116]. Additionally, there were some subvariants reported, carrying the E484K Spike mutation connected with immune evasion[117,118]. Additionally, Alpha showed sparce mutations in the Nucleocapsid as well as multiple mutations in the ORF1a and b region, with only limited knowledge on their biological function[119].

The Alpha variant was quickly followed by the **B1.351/Beta and B1.1.248/P.1/Gamma** variants in South Africa and Brazil, respectively, though both variants remained geographically constrained to South America or Africa and some Asian countries [120–123]. Both variants Spike proteins had the previously mentioned N501Y for enhanced receptor binding as well as the E484K and the novel K417N/T mutation, connected with immune evasion[117,118,124]. Both variants showed a significant escape from neutralization by plasma from convalescent individuals[125,126].

In contrast to the geographically constrained spread of Beta and Gamma, the following **Delta/B1.617.2** Variant first appeared in India and rapidly became the dominating variant worldwide in late 2021[127,128]. Delta was characterized by the mutations L452R, P681R, and T478K in the S-protein, associated with immune evasion, increased transmissibility and modified furin processing[128,129]. Delta progressed into various sublineages (AY.X), thereof most notable was the “Delta Plus”/AY.1 subvariant, carrying the K417N mutation known from beta for immune evasion. Reportedly “Delta Plus” was even more contagious than Delta[130]. Off note, despite the ongoing vaccination campaign, the Delta wave of infections caused the highest number of total registered infections during the whole SARS-CoV-2 pandemic[52,102]. However, those registered numbers might be highly biased due to different reporting and surveillance strategies, with lower surveillance in following waves[23,131].

The following **B.1.1.529/Omicron** VOC marked a change in novel arising variants. Similar to all other variants the initial Omicron BA.1 variant was an independent descendant of the common wildtype ancestor and no evolution from an already existing VOC[132]. However, Omicron started a new sublineage of SARS-CoV-2 with BA.1 being followed by direct evolutionary descendants and recombinants of multiple Omicron subvariants. This resulted in a variety of Omicron subvariants/sublineages, like e.g. BA.1.1, BA.2, BA.4/5, XBB.1, BQ.1, EG.5, JN.1 and XE.[102].

BA.1 was **characterized** by a variety of Spike, N, M, ORF1ab and ORF9b mutations. Hereof most notable the patch of Spike mutations near the S1-S2 furin cleavage site (H655Y, N679K, P681H) which increased transmissibility and the combination of Q498R and N501Y in the Spike-RBD which increased ACE2 Receptor binding affinity[133,134]. Additionally, BA.1 carried an E484A Spike mutation similar to the E484K mutation, associated with immune evasion. The Omicron BA.1 N Protein carried the R203K G204R double mutation, similar to previous VOCs, associated with enhanced RNA expression, higher viral loads and different sumoylation of the proteins[49,135]. Finally, BA.1 carried a variety of mutations in the ORF1a, most notably a three aminoacid deletion in NSP6, connected to innate immune evasion[136,137]. The Omicron sublineages (all descendants of BA.2) kept acquiring additional mutations, some of which already known from previous VOCs, resulting in enhanced receptor binding, possibly different receptor usage, different tissue-localization, immune evasion and major changes in antigenicity[49,136].

Off note, SARS-CoV-2 has previously been known to **infect** a variety of **animals** like deer, cats, dogs, minks and bats[5,138], hence Omicrons vast number of novel mutations as well as an adaption to enhanced Mouse ACE-2 binding [139,140] sparked discussion about a possible rezoonotic origin from rodents. Other theories claimed the origin to be an "undisturbed" evolution of the virus in an immunocompromised patients[141–143], while a (now retracted publication) declared a normal/natural evolution of Omicron over months in Africa, undetected due to missing surveillance[144].
Today, genetic diversity of Omicron sublineages vastly exceeds the genetic diversity of the initial Alpha, Beta, Gamma and Delta VOCs as visualized in **Figure 3**[132].

Additionally, the **phylogenetic tree** visualizes the antigenic drift and immune evasive evolution of variants in regard of SARS-CoV-2 vaccination. Since the emergence of Omicron, the vaccine was regularly adjusted to use the Spike of current circulating variants[145], after introduction of each novel vaccine, the corresponding variant branch aborted and the main circulating variant was replaced by another branch (**Figure 3 B**).

In conclusion, since the start of the pandemic, the **SARS-CoV-2 virus evolved** rapidly, showing constant immune evasion and host adaption. Its' evolutionary pattern resembles antigenic drift (evolution from WT to Alpha) but also antigenic shifts (emergence of Omicron after Delta) known from influenza research, yet without the segmented genome of influenza[146]. Thus, constant monitoring and surveillance is mandatory to track potential novel threats and a regular adaption of vaccines similar to influenza could be highly advised to keep immunity up to date[147].

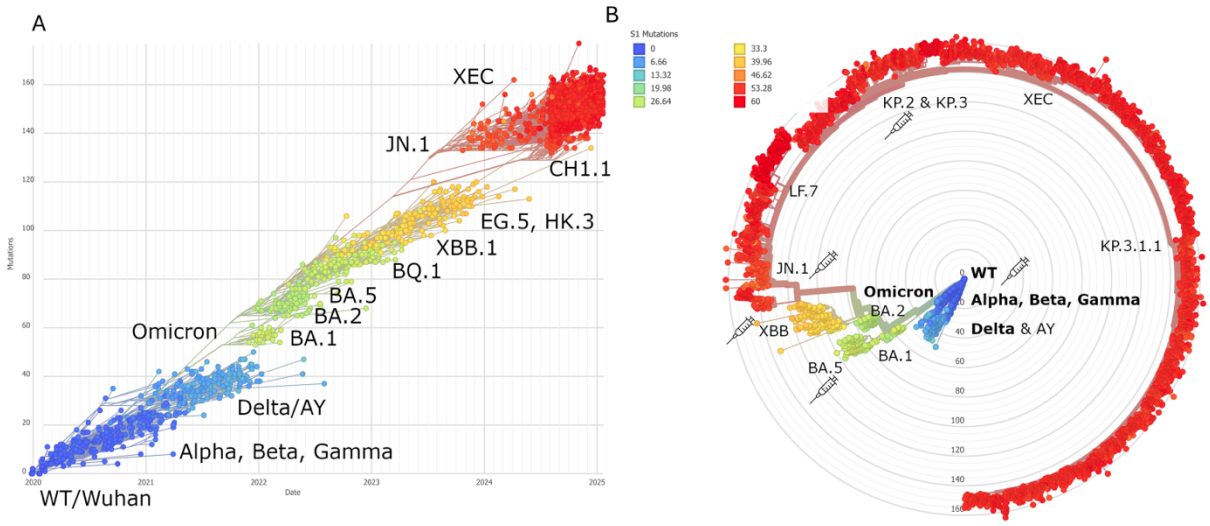

Figure 3 A Linear phylogenetic tree of SARS-CoV-2, annotated with a selection of VOCs and subvariants. The x-axis denotes time (of emergence) in years, the y-axis denotes total aminoacid mutations compared to the wildtype reference. B Circular phylogenetic tree of SARS-CoV-2 with a selection of VOCs and subvariants annotated. Circles denote total aminoacid mutations compared to the wildtype reference. Variants which Spikes have been used in the BNT162 vaccine are marked with a syringe. Both trees are color coded using a heatmap of the number of S1 aminoacid mutations (blue = 0, red = 60, as denoted by the legend in B). Trees were generated using GISAID data on Nextstrain.org[132] on 05.02.2025.

3.3 Antibody response to SARS-CoV-2

3.3.1 Antibodies and Neutralization

A major part of the **humoral immune response** to SARS-CoV-2 is the antibody response, which can be divided in the extrafollicular (EF) phase and the germinal center (GC) phase[148,149]. The EF phase is started within days after infection and mainly results in short lived EF plasma cells which underwent only little somatic hypermutation, GC B-Cells as well as EF memory B-Cells. The EF plasma cells primarily produce IgM but may still switch to IgG or IgA. Despite the few mutations, the EF response may still result in (neutralizing) antibodies with high affinities[150]. Approximately one week after initial antigen contact, the GC B cells then enter the dark zone of the germinal center to proliferate and hypermutate. After affinity selection, the GC B-cells differentiate to memory B-cells, long lived plasma cells or re-enter into the GC. Finally resulting in a high affinity, highly specific and isotype switched (IgG) antibody response[148]. (**Figure 4A&D**)

In case of **SARS-CoV-2**, nearly 100 % of infected individuals seroconvert within two weeks[151], with the main **antibody response** being directed against the viruses' Nucleocapsid and Spike proteins. The antibody response can further be differentiated based on the properties of specific antibodies, e.g. binding antibodies or neutralizing antibodies.

Most **neutralizing antibodies** inhibit SARS-CoV-2 infection by binding to the viral spike protein, especially its receptor-binding domain (RBD), and blocking the interaction with the ACE2 (or potential other receptors) on host cells, thereby preventing viral entry and subsequent replication. Other mechanisms include sterical hindrance of conformational changes in the spike protein during membrane fusion or inhibition of TMRSS2 cleavage[152]. Those nAbs can target a variety of more conserved spike regions including the N-terminal domain, stem helix, or fusion peptide and are known for enhanced breadth and retaining activity even against immune-evasive variants[153]. During the (early) SARS-CoV-2 pandemic, **monoclonal neutralizing antibodies** (nAbs), combination antibody cocktails, and convalescent plasma were used to confer immediate immunity in vulnerable individuals[154,155]. However, most of these passive immunization attempts showed only limited efficacy and lost neutralizing efficacy against the Omicron variant and its sub-lineages (e.g. bamlanivimab/etesevimab and casirivimab/imdevimab)[156,157].

Antibodies binding viral antigens but incabable of inhibiting viral infection are usually called **binding antibodies**. Yet those antibodies might exhibit a variety of other (Fc-domain dependent) effector functions to support viral clearance beyond neutralization[158].

First, they can trigger **antibody-dependent cellular phagocytosis** (ADCP) by opsonizing virions or infected cells and engaging macrophages and neutrophils via their Fcγ-receptor, enhancing pathogen ingestion and antigen presentation. Second, they can activate **antibody-dependent cellular cytotoxicity** (ADCC), in which antibody (IgG) marked cells are recognized by FcγRIIIa on NK cells, leading to the release of perforin and granzymes and targeted cell death. Third, binding antibodies can induce **complement dependent cytotoxicity** (CDC) by activating the classical complement cascade via C1q binding, ultimately leading to membrane attack complex formation and lysis. Finally, there is a multitude of **additional antibody derived effects**, like biofilm formation, antibody dependent antigen uptake or antibody driven antigen presentation, to name a few examples, but also possibly negative functions like **antibody dependent enhancement** (ADE) of viral infections[158–160].
Off note, in contrast to neutralizing antibodies, those additional effector functions can also be elicited by antibodies targeting other SARS-CoV-2 proteins than Spike. Additionally, all the aforementioned effector functions including neutralization are not inherently exclusive and one e.g. Spike antibody might be both, neutralizing and CDC activating.

3.3.2 Immune Imprinting/Original Antigenic Sin

A major concern accompanying the rise of VOCs, was the phenomenon of "**original antigenic sin**" (OAS) or recently more neutrally phrased "**immune imprinting**". The phenomenon was initially observed in Influenza research and described as the inability of the adaptive immune response to adapt to a novel antigen, after initial prime with an antigenically close antigen[161,162].

To elaborate in more detail: At first, an **initial** infection or **immunization** with a novel antigen, results in a primary/EF B-Cell response specific for the epitopes of the immunizing antigen, which consists of GC-B-cells, GC independent memory cells as well as short lived plasma cells. The GC B-Cells proliferate and undergo somatic hypermutation until they differentiate to memory B-Cells, long lived plasma cells or reenter the GC[149,150] (see **Figure 4A**, also see 3.3.1).

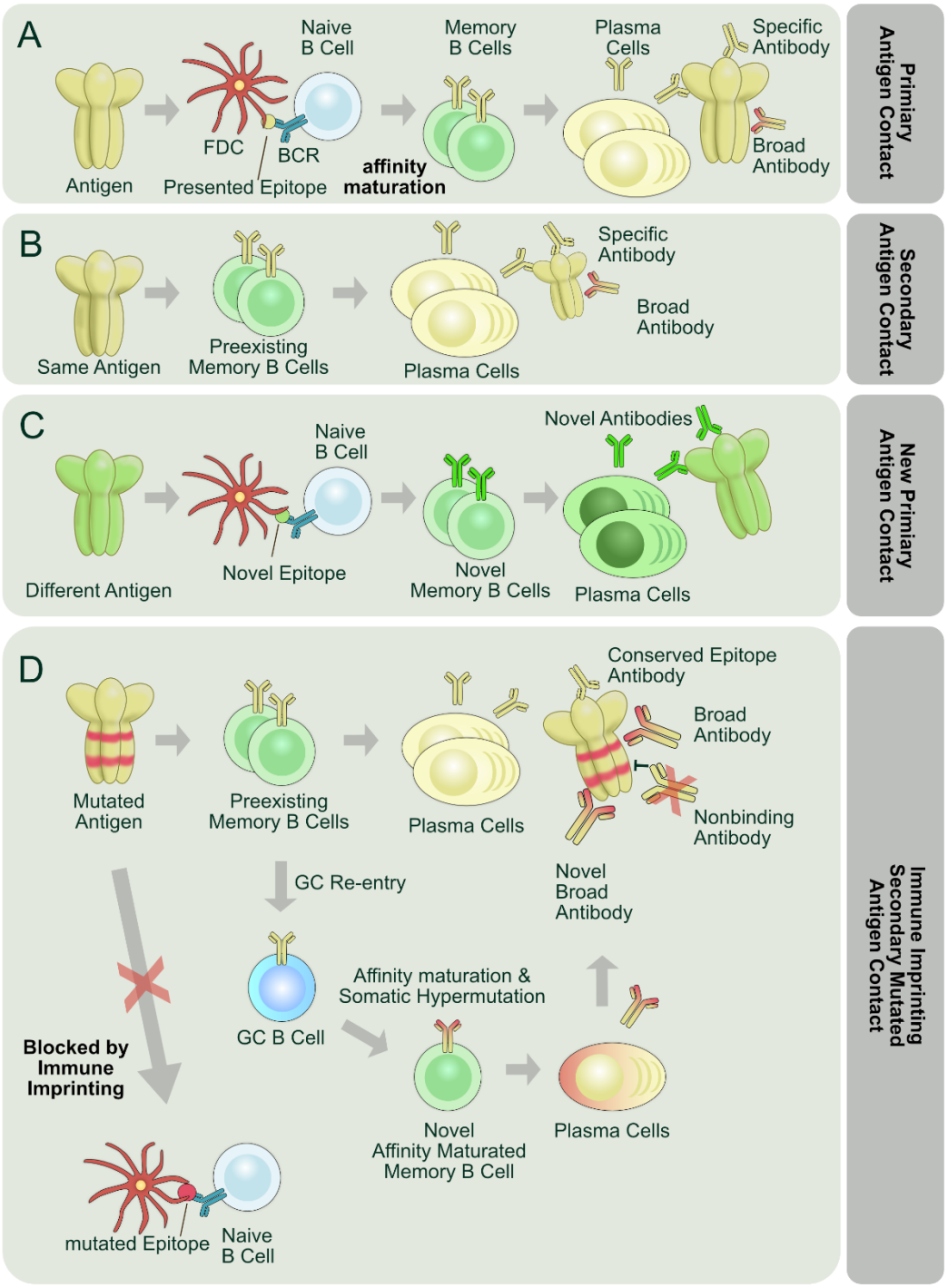

Figure 4 A Primary B-Cell response after first antigen exposure. Folicular Dendritic Cells (FDC) present the antigen's epitopes to the B-Cell receptor (BCR) of naïve B-Cells, subsequently generating antigen specific memory B-Cells, plasma cells and antibodies, some of which might even be broadly binding/neutralizing. B Secondary antigen contact with a previously encounterd antigen. Preexisting memory B-Cells expand and quickly differentiate into Plasma Cells resulting in the same antibody response as for the first antigen contact but with a significantly faster onset time. C "Secondary" antigen contact for a very different/new antigen triggers a new primary response analog to A for the novel antigen. D Immune imprinting effects after a secondary antigen encounter with a slightly mutated version of the previously encountered primary antigen. Immune Imprinting blocks novel priming of naïve B-cellswith the mutated Epitopes. Conserved epitopes trigger a memory response similar to B, while some memory Cells reenter into the germinal center (GC) for further affinity maturation towards the novel epitopes.

In case of a **secondary antigen contact**, either by infection or immunization, with the exact same antigen, the memory cells would be reactivated for a secondary plasma cell response mainly dependent and GC dependent memory B-Cells and potentially further expand or maturate[150] (**Figure 4B**).

In contrast, a "**secondary" antigen contact with a completely different antigen**, e.g. from a completely different virus, would not reactivate, but mount another primary response (**Figure 4C**).

Interestingly, a **secondary contact with an antigenically close antigen** (**Figure 4D**), carrying only some different epitopes (e.g. derived by antigenic drift), would only reactivate memory cells specific for shared epitopes or crossreactive memory cells. However, the majority of **novel epitopes** neither prime a novel response, nor activate any existing memory cells[150,162,163]. This could result in an impaired protection against the novel pathogen caused by missing adaption to functional changes in the pathogen, a loss of function for previously neutralizing antibodies, or other effects like antibody dependent enhancement[158,164]. To put this into perspective, though B-Cell sequencing and antibody depletion studies could prove a strong **bias towards pre-existing immunity**, it remains obscure if novel B-Cell priming doesn't occur at all or is just extremely sparse.[163] In the second case, repeated exposure with the novel antigenically close antigen, or a designed sequence of antigenic exposures, could indeed prime new B-Cells and reshape the imprinted response to overcome the "original antigenic sin" as repeatedly proposed by others[165–167].

On the other hand, **immune imprinting** does not only imply negative consequences but might harbor a variety of **positive effects**. As of such, immune imprinting could favor the development of cross-reactive antibodies through positive selection of B-Cells over repeated exposures with evolving or variant derived antigens. Second, immune imprinting enhances targeting of conserved epitopes. Together, this allows for a broad immunity against multiple previously encountered or even future and unencountered variants of a pathogen[162,163,168].

In conclusion, immune imprinting evolutionary favors **one preexisting, fast and broad antibody response** over multiple novel, slower but very specific antibody responses. Notwithstanding an impaired immunity in case of an unfavorable prime and the **potential risk of a complete failure** in case of an unfortunate antigenic shift.

3.3.3 Vaccination

As of today, there are several approved SARS-CoV-2 vaccines on the market (this thesis focused on the EU), using a variety of different approaches and novel technological platforms[145]. An overview of the vaccines applied in the EU and the US is shown in **Figure 5**.

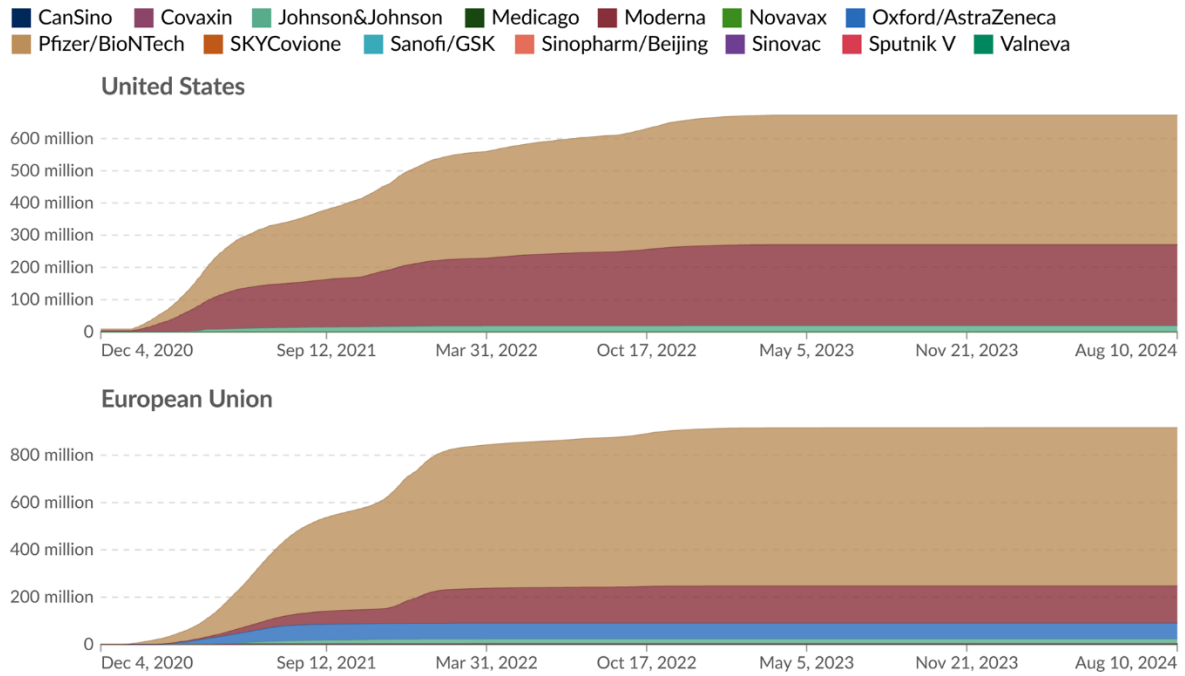

Figure 5 SARS-CoV-2 vaccines by brand administered in the United States and the European Union over time. Charts include all doses, including booster vaccination as individual counts. Figure adapted from Our World in Data[169].

mRNA vaccines, such as those developed by BioNTech/Pfizer and Moderna, utilize messenger RNA to produce viral spike protein in host cells, thereby stimulating immunity. mRNA vaccines have demonstrated high efficacy and have been pivotal in the EU's vaccination campaigns. Clinical trials reported efficacy rates of 95% for Pfizer-BioNTech and 94.1% for Moderna against symptomatic COVID-19. Real-world studies corroborate these findings, showing effectiveness exceeding 90% in preventing infection and severe disease.[37,38,42,43,170,171]

Viral vector vaccines, including AstraZeneca's ChAdOx1 and Johnson & Johnson's Ad26 vaccine, employ replication deficient adenoviruses to deliver spike protein encoding DNA into host cells, while the adenoviral particles employ adjuvantive effects. The AstraZeneca vaccine demonstrated an overall efficacy of approximately 70% in clinical trials. Real-world data indicated effectiveness ranging from 70% to 85% in preventing symptomatic infection[39,170–172].

Protein subunit vaccines, like Novavax's NVX-CoV2373 and Sanofi-GSK's VidPrevtyn Beta, contain purified recombinant spike protein or RBD, combined with adjuvants to enhance the immune response. Novavax's vaccine showed efficacy rates of 73.5 % in clinical trials, though it should be noted that Novavax was tested for prevention of infection instead of efficacy against severe/symptomatic disease[173]. Sanofi-GSK's vaccine did show 100 % efficacy against severe disease and 57.9 % against symptomatic disease[174].

Inactivated virus vaccines, such as Valneva's candidate, consist of whole viruses rendered non-infectious through chemical processes[175]. This traditional approach presents the entire virus to the immune system, promoting a broad immune response against other viral proteins. Efficacy rates for inactivated vaccines have varied, with clinical trials reporting efficacy around 65% against symptomatic infection, and higher effectiveness against severe disease[175,176].

Beyond those already approved vaccines, **experimental platforms** are under investigation, including self-amplifying RNA (saRNA) vaccines, which aim to enhance protein expression and immune response with lower doses. Other approaches involve nanoparticle-based vaccines and live attenuated viruses, each offering unique advantages and challenges.
With the introduction of **VOCs**, especially omicron, vaccine efficacies against both, severe disease and infection drastically changed, with sometimes increased efficacy against severe disease but decreased effectiveness to prevent infection[177]. These changes could likely be attributed to variant specific changes in the morbidity of SARS-CoV-2 as well as immune evasion of omicron variants[177,178]. At the same time, the populations immunization situation to reliably determine effects of certain vaccines, becomes more and more obscure, as most of the world's population received multiple shots, possibly of multiple vaccine brands, and experienced multiple (breakthrough) infections.

3.3.4 Correlates of Protection

In this complex immunological landscape, identifying reliable correlates of protection has become increasingly challenging. **Neutralizing antibody titers**, particularly those targeting the spike protein's S1 unit or specifically the receptor-binding domain, have been consistently associated with protection against (symptomatic) infection[179]. Furthermore, multiple studies have demonstrated that higher (pseudovirus) neutralizing antibody titers and spike protein binding antibody concentrations correlate with greater (vaccine-induced) protection[180]. Yet, until today **no reliable cutoff** values could be determined to provide true sterile immunity. On top, the emergence of variants like Omicron, which

possess mutations that reduce antibody binding, has led to decreased vaccine effectiveness against infection[181], though protection against severe disease often remained robust[152,182].

Additionally, **CD8+T-cell mediated immunity** plays a crucial role, especially in preventing severe outcomes[179]. T-cell responses tend to be more conserved across variants, providing a layer of protection even when antibody neutralization is compromised[183]. Additionally, T-cells expand the repertoire of target proteins from spike to other viral proteins, e.g. NSP-12 which could successfully abort infection[184].

Moreover, **hybrid immunity**, resulting from a combination of vaccination and natural infection, has been shown to elicit broader and more potent immune responses, enhancing protection against diverse SARS-CoV-2 variants. Furthermore, current studies could show promising effects of mucosal immunization regarding prevention of infection in macaques, yet more research is needed to translate those results to humans[185].

Overall, these insights underscore the **multifaceted nature** of the immune response and the importance of considering both, humoral and cellular responses when evaluating vaccine efficacy or protection in an epidemiological setting.

3.4 Terminology and Methodological Frameworks in Epidemiology

When SARS-CoV-2 began spreading globally, numerous (sero-)**epidemiological studies** were launched to assess various aspects of the virus and viral infection, including (sero-)prevalence, surveillance accuracy, and other population-level factors. Over time, with the virus evolving and vaccines being introduced, research objectives expanded. New studies emerged to investigate topics such as antibody durability, variant-specific immunity, correlates of protection, and viral behavior in immunocompromised groups. To accurately interpret these studies, it is essential to understand the **terminology, tools, and methods** they employ, which this chapter aims to clarify.

3.4.1 Representativeness

Representativity/Representativeness refers to how well the sample population in an epidemiological study reflects the broader population from which it was drawn or, even more important, the population it aims to describe[186]. Off note, the target population does not necessarily need to be the general population, but could be a certain subset thereof, e.g. individuals with a certain disease. Additionally, it should be emphasized, that a cohort though representative for the general population might still not be representative for a certain subgroup of said general population and vice versa.

In the case of **epidemiological studies**, representativity is highly desired, as it determines the generalizability of the study's findings with a high risk of bias in a nonrepresentative sample. A representative sample accurately mirrors the distribution of key characteristics, such as age, gender, socioeconomic status, and health behaviors of the target population, while other custom characteristics can be included dependent on the particular research question.[186]

However, one major **drawback in representativity** of epidemiological studies is, that the target populations' characteristics ought to be known, which might not always be the case. Furthermore, characteristics might change over time, impairing a once representative sample unrepresentative for future inference[187,188]. One apparent example for unknown and changing population characteristics would be the vaccinated population during the SARS-CoV-2 pandemic in Germany. This population was assumedly highly divergent from the general population due to vaccination priorities, yet no data was available on the vaccinated individuals' demographics, while the ongoing vaccination campaign lead to constantly changing population characteristics.

Another widely used term, but less strictly defined, are **population-based studies**. The term population-based refers to research which includes a defined population, often within a specific geographic area, and aims to study the entire population or a significant portion of it. Though population- based studies strive for representativeness, they are not inherently representative just by being population-based[189].

To clarify further, a population-based study might include a **significant proportion of the population**, but still suffer from underrepresentation of certain groups, due selection or recruitment bias. For example, the elderly population might receive the study invitation but could be physically unable to travel to a study center. Certainly, **selection bias** could be counteracted in most cases, but this requires proper identification of possible bias, application of correctional models to the study results or more complex (and costly) sampling procedures such as multiple options of study inclusion, multiple study centers or home visits[190].

Sampling procedures to achieve representativity include random sampling, where the individuals of the sample population are randomly selected to be invited in the study[187]. Another technique would be stratified sampling, where the population is divided into subgroups (strata) based on certain target characteristics, and samples are drawn proportionally for the different strata. Finally, the population could be divided into clusters (e.g. geographic areas) of which a random sample is selected, to perfom a technique called cluster sampling. In reality, the aforementioned techniques are often combined in a multitude of different ways[190,191]. Off note, a non-representative but properly sampled and conducted study may still provide valuable insights, albeit within limits[192].

Another, widely used sampling technique during the SARS-CoV-2 pandemic, was "**convenience sampling**". Here, study participants get selected from readily available populations, such as health-care workers or students, to quickly generate (large) cohorts. However, this procedure, depending on the specific research question, often yields highly biased or even ungeneralizable cohorts and study results[193–195]. A preferred option, providing similar speed and convenience during sampling but with less risk of bias, would be to **repurpose existing**, properly sampled cohorts or subgroups thereof[196].

In conclusion, representativeness is often aimed for, but quite hard to achieve, while population-based sampling is easier to accomplish, yet prone to selection bias. A proper sampling procedure as well as the analysis and counteraction of potential bias remains crucial to obtain valid and generalizable study results.

3.4.2 Standardization

Standardization is a statistical method used to remove the effects of confounding variables when comparing different populations or groups within a study. It allows for fair comparisons by adjusting the data to a common predefined standard (e.g. the true population of a given area). In epidemiological studies, standardization is often used to control for differences in age, sex, lifestyle and geographical distribution between populations[197].

Standardization can be applied using **two different methods**, namely direct and indirect standardization. For **direct standardization**, the e.g. age-specific rates of the study population are applied to a standard population structure. The overall standardized rate is a weighted average of these rates, with the weights being the proportions of each age group in the standard population. Direct standardization can only be used if the e.g. age-specific rates are available for the study population. If the e.g. age-specific rates are not available for the study population but are known for the standard population, **indirect standardization** can be used for analysis. Here, the standard population's age-specific rates are applied to the study population's structure to estimate the expected number of events. This enables to calculate e.g. a standardized mortality ratio to be reported[197,198].

In case of **multiple variables to standardize** for, methodology needs to be adjusted, while each of the adjustments comes with different implications and consequences to consider. First, one might perform a **complete direct standardization** by building combined multivariable subgroups (e.g. for sex and age groups: 50-60 years-old females). However, this method is only possible if the according combined subgroup information is known for the study population as well as standard population. Furthermore, the major problem to consider with this procedure (especially with an increasing number of variables to consider) is the high risk of extremely small or even empty subgroups. Hence, this method could result in highly biased or even incalculable results which can only be avoided by selecting broader subgroups or increasing the study population[199,200].

An **alternative procedure**, less prone to small or empty subgroups, calculates every standardization for a single variable and yields a **weight/ratio** of standardized value to non-standardized value, those weights can then be applied together with the other standardizations to yield standardized values for multiple variables[201]. Yet, this method might still introduce bias, as by design it ignores and overrides any interaction effects between the variables[200,202].

In **conclusion**, standardization is crucial for valid comparisons between (sub)populations, generalizability of study results and control for confounding factors in the face of imperfect cohorts. Nonetheless, there are several drawbacks and implications to consider when choosing the right methodology for standardization of a specific cohort.

3.4.3 Testing, Accuracy and Comparisons

The SARS-CoV-2 pandemic spiked the **development** and implementation of a **variety of tests** into diagnostics and research. To correctly interpret and evaluate the test results, it is important to understand the tests' biological targets as well as the tests' accuracy and relevance of a potential quantitative readout.

Additionally, one should consider, that some tests can be treated nearly identical regarding their application and results, while other tests have similar **targets** but use different **readouts**, resulting in most probably correlated results and even other tests use completely different targets and thus could provide either correlated or completely different (uncorrelated) insights, dependent on biological connection. Finally, it should be considered, that any previously found correlations might drastically change over time due to the **evolution of the test targets** (e.g. the SARS-CoV-2 Spike protein). An overview of widely used tests, readouts and targets is provided in Table 2.

Table 2 Overview of SARS-CoV-2 tests for detection of both viral infection as well as antibodies. Denoted are the objective of the test, the (most commonly) used readout, available brands, the target the test is detecting as well as an estimate of test accuracy. Accuracy estimates may be different for certain brands and are highly dependent on the sample quality.

Objective	Readout	Brand	Target	Accuracy
Direct Virus (Antigen) detection	Lateral Flow Assay (LFA)	Multiple commercial suppliers, e.g. Siemens, Roche, R-Biopharm, Healgen	SARS-CoV-2 N	Sensitivity: appx. 95% Specificity: 88.9 % to 100%[203]
Direct Virus (Genome) detection	RT qPCR	Multiple, e.g. Thermo Fisher, Roche	SARS-CoV-2 Genome (typically, M and E Genes)	Sensitivity: 80 - 100 % (LOD appx. 500 genome copies) Specificity: 98 – 99 %[204,205]
Spike/RBD Binding Antibodiy detection	ECLIA, ELISA, LFA	Multiple commercial suppliers, e.g. Roche, YHLO,	Antibodies against SARS-CoV-2 Spike or SARS-CoV-2 RBD	Sensitivity: >90 % Specificity: Up to 99 %[206]

		Euroimmun. Multiple in-house solutions	(can be variant specific, detect total Ig, IgG/A/M or even Ig-subtype specific (e.g. IgG2)	
N binding Antibody detection	ECLIA, ELISA	Multiple commercial suppliers, e.g. Roche	SARS-CoV-2 N (sometimes variant specific)	Sensitivity: >98 % Specificity: >99 %[207]
Surrogate Neutralizing Antibody detection	ACE2 Binding inhibition ELISA	Multiple commercial or selfmade versions.	SARS-CoV-2 Spike or RBD	Sensitivity: > 95 % Specificity: > 99 %[208]
Neutralizing Antibody detection	Lentiviral or VSV based Pseudovirus Assay, live virus SARS-CoV-2 Focus forming assay, SARS-CoV-2 MNES particles[209,210]	Multiple lab specific versions. E.g. VSV system, Lentiviral system, Live Virus system, MNES system	SARS-CoV-2 Spike or full SARS-CoV-2 virions including other Proteins (Matrix and Envelope)	often viewed as gold standard, up to 100 % accuracy[211], highly dependent on lab specific assay conditions

To put the this into the perspective of SARS-CoV-2: similar to other viruses, SARS-CoV-**2 binding antibodies** against the WT Spike protein have been significantly correlated with WT **virus neutralization**[212] thus Spike binding would, in most cases provide a sufficient surrogate assay. However, e.g. for HIV, this correlation couldn't be shown, probably due to its extremely fast immune escape and the high number of mutations in its' envelope protein[213]. Consequently, it's fair to assume, that SARS-CoV-2 variant specific neutralization could be correlated differently or even uncorrelated with WT or other VOC specific binding antibodies and vice versa.

Apart from quantitative test readouts, also **qualitative test results** were of great importance during the SARS-CoV-2 pandemic, as e.g. the qualitative results of SARS-CoV-2-N-targeted lateral flow tests or SARS-CoV-2 qPCR tests were used to determine prevalences and impose pandemic counter measures.

Though understandable at the time being, this procedure has been reviewed critically, since the large number of tests combined with a low true prevalence might have led to a low positive **predictive value** and finally to a biased calculation of the prevalence[214].

Testing accuracy, defined as

$$accuracy = \frac{true\ positives + true\ negatives}{true\ positives + false\ positives + true\ negatives + false\ negatives} \quad \textbf{(Equation 1)}$$

can be additionally specified to sensitivity, the amount of positive tests within the true positive population, denoted as

$$sensitivity = \frac{true\ positives}{true\ positives + false\ negatives} \quad \textbf{(Equation 2)}$$

and specificity, the number of negative tests within the true negative population, denoted as

$$specificity = \frac{true\ negatives}{true\ negatives + false\ positives} \quad \textbf{(Equation 3)}$$

While **accuracy, sensitivity and specificity are constants** intrinsic to the test (at least theoretically, as long as e.g. the target doesn't evolve and the test population is biologically the same), the positive and negative **predictive values** (PPV, NPV) of tests are directly influenced by the true target prevalence as they are denoted by the fraction of true positives/negatives divided by the sum of true and false positives/negatives. Alternatively, according to Bayes theorem, the PPV & NPV can also be calculated as follows:

$$PPV = \frac{\text{sensitivity} * \text{prevalence}}{\text{sensitivity} * \text{prevalence} + (1 - \text{specificity}) * (1 - \text{prevalence})} \quad \textbf{(Equation 4)}$$

and

$$NPV = \frac{specificity * (1 - prevalence)}{specificity * (1 - prevalence) + (1 - sensitivity) * prevalence} \quad \textbf{(Equation 5)}$$

PPV and NPV can further be used to calculate the False Discovery Rate (1-PPV) or False Omission Rate (1-NPV)[215,216].

Hence, despite the extraordinary high specificity of the **SARS-CoV-2-RT-qPCR** of up to 99%[205], the low true prevalence in between waves combined with mandatory testing lead most likely to an overestimation of the calculated prevalence[217,218]. Consequently, those **potential biases** also apply and should be considered when using serological tests in an epidemiological seroprevalence setting.

In general, often one particularly accurate or otherwise well-suited test (e.g. Neutralization as a possible correlate of protection) would be defined as a **golden standard**, which could be referenced on the introduction of novel tests. However, the pandemic situation with a novel virus sparked the introduction of a variety of tests without any known or defined reference.

Here, statistical tools like **Latent Class Analysis**, a model assuming the observed distribution as a mixture of underlying latent distributions, [219] can be used to infer a final status from a multitude of tests. Another widely used approach was to define a test of biological relevance as the reference, e.g. testing for neutralizing antibodies with a focus forming or pseudoviral assay, and benchmark other tests on this basis[209,220,221]. However, the reliability of results following from this approach are highly dependent on the quality of the first test and thus should be interpreted with caution.

In the face of thousands of different, often "homebrew" tests, the **WHO** introduced (multiple) **standards** (e.g. for neutralizing or binding antibodies or genome copies), which were made accessible for the diagnostic and research labs worldwide. This allowed for unit standardization, bridging and comparison between the multitude of different assays and aimed to ensure reproducibility of scientific results[222].

3.4.4 Antigenic Cartography

The concept of antigenic cartography was introduced into the scientific community in 2004 during influenza research[223]. The concept relies on **mapping antigenetic properties** onto a 2D-space using multidimensional scaling.

Multidimensional scaling itself, as proposed by Lapedes & Farber[224] relies on the concept of a theoretical multidimensional **shape space**, in which unknown physical properties, such as tertiary structure, charge, hydrophobicity and more, related to binding/neutralization are mapped to antigens and antibodies. Herein, small distances between antigen and antibody would correspond to high affinity, while small distances between antigens would correspond to similar antigenicity and small distances between antibodies correspond to similar binding properties.
Though the unknown variables are not directly measured, the **distances** as well as explicit coordinates in the assumed shape space, or at least a true to scale **projection** of them, can be computed from measured binding properties by e.g. hemaglutinin inhibition assays, ELISA or neutralization[224,225].

This can perfomed either **metric or ordinal/parametric**, although the ordinal algorithm is theoretically preferrable, since it avoids dimension inflation and deviances of reconstructed distances against true distances. After random initialization of coordinates, the objective of the ordinal reconstruction is to minimize:

$$E = -\sum_{\alpha=1}^{\alpha=MN} \log\big(g(D_{\alpha+1} - D_{\alpha})\big)$$ **(Equation 6)**

With the function g(x) being a sigmoidal activation function, N the number of experimental samples/sera, M the number of antigens tested against and D the Euclidean distances of a points[224].

However, in **current scientific reality**, e.g. when using the racmacs package for antigenic mapping, metric distances are used to gain a map with a meaningful scale. Here, distances are simply calculated by subtraction of the measured logarithmic titer against a specific antigen from the logarithmic maximum titer of a serum (either experimental or a larger, predefined value)[226] :

$$distance_{AgS} = \log_2\left(\frac{maximum\ titer_S}{10}\right) - \log_2\left(\frac{measured\ titer_{AgS}}{10}\right)$$ **(Equation 7)**

Since from the experimental data, **serum to serum and antigen to antigen distances** are unknown, all points (antigens and sera) are initialized randomly, and coordinates are adjusted using a limited-memory Broyden-Fletcher-Goldfarb-Shanno (BFGS) algorithm[227] to minimize the stress function:

$$x = d_t - d_m + 1$$ **(Equation 8)**

$$s = x^2\left(\frac{1}{1+e^{-10x}}\right)$$ **(Equation 9)**

With d_t being the previously calculated distance, d_m the current map distance and s the stress[226].

Ultimately this enables the generation of a **n-dimensional** (for viewability, most of the times 2D) **map**, to evaluate viral antigens, e.g. from Influenza or SARS-CoV-2, not by their genetic or sequence similarity, but by their antigenic properties, while at the same time it enables to analyze binders, such as antibodies or sera, to be evaluated on their effector properties against multiple antigens.

One major downside of this procedure is, that the **absolute amplitude** of serum responses towards a specific antigen **is lost**, as the distances are processed separately for each serum. As visualized in **Figure 6**, Serum S2 has a 10-times increased titer to each variant, compared to S1, yet both points on the antigenic map share the same coordinates. This problem can be overcome by **reintroduction of the** actual titer **amplitude** as a third dimension and fitting of a shape through the titers per antigen for each group of sera, a procedure called **antibody landscaping**[228,229].

Admittedly, there are several **different options to fit** the shape each with its' own pros and downfalls. Both locally estimated scatterplot smoothing (Loess) or bell-shaped curves are used in published packages[228] yet different options like planes from linear models or other shapes from nonlinear models (e.g. gams) could provide superior options for specific cases. Thus, the choice of the right shape needs

to be considered case by case, depending on the target research question[230,231]. One major aspect of antibody landscaping, is the possible **prediction of antibody titers** against novel or unmeasured variants, given a valid map placement of said variant. Another valuable aspect could be to judge and compare different immunization antigens or schemes for vaccine development or to improve mAbs for passive immunization[232,233].

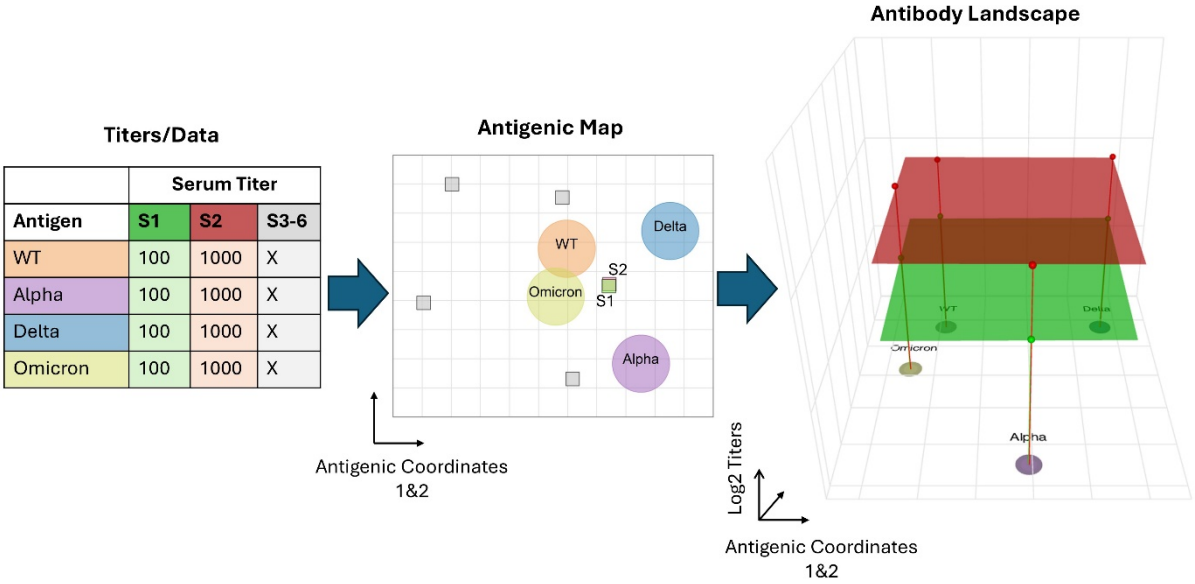

Figure 6 Demonstration of antigenic cartography principles, starting from a titertable (S3-6: X indicates multiple different titers introduced for a visually more appealing map), an exemplary antigenic map was generated, visualizing the color coded antigens (WT in orange, Alpha in purple, Delta in blue, Omicron in yellow) and sera (S1 in green, S2 in red, S3-6 in grey). Despite different titer amplitudes, S1 and S2 were mapped into the same coordinates due to similar titer ratios for each antigen within each serum and a loss of absolute titer amplitude in the mapping process. Antibody landscaping reintroduced the titer amplitude to each antigen, by taking the map coordinates as a footprint and fitting a shape through the titers of each serum for the respective antigen (in this example simple shapes were used for visual purposes). In contrast to the sole map, this allows a split of S1 and S2 in two seperable landscapes. The map grid represents antigenic coordinates, representing a fold-change in titers, the third axis denotes absolute log2 titers against the denoted variants. The map was modified with the grey Sera S3-6 (titers not shown in table and landscape), to generate a more spread out and optically appealing map.

3.4.5 Machine learning, Classification Modeling and Regression

Machine learning or modeling has become an **essential tool** in biosciences for uncovering patterns in complex biological data. Hence, it was applied for a variety of tasks within the SARS-CoV-2 pandemic, off note, the aforementioned multidimensional scaling in antigenic cartography can already be considered a form of machine learning. In general, machine learning tasks can be distinguished to supervised and unsupervised learning, as well as semi-supervised approaches as a mixture of both worlds[234](**Figure 7**).

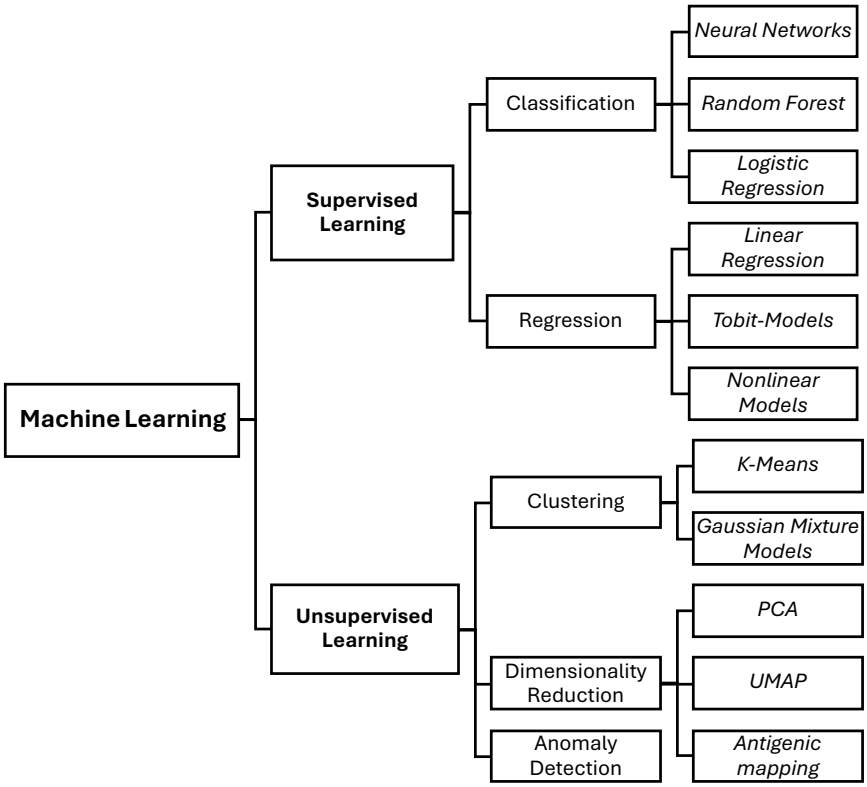

Figure 7 Schematic overview of machine learning techniques, use cases, and models. This figure does not claim to be exhaustive but aims to provide a structured overview of the models and methods applied within this thesis (and more), supporting a broader understanding of their roles and relationships.

Unsupervised learning is characterized by the lack of a target class, hence it is often intuitively associated with clustering tasks such as k-means or k-medoids. However, there are a variety of other technically unsupervised tasks, such as dimensionality reduction, e.g. UMAP or PCA, anomaly detection and matrix factorization[235–237].

Supervised machine learning is characterized by the availability of a target class. Additionally, supervised learning tasks can be split into **classification** tasks, such as predicting e.g. positive or negative test results or e.g. the infecting VOC, and **regression** tasks, such as predicting antibody loss with time/antibody durability or neutralizing antibody titers against a novel variant as previously

described for antibody landscapes. Additionally, appropriate regression models can also be used to identify effects and correct for confounding variables, e.g. antibody titers corrected by age[238,239].

In any use case, **correct model choice** is crucial for valid prediction or effect determination. In regression models, multiple factors need to be considered, starting with the scale and distribution of the target variable, potential censoring of the data and the supposed form of connection such as linear, logistic, cubic or other nonlinear connections. Other things to consider are the nature and type of the predictors/features, homoscedasticity, the number of predictors relative to the sample size and multicollinearity among the feature variables[240].

For regression models, **assessing quality** involves evaluating both the goodness of fit and the proportion of variance explained, as these reflect how well the model captures the underlying data structure and how accurate its predictions are. Depending on the type of regression model used, different metrics and diagnostic tools may be appropriate, ranging from R^2 and adjusted R^2 in linear models, to deviance or pseudo-R^2 or parameter confidence intervals in logistic and other generalized models. Additionally, information criteria such as AIC (Akaike Information Criterion) and BIC (Bayesian Information Criterion) are useful for comparing models, as they balance model fit with complexity and help prevent overfitting[241,242].

Classification modeling can be split into (non)linear classifiers and tree-based approaches, while both can be used in very simple single forms or as more complex ensembles[243].

Linear classifiers, such as perceptron or support vector machines with linear kernels, are generally interpretable and computationally efficient, but struggle with complex, non-linear boundaries, as they rely on linear separability of the data. On the other hand, non-linear classifiers, such as kernel-based support vector machines, are capable of capturing more complex patterns in the data. Similarly, neural networks—more specifically, feedforward neural networks—use multiple layers of interconnected perceptrons with activation functions like ReLU or sigmoid functions to transform input features and model intricate, non-linear relationships. However, these non-linear approaches often require careful hyperparameter tuning and come at the cost of reduced interpretability and increased computational demands, especially as model or kernel complexity grows. Another consideration with the aforementioned methods, is the need for balanced classes to ensure an unbiased fit[234,243,244].

Tree-based methods, such as single decision trees, random forests, and gradient boosting machines, provide a versatile framework for classification tasks, as they can naturally handle both linear and non-linear relationships without requiring extensive preprocessing and are less sensitive towards class imbalance problems. Single decision trees are intuitive and interpretable but prone to overfitting,

especially on complex datasets. To address this, ensemble techniques like bagging (used in random forests) and boosting (as in gradient boosting machines) aggregate multiple weak learners to produce more robust and accurate models. More advanced ensemble strategies, e.g. model stacking, combine different types of models to leverage their individual strengths, often achieving improved predictive performance through reduced variance, bias, or both. All those techniques need a sufficiently large dataset combined with a proper feature selection, feature transformation and feature scaling to be learned well[234,245,246].

Additionally, to **ensure generalizability**, it is good practice, to perform model cross-validation and at least use a training and a testing dataset, which can be achieved by using either two separate datasets or splitting the dataset in the beginning. A more advanced technique would be k-fold cross-validation, performing multiple different test and train splits with separate models, to ensure that results are not dependent on a particular train-test split[247,248]. To further reduce the **risk of overfitting**, regularization techniques such as L1/Lasso[249] or L2/Ridge[250] penalties can be applied, especially in high-dimensional settings. Another effective strategy for overfitting reduction, particularly useful in iterative models like neural networks, is early stopping, where training is halted once performance on a validation set begins to degrade or is reaching a plateau[251].

Finally, to help balance fit and generalizability, **model complexity** should be kept as low as possible, while still achieving the desired result, a principle known as the principle of parsimony or Occam's razor[252]. This can be achieved by limiting model parameters (e.g. neural network layers or random forest tree depth) or reducing the number of included variables.

4 Objective of this thesis

As illustrated in the introduction, the SARS-CoV-2 pandemic posed a **variety of challenges** to the global public and research community, everchanging dependent on the current state of the pandemic. Hence, the general objective of this thesis was to provide insight to a variety of the occurring **epidemiological and immunological questions** as clarified within the next paragraph.

In the beginning of the **SARS-CoV-2 pandemic**, one of the major tasks was to determine the current epidemiological state as well as to retrieve basic epidemiological reference values such as seroprevalence, surveillance detection ratios and infection fatality ratios. In the same scope, it was important to set up, compare and evaluate tests used in those epidemiological studies and diagnostics, to verify validity of the retrieved insights. After introduction of **SARS-CoV-2 vaccination**, the focus shifted towards the immunogenicity of the different vaccine types, effects of vaccine breakthrough infection and the derived "hybrid immunity" as well as antibody durability. The **emergence of VOCs**, especially the omicron variant BA.1 marked another shift in interest, towards investigation of effects of variant specific immunity connected with potential immune imprinting effects from vaccination or initial infection.

In the first manuscript, references such as seroprevalence, symptoms and neutralizing antibody levels ought to be evaluated in a cross-sectional, semi-population-based approach, after the first pandemic wave in spring 2020. Here, the major goal was understanding **the role of** rather mildly affected and largely not tested **children** in the pandemic.

The second manuscript aimed to analyze and to **compare** widely used SARS-CoV-2 **serological tests** following international guidelines using a population-based cohort. On top, the study strived to provide insight into the transferability of said serological test results towards the level of neutralizing antibody levels, the best predictive immunological correlate of protection. Finally, the manuscript tried to set sight to potential problems in artificially designed test establishment settings and implications when moving those tests to the real world.

The third manuscript's scope was to expand on the knowledge of the first **TiCoKo19 study** visit by providing insights into the time trend of representative epidemiological reference values such as seroprevalence, SDR and IFR between 2020 and 2021 again using the population based TiKoCo19 cohort. Furthermore, the manuscript aimed to explore the role of senior care homes towards those measures at the different timepoints. Finally, the manuscript provided insight into the progress of the starting vaccination campaign within the municipality of Tirschenreuth.

The fourth manuscript aimed to better understand the **immunity** derived from **SARS-CoV-2 infection, vaccination** as well as combinations of both. It further strived to evaluate differences between the

available vaccine types (adenoviral vector and mRNA-based vaccines) and elaborate on the durability of the elicited antibody responses post vaccination.

The fifth manuscript tried to elaborate on the **variant specific immunity** derived after VOC stratified infection or vaccine breakthrough infection, especially in terms of immune imprinting, using the cross-sectional CoVaKo19 cohort. Here, advanced bioinformatic techniques such as antigenic cartography and machine learning were used to work out differences in longitudinal neutralizing antibody responses, bias towards certain antigens and imprinted patters based on the infecting VOC.

Finally, the appendix manuscripts ought to expand on the previously mentioned topics and provide additional insights on epidemiological status, correlates of protection, reactogenicity of SARS-CoV-2 vaccination, SARS-CoV-2 vaccine development and serological testing.

5 Manuscripts

5.1 Overview

This dissertation is comprised of five main manuscripts, all of which are published in peer-reviewed, open-access journals. First authorship was shared with others in the first, second and fourth manuscript, the third and fifth manuscript were authored as sole first author.

To comply with university regulations, the formatting of the original, published manuscripts and the style of the references was changed to provide a uniform picture within the thesis itself. Furthermore, the indexing and layout of the figures, supplementary figures and tables was adjusted to have a uniform indexing within the thesis. Neither data nor other content was changed in any form, however, typos in the manuscripts were corrected when encountered.

An additional 17 manuscripts were co-authored. Due to limited space, only the abstracts are shown within this thesis (9.1 Appendix Publication Abstracts), but the results are included in the summary of results and the discussion. The full publications can be accessed using the DOI provided in 0 B) Appendix publications.

5.2 Manuscript 1: "Symptoms, SARS-CoV-2 antibodies and neutralization capacity in a cross sectional population of German children"

5.2.1 Abstract

Background: Children and youth are affected rather mildly in the acute phase of COVID-19 and thus, SARS-CoV-2 infection infection may easily be overlooked. In the light of current discussions on the vaccinations of children it seems necessary to better identify children who are immune against SARS-CoV-2 due to a previous infection and to better understand COVID-19 related immune reactions in children.

Methods: In a cross-sectional design, children aged 1-17 were recruited through primary care pediatricians for the study (a) randomly, if they had an appointment for a regular health check-up or (b) if parents and children volunteered and actively wanted to participate in the study. Symptoms were recorded and two antibody tests were performed in parallel directed against S (in house test) and N (Roche Elecsys) viral proteins. In children with antibody response in either test, neutralization activity was determined.

Results: We identified antibodies against SARS-CoV-2 in 162 of 2,832 eligible children (5.7%) between end of May and end of July 2020 in three, in part strongly affected regions of Bavaria in the first wave of the pandemic. Approximately 60% of antibody positive children (n = 97) showed high levels (>97th percentile) of antibodies against N-protein, and for the S-protein, similar results were found. Sufficient neutralizing activity was detected for only 135 antibody positive children (86%), irrespective of age and sex. Initial COVID-19 symptoms were unspecific in children except for the loss of smell and taste and unrelated to antibody responses or neutralization capacity. Approximately 30% of PCR positive children did not show seroconversion in our small subsample in which PCR tests were performed.

Conclusions: Symptoms of SARS-CoV-2 infections are unspecific in children and antibody responses show a dichotomous structure with strong responses in many and no detectable antibodies in PCR positive children and missing neutralization activity in a relevant proportion of the young population.

5.2.2 Introduction

Early in the COVID-19 pandemic, children and adolescents were thought to be important transmitters of the disease but were also believed to be only mildly affected[253]. Later, evidence increased that children are not major spreaders[254–256]. However, a pediatric multiorgan immune syndrome in children and youths was reported[257], occurring weeks to months after the SARS-CoV-2 infection, also in children with mild or no symptoms in the initial phase of the disease. Recent studies linked PIMS to the presence of antibodies to SARS-CoV-2 and some authors suggested that high levels of antibodies against SARS-CoV-2 may in fact contribute to the occurrence of the full-fledged syndrome[258]. These observations

indicate that immune reactions to SARS-CoV-2 exposure may differ, at least in strength, between children and adults.

When vaccination for SARS-CoV-2 was first administered to adults, stronger systemic vaccination reactions to the vaccine were reported in younger individuals [37]. In some of our cases, high antibody levels were already observed directly after vaccination when these symptoms occurred (own observation), suggesting a possibility that these individuals may have had an unnoticed SARS-CoV-2 infection previously. With vaccination of children against SARS-CoV-2 in sight, it is important to better identify those that were already infected and to improve our understanding of SARS-CoV-2 related immune responses in children overall.

In many children allegedly mild or inapparent infections occurred and PCR testing was performed rarely. Therefore, we screened a large number of children in rather severely affected areas of Bavaria (Southern Germany) for symptoms as well as overall and neutralizing antibody levels against SARS-CoV-2 in the first pandemic wave in spring of 2020, in a population-based approach.

5.2.3 Material and Methods

5.2.3.1 Study Design and Population

In a cross-sectional design we investigated children from three distinct regions of South East Germany to assess the true prevalence of SARS-CoV-2 infections in areas with very differently reported infection rates by antibody testing. We established a network of pediatricians who volunteered to take part in the study and focused on three areas/counties within Bavaria with very high, moderate, and average infection rates as indicated by positive PCR tests per 100,000 inhabitants according to the Robert Koch Institute, the German center for disease prevention (**Figure 8**). The assessment and sample collection took place in three study areas: Tirschenreuth; Regensburg city and county; and Oberbayern/ alpine region from May 22nd to July 22nd, 2020. In areas where the number of willful study participants exceeded the capacity of local pediatricians, a study team supported sample collections.

Invitation to participate for children aged 1–14 years was based on two approaches: (a) All children of that age group who were scheduled for a prevention program visit in 2020 with the respective pediatrician were invited to participate (random selection) and (b) all children of families who actively wanted to participate were also tested (own intention to participate). In approach (b), also siblings older than 14 years were allowed to participate in the study, as for ethical reasons, children older than 14 could not be excluded from antibody testing if families presented them together with younger siblings for testing. The study was approved by the Ethics Committee of the University of Regensburg (file-number: 20-1865-101).

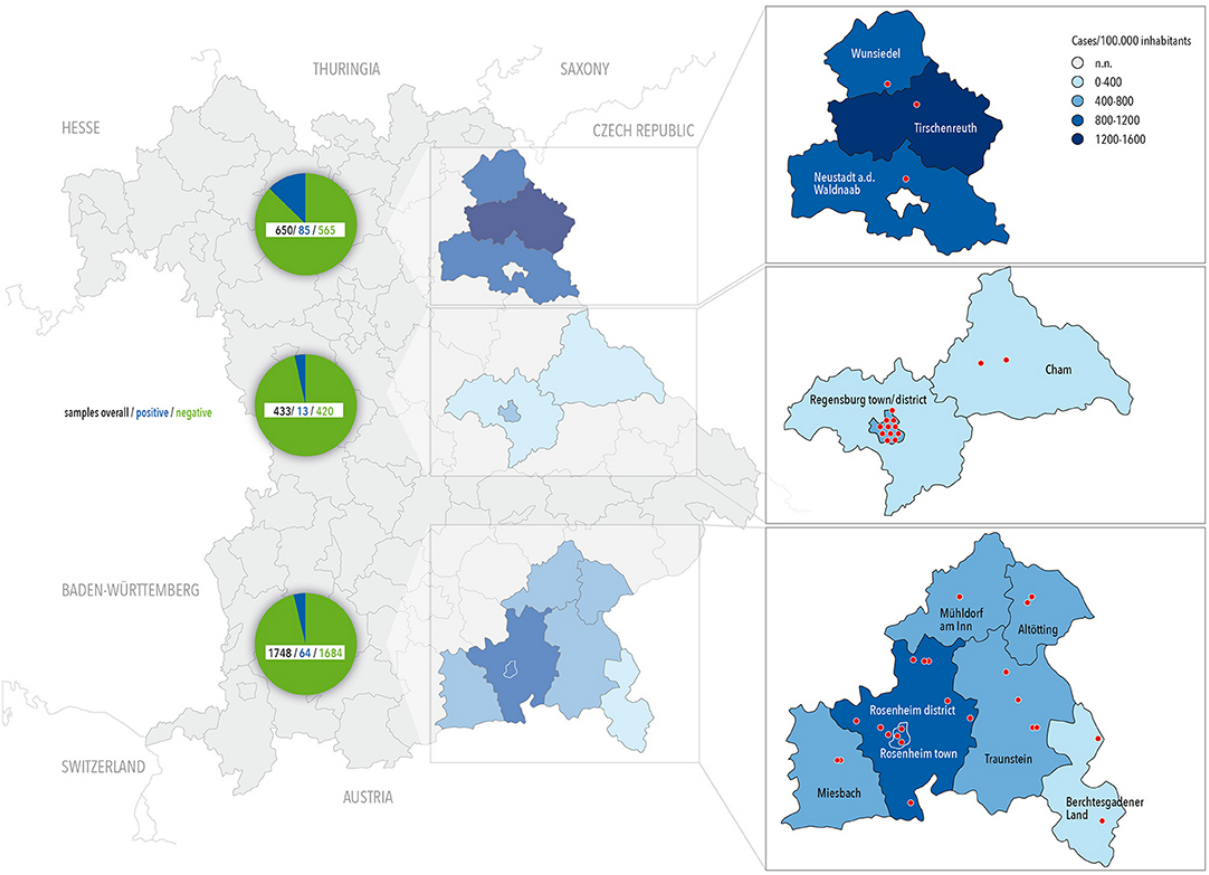

Figure 8 Map of Bavaria with location of centers contributing to the survey (red dots) and COVID-19 prevalence until July 2020 (color coded by county). Number for overall, negatively and positively tested children are given in the circle chart.

5.2.3.2 Data Collection and Management

All data were collected in an online survey using self-administered parental questionnaires. The questionnaires can be obtained upon request from the authors. All acquired data was fully anonymized and only accessible at an individual level to the participant using an individual code on the Qnome platform (www.qnome.eu) as previously described in detail[259]. Clinical data was entered by the parents in an online survey. That way, anonymization of data on the level of the dataset was achieved while the test values were directly accessible to parents.

5.2.3.3 SARS-CoV-2 Antibody Tests

Blood was taken from all participants by venipuncture. Specific antibody response to SARS-CoV-2 was evaluated by the use of two different test kits: the commercially available, licensed qualitative Elecsys Anti-SARS-CoV-2 (Roche Diagnostics, Rotkreuz, Switzerland; https://diagnostics.roche.com) with a sensitivity of 99.5% and a specificity of 99.8%, according to the manufacturer; and a validated and published in-house ELISA with a sensitivity of 96% and a specificity of 99.3% as previously reported[260]. The Elecsys Anti-SARS-CoV-2 assay does not discriminate between the antibody type(s) present and can detect IgA, IgM, and IgG. The test is based on a recombinant nucleocapsid (N) antigen and has a

cutoff value of 1.0 (S/Co). The in-house ELISA is based on SARS-CoV-2 S-protein's receptor-binding domain, quantifies total IgG and has a cutoff value of 1.0 (S/Co). The detected reactivity correlates with the SARS-CoV-2 neutralization titer as described previously[260]. All samples with S/Co <1.0 were considered negative.

5.2.3.4 SARS-CoV-2 Neutralization Test

Neutralizing antibodies were evaluated by titration of sera against SARS-CoV-2 pseudotyped Vesicular Stomatitis Virus (VSV). The test is based on VSV-ΔG*FLuc pseudotyped with SARS-CoV-2-Spike-ΔER, which correlates with SARS-CoV-2 neutralization as described previously[72,209]. Pseudoviral titers were determined by limited dilution and fluorescence microscopy. For all samples, a fixed inoculum of 25,000 ffu was neutralized for 1 h and luciferase activity was determined 20 h post infection of HEK293T-ACE2+-cells. IC50 values were fitted using the algorithm: 'log (inhibitor) vs. normalized response'. Data were analyzed and Spearman's correlations (R) were calculated in GraphPad Prism 8 software (GraphPad Software, San Diego, USA).

5.2.3.5 Statistical Analyses

Descriptive statistics were calculated using frequencies (percentages) for categorical data and median (interquartile range) for metric data. Participants' characteristics and symptoms are presented stratified by antibody response. Differences between groups were analyzed using χ2-tests for categorical variables and t-test for independent groups, respectively. All analyses were performed using SPSS.23.

5.2.4 Results

Overall, 2,934 children participated in the study of whom 2,906 were tested successfully with at least one of the two applied antibody tests and 2,832 (96.5%) had also entered necessary study data in the online tool. Demographic data of the children participating in the study are given in **Table 3** and locations of test-centers across counties are depicted in **Figure 8**.

Table 3 Characteristics of study participants stratified for antibody (AB) test result.

GENERAL CHARACTERISTICS	**Negative AB test (N=2670)**	**Positive AB test (N=162)**	***p***
Study participation due to...			
random selection (health check-up), % (N)	66.0 (1763)	32.1 (52)	
own intention to participate, % (N)	34.0 (907)	67.9 (110)	<.001*
Sex (male), % (N)	51.7 (1380)	50.6 (82)	.792
Age (years) (Md, IQR)	7 (4.0-10.0) (range 0-17)	8 (4.7-11.0) (range 0-16)	.070
Any chronic disease, % (N)	12.3 (329)	9.3 (15)	.247
Does your child usually attend...			
Nursery, % (N)	6.1 (163)	4.9 (8)	
Kindergarten, % (N)	27.5 (733)	23.5 (38)	
Elementary school, % (N)	30.3 (809)	29.0 (47)	
Secondary school (Mittelschule), % (N)	4.9 (130)	9.9 (16)	
Secondary school (Realschule), % (N)	8.5 (227)	11.1 (18)	
Grammar school, % (N)	11.0 (295)	9.9 (16)	
School for special needs, % (N)	0.6 (17)	1.2 (2)	
None of them, % (N)	11.1 (296)	10.5 (17)	.138
SARS-CoV-2 PCR testing, % (N)	8.8 (234)	17.9 (29)	<.001*
Positive SARS-CoV-2 PCR test, % (N)	0.2 (6)	9.3 (15)	<.001*
Hospitalization due to COVID-19, % (N)	0.2 (6)	1.2 (2)	.019*
Household member COVID-19, % (N)	6.0 (161)	47.5 (77)	<.001*
Any symptom, % (N)	70.1 (1871)	76.5 (124)	.080

Notes: *p< .05; chi² test, t-test for independent groups. IQR, interquartile range. Md, median

Overall, 161 participants were classified seropositive with any test*, of which 158 were ELISA positive and 139 showed a positive ELECSYS signal, yielding a total concordance of 83.9 % (n = 135 positive in both tests) and a total discordance of 16.1 % (n = 23 ELECSYS-positive/ELISA-negative; n = 3 ELECSYS-positive/ELISA) (**Figure 9**). A positive result in at least one of the two tests defined a positive case.

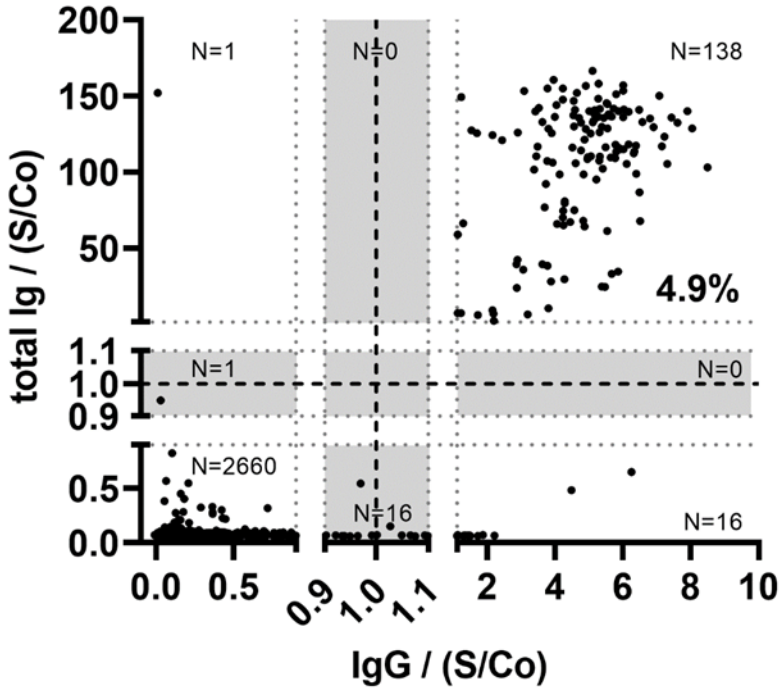

Figure 9 Comparison between the N protein directed Elecsys Anti-SARS-CoV-2 assay (total Ig) and the S protein directed in-house SARS-CoV-2 assay detecting IgG (IgG) in the total study population (N = 2,832). Strong dotted lines represent the assay cutoff values, ±10% borderline intervals (gray areas). Signal-to-cutoff (S/Co) ratios are given for both assays.

Strong regional differences were observed in the prevalence of SARS-CoV-2 antibodies in children (**Figure 8**). Overall, children in the heavily affected county of Tirschenreuth (with 1,638 positive PCR tests/100,000 inhabitants when the survey was performed) had positive antibody response 3–4 times more often than in the two other test regions, with 586 positive PCR tests/100,000 inhabitants in Regensburg and 1,111 positive PCR tests/100,000 inhabitants in Rosenheim (September 2020). When only those children randomly selected [approach (a)] and only one child (the youngest) per family were included in the analysis, 7.2% of tested children where positive in Tirschenreuth, 3.1% in Regensburg and 1.8% in Oberbayern/Alpine region. In those who participated on their own intention, e.g., due to symptoms that may have been related to COVID-19 or suspected contact to a COVID-19 patient [approach (b)], 15.9% were found positive in Tirschenreuth, 2.3% in Regensburg and 7.8% in Oberbayern/Alpine region, again taking only one child per family into account.

The older the children, the more positive SARS-CoV-2 tests were found, with 4.9% positive in the 0–6 year-olds (n = 1,299), 5.7% in the 7–10 year-olds (n = 849) and 7.3% positive in the 11–17 year-olds (n = 684). Children with chronic diseases tended to be slightly less often positive (4.3% of 344) than those without chronic diseases (5.9% of 2,488). Within the study population, only 263 children had already received a SARS-CoV-2 PCR test previously and 21 had a positive test result. Of these, 15 individuals showed elevated antibody responses (71.4%) while in 6 subjects no antibody response in any of the two tests could be found. Two hundred and thirty-eight children lived in a household with a positively

tested family member and of these, 32.4% developed antibodies against SARS-CoV-2. Thus, living with a SARS-CoV-2 positive family member is the single most prominent association with a SARS-CoV-2 infection in children in our study population. We assessed symptoms potentially related with SARS-CoV-2 infections in our study population but found very few specific features (other than the loss of smell and taste) which would allow to discriminate COVID-19 from common viral infections in children (**Table 4**).

Table 4 Symptoms of study participants after antibody measurement: stratified for antibody (AB) test result.

Symptoms	Negative AB test (N=2670)	Positive AB test (N=162)	*p*
No symptoms, % (N)	30.1 (804)	23.5 (38)	.072
Runny nose, % (N)	42.5 (1135)	32.7 (53)	.014*
Sore throat, % (N)	28.2 (753)	18.5 (30)	.007*
Headache, % (N)	24.3 (648)	24.1 (39)	.955
Dizziness, % (N)	6.5 (173)	4.9 (8)	.436
Exhaustion/ fatigue, % (N)	24.0 (640)	25.3 (41)	.699
Muscle aches, % (N)	14.0 (373)	16.0 (26)	.460
Inflammation of the eyes, % (N)	4.4 (117)	3.1 (5)	.430
Loss of smell, % (N)	1.0 (27)	4.9 (8)	<.001*
Loss of taste, % (N)	2.4 (64)	6.8 (11)	.001*
Shortness of breath, % (N)	5.1 (137)	3.7 (6)	.420
Coughing, % (N)	41.0 (1096)	30.9 (50)	.010*
Fever, % (N)	37.6 (1004)	38.3 (62)	.865
Chills, % (N)	7.3 (194)	3.7 (6)	.086
Rash, % (N)	5.3 (142)	2.5 (4)	.111
Diarrhea, % (N)	16.5 (441)	13.0 (21)	.235
Nausea, % (N)	11.4 (304)	9.9 (16)	.556
Loss of appetite /difficulty feeding, % (N)	11.2 (298)	5.6 (9)	.026*
Other symptoms, % (N)	2.5 (66)	2.5 (4)	.998

Notes: * $p < .05$; chi^2 test.

Despite the good level of concordance (83.9%) between the occurrence of N-protein specific (Roche Elecsys) and S-protein specific antibodies (in house ELISA), N-specific titers (ELECSYS) did not correlate with our in-house S-protein ELISA in the overall analysis (**Figure 9**). Considering this obvious discordance regarding N- and S-protein specific antibody titers, the positive population in any test with sufficient material for further testing (n = 161) was analyzed for neutralizing antibodies (nAbs).

In the following neutralizing activity was detected for n = 135 participants, providing a total concordance of 95.7 % (n = 133 positive; n = 21 negative) and a discordance of 4.3 % (n = 2 N-seropositive/neutralization-negative; n = 5 N-seronegative/neutralization-positive) of the Elecsys result with the presence of nAbs. For comparison, the ELISA showed 83.2 % concordance (n = 133 positive; n = 1 negative) and 16.8 % discordance (n = 25 S-seropositive/neutralization-negative; n = 2 S-seronegative/Neutralization-positive) with the result of the neutralization assay (**Figure 10** and **Supplementary table 1**). As internal control, n = 81 randomly chosen negative sera (matching the age and sex distribution of the positive population) were tested for the presence of neutralizing antibodies, of which none exhibited a positive result yielding a specificity of 100% (**Supplemental Figure 1**).

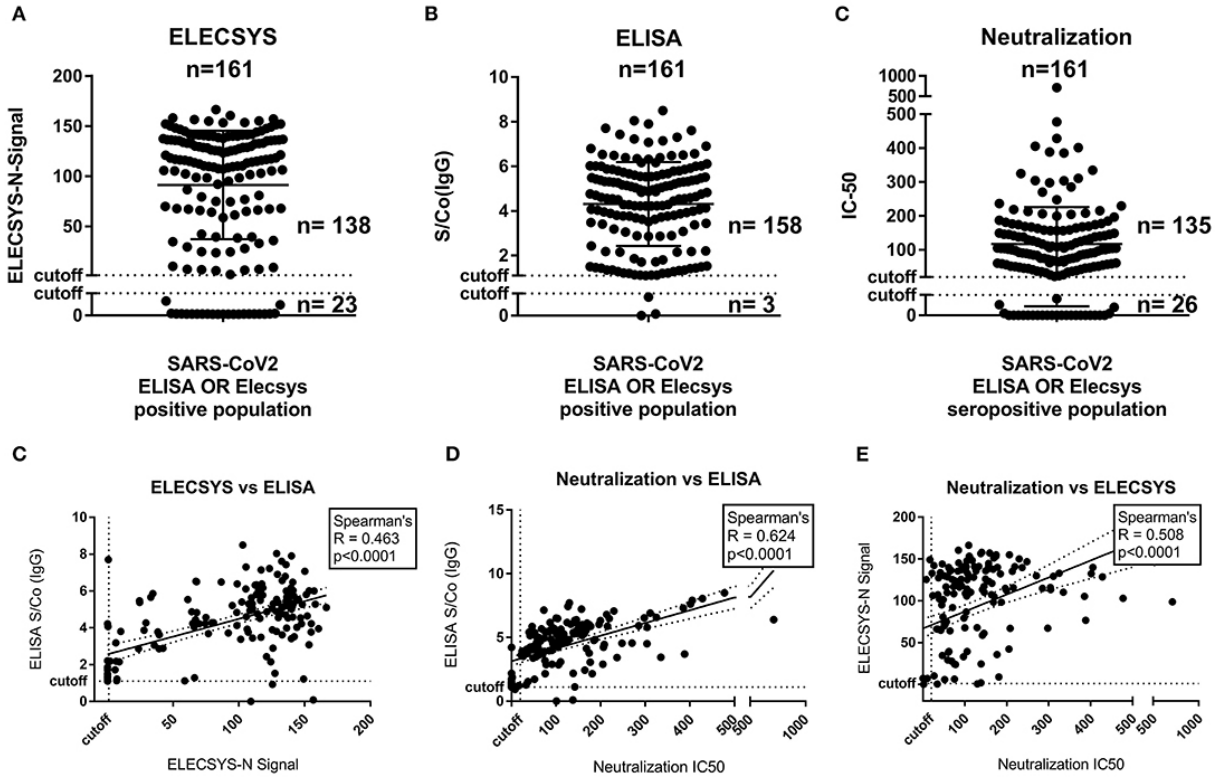

Figure 10 N- and S-protein specific binding antibody titer and neutralization capacity analysis of in any test positive children (n = 161). (A) Distribution of N-specific antibody signal (Elecsys, S/Co). (B) Distribution of SRBD-protein ELISA binding antibody titers (S/Co). (C) Distribution of Neutralization titers (IC50). (D) Correlation of N-specific antibody signal (Elecsys, S/Co) with SRBD-protein ELISA binding antibody titers (S/Co). (E) Correlation of N-specific antibody signal (Elecsys, S/Co) with SRBD-protein ELISA binding antibody titers (S/Co).

Correlating (Spearman) the quantitative results of the three assays showed a significant correlation for each pair, while the ELISA correlated best (R = 0.62) with the IC-50 of the neutralization assay, the quantitative readout of the Elecsys showed inferior correlation with both the ELISA (R = 0.46) and the neutralization (R = 0.50). This was not surprising, as the manufacturer doesn't recommend any quantitative readout of the ELECSYS assay. Furthermore, no significant effects could be found on any of the three (quantitative) test results regarding age or sex of the participants (**Supplemental Figure 2**). Neither antibody levels nor neutralization capacity did correlate with any of the classical symptoms named in **Table 4**(detailed analysis in **Supplemental Figure 3**).

5.2.5 Discussion

In our study, performed in regions of Germany with a relatively high incidence of COVID-19 in adults in the first phase of the pandemic, approximately 6% of tested children were positive for SARS-CoV-2 antibodies in two tests directed against the N- and S-proteins of the virus. Symptoms of COVID-19 were found to be rather unspecific in children while antibody response was strong in most cases. SARS-CoV-2 neutralization capacity was independent of age, sex or symptoms in those children with antibodies and absent in those without antibodies.

This study showed an unexpected high prevalence rate of SARS-CoV-2 infections in children in Germany in the first wave, comparable to similar studies in Germany[261]. The antibodies in our study were determined approximately 2 months after the peak of the first pandemic wave. Despite the closing of schools, kindergartens, and nurseries very early on in the pandemic in Germany, a surprisingly high number of children showed antibodies in our study. One possible explanation for that could be that many parents who participated in the study suspected a coronavirus infection in their children due to symptoms or outbreaks in their community. Indeed, children were explicitly not tested in the beginning of the pandemic when PCR test capacities were limited. Thus, the study may have addressed an unmet need of parents to get their children tested, which was further supported by the observation that participation in the study was overwhelming.

About 70% of the positive children showed S/Co >100 in the ELECSYS test, a value approximately representing the 97th percentile of all previously available test values (provided by Roche, personal communication). We are aware that the assay is not registered for quantitative readout, nevertheless the measures give an indication for a strong antibody response in children. Compared to the 70% of seropositive children with a mild to asymptomatic course of the initial SARS-CoV-2 infection only 21% of seropositive adults with mild symptoms showed such high values in one of our studies conducted at the same time[262]. A similar observation was made for the S protein based in-house ELISA test, where also high values were observed in more than half of the positively tested children. These data may suggest that children mount stronger antibody responses to SARS-CoV-2 than adults on a regular basis.

We used two different antibody tests, one directed against the N-protein and one targeting the S-protein, which explains the slight differences and discordance in test results. With two capable antibodies used for testing at the same time, we have good confidence that we were able to catch all truly seropositive children after SARS-CoV-2 infection. Interestingly, in those few cases where children were initially positive in PCR testing, approximately 30% did not show antibody responses in our tests. This is a higher percentage than observed in our studies in adults[262]. Furthermore, approximately 15% of antibody positive children showed no neutralization capacity.

Taken together, it seems that children show a somewhat dichotomous response to SARS-CoV-2 in terms of antibody generation and neutralization. While a great majority mounts exceptionally high antibody responses, a significant subgroup shows no antibodies after infection or no neutralization capacities. Both, strong-responders and non-responders, represent larger fractions of the population than in our adult study populations[262]. It could be speculated that strong antibody responses may contribute to the milder acute course of the initial infection observed in children, but in adults, high levels of S-specific (and neutralizing) antibodies seem to be connected to severe courses of COVID-19[263]. On the other hand, considering the lower neutralizing antibody levels in a substantial group of children, a lower protection from reinfection is much more probable, as neutralizing antibody levels were found to be highly predictive to prevent future (symptomatic) infection[180].

Our study indicates that very few symptoms are specific for COVID-19 in children. On the other hand, only 23% of children with detectable SARS-CoV-2 antibodies were free of symptoms in the weeks before the antibody test. Interestingly, even children as young as 6 years of age were able to indicate loss of smell and taste—the only specific symptom for COVID-19 we could identify in children. It is currently debated, if a loss of smell and taste is also a feature of future mutants of SARS-CoV-2, as data for the SARS-CoV-2 delta variant suggest otherwise. Thus, screening for SARS-CoV-2 infections in children by symptoms does not seem to be useful.

A large number of children acquired antibodies against SARS-CoV-2 when family members had developed COVID-19. Therefore, we suggest that children confronted with COVID-19 in the household should systematically be screened for SARS-CoV-2 antibody responses e.g., 4 weeks after the diagnosis in the index case, thereby not missing out on potential childhood SARS-CoV-2 infections despite of mild or absent symptoms in children. Especially with new, more contagious virus variants, infections in families become even more relevant.

Based on our results we propose to screen children from households with COVID-19 cases on a regular basis for SARS-CoV-2 antibodies as well as children from areas with high prevalence of COVID-19, if any symptoms suggestive for COVID-19 occur. Alternatively, prospective PCR based test systems in schools

seem to be reasonable and feasible[264]. Therefore, we would recommend longitudinal antibody testing as well as vaccination; if found to be safe; for children to ensure full protection from future disease.

5.2.6 Appendix & Declarations

Data Availability Statement

The raw data supporting the conclusions of this article will be made available by the authors, without undue reservation.

Ethics Statement

The studies involving human participants were reviewed and approved by Ethics Committee of the University of Regensburg (file-number: 20-1865-101). Written informed consent to participate in this study was provided by the participants' legal guardian/next of kin.

Author Contributions

OL, GL, SG, KÜ, RW, and MK were responsible for the study design. OL, GL, HB-D, SL, AS-K, DE, MH, JN, and MK performed the data collection. AT, DP, SE, PN, NB, ES-V, PK, PS, RW, and AA carried out the laboratory analysis and the data interpretation. Data Analysis was performed by DP, SE, PN, SB, RW, and MK. OL, GL, DP, SE, SB, RW, and MK wrote this manuscript. All authors contributed to the article and approved the submitted version.

Funding

This work was supported by institutional and charity funds, RW and KÜ by the Bavarian States Ministry of Science and Arts (Grant Prospective Covid-19 Cohort Tirschenreuth, TiKoCo19). Roche Diagnostics provided Elecsys Anti-SARS-CoV-2 assay free of charge.

The CoKiBa Study Group are (in Alphabetical Order)

Bettina Aichholzer, Georg Mair, Michaela Wruk, Imke Reischl, Paediatric Office, Dr. Aichholzer, Dr. Mair, Dr. Wruk, Reischl, Bad Endorf, Germany; David Antos, Paediatric Office Dr. Antos, Traunstein, Germany; Stephan von Koskull, Christian Becker, Paediatric Office Dr. von Koskul, Becker, Bad Aibling, Germany; Elisabeth Beer, Hubert Schirmer, Paediatric Office Dr. Beer, Dr. Schirmer, Marktredwitz, Germany; Georg Birkinger, Paediatric Office Dr. Birkinger, Wasserburg am Inn, Germany; Andreas Blueml, Paediatric Office Blueml, Trostberg, Germany; Mona Castrop, Paediatric Office Dr. Castrop, Regensburg, Germany; Jost Dieckerhoff, Paediatric Office Dr. Dieckerhoff, Rosenheim, Germany; Renate Eichhorn, Paediatric Office Dr. Eichhorn, Regensburg, Germany; Dominik Ewald, Paediatric Office Dr. Heuschmann & Dr. Ewald, Regensburg/Regenstauf, Germany; Gudrun Fleck, Alfred Heihoff, Paediatric Office Dr. Fleck, Dr. Heihoff, Regensburg, Germany; Jürgen Geuder, Paediatric Office Dr. Geuder, Freilassing, Germany; Jens Grombach, Paediatric Office Dr. Grombach, Neuoetting, Germany; Peter Gutdeutsch, Florian Segerer, Paediatric Office Dr. Gutdeutsch, Dr. Segerer, Regensburg, Germany; Thomas Habash, Sonja Habash, Paediatric Office Dres. Habash, Cham, Germany; Susanne Harner, University Childrens‘Hospital Regensburg (KUNO) at the Hospital St. Hedwig of the Order of St.

John University of Regensburg, Regensburg, Germany; Christoph Herbst, Paediatric Office Dr. Herbst, Edling, Germany; Daniela Heuschmann, Paediatric Office Dr. Heuschmann & Dr. Ewald, Regensburg/Regenstauf, Germany; Meike Hofmann, Paediatric Office Hofmann, Mitterteich, Germany; Michael Horn, Paediatric Office Dr. Horn, Schoenau am Chiemsee, Germany; Birgit Jork-Kaeferlein, Monika Schwarz, Reinhard Hopfner, Paediatric Office Dr. Jork-Kaeferlein, Dr. Schwarz, Dr. Hopfner, Prien, Germany; Guido Judex, Bastian Baumgartner, Monika Corbacioglu, Sabrina Lindner, Bettina Meinel, Alena Bauer, Hannes Löw, Annamaria Szulagyi-Kovacs, Paediatric Office Dr. Judex, Dr. Baumgartner, Dr. Corbacioglu, Dr. Lindner, Dr. Meinel, Bauer, Löw, Szulagyi-Kovacs, Regensburg, Germany; Michael Kabesch, University Childrens'Hospital Regensburg (KUNO) at the Hospital St. Hedwig of the Order of St. John University of Regensburg, Regensburg, Germany; Annegret Klein, Paediatric Office Dr. Klein, Oberaudorf, Germany; Cosima Koering, Paediatric Office Dr. Koering, Altoetting, Germany; Niclas Landvogt, Claudia Soehngen, Karin Rasp, Gudrun Schick-Niedermeier, Paediatric Office Dr. Landvogt, Dr. Soehngen, Traunreut, Germany; Marinus Laub, Paediatric Office Laub, Rosenheim, Germany; Otto Laub, Paediatric Office Laub, Rosenheim, Germany; Georg Leipold, Petra Schmid-Seibold, Paediatric Office Dr. Leipold Schmid-Seibold, Regensburg, Germany; Johannes Pawlak, Michaela Reitz, Paediatric Office Dr. Pawlak, Dr. Reitz, Rosenheim, Germany; Georg Puchner, Paediatric Office Dr. Puchner, Regensburg, Germany; Christiane Razeghi, Stefan Razeghi, Paediatric Office Dres. Razeghi, Miesbach, Germany; Christine Rehe, Klaus Rehe, Paediatric Office Dres. Rehe, Kolbermoor, Germany; Matthias Scheffel, Ludwig Kaesbauer, Paediatric Office Dr. Scheffel, Dr. Kaesbauer, Muehldorf, Germany; Roland Schmid, Michael Strobelt, Paediatric Office Dr. Schmid, Dr. Strobelt, Bruckmuehl, Germany; Nina Schoetzau, Paediatric Office Dr. Schoetzau, Miesbach, Germany; Marko Senjor, Paediatric Office Dr. Senjor, Wasserburg, Germany; Michael Sperlich, Paediatric Office Dr. Sperlich, Ampfing, Germany; Guenter Theuerer, Guenter Steidle, Paediatric Office Dr. Theurer, Dr. Steidle, Traunstein, Germany; German Tretter, Paediatric Office Dr. Tretter, Altenstadt an der Waldnaab, Germany; Victor von Arnim, Paediatric Office Dr. von Arnim, Roding, Germany; Marlene Volz-Fleckenstein, Paediatric Office Dr. Volz-Fleckenstein, Regensburg, Germany.

Conflict of Interest

JN was employed by the company Maganamed Limited. The remaining authors declare that the research was conducted in the absence of any commercial or financial relationships that could be construed as a potential conflict of interest.

Publisher's Note

All claims expressed in this article are solely those of the authors and do not necessarily represent those of their affiliated organizations, or those of the publisher, the editors and the reviewers. Any product that may be evaluated in this article, or claim that may be made by its manufacturer, is not guaranteed or endorsed by the publisher.

Acknowledgments

We are grateful to all participants for their bravery in giving blood and their parents for their great support, the Bavarian red cross for support in Tirschenreuth and especially Mr. Schedel; the students who helped organizing the study, packing study sets, transporting sets and samples across the study areas; the assistants and helpers in all pediatric outpatient clinics who did a tremendous job on top of their routine work; all lab personal in the involved laboratories for extra and weekend hours; and Birgit Kulawik for providing graphic design. We thank the WECARE research and development campus at the KUNO hospital St. Hedwig in Regensburg for the generous logistical support.

Keywords: antibody, neutralizing, COVID-19, SARS-CoV-2, children

5.2.7 Supplementary Materials

The Supplementary Material for this article can also be found online at: https://www.frontiersin.org/articles/10.3389/fped.2021.678937/full#supplementary-material

Supplementary table 1 Comparative analysis of three serological test results (Cutoffs: Roche ELECSYS N S/Co≥1; SRBD-ELISA S/Co≥1.1; Neutralization IC50≥20) of the seropositive population in any test (n=161) visualizing the positive, negative as well as concordant and discordant results.

ELECSYS vs Neutralization			**ELISA vs Neutralization**			**ELECSYS vs ELISA**		
	Neutralization			Neutralization			ELISA	
Elecsys	positive	negative	ELISA	positive	negative	ELECSYS	positive	negative
positive #; %	133; 82.6	5; 3.1	positive #; %	133; 82.6	25; 15.5	positive #; %	135; 83.9	3; 1.9
negative #; %	2; 1.2	21; 13.0	negative #; %	2; 1.2	1; 0.6	negative #; %	23; 14.3	0; 0
total concordance %	**95.7**		**total concordance %**	**83.2**		**total concordance %**	**83.9**	
total discordance %	**4.3**		**total discordance %**	**16.8**		**total discordance %**	**16.1**	

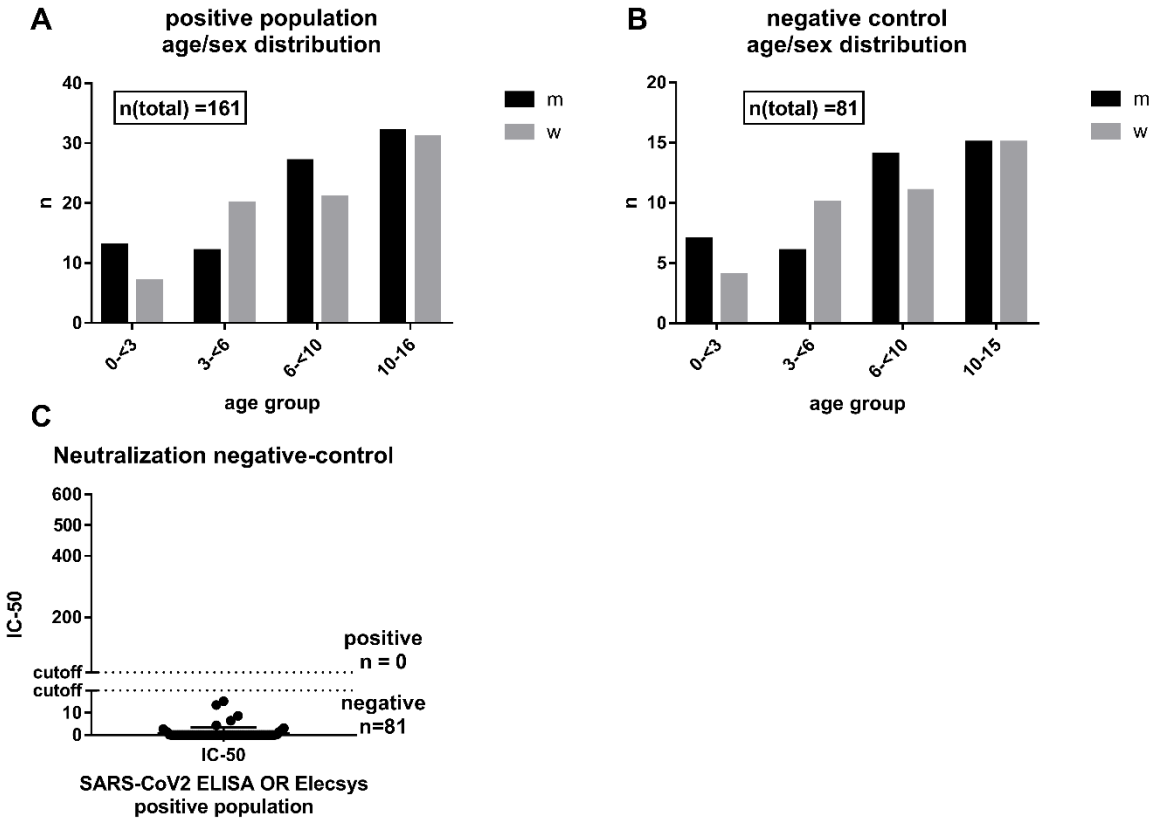

Supplemental Figure 1 Age and sex distribution of A the seropositive population in any test (n=161), B the negative control (n=81; randomly picked based on age and sex of the pos. population) and C the neutralization test result of the negative control (n= 81, all negative)

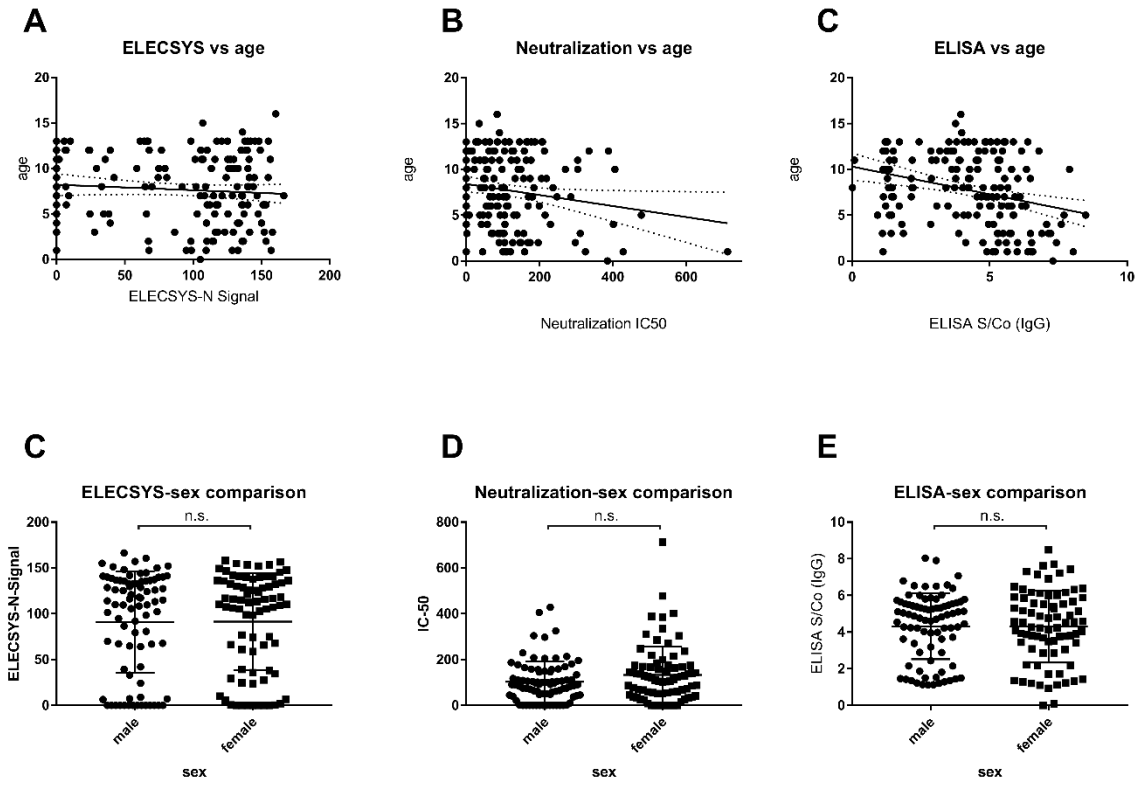

Supplemental Figure 2 Spearman Correlation of A ELECSYS N (S/Co; n.s.; R= -0.05), B Neutralization (IC50; n.s.; R=-0.11) and C SRBD-ELISA (S/Co; n.s.; R=-0.32) with the age of the participants. And comparison of the male and female population (unpaired t-test) for D Neutralization (IC50; n.s.), E SRBD-ELISA (S/Co; n.s.) and F ELECSYS N (S/Co; n.s.)

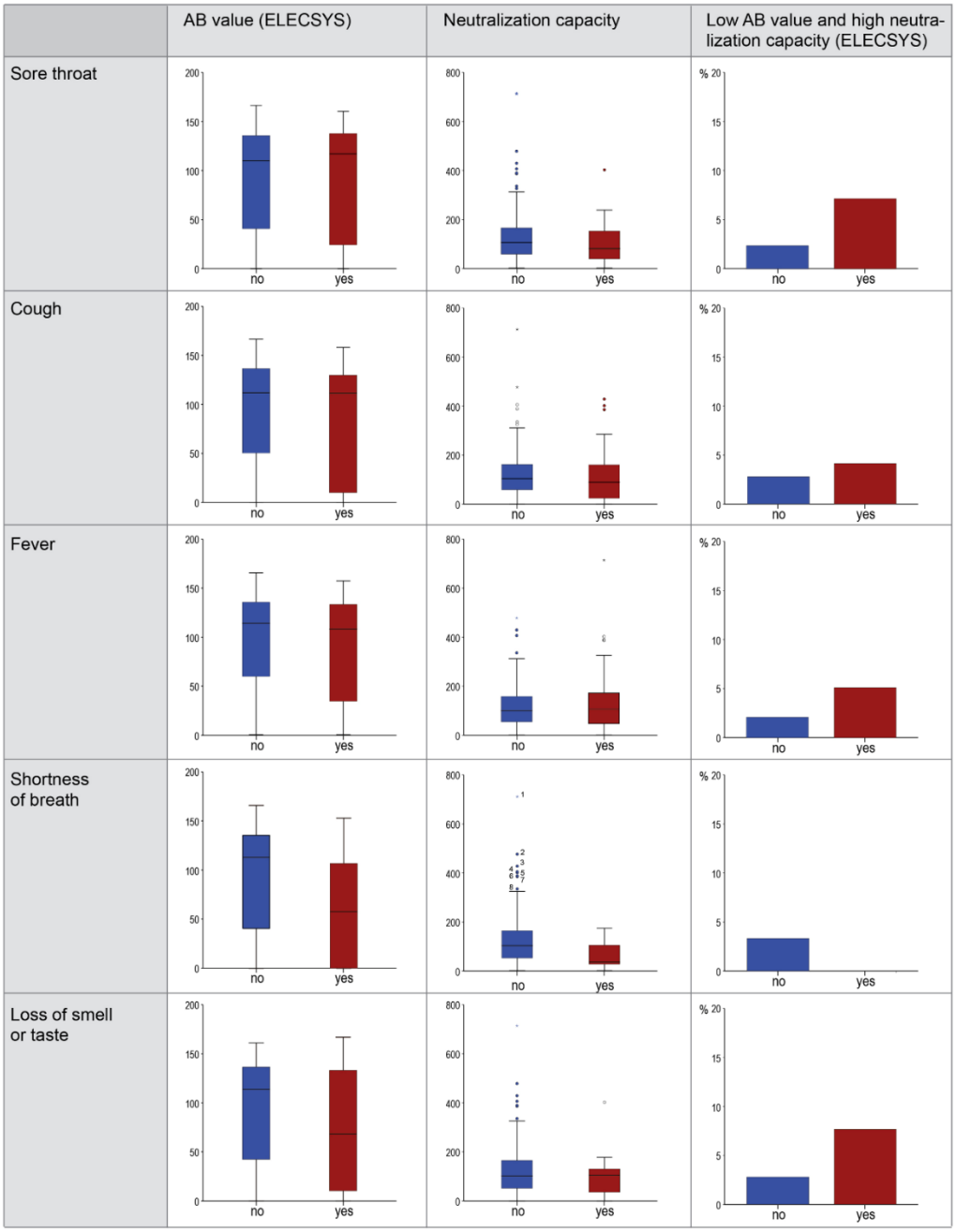

Supplemental Figure 3 Association of Antibody Values, Neutralization Capacity and the Antibody to Neutralization Ratio with Classical Symptoms of COVID19. Legend: AB value (ELECSYS), neutralization capacity and a combined measure of AB value (ELECSYS) and neutralization capacity (ELECSYS >130, neutralization capacity <50) are presented in columns, selected SARS-CoV-2 infection related symptoms are presented in rows. All AB positive children with questionnaire data on symptoms were included in the analyses (N=161/162). T-tests and chi²-tests revealed no statistically significant difference in any of the displayed comparisons.

5.3 Manuscript 2: "Spectrum Bias and Individual Strengths of SARS-CoV-2 Serological Tests-A Population-Based Evaluation"

5.3.1 Abstract

Antibody testing for determining the SARS-CoV-2 serostatus was rapidly introduced in early 2020 and meanwhile is gaining special emphasis regarding correlates of protection. With limited access to representative samples with known SARS-CoV-2 infection status during the initial period of test development and validation, spectrum bias has to be considered when moving from a "test establishment setting" to population-based settings, in which antibody testing is currently implemented. To provide insights into the presence and magnitude of spectrum bias and to estimate performance measures of antibody testing in a population-based environment, we compared SARS-CoV-2 neutralization to a battery of serological tests and latent class analyses (LCA) in a subgroup (n=856) of the larger population based TiKoCo-19 cohort (n=4185). Regarding spectrum bias, we could proof notable differences in test sensitivities and specificities when moving to a population-based setting, with larger effects visible in earlier registered tests. While in the population-based setting the two Roche ELECSYS tests outperformed every other test and even LCA regarding sensitivity and specificity in dichotomous testing, they didn't provide satisfying quantitative correlation with neutralization capacity. In contrast, our in-house ELISA though inferior in dichotomous testing, provided satisfactory quantitative correlation and may thus represent a better correlate of protection. In summary, all tests, led by the two Roche tests, provided sufficient accuracy for dichotomous identification of neutralizing sera, with increasing spectrum bias visible in earlier registered tests, while the majority of tests, except the RBD-ELISA, didn't provide satisfying quantitative correlation.

5.3.2 Introduction

Coinciding with the onset of the SARS-CoV2 pandemic early 2020 there was an urgent and strong quest for serological tests addressing a number of different needs, for example, to determine the number of undetected infections enabling the calculation of infection fatality ratios, to survey virus spread on the population level and also to serve immediate medical needs namely to qualify convalescent plasma for treatment of severely diseased patients. Alongside with others and in order to meet such needs, we established and validated a SARS-CoV-2 ELISA for the detection and quantification of antibodies targeting the receptor binding domain (RBD) of the spike (S) protein for in-house diagnostic use. The assay itself was validated, using sera from the pre-pandemic era to determine test specificity as well as available positive sera, which at that time were derived from PCR positive, symptomatic and partially hospitalized COVID-19 patients to calculate test sensitivity[260]. A similar strategy, though using the SARS-CoV-2 nucleoprotein (N) instead of the spike protein for antibody detection, was applied – like for many other now commercially available SARS-CoV-2 antibody tests – for validation and approval of

the Roche COBAS/ELECSYS SARS-CoV-2-N (nucleoprotein) platform, where 204 samples of 69 PCR-positive patients were tested at various time points, and 5272 pre-December 2019 samples were used to test for specificity[265]. Though various studies and meta-analyses have been carried out comparing different serological tests during the pandemic[266–268], most of these studies used predefined clinical samples relying on pre-COVID-19 and symptomatic/PCR-verified cohorts or other, non-population based sera or convenience samples to derive performance metrics for test accuracy.

Despite being methodologically correct from a laboratory and experimental perspective, such comparative studies may harbor the risk of a potential "spectrum bias", a phenomenon described by Ransohoff and Feinstein already more than 40 years ago when scrutinizing the evaluation process of the accuracy of diagnostic tests[269]. After repeated observations of failure of initially promising new diagnostic tests when introduced in clinical practice, this discrepancy could be attributed to differences in the composition of samples used for test validation and the final target population. Although in statistical theory measures like sensitivity and specificity are population-independent test-specific constants, in biological reality these measures vary between test populations, as often the condition to be detected is not inherently dichotomous[270,271]. Thus, it is crucial to use an appropriate test population, resembling the setting in which the diagnostic test is used in later practice, when evaluating diagnostic tests. Therefore, population-based studies are critically important to determine and compare performance measures like sensitivity and specificity of SARS-CoV-2 antibody assays.

With an increasing number of individuals recovered from COVID-19 and the success of vaccination campaigns, the initial quest for tests accurately determining the serostatus in a dichotomous fashion is currently being complemented by a growing demand for a simple and quantitative surrogate, which can predict protection from infection or disease in convalescent and vaccinees[272]. To avoid any spectrum bias, such surrogates should be validated based on a representative and properly powered set of samples from the population.

The objective of this study therefore was to analyze and to compare different SARS-CoV-2 serological tests in a population-based setting following STARD guidelines[201,273]. Furthermore, we opted to determine the quantitative agreement of the obtained test results with virus neutralization representing the currently best predictive immunological correlate for protection. For didactical reasons we also aimed to highlight the impact of potential spectrum bias on diagnostic performance measures.

5.3.3 Material and Methods

5.3.3.1 Study design & participants

For this retrospective analysis we used a subgroup of the well described population-based TiKoCo-19 study cohort[201]. In brief, a representative sample of 6608 residents of Tirschenreuth aged 14 years and

older, selected by means of a sex- and municipality-stratified random sample, were invited and 4203 (64.27%) fully participated in the study by filling out a questionnaire and giving blood samples. Three independent antibody tests were applied (complete data from 4185 participants) and the "true" serostatus was predicted by latent class analysis, to finally estimate key epidemiological parameters like seroprevalence and infection fatality ratio[201].

Out of these 4185 participants, 432 tested positive for SARS-CoV-2 antibodies in at least one of the three antibody tests and thus were defined as "any-test-positive". As neutralization testing remains time and work intensive, 430 of these, which yielded sufficient material for further testing were analyzed for their age and sex distribution and equivalent number (426) of age- and sex-matched samples were then randomly selected from the remaining "all-tests-negative" participants. Being aware that a reduction of the SARS-CoV-2 antibody negative samples while keeping the positive population constant will induce a bias in the subgroup analysis, we estimated all diagnostic performance measures after applying a reweighting procedure to yield a subgroup for the analysis resembling the full TiKoCo-19 study cohort (n=4185). This weighting technique uses weights inverse proportional to the probability of being included in the subgroup and, in general, will avoid the bias in the estimation of diagnostic performance parameters otherwise encountered[274]. Thus, a final population-based subgroup of n = 856 was defined with the following characteristics: male (n; %) = 410; 48; age (median; range) = 52; 14 – 100.

Of note, by the nature of the study design, it was impossible to assess exact time intervals between SARS-CoV-2 infection and taking blood samples, while epidemiological data from Robert Koch Institute (RKI) strongly suggests that nearly all infections during that first wave in the county of Tirschenreuth happened 2-4 months prior to 1st day of taking blood samples allowing for seroconversion[275]. No timepoint differences have to be assumed between the tests, as all analyses were performed from the same blood sample.

5.3.3.2 "Wetlab"-Methods

5.3.3.2.1 Independence of testing

All serological tests were performed by independent experimentators in a randomized and pseudonymized manner, while the experimentators were blinded for any other test result during testing. Neutralization and COBAS_S was separately performed on the "any-test-seropositive/negative" (ELISA_G; YHLO; COBAS_N) subgroup (**Table 5**; detailed test descriptions below). Experimentators were neither aware which specific test delivered seropositive results nor did they have insight into any quantitative values.

5.3.3.2.2 SARS-CoV-2 in-house SRBD-ELISA

Our validated in-house ELISA detecting IgG (or IgA or IgM) antibody responses to the SARS-CoV-2 spike protein's receptor binding domain (RBD) was performed as described earlier [260]. Results from the different immunoglobulin classes were either used on their own (ELISA_G (IgG); ELISA_A (IgA); ELISA_M (IgM)) or combined to ELISA_GAM using the "believe-the-positive" rule, i.e. only if the results of all three immunoglobulin classes were negative, ELISA_GAM was defined negative. Cutoff values were chosen as published earlier. Test characteristics are shown in **Table 5**.

5.3.3.2.3 Roche SARS-CoV-2 ELECSYS N antibody test

The Elecsys Anti-SARS-CoV-2 test (Roche Diagnostics GmbH, Penzberg, Germany)[276] detecting Nucleoprotein-(N)-directed complete Ig was operated on the Cobas pro e 801 module according to the manufacturer's recommendations. Cutoff values were chosen as specified by the manufacturer. Test characteristics are shown in **Table 5**.

5.3.3.2.4 Roche SARS-CoV-2 ELECSYS S antibody test

The Elecsys Anti-SARS-CoV-2 S test (Roche Diagnostics GmbH, Penzberg, Germany)[277] detecting complete Ig directed to Spike-(S) protein receptor-binding-domain (RBD) was operated on the Cobas pro e 801 module according to the manufacturer's recommendations. Cutoff values were chosen as specified by the manufacturer. Test characteristics are shown in **Table 5**.

5.3.3.2.5 YHLO SARS CoV-2 test

The YHLO SARS CoV-2 test (Shenzhen Yhlo Biotech Co. Ltd., Shenzen, China) detects IgG antibodies to the N- and S-protein and was performed on the iFlash 1800 according to the manufacturer's recommendations. Cutoff values were chosen as specified by the manufacturer. Test characteristics are shown in **Table 5**.

5.3.3.2.6 SARS-CoV-2 neutralization test

SARS-CoV-2 neutralization capacity was evaluated using the Vesicular Stomatitis Virus (VSV-Δ G*FLuc) pseudotyped with SARS-CoV-2-Spike-ΔER [72], which is an established and widely used surrogate for WT SARS-CoV-2 neutralization[209,278](**Supplemental Figure 4**) while providing enhanced (bio)safety. Pseudoviral titers were determined by limited dilution and fluorescence microscopy. For all samples, an inoculum of 25 000 ffu was neutralized with a 2-fold serum dilution series starting at 1/20 dilutions in triplicates for 1 h, and luciferase activity was determined 20 h post infection of HEK293T-ACE2+-cells using BrightGlo (Promega Corp, Madison, USA). IC50 values (50% maximal inhibitory concentration) were calculated using the algorithm: 'log (inhibitor) vs. normalized response' in GraphPad Prism 8

software (GraphPad Software, San Diego, USA). For dichotomous analysis, values above IC50 ≥ 20 were defined positive.

Table 5 Applied antibody tests with manufacturer, test principle, test target, test strategy, antigen, cutoff, sensitivity and specificity as provided by the manufacturer

Manu-facturer	Principle	Target	Abbreviation	Antigen	Time after PCR	Sensi-tivity	Speci-ficity	Ref-erence
in house ELISA	ELISA	IgG; (IgA; IgM)	ELISA_G ELISA_A ELISA_M	Spike-RBD	>10d	96% 92% 98%	99.3%	Peterhoff *et al.* 2021[260]
Roche ELECSYS COBAS	ECLIA	total Ig	COBAS_S	Spike	≥14 d	99.5%	99.8%	IFU*[279]
Roche ELECSYS COBAS	ECLIA	total Ig	COBAS_N	Nucleoprotein	≥14 d	98,81%	99,98%	IFU*[280]
YHLO Biotech	ECLIA	total Ig	YHLO	Nucleoprotein & Spike	not specified	97.3%	96.3%	Wagner *et al.* 2021[201]

*IFU: Manufacurers Instructions For Use

5.3.3.3 Statistical Analysis

5.3.3.3.1 Dichotomized data on serostatus

Data from antibody testing were dichotomized following guidance from the manufacturers' manuals to define serostatus and thereby distinguishing seropositive from seronegative samples for each antibody test separately. Agreement on serostatus between the different antibody testing procedures was quantitatively assessed by estimates of Cohen's kappa, a measure of chance-corrected agreement ranging between 0 and 1 that avoids the pitfall of simply quantifying total agreement percentages[281]. Estimates of Cohen's kappa are accompanied by 95% confidence intervals (CIs) to depict the precision of the point estimates.

The diagnostic performance of single antibody tests is evaluated based on the dichotomized results of the neutralization assay. In addition to quantifying agreement using Cohen's kappa we also estimated sensitivity, specificity and the Youden index combining these two measures of diagnostic performance taking the neutralization assay as the gold standard to define true serostatus. Estimates of these measures are accompanied by 95%-CIs derived by Wilson's method [282].

In a further step we also analyzed the diagnostic performance of model-predicted serostatus derived from various latent class models that use the information from all or subsets of the single antibody tests. Latent class analysis (LCA), a classical modeling approach for discrete data developed more 70 years ago by Lazarsfeld[283], has increasingly been applied during recent decades in the context of infectious disease data when a number of different diagnostic tests but no established gold standard

are available[284]. In general, LCA identifies a set of discrete, mutually exclusive latent (i.e., unobserved) classes based on the observed pattern of a set of categorical variables. The basic idea of LCA in this setting is to treat the unobservable true serostatus as being equivalent to two latent classes (seropositive vs. seronegative) and to relate the observed pattern of antibody test results to it via a statistical model. The model derived from LCA provides an objective way of classifying the partially contradictory pattern of results from antibody testing into the two groups of seropositives and seronegatives. We estimated agreement between LCA classification and dichotomized results of neutralization assays using Cohen's kappa and also sensitivity, specificity and the Youden index taking the neutralization assay as the gold standard for serostatus.

5.3.3.3.2 Raw data on seropositivity

We analyzed the raw (undichotomized) data of the antibody tests to elucidate the correlation structure of the quantitative readouts between different antibody tests. We restricted this correlation analysis to the subsample of seropositives that have been classified seropositive by all four antibody tests as inclusion of seronegatives would bias this analysis. We eliminated three samples where the quantitative value of an antibody test exceeded the upper cutoff defined by the manufacturer leaving a remaining subgroup of 310 seropositives contributing to this analysis. Raw data of the COBAS_S, COBAS_N and YHLO were log-transformed, raw data of the Elisa remained untransformed. Estimates of Pearson's correlation coefficient (accompanied by 95%-CIs) are reported to quantify the strength of a linear association between quantitative test results. Additionally, estimates of Spearman's rank correlation coefficient (accompanied by 95%-CIs) are shown to give a quantitative impression of the strength of a more general monotonous association between test results.

5.3.3.3.3 Illustration of spectrum bias

Our data set for previous analyses comprised a randomly selected (weighted) population-based study group. Thus, the evaluation of the diagnostic performance of a serological testing using different specific procedures avoids spectrum bias that is inherent in many other settings. To illustrate the effect of spectrum bias on measures of diagnostic performance (sensitivity, specificity, Youden index) we generated a selected subgroup for an alternative analysis. The data set for the illustration is constructed by eliminating all 241 observations where the neutralization assay yielded values above 1 but below 100. The remaining sample of 615 observations comprises only clear-cut seronegatives and seropositives and serves as an instructive example of the effects of spectrum bias. We withstood the temptation to vary the exclusion criteria with respect to the width of the interval of values to be excluded in an effort to find a stark example, we only performed our analysis once with the pre-specified eligibility criteria stated above and report the corresponding results.

5.3.3.3.4 Software and tools

The statistical software SAS version 9.4 (SAS Institute Inc., Cary, NC, USA) was used for all computations, and LCA modeling was performed by employing a SAS extension from the Penn State University[285].

5.3.4 Results

5.3.4.1 Agreement between dichotomized serological tests

We compared the dichotomized (seropositive vs. seronegative) results of the different serological tests to assess agreement regarding the identification of the serostatus. Though targeting antibodies to a different antigen (**Table 5**) but using the same test system we found a nearly perfect agreement between the two COBAS tests (κ = 0.96), while both, the IgG ELISA and the YHLO provided very good agreement with both COBAS tests (each κ ~ 0.9) and the YHLO and the ELISA showed a similar degree of agreement (κ = 0.87).

Expectedly, as could be anticipated from earlier reports analyzing the occurrence and durability of IgA and IgG antibody isotypes, the IgA and IgM ELISA on their own showed only weak agreement with every other test (each κ ≤ 0.21), respectively. In an attempt to improve the IgG ELISA's performance, we combined the three ELISAs (G, A, M) with an OR-function, rendering every participant with at least one positive result in any test as seropositive. Though the results were strongly reliant on the IgG ELISA (κ = 0.93), the combination did not improve but rather decreased the overlap with the other tests. (**Table 6**)

Table 6 Agreement of dichotomous (seronegative vs. seropositive) test results within the complete group (n = 856 weighted to n =4185) estimated by Cohen's kappa with 95%-CIs

Kappa 95% KI	COBAS_S	COBAS_N	ELISA_G	ELISA_A	ELISA_M	ELISA_GAM	YHLO
COBAS_S							
COBAS_N	**0.9646** 0.9467; 0.9825						
ELISA_G	**0.9116** 0.8836; 0.9396	**0.9163** 0.8889; 0.9437					
ELISA_A	**0.1916** 0.1395; 0.2438	**0.2097** 0.1560; 0.2634	**0.2114** 0.1559; 0.2669				
ELISA_M	**0.1140** 0.0768; 0.1513	**0.1208** 0.0818; 0.1598	**0.1235** 0.0826; 0.1644	**0.1617** 0.0716; 0.2519			
ELISA_GAM	**0.8488** 0.8129; 0.8847	**0.8579** 0.8230; 0.8928	**0.9262** 0.9006; 0.9519	**0.3216** 0.2707; 0.3725	**0.1298** 0.0928; 0.1668		
YHLO	**0.8853** 0.8537; 0.9170	**0.9146** 0.8868; 0.9423	**0.8741** 0.8405; 0.9076	**0.2402** 0.1823; 0.2981	**0.1225** 0.0794; 0.1657	**0.8116** 0.7719; 0.8513	

5.3.4.2 Relationship between dichotomized serological tests and neutralization

Next, we compared the test results obtained for the individual binding antibody assays with the presence or absence of neutralizing antibodies. The COBAS_S test, designed to detect and quantify antibodies directed towards the ACE-2 receptor-binding-domain (RBD) of the Spike (S) protein, was able to identify neutralizing sera on a near to perfect level as expressed by the Youden Index (J) (J = 0.97) with high sensitivity (97.2%) and specificity (99.7%).

The COBAS_N test scored second best on both parameters resulting in a Youden-Index of 0.94. This was not necessarily expected as N is not presented on the virion's surface and most likely only S-protein directed antibodies exhibit neutralization capacity. The YHLO and the ELISA test showed comparable overall performance (J= 0.85 and 0.88, respectively), whereas the ELISA demonstrated a notable higher sensitivity (89.2% vs 85.3%), and the YHLO exhibited slightly enhanced specificity (99.4% vs 98.9%). While the IgA and IgM ELISA only showed minimal suitability for this issue (both J < 0.2), the combined ELISA data (ELISA_GAM J=0.87) increased test sensitivity to 92.2%. This was, however, on high cost of assay specificity and couldn't further improve the already good ELISA_G estimates (J=0.88) (**Table 7**).

5.3.4.3 Illustration of the effect of spectrum bias on diagnostic performance measure

Since previous studies suggest that hospitalized COVID19 patients yield higher titers of neutralizing antibodies[286], while pre 2019 sera, by definition should not and also in reality have not been found to neutralize SARS-CoV-2 so far, we defined an artificial "establishment sample setting" within our study sample, by defining a subgroup comprising only including participants with a very definite neutralization titer of either IC50 < 1 or >100 (n=615) and normalized those results back to the full cohort (n=4185) for proper comparability.

To illustrate the potential impact of a spectrum bias we compared this "artificial establishment cohort" to the real population-based findings. By this procedure, we found clearly enhanced performance of every test, especially regarding test sensitivity. The highest impact was determined for the YHLO, which gained nearly 10% sensitivity compared to the population-based setting, followed by the ELISA_G (Δ(sens)=9%). The COBAS_N test gained approximately 7 % in sensitivity, with only minor gains in specificity, impressively even reaching 100% sensitivity, while the COBAS_S still gained 2% sensitvity, but nearly no specificity (**Table 7**).

Interestingly, this pattern resembles the time of licensing of the tests, with the biggest gains to be recorded for the earlier licensed tests. Overall, in this artificial setting, all test determinants closely resembled the manufacturer's information (**Table 5**) regarding sensitivity and specificity.

Table 7 Relationship between dichotomized antibody test results and dichotomized neutralization results. For each antibody test Cohen's kappa, sensitivity, specificity and accompanying 95%-CIs as well as the Youden-Index are shown for the complete sub-group (n=856 weighted to n=4185) in the corresponding first row (labelled "all") and for the reduced subgroup (n=615 weighted to n=4185) representing the test establishment setting (only participants with neutralization IC-50 < 1 or >100 included) in the second row labelled "Spectrum".

		Neutralization						
Test	**Cohort**	**Kappa**	**95% CI**	**Sensitivity**	**95%-CI**	**Specificity**	**95% CI**	**Youden-Index J**
COBAS_S	all	0.9719	0.9560; 0.9879	0.9719	0.9496; 0.9845	0.9971	0.9871; 0.9994	0.9690
	Spectrum	0.9961	0.9886; 1.0000	0.9954	0.9737; 0.9992	0.9997	0.9900; 1.0000	0.9951
COBAS_N	all	0.9418	0.9190; 0.9646	0.9386	0.9093, 0.9589	0.9966	0.9862; 0.9991	0.9352
	Spectrum	0.9986	0.9942; 1.0000	1.0000	0.9820; 1.0000	0.9990	0.9888; 0.9999	0.9990
YHLO	all	0.8619	0.8275; 0.8963	0.8526	0.8127, 0.8852	0.9944	0.9830; 0.9982	0.8470
	Spectrum	0.9614	0.9383; 0.9845	0.9587	0.9225; 0.9784	0.9952	0.9824; 0.9987	0.9539
ELISA_G	all	0.8915	0.8607; 0.9222	0.8917	0.8558; 0.9195	0.9894	0.9758; 0.9954	0.8811
	Spectrum	0.9734	0.9543; 0.9926	0.9817	0.9530; 0.9930	0.9914	0.9767; 0.9969	0.9731
ELISA_ GAM	all	0.8736	0.8406; 0.9066	0.9224	0.8905; 0.9456	0.9500	0.9269; 0.9661	0.8724
	Spectrum	0.9206	0.8884; 0.9528	0.9908	0.9664; 0.9975	0.9495	0.9236; 0.9669	0.9403
ELISA_M	all	0.1092	0.0732; 0.1453	0.1043	0.0770; 0.1397	0.9930	0.9809; 0.9975	0.0973
	Spectrum	0.1993	0.1380; 0.2605	0.1651	0.1209; 0.2214	0.9944	0.9812; 0.9984	0.1595
ELISA_A	all	0.2315	0.1805; 0.2824	0.2445	0.2034; 0.2909	0.9667	0.9468; 0.9794	0.2112
	Spectrum	0.3326	0.2595; 0.4058	0.3211	0.2615; 0.3871	0.9627	0.9395; 0.9773	0.2838

5.3.4.4 Relationship between serostatus predicted by latent class modelling and neutralization results

Lacking a suitable gold standard to determine seroprevalence in our population based TiKoCo-19 baseline study, we applied latent class modelling by combining test results derived from the COBAS_N test with the YHLO assay and our in-house IgG ELISA as the best approximation to determine true serostatus. Using our neutralization data as functional reference, we were asking (i) how the LCA performs regarding the identification of neutralizing sera and (ii) whether the performance of the LCA based on initial criteria can be further improved by adding data from additional serological tests (e.g. COBAS_S; ELISA IgM (ELISA_M) and IgA (ELISA_A)) to the LCA analysis. The first LCA-model (LCA1)

mimicked the model used in the TiKoCo-19 baseline study and provides a very good prediction of the presence of neutralizing antibodies (J = 0.913). Whereas the inclusion of ELISA_A and M results per se did not influence the model's parameters at all (data not shown), the replacement of ELISA_G by ELISA_GAM was able to minimally improve the model's performance (LCA2; J = 0.915).

As the Roche COBAS_S wasn't available in June 2020 when the baseline study was conducted, we couldn't include its results at the time of the TiKoCo-19 baseline study. Whilst now we found a noticeable improvement of the baseline model (LCA1) when including this test in the latent class modelling of the subgroup (LCA3) (J = 0.946). Again, as for the above, including the IgA and IgM ELISA data in any combination couldn't further improve the model at all (LCA4&4b, J = 0.946) (**Table 8**). This is expected since the IgM ELISA due to early occurrence of IgM antibodies is only sensitive in an early time-interval after infection and thus not suited to predict general seropositivity[287].

Interestingly, comparing the best-in-class LCA model (**Table 8**, LCA3) with the best-in-class individual test (**Table 7**, COBAS_S), the performance regarding assay sensitivity and specificity turned out to be similar. In conclusion, the COBAS_S test provided the most feasible surrogate for the dichotomous antibody detection in neutralizing sera. Prediction of serostatus by latent class modelling incorporating further serological tests could not improve the performance of the single COBAS_S test.

Table 8 Agreement of seropositivity determined through various LCA-models and dichotomized neutralization results within the complete group (n = 856 weighted to n =4185). Shown are: Tests included in the model, Cohen's kappa, sensitivity, specificity and Youden-Index accompanied by 95%-CIs

					Neutralization				
	included in Model	**Kappa**	**95% CI**	**Sensitivity**	**95% CI**	**Specificity**	**95% CI**	**Youden-Index**	**95%-CI**
LCA 1*	ELISA_G; Cobas_N; YHLO	0.9220	0.8958; 0.9483	0.9152	0.8822; 0.9395	0.9976	0.9879; 0.9995	0.9128	0.8701; 0.9390
LCA 2	ELISA_GAM; Cobas_N; YHLO	0.9244	0.8985; 0.9503	0.9178	0.8852; 0.9417	0.9976	0.9879; 0.9995	0.9154	0.8731; 0.9412
LCA 3	ELISA_G; Cobas_N; YHLO; Cobas_S	0.9514	0.9305; 0.9722	0.9491	0.9216; 0.9672	0.9968	0.9866; 0.9993	0.9459	0.9082; 0.9665
LCA 4**	Elisa_GAM; Cobas_N; YHLO; Cobas S	0.9514	0.9305; 0.9722	0.9491	0.9216; 0.9672	0.9968	0.9866; 0.9993	0.9459	0.9082; 0.9665

* Identical to model LCA 2b: Elisa_G, Elisa_A, Elisa_M, Cobas_N, and YHLO

** Identical to model LCA 4b: Elisa_G, Elisa_A, Elisa_M, Cobas_N, Cobas S and YHLO

5.3.4.5 Correlation of quantitative serological test results and neutralization

In view of globally ongoing vaccination campaigns, emerging variants of concern and the desire of our societies, opinion leaders in economy and politics to relief restrictions and return “back to normal”, there is an increasing quest for feasible surrogates to predict protection from infection or disease. Whilst the levels of neutralizing antibodies currently represent the best correlate of protection, such assays are cumbersome to conduct, low to medium throughput, time consuming and expensive. The quantification of binding antibodies might represent a feasible surrogate, provided the quantitative date show a sufficiently good correlation.

Herein, we used Pearson’s correlation coefficients to evaluate quantitatively the association between test results for binding antibodies and neutralization, respectively. This analysis proved a satisfactory correlation between the two tests designed to quantify the levels of antibodies binding to the ACE-2 receptor-binding domain (RBD) of the S protein (ELISA_G; COBAS_S; R=0.74) as well as for the two N-based readouts (COBAS_N; YHLO; R=0.77). As expected, since they test for different antigen-targets, we couldn’t find a sufficient correlation between the S and the N based tests, though the YHLO-test claims to include Spike antibodies as a target, which results in a slightly better correlation coefficient to the ELISA_G and the COBAS_S as compared to the COBAS_N (R (YHLO-ELISA) = 0.56; other R < 0.5). Comparing the levels of binding antibodies quantified by the various serological tests to virus neutralization (IC50), we found a satisfactory correlation of the S-RBD-ELISA with neutralizing antibodies (R=0.65), followed by an only moderate correlation of the COBAS_S (R=0.53), while both, YHLO and COBAS_N showed only minor quantitative correlation to the determined IC50 values (R<0.5) (**Figure 11**). Off note, the COBAS_N is not registered for quantitative readout and measurements often provided maximum reads, which may have negatively impacted correlations calculated for that test with other assays. We further investigated for non-linear monotonic associations, by using Spearman correlations, which overall didn’t lead to different results (**Supplementary Table 2**).

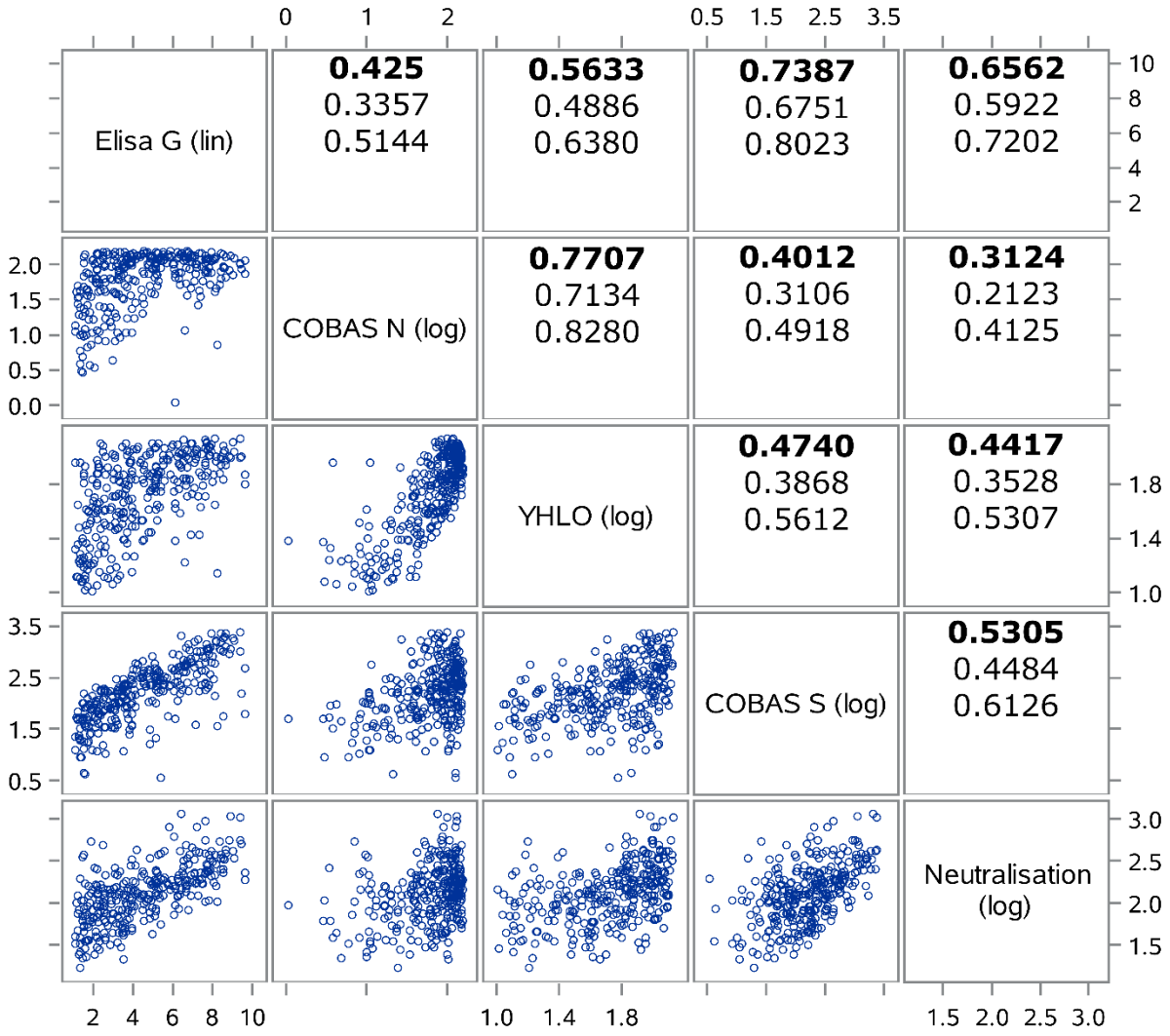

Figure 11 Scatterplot matrix of correlation between the different positive test results using logarithmic results for ECLIA based tests and neutralization. Also shown are Pearson correlation coefficients (bold type, 95%-CIs in the two rows below) to quantify the magnitude of linear association between antibody tests and neutralization within the subgroup (n = 310) where all tests (ELISA_G, COBAS_N, COBA_S; YHLO; neutralization) were positive. (Further experimental inclusion constraints: COBAS_S ≤ 2500; ELISA_G ≤ 15; Neutralization IC_{50} ≤ 2560).

5.3.5 Discussion

While PCR testing is still the reference to identify acute COVID-19 cases[288], serological testing is widely used in epidemiological studies to gather information on the dynamics of the pandemic[289], regarding the impact of political and health care measures, the number of undetected infections, the infection fatality ratio[201] or even identification of high antibody-titer convalescent sera for the treatment of severe COVID cases[266,290]. Manufacturers' information on test performance relies on the composition of the test population that was available at the time of development and validation of these tests. While pre-pandemic sera were used to determine test specificity, test sensitivity was presumably evaluated based on - at that time - available samples of symptomatic and in part hospitalized COVID-19 cases with positive PCR tests largely missing e.g. asymptomatic infected. Based on such a

composition of the test population in this “test establishment and validation setting” – which is fundamentally different from a population-based setting in which these serological tests are later on applied any statement on test performance is prone to spectrum bias. Our results demonstrate that spectrum bias is not only a theoretical threat to the validity of manufacturers’ initial claims on test performance. An unbiased assessment of the properties of serological tests in identifying neutralizing capacity in a population-based setting yields slightly less perfect but still remarkably good test performance of these assays.

A new scope of application of serological testing is gaining increasing importance. With the ongoing SARS-CoV-2 vaccine programs worldwide, there is an increasing need for surrogate markers providing information to predict protection from reinfection or at least severe COVID-19 following natural infection and vaccination[291,292]. Therefore, we compared five serological assays not only with regard to dichotomized test accuracy but also analysed the degree of quantitative correlation with neutralizing capacity.

Regarding dichotomized results, the two COBAS assays proved superior to every other assay and delivered test results with a high accuracy. Therefore, both Roche assays can be proposed as a gold standard for dichotomous testing in a population-based setting. Our population-based results contradict the earlier findings by others reporting a sensitivity of 76% and non-determinable specificity for the COBAS_N based on convenience samples[293]. As those findings also strongly differ from the manufacturer’s information[294], one might attribute those results to assessed timepoints or cohort composition. All of our findings regarding sensitivity and specificity settle completely in line to larger metaanalyses attributing a general sensitivity of approximately 80 to 90% as well as a specificity of well over 95% to ELISA and CLIA based assays[267,288].

Comparing different tests to each other, we found similar concordance of our ELISA_G with the COBAS_N, whereas those previous findings also suggested high comparability of our ELISA_G with the commercially available Euroimmun test[268]. In contrast to others reporting lower agreement for the COBAS_S with neutralization[295], we found a high concordance of the COBAS_S with neutralization, in line with the manufacturers statement in the IFU [296] and also in agreement with others comparing COBAS_S to ACE-2 Inhibition as a surrogate for neutralization[297]. This might be attributed e.g. to higher sensitivity of our luciferase-reporter based neutralization assays as compared to a neutralization assay relying on a cytopathic effect as readout [295].

Regarding the quantitative effects of spectrum bias, we could show small to midrange decreases in both sensitivity and specificity of all tests, when moving from our artificial, “test establishment setting” to a population-based setting, while the earlier admissioned tests recorded the higher benefits in comparison to newer tests. This reflects the logical assumption that in the beginning of 2020 only

limited access to positive sera was given[265], while later on manufacturers were able to utilize a more diverse pool of samples for determining assay performance[298].

That said, the impact of spectrum bias should definitely be considered in future population-based approaches, especially, when results are reliant on a single test. While in the past we applied latent class analysis comprising several different tests to determine the seroprevalence in our study population [201], we couldn't show in this analysis any advancement of predicting serostatus from our LCA models as compared to the best single test in this study, thus rendering the LCA approach obsolete in this situation. Nonetheless, in the absence of a golden standard and without prior information on the actual and/or relative performance of different available tests, LCA can still provide a good opportunity to define epidemiological seroprevalence.

With international standardization of protective correlates on the horizon[292], quantitative readouts and the scope of their statement are gaining importance. Though only a surrogate, the SARS-CoV-2-VSV pseudovirus assay first introduced by Hoffmann et al. [73] as well as the lentiviral pseudotype system used by many others and us were found to correlate very well with real virus SARS-CoV-2 neutralization, while providing enhanced biosafety and throughput[209,278]. In contrast to the dichotomous assessment of the various tests with regard to their sensitivity and specificity, where the Roche COBAS_S as well as the Roche Cobas_N test behaved really well, both assays couldn't provide a sufficient quantitative correlation to neutralization IC50s, and also the YHLO test didn't reach satisfying correlation. Regarding the COBAS_S test, others found in agreement with this study a significant connection of dichotomous COBAS_S results with neutralization, but also in their hands the quantitative correlation between binding antibodies and virus neutralization proved to be not sufficiently good[295].

Overall, only the S-RBD-ELISA provided a satisfactory quantitative correlation, in the same ballpark as others found, with quite comparable assay formats such as the Euroimmun ELISA [266] or in house S-RBD-CLIA tests[299]. Consequently the S-(RBD)-ELISA formats such as e.g. our in-house assay or commercially available Euroimmun- or Diasorin-tests are, amongst the analyzed tests, best suited to predict neutralization capacity and thus possibly for protection from infection or disease.

5.3.6 Conclusion

Whilst all used serological assays provide a solid test result for SARS-CoV-2 antibody seropositivity, the two Roche assays (ELECSYS anti-SARS-CoV-2 S&N) outperformed every other test in terms of identifying neutralizing sera. Regarding quantitative readouts, only our in-house ELISA yielded satisfactory correlation to neutralization and thus to a predictive parameter of protection. In terms of a potential spectrum bias during validation of assays with inpatient material we could show that a reconsideration of assay performance is necessary when moving from strictly defined clinical samples to a population based setting, as otherwise estimates of specificity and sensitivity derived in such "test establishment settings" are biased upwards.

5.3.7 Appendix & Declarations

Author Contributions: Conceptualization, R.W., O.G., D.P., S.E., K.Ü; Data curation, S.E., D.P., S.B., R.W., O.G.; Formal analysis, S.E., D.P., A.P. and O.G.; Funding acquisition, R.W. and K.Ü.; Investigation, S.E., D.P., S.B., H.H.N., P.S., R.B.; Methodology, S.E., D.P., A.P., O.G., R.W.; Project administration, R.W. and K.Ü.; Resources, R.W., R.B., I.M.H., O.G., and K.Ü.; Software, O.G., A.P., F.G., S.E.,; Supervision, R.W., D.P., O.G., and K.Ü.; Validation, R.W., D.P., O.G.; Visualization, S.E., O.G.; Writing—original draft, O.G. and S.E.; Writing—review & editing, R.W., D.P., S.E. , O.G., K.Ü.. All authors have read and agreed to the published version of the manuscript.

Funding: This work was supported by the Bavarian States Ministry of Science and Arts (StMWK; grant to R.W and K.Ü.) as well as by the National Research Network of the University Medicine (NUM; applied surveillance and testing; B-FAST) to KÜ and RW. The funders had no role in study design, data collection and analysis, decision to publish, or preparation of the manuscript.

Institutional Review Board Statement: The TiKoCo study was approved by the Ethics Committee of the University of Regensburg, Germany (vote 20-1867-101) and adopted by the Ethics Committee of the University of Erlangen (vote 248_20 Bc). The study complies with the 1964 Helsinki Declaration and its later amendments. All participants provided written informed con[299]sent.

Informed Consent Statement: Informed consent was obtained from all subjects involved in the study.

Data Availability Statement: All authors declare that data and materials will be made available according to the guidelines of the journal.

Acknowledgments: We are particularly grateful to all the study participants. We would like to thank the office staff and numerous students of the University of Regensburg and the University Erlangen as well as the employees of the Bavarian Red Cross, the members of the civil protection, the county office, and the public health office of county Tirschenreuth, respectively, for their tremendous support. We are also grateful to Christine Wolff from wECARE and Jakob Niggel from MaganaMed for providing questionnaires and the database for the baseline-study. Furthermore we would like to thank Stephan

Pöhlmann for providing the VSV ΔG pseudovirus system and Janine Kimpel for providing their ACE-2 and SARS-CoV-2 Spike expressing cell-line.

Conflicts of Interest: The authors declare that no competing interests or conflicts of interest exist. The authors have no financial or proprietary interests in any material discussed in this article. The funders had no role in the design of the study; in the collection, analyses, or interpretation of data; in the writing of the manuscript, or in the decision to publish the results

5.3.8 Supplementary Materials

The following are also available online at https://www.mdpi.com/article/10.3390/diagnostics11101843/s1.

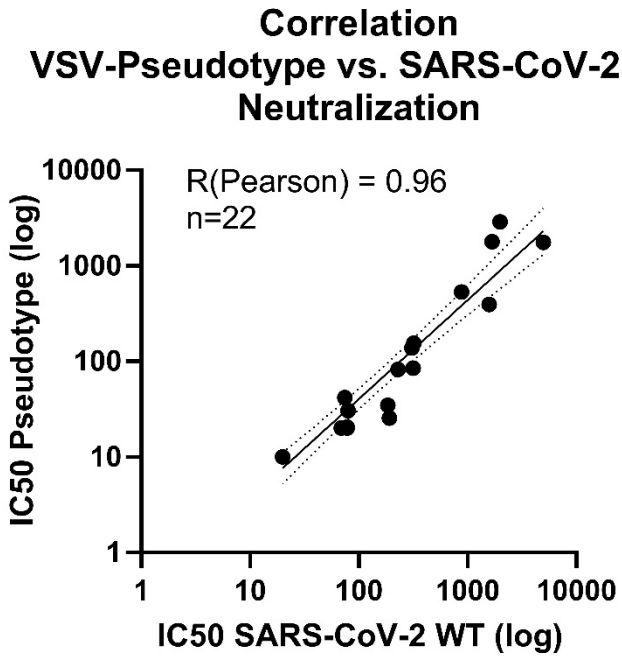

Supplemental Figure 4 Correlation of VSV pseudoviral versus SARS-CoV-2 neutralization (as described in (1)) for n=22 sera (Pearson R=0.96)

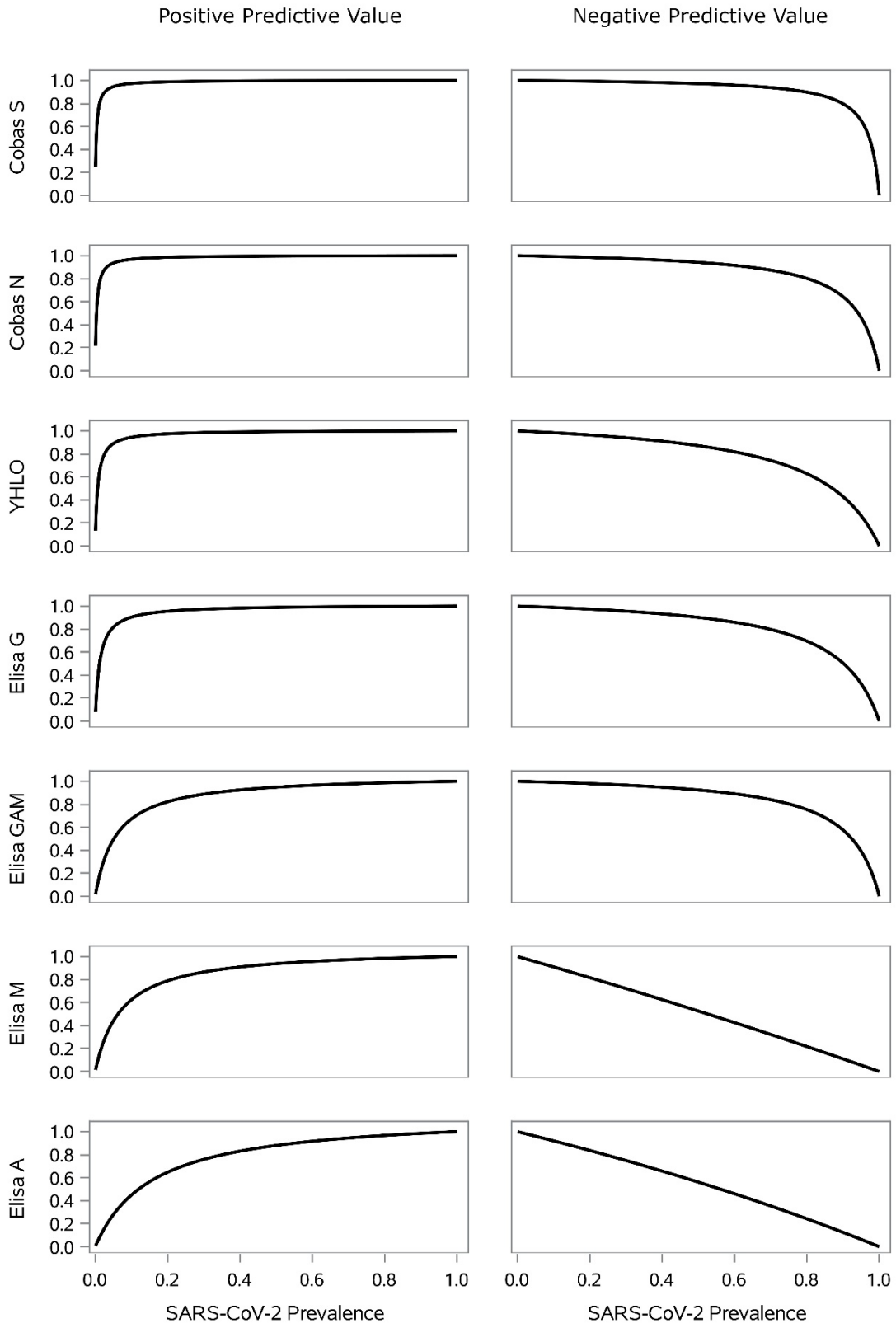

Supplemental Figure 5 Model of positive and negative predictive values of each serologicial assay with respect to seroprevalence

Supplementary Table 2 Spearmans rank-correlation coefficients of serological assays and neutralization, within in all tests (ELISA_G, COBAS_N, COBA_S; YHLO; Neutralization) positive population (n = 310) to quantify general monotonous connection with 95% CI. (Further experimental inclusion constraints: COBAS_S ≤ 2500; ELISA_G ≤ 15; Neutralization IC50 ≤ 2560)

Spearman 95% CI	COBAS_S (log)	COBAS_N (log)	Elisa_G (lin)	YHLO (log)	Neutra-lization (log)
COBAS_S (log)					
COBAS_N (log)	**0.3667** 0.2692; 0.4641				
Elisa_G (lin)	**0.7714** 0.7136; 0.8291	**0.4256** 0.3316; 0.5196			
YHLO (log)	**0.4903** 0.4036; 0.5770	**0.7323** 0.6764; 0.7882	**0.5772** 0.4988; 0.6555		
Neutra-lization (log)	**0.5300** 0.4451; 0.6148	**0.3028** 0.2039; 0.4017	**0.6592** 0.5872; 0.7312	**0.4658** 0.3760; 0.5555	

5.4 Manuscript 3: "Time Trend in SARS-CoV-2 Seropositivity, Surveillance Detection- and Infection Fatality Ratio until Spring 2021 in the Tirschenreuth County-Results from a Population-Based Longitudinal Study in Germany"

5.4.1 Abstract

Herein, we provide results from a prospective population-based longitudinal follow-up (FU) SARS-CoV-2 serosurveillance study in Tirschenreuth, the county which was hit hardest in Germany in spring 2020 and early 2021. Of 4203 individuals aged 14 years or older enrolled at baseline (BL, June 2020), 3546 participated at FU1 (November 2020) and 3391 at FU2 (April 2021).

Key metrics comprising standardized seroprevalence, surveillance detection ratio (SDR), infection fatality ratio (IFR) and success of the vaccination campaign were derived using the Roche N- and S-Elecsys anti-SARS-CoV-2 test together with a self-administered questionnaire. N-seropositivity at BL was 9.2% (1st wave). While we observed a low new seropositivity between BL and FU1 (0.9%), the combined 2nd and 3rd wave accounted for 6.1% new N-seropositives between FU1 and FU2 (ever seropositives at FU2: 15.4%). The SDR decreased from 5.4 (BL) to 1.1 (FU2) highlighting the success of massively increased testing in the population. The IFR based on a combination of serology and registration data resulted in 3.3% between November 2020 and April 2021 compared to 2.3% until June 2020. Although IFRs were consistently higher at FU2 compared to BL across age-groups, highest among individuals aged 70+ (18.3% versus 10.7%, respectively), observed differences were within statistical uncertainty bounds. While municipalities with senior care homes showed a higher IFR at BL (3.0% with senior care home vs. 0.7% w/o), this effect diminished at FU2 (3.4% vs. 2.9%). In April 2021 (FU2), vaccination rate in the elderly was high (>77.4%, age-group 80+).

5.4.2 Introduction

Despite a slight relief in new SARS-CoV-2 infections in summer 2020 following the 1st wave and several highly effective vaccines becoming available[37,40,43], most European countries including Germany were facing new waves of infections from autumn 2020 till now and emerging variants of concern, namely alpha[300] , delta [301], and omicron[302,303].

Early during the SARS-CoV-2 pandemic, multiple population-based cross-sectional seroprevalence studies have been initiated across the globe in order to calculate the proportion of undetected infections and the infection fatality ratio (IFR)[304]. The ratio of actual infections to the number of registered infections is a measure of the surveillance success (surveillance detection ratio, SDR) and differs between populations and age groups, e.g. due to the intensity of testing and symptom severity[201]. The IFR is a hallmark of the severity of the pandemic and one of the prime reasons for containment measures. IFR has been shown to depend substantially on age[304] and the extent that the

particularly vulnerable part of the population, like senior care home residents, were included[201]. An upper bound for the IFR is the case-fatality-ratio (CFR) derived from the proportion of registered COVID-19 deaths to registered infected. As long as registered infected underreport the true number of infected, the CFR is an overestimate of the IFR.

SDR and IFR are highly relevant as key metrics to guide and judge political action such as testing strategy, containment measures, and vaccination campaigns. To understand changes over time, longitudinal studies investigating a defined group of individuals (cohort) over time are required to adequately address the longitudinal dynamic in SDR and IFR.

However, systematic longitudinal seroprevalence studies reporting interval-related incidences of new infections, SDR, and IFR are scarce. Most studies assessing population-based seropositivity over time repeat cross-sectional analyses at consecutive time points in different panels, focus on the increase in total seroprevalence and rarely report IFRs[32,305–307]. For Germany, the Robert-Koch Institute (RKI, CDC equivalent) reports 26 population-based cross-sectional seroprevalence studies in Germany in mostly low-incidence populations[308–310], selected hotspots[311] or distinct subgroups[261,312–314]. On top there is the recently pulished, federal state wide SaarCoPS study[315] which thoroughly assessed key metrics during the first wave. Only two studies included serial assessments over time. The KoCo19 study 16 assessed households longitudinally between Nov 2020 until Oct 2021. MuSPAD, the "Multilocal and Serial Prevalence Study of Antibodies against SARS-2 Coronavirus" provided estimates of seropositivity, SDR, and IFR across different regions for up to 2 time points, but for different panels of individuals, which hampers the comparison over time (serial study, between July 2020 and May 2021)[307]. While SaarCoPS rather focused on the influence of various tests on key metrics than on different time points.[315] In addition to the above-mentioned metrics, population-based longitudinal studies can also provide important insights with regard to infection- and vaccine-induced immunity over time[316].

Results of longitudinal population-based studies are impacted e.g. by triggering events or regional differences in the infection intensity. KoCo19, SaarCoPS and also MuSPAD for example describe serology-based metrics in populations with low incidence during the first wave in spring 2020, and so far only MuSPAD has computed SDRs and IFRs for multiple time points capturing also the rising infections in winter 2020/21.

We thus set out to investigate the time trend in SARS-CoV-2 seropositivity, seroconversion from positive to negative, SDR and IFR over time in the Tirschenreuth county in Northeastern Bavaria, Germany. Tirschenreuth was one of the hardest hit counties in Germany during the 1st wave in spring 2020[317,318] and in early 2021 (combined 2nd and 3rd wave caused by the SARS-CoV-2 wild type variant D416G and the alpha variant). For this, we conducted two follow-up investigations in November 2020 and April 2021 (FU1, FU2, respectively) in our established seroprevalence cohort study with baseline

assessment in June 2020[201]. We invited >4100 study participants aged 14 to 102 years for these two follow-up blood draws in the same fashion as for baseline and yielded measured N- directed SARS-CoV-2 antibodies of up to three time points. We also measured S-directed antibodies for the same individuals and time points to compare S-test with N-test derived seropositivity and seronegativity. Since vaccination started in Germany at Dec 27th, 2020, our S-test measurements provide additional insights into vaccination rates at FU2.

5.4.3 Material and Methods

5.4.3.1 Cohort design, inclusion criteria, and study program

The cohort at baseline (BL) was described in detail in Wagner et al. 2021[201]. In brief, 4203 randomly selected inhabitants of Tirschenreuth aged 14 years or older participated in the baseline survey of the TiKoCo study (response rate: 64.3%). Study participants came to the study center or requested a visit at home between June, 28th and July 13th 2020.

For the longitudinal follow-up (FU), 4173 of the 4203 BL participants who had agreed to be re-contacted were reinvited for a second (November 16th to27th, 2020; FU1) and third blood sampling (April 19th and 30th, 2021; FU2) in the same fashion as for BL assessment[201]: Handicapped or otherwise immobile participants (n=112 and 79 at FU1 and FU2, respectively) were visited at home; invited individuals with flu-like symptoms were asked to stay at home and use the installed hotline to arrange an appointment for a home visit. At BL, FU1, and FU2, participants were asked to provide blood (5.7ml) and to fill out a questionnaire (see below).

The TiKoCo study was approved by the Ethics Committee of the University of Regensburg, Germany (vote 20-1867-101) and adopted by the Ethics Committee of the University of Erlangen (vote 248_20 Bc). The study complies with the 1964 Helsinki declaration and its later amendments. All participants provided written informed consent.

5.4.3.2 Data on registered COVID-19 related deaths, registered infected, and Tirschenreuth county inhabitants

From local health authorities, we obtained sex-, age- and municipality-specific numbers of COVID-19 related deaths and registered infections. The number of inhabitants of the Tirschenreuth county, by sex, age-groups, and municipalities, were obtained by the municipal administration (as of Dec 2019). For the Tirschenreuth county population, we assumed a steady state, i.e. a similar number of inhabitants and sex- and age-group distributions across years. We also derived the number of Tirschenreuth county inhabitants living in a care home as well as respective COVID-19 related deaths and registered cases by the county administration.

5.4.3.3 Observation periods

Our longitudinal seroprevalence study consisted of three observation periods: (i) from pre-pandemic until BL blood draw; (ii) between BL and FU1 blood draw; (iii) between FU1 and FU2 blood draw.

To define precise observation periods for registered COVID-19 cases and COVID-19 deaths, the time interval from first symptoms to seroconversion was assumed to be 12 days[319], from first symptom to registration as COVID-19 case with the RKI 8 days[320] , and from first symptoms to COVID-19 associated death 16 days[321]. The cut-off date for registered COVID-19 cases and COVID-19 associated deaths were therefore defined as the fourth day prior to the median day of sampling and the fourth day after the median day of sampling, respectively.

This resulted in the following observation periods for registered COVID-19 cases: observation period 1 (until BL): Februar 1st to Juli 4th, 2020; observation period 2 (BL to FU1): July 5th to November 18th, 2020; observation period 3 (FU1 to FU2): November 19th to April 21st, 2021. The observation periods for COVID-19 associated deaths were February 1st to July 12th 2020, July 13th to November 26th, 2020, and November 27th to April 29th, 2021, respectively.

5.4.3.4 Assessment of educational status, comorbidities, self-reported previous infections, and vaccination status

A questionnaire was designed and administered at BL as previously described[201] and analogously administered for FU1 and FU2. In brief, the self-administered questionnaire was sent out with the invitation and collected at the study center (or at home), with the possibility of personal counseling by trained staff in case of questions. At BL, participants were asked if they had been tested for SARS-CoV2, whether the test was positive, which current diagnoses of chronic diseases they had, which school and further education they had undergone, and whether they were living in a care home. At FU1 and FU2, participants were further asked with regard to testing, if tested positive since last visit, and with regard to existing chronic disease diagnoses. At FU2, individuals were also asked about the number of received vaccinations, including respective date(s) and type(s).

5.4.3.5 Blood sampling, transport and antibody measurements

Blood sampling and transport of samples was performed as previously described 9. In brief, after blood drawal by qualified study personnel into a barcoded serum monovette (Sarstedt AG Co.KG, Nümbrecht, Germany), the serum sample was processed on the same day. To assess SARS-CoV-2 antibodies, we used an Elecsys Anti-SARS-CoV-2 N test (Roche Diagnostics GmbH, Penzberg, Germany) detecting nucleoprotein-(N)-directed complete Ig as well as the Elecsys Anti-SARS-CoV-2 Spike test (Roche Diagnostics GmbH, Penzberg, Germany) detecting Spike-protein (receptor-binding-domain; RBD) directed complete Ig (referred to as “N-test” and “S-test”, respectively). Both tests were operated on the Cobas pro e 801 module. Sensitivities and specificities provided by the manufacturers in the

instructions for use are 99.5% and 99.8%, respectively, for the ELECSYS anti-SARS-CoV-2 N (Roche Diagnostics) or 98.8% and 99.98% for the ELECSYS an-ti-SARS-CoV-2 S (Roche Diagnostics). We decided to focus our follow-up analyses on these two Roche, ELECSYS tests because: in the BL analysis, we observed that ELECSYS N results were most in line with the results from latent class modeling using information from three antibody tests, including the YHLO and our in-house SRBD-ELISA[201,260]; ELECSYS S test provided excellent concordance with a latent class model and neutralization as published earlier[322]. Finally, the use of these two tests also enabled the discrimination of serostatus resulting from infection versus vaccination. Test results were also reported to study participants to incentivise participation in the study.

5.4.3.6 Statistical analysis

From these longitudinal analyses, we excluded 17 individuals without successful N-test measurement at BL and 33 and 17 individuals without successful N-test measurements at FU1 or FU2, respectively (**Figure 12**). We compared BL characteristics of FU1 and FU2 participants with those of drop-outs, using a t-test or Chi-square test (judged at 5% significance level).

For each of the three observation periods (until BL, BL to FU1, FU1 to FU2), we computed the % new seropositives in the study sample using the anti-SARS-CoV-2 N-test to estimate the probability of a participant to be seropositive at the end of the observation period given that the person was seronegative at the end of the previous observation period (i.e. at risk for seroconversion into positive): (i) % (new) seropositives at BL as the number of seropositives at BL divided by all participants with N-measurement at BL, (ii) % new seropositives at FU1 (compared to BL) as the number of individuals seropositive at FU1 AND seronegative at BL divided by the number of seronegatives at BL, and (iii) % new seropositives at FU2 (compared to FU1) as the number of individuals seropositive at FU2 AND seronegative at FU1 divided by the number of seronegatives at FU1 (restricted to those with N-test available at FU2). We did this overall, by sex and by age-groups.

Given the time points of BL, FU1 and FU2 at June 2020, November 2020, and April 2021, these % new seropositives reflect the % infected during the 1st wave until Juli 2020, during the low incidence period in summer 2020, and during the 2nd/3rd wave of autumn/winter 2020/21, respectively. Of note, the total seropositivity at FU2 does not reflect the % infected until FU2, if individuals seroconverted from positive to negative.

The total % seropositives at a specific time point, t, can also be derived in a sequential approach: let t=1, 2, 3 for BL, FU1 and FU2, respectively; t=0 reflects the time before the pandemic. The probability (P) for a person to be seropositive at time t can be written, according to Bayes' theorem as

*P(seropos. at t) = P(seropos. at t | seroneg. at t-1) * P(seroneg. at t-1) +*

*P(seropos. at t | seropos. at t-1) * P(seropos at t-1),*

with P(seropos at t=0)=0. The probability P(seropos. at t | seroneg. at t-1) can be estimated from serology data as the % new seropositives in the time period between t-1 and t (assuming the number of seroconverters from positive to negative within the time period t—1 to t to be few and thus negligible). Accordingly, 1- P(seropos. at t | seropos. at t-1) is reflected by the % new seronegatives (i.e. the seroconverters from positive to negative). Thus, the sequential approach to derive the % total seropositivity can be derived as

*% total seropos. (at t) = % new seropos (t-1 to t) * (100%-%total seropos(at t-1)) +*

(100%- % new seroneg(t-1 to t)) %total seropos (at t-1).*

The % ever seropos. until t includes the individuals seroconverting from positive to negative and can be approximated by

*% ever seropos. (at t) = % new seropos (t-1 to t) * (100%-%total seropos(at t-1)) +*

%total seropos (at t-1).

The % ever seropos. until FU1 or FU2 are thus an estimate of the % infected until FU1 or FU2, respectively that can't be estimated based on the cross-sectional data of FU1 or FU2 alone. In contrast, the % total seropositives (at t) can in principle be estimated based on cross-sectional data as the fraction of seropositives at the respective time point. However, the sequential estimation approach has a considerable advantage: usually, study participants in a longitudinal seroprevalence study are informed of their antibody status after each study time point. However, knowledge of the test result may have an effect on future willingness to participate at follow-up assessments. For example, if a study participant only learns of a previous infection through a positive antibody test and wishes to have this result confirmed in a later assessment. In this case, the cross-sectional estimate of % total seropositives (at t) can be substantially biased. The sequential approach can still yield unbiased estimates when participation at follow-up assessments is associated with antibody status at previous time points.

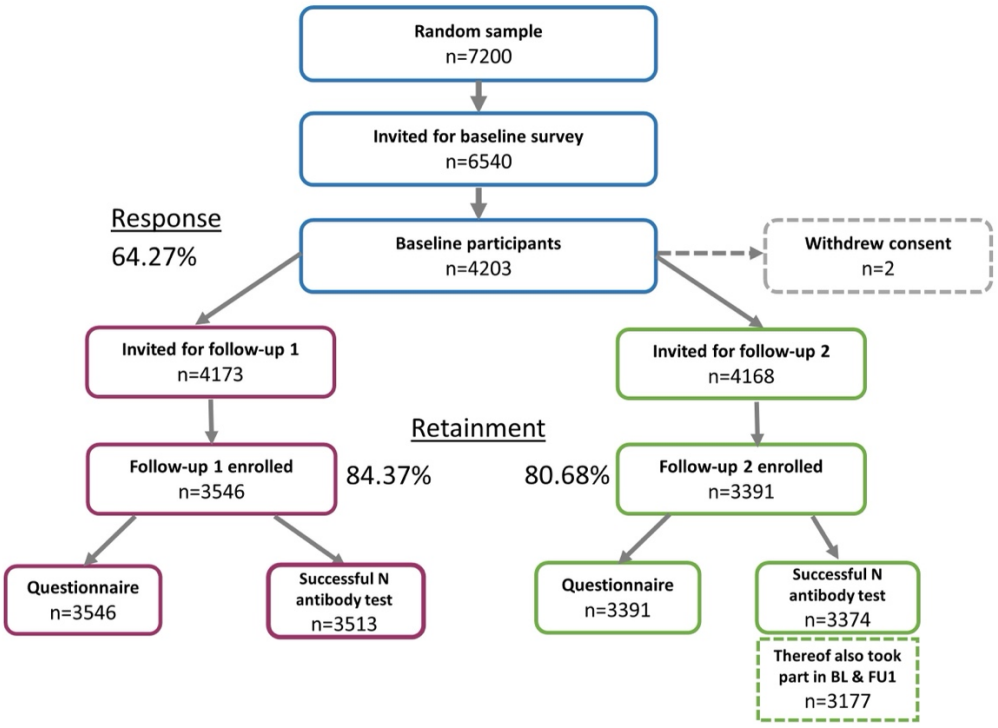

Figure 12 Summary of the TiCoKo longitudinal study design – follow-up 1 and follow-up 2. Shown are the numbers of invited individuals (14 years and older), follow-up participants, information via questionnaire, successful blood-draws and available N-test measurement for follow-up 1 and 2, respectively.

5.4.3.7 Standardization

For each of the three observation periods, we standardized the observed (crude) % new seropositive to the Tirschenreuth population as described previously for baseline[201]. In brief, we standardized crude seropositivity by age-group-, sex-, and municipality-specific weights according to Tirschenreuth county administration data. We also accounted for the COBAS test's sensitivity and specificity by the approach of Sempos and Tian[323].

From the standardized % new seropositives at BL, FU1, and FU2, we derived the estimated number of infected individuals in the Tirschenreuth population for the respective observation periods (overall, by sex, and by age-groups). However, a specific challenge is the high COVID-19 related mortality particularly among older individuals: the individuals having died from COVID-19 were infected, but not covered by this – or any – seroprevalence study. We thus added the number of registered COVID-related deaths in the Tirschenreuth county for the respective observation period to our derived expected number of infected. Dividing this expected number of infected accounting for deaths by the number of inhabitants (overall, by sex, by age-groups), we obtained estimates for infection incidence during the three observation periods.

For each of the three observation periods, we derived the SDR as the expected number of infected accounting for deaths divided by the number of registered infected in the Tirschenreuth county. The SDR is a measure with a lower bound of 1.0. When the number of expected infected in the county based on serology was lower than the number of registered cases, the SDR was set to 1.0. We did this overall, by sex, and by age-groups.

The CFR compares registered COVID-19 related deaths with the registered infected ("cases") and overestimates fatality when testing strategies are incomplete and not all infected are registered. The IFR is the number of deaths divided by the true number of infected in the population. Standardized seroprevalence estimates from population-based studies are considered state-of-the-art to determine the number of infected in populations. For each of the three observation periods, we derived the IFR (overall, by sex, and by age-groups) as the registered number of SARS-CoV-2 related deaths in the Tirschenreuth county divided (i) by the number of infected calculated based on our serology data, or (ii) by the number of registered infected if this number was higher than the number resulting from serology (the latter is, in fact, the CFR).

Despite the offer of a home visit by the study team, participation rate of senior care home residents was low rendering the calculation of estimates for this group impossible. As an approximation, we approached a possible impact of senior care homes on the overall IFR by dividing the municipalities of the county into two subgroups: municipalities with at least one senior care home versus municipalities without any senior care home (as described previously for the BL analysis[201]).

5.4.3.8 Confidence and Credibility Intervals

All 95%-CIs for standardized seropositivity were computed using Wilson's method for binomial proportions assuming the weights as fixed constants. For the standardized IFRs and SDRs, we computed Bayesian credibility intervals accounting also for variation in the number of reported cases or deaths (following the reasoning of and using a similar method as Streeck et al.[311]). For the IFR, we first obtained 100 000 random draws from two Beta-distributions with parameters a_1=#(reported deaths)+1 and b_1= #(at risk in population)-#(reported deaths)+1 and a_2= #(est.new seropos.in study)+1 and b_2= #(at risk in study)-#(est.new seropos.in study)+1, where #(est.new seropos.in study) is the expected number of new seropositive cases in our study (i.e. after standardization and accounting for COVID-19 related deaths and for imperfect sensitivity/specificity of the N-test). These Beta-distributions correspond to posterior distributions of the binomial proportions for the number of deaths among the population and the number of seropositives among the study participants, respectively. We divide samples from these posteriors and calculate the 2.5% and 97.5% quantiles of the ratio to derive approximate 95% credible intervals for the IFR. When using registered cases instead of the expected number of new sero-positives in the population as denominator (i.e. the CFR), a_2 and b_2 are replaced by a_2= #(reg.cases in population)+1 and b_2= #(at risk in population)-#(reg.cases in

population)+1. Credible intervals for SDRs are constructed in a similar fashion by dividing samples from the Beta-posterior of the binomial fraction of new seropositives in our study and new registered cases in the population. We refrain from providing credible intervals for the SDRs when there are fewer expected new infections in the population (based on serology) than registered infections.

5.4.3.9 Vaccination

To obtain the proportion of individuals that were vaccinated in the study sample, we considered the questionnaire-based information on vaccination status: an individual was considered fully vaccinated when having received two doses of Comirnaty at least 14 days prior to blood draw. To obtain the antibody profile in vaccinated and / or infected, we also derived the individuals' status of being seropositive for S, but not for N (i.e. seroconversion due to vaccination, not due to infection) and the individual's status of being seropositive for S and N (infected or infected and vaccinated) at FU2, divided this by the number of individuals with S-measurement at FU2 and standardized this proportion to the Tirschenreuth county population as described above.

5.4.4 Results

5.4.4.1 Participant Characteristics and dropout analysis

Among the 4203 participants enrolled at BL, 3546 participated in FU1 (November 2020; 84.1%) and 3391 in FU2 (April 2021; 80.4%). Overall 3196 participants took part in all BL, FU1 and FU2, resulting in a full participation ratio of 76.0 %. (**Figure 12** and **Figure 13**).

Among the 4203 enrolled participants at BL, 4181 had N-test measurements available at BL. Among these, 4181, 3513 and 3374 participants had N-test measurements available at BL, FU1, or FU2, respectively, and comprised the analyzed individuals for each of the three observation periods. For 3177 participants, N-test measurements were available for all three time points. Analyzable participants at BL were 48% men and aged 14 to 102 years with a median age of 52.0 years (**Table 9**).

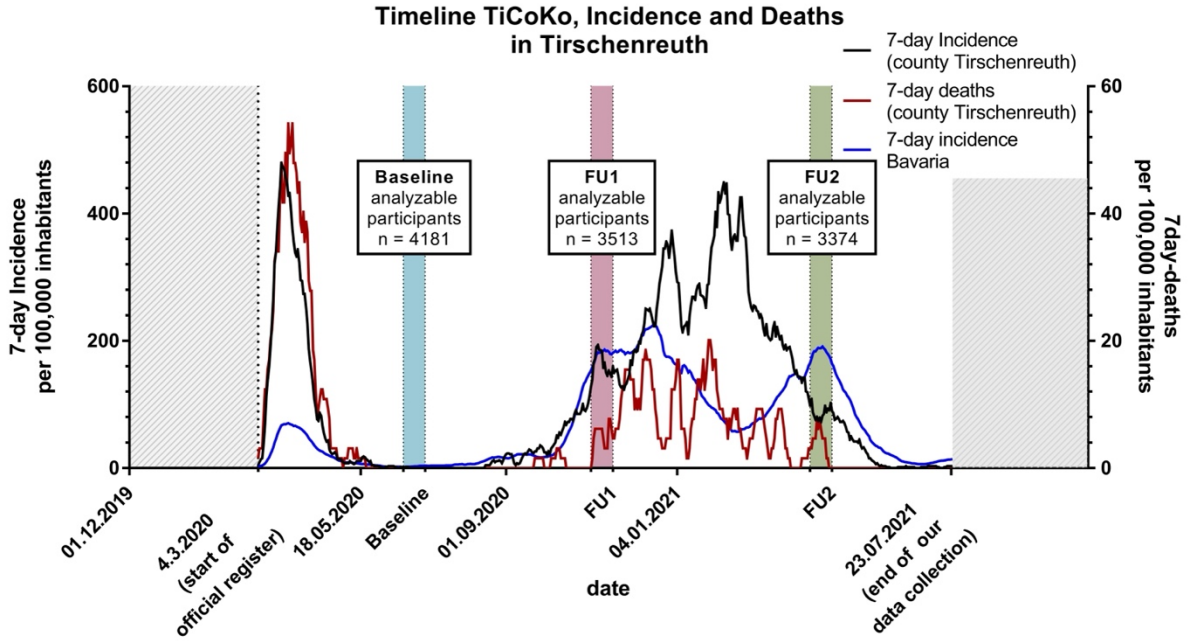

Figure 13 Overview of the time of assessments in the context of Tirschenreuth county SARS-Cov-2 infection waves. Shown are, over time, the 7 day registered infection incidence, the 7-day registered COVID-19 related death incidence per 100,000 of Tirschenreuth county inhabitants and the time of study assessments. Also shown are the numbers of enrolled participants and the number of analyzable participants, i.e. with successful N test measurements at BL, at FU1 and BL, and at FU2 and BL, respectively. N-test measurements for all three time point were available for n=3177 .

When comparing the characteristics of FU1 and FU2 participants with respective dropouts, we found significant difference regarding age and sex, but not with regard to reported comorbidity or education ($P< 0.05$) (**Table 9** and

Supplementary Table 3). A significant difference was also found with regard to seropositivity at BL, which was consistently higher in those returning at FU1 and FU2 (**Table 9** and

Supplementary Table 3), reasoning individuals seropositive at BL were more interested in the follow-up than individuals seronegative at BL. Total N-seropositivity at FU1 or FU2 can thus be biased by the confounding effect of differential response with regard to seropositivity at BL. Estimation of new seropositivity at FU1 among those seronegative at BL and at FU2 among those seronegative at FU1 is not biased by this differential response. This further supported our approach to derive total % of ever seropositives and the % seropositives at FU1 or FU2 in a stepwise approach (see Methods).

Table 9 Participant characteristics Shown are, as indicated, median and IQR or percentage and number of individuals for the given characteristic for analyzable participants at BL, FU1, and FU2.

Variable	BL [participants]	FU_1 [participants]	FU_2 [participants]
Age median (min, max, IQR)	52.0 (14.0, 102.0, 35.0-64.0) [n=4181]	53.0 (14.0, 102.0, 37.0-64.0) [n=3513]	53.0 (14.0, 102.0, 37.0-64.0) [n=3374]
Age 14-20 % (n)	5.4 (225) [n=4181]	5.0 (176) [n=3513]	5.2 (177) [n=3374]
Age 20-49 % (n)	40.8 (1707) [n=4181]	38.3 (1345) [n=3513]	38.1 (1284) [n=3374]
Age 50-69 % (n)	38.8 (1624) [n=4181]	41.2 (1449) [n=3513]	41.2 (1389) [n=3374]
Age 70+ % (n)	14.9 (625) [n=4181]	15.5 (543) [n=3513]	15.5 (524) [n=3374]
Female % (n)	51.6 (2158) [n=4181]	53.0 (1861) [n=3513]	53.7 (1813) [n=3374]
BMI median (min, max, IQR)	26.6 (13.9, 62.1, 23.7-30.4) [n=4134]	26.6 (13.9, 62.1, 23.7-30.3) [n=3474]	26.6 (13.9, 62.1, 23.7-30.4) [n=3339]
Disease[1]			
autoimmune % (n)	7.1 (289) [n=4081]	7.3 (250) [n=3435]	7.4 (243) [n=3300]
cancer % (n)	4.9 (202) [n=4081]	5.2 (178) [n=3435]	5.0 (164) [n=3300]
diabetes % (n)	7.6 (312) [n=4081]	7.5 (259) [n=3435]	7.4 (245) [n=3300]
cardiovascular % (n)	9.9 (402) [n=4081]	9.6 (331) [n=3435]	9.5 (314) [n=3300]
none[4] % (n)	75.8 (3093) [n=4081]	75.6 (2596) [n=3435]	76.0 (2507) [n=3300]
Education			
Years[2] median (min, max, IQR)	11.0 (6.0, 22.0, 10.0-14.0) [n=4085]	11.0 (6.0, 22.0, 10.0-13.0) [n=3433]	11.0 (6.0, 22.0, 10.0-14.0) [n=3301]
High[3] % (n)	30.0 (1225) [n=4085]	29.5 (1013) [n=3433]	29.8 (985) [n=3301]
antibody status			
N-antibody positive at BL % (n)	8.9 (374) [n=4181]	10.0 (351) [n=3513]	10.3 (349) [n=3374]

[1] diseases = self-reported disease from questionnaire; [2] education years = years of schooling and university/vocational training; [3] high education ≥12 education years; [4] no autoimmune disease, no cancer, no diabetes, no cardiovascular diseases as per self-report

5.4.4.2 Crude N-Antibody seropositivity over time

For the three observation periods, we analyzed the 4181, 3513, and 3177 participants with N-test measurements available for BL, for both FU1 and BL, and for all three visits at FU2, FU1 and BL, respectively. We found % (new) seropositives of 8.95%, 0.66%, and 5.80% for the three observation periods, respectively (**Table 10**), with little differences by sex, but larger differences by age-groups (**Supplementary Table 4**). This reflects the low spread of SARS-CoV-2 during summer and autumn 2020 and the high infection occurrence in the combined 2nd and 3rd wave during winter and spring 2021. The % ever seropositives in our cohort was 9.55% at FU1 and 14.80% at FU2.

Among the 351 individuals positive at BL analyzable also at FU1 and FU2, 13 were seronegative at FU1 (3.70%) and 15 at FU2 (4.30%). Thus, > 5 months after infection (i.e. the time between BL and FU1 as well as between FU1 and FU2), approximately 4% were seroconverters from N-antibody positive to negative (**Table 10**). Computing the % total seropositives by the sequential approach (Methods) resulted in 9.22% at FU1 and 14.09% at FU2 (8.95% at BL).

Of note, the total N-antibody positivity estimated directly from antibodies at FU1 and FU2 rather than estimated by the sequential approach was 10.22% (FU1) and 15.68% (FU2), respectively. This is higher than the 9.22% or 14.09% from the sequential approach as a result of the above noted differential response with regard to seropositivity at BL (**Table 10**).

Table 10 Crude N-test seropositivity among analyzed participants and changes over time. Shown are the number of total N-antibody positives, newly seropositive, and newly seronegative participants for N-protein specific antibodies at baseline (June 2020), at FU1 (November 2020), and at FU2 (April 2021). Also shown is the percentage of the according participants group as well as ever N-seropositives and total N-seropositives.

Time of analysis Sex	Analyzable participants[1] #	Total N antibody positive % (#)[2]	Analyzable participants # previously pos/neg	Newly N antibody positive % (#)[3]	Newly N antibody negative % (#)[4]	Ever seropositive (%)[5]	Total N antibody positives (%)[5]
Baseline	4181	8.95 (374)	0/4181	8.95 (374)	(n/a)		
women	2158	9.08 (196)	0/2158	9.08 (196)	(n/a)		
men	2023	8.80 (178)	0/2023	8.8 (178)	(n/a)		
FU1	3513	10.22 (359)	351/3162	0.66 (21)	3.70 (13)	9.55	9.22
women	1861	10.26 (191)	187/1674	0.66 (11)	3.74 (7)	9.54	9.21
men	1652	10.17 (168)	164/1488	0.67 (10)	3.66 (6)	9.58	9.23
FU2	3177	15.68 (498)	349/2828	5.80 (164)	4.30 (15)	14.80	14.09
women	1710	15.56 (266)	186/1524	5.91 (90)	5.38 (10)	14.89	14.08
men	1467	15.81 (232)	163/1304	5.67 (74)	3.07 (5)	14.69	14.10

[1] analyzable for the respective observation period and all periods before. 2 derived directly from antibodies at BL, FU1, or FU2, respectively 3 compared to previously negative. 4 compared to previously positive. 5 derived from the sequential approach (Methods).

5.4.4.3 Serology vs positive PCR (self-reported and confirmed by health authorities) across the observation periods

We compared our serological results (anti-N serostatus) with a participants' self-reports of positive SARS-CoV-2 test confirmed by health authorities (i.e. based on positive PCR tests).

Until BL, 66 positive tests among the study participants were recorded by Tirschenreuth health authorities, of which 6.06 % (n=4) couldn't be confirmed by serology. Between BL and FU1, those numbers increased to 31.58 % (n=6) antibody negative tests among 19 registered PCR positives, settling back to 5.23 % (n= 8 of 161) unconfirmable results between FU1 to FU2. Though these inconsistent serostatus observations (especially at FU1) seemed to be substantial at first, they are in line with a reduced positive predictive value, even for highly specific diagnostic tests, in times of large testing activity and low disease prevalence. When focusing on individuals with a "false-positive" PCR test (individuals with positive PCR tests but negative antigen test) among all tested persons (i.e., self-reported PCR-tested in the respective observation period), we found such inconsistent results in 0.80, 0.56, and 0.51 % of all tested for BL, BL to FU1, and FU1 to FU2, respectively. Such a joint probability of positive PCR-test and a negative antibody test, P(non-infected., PCR-pos.)=P(PCR-pos.|non-infected)*P(non-infected) = (1-specificity)*P(non-infected), is in line with the high published specificity[324] of the SARS-CoV-2 RT-qPCR of 99.5% and low infection occurrence. A part of the inconsistent observations can also be due to false-negative N-serology.

In conclusion, the overall 238 individuals with positive test until FU2 (reported via questionnaire and confirmed by local health authority), the serological test was positive at FU2 for n=220 (92.44%), but negative for 18 (7.56%). The vast majority of these can be attributed to loss of antibodies over time or a false-positive PCR test, emphasized by increased impact in times of high testing frequency combined with low incidences. (**Table 11**).

Table 11 PCR-test report. Via questionnaire, 66, 19 and 153 participants reported a positive PCR-test for the period until BL, between BL and FU1, or between FU1 and FU2, respectively, which were confirmed by health authorities. We derived the % N-antibody negatives and N-antibody positives at BL, FU1, FU2, respectively, for these individuals. Additionally, we derived the % N-antibody negatives and N-antibody positives at FU2 for all individuals with self-reported positive PCR-test (health authority confirmed) at any time until FU2 assessment (April 2021).

Timepoint	**# confirmed positive registered PCR test** (# total self-reported PCR tests)	**N-antibody negative** **#** (%[group]; %[all tests])	**N-antibody positive** **#** (%[group]; %[all tests])
Until BL 12/2019-4/2020	n=66 (n=501)	4 (6.06; 0.80)	62 (93.94; 12.38)
between BL and FU1 6/2020-11/2020	n=19 (n=1064)	6 (31.58; 0.56)	13 (68.4; 1.22)
between FU1 and FU2 11/2020-4/2021	n=153 (n= 1568)	8 (5.23; 0.51)	145 (94.77; 9.25)
until FU2 12/2019-4/2021	n=238 (n= 3133)	18 (7.56; 0.57)	220 (92.44; 7.02)

5.4.4.4 Dynamics of standardized N-antibody seropositivity across the observation periods

Based on the crude % new seropositives for each of the three observation periods, we accounted for antibody test misclassification, standardized to the Tirschenreuth county population aged ≥ 14 years, and added the (unobservable) deaths, in order to approximate the proportion of the Tirschenreuth county individuals that were infected within the respective periods. We refer to this as (standardized) % new seropositives in each of the three observation periods, which estimates the Tirschenreuth county (aged ≥ 14 years) cumulative incidence of infection of the respective time period. We found the highest proportion of (new) seropositives at BL (9.18 %; 95%-CI 8.34-10.09; before June 2020), which captured the 1st SARS-Cov-2 wave as reported previously. We found only minor new N-seropositives (0.87 %) between BL and FU1, which reflects the low-incidence period during summer 2020. Between FU1 and FU2, which captures the 2nd and 3rd wave, the new seropositivity was 6.06 % (95%-CI 5.24-7.00) (**Figure 14A¸ Supplementary Table 5** and **Supplementary Table 6**)

There were only little differences by sex, but age-stratified analysis revealed different patterns for different observation periods. While the seropositivity at BL was comparable across age groups, the new seropositivity between FU1 and FU2 was lower among the older aged population compared to the younger (**Figure 14A,D; Supplementary Table 5 and Supplementary Table 6**).

The % ever seropositives at the respective observation periods at BL, FU1 and FU2 was 9.18% [95%-CI 8.34-10.09], 9.97% [95%-CI 9.03-11.01] and 15.43% [95%-CI 14.25-16.69], respectively (**Supplemental Figure 6** and **Supplementary Table 7**).

We also calculated % new seropositivity for each of the three observation periods as described above for each of the 26 municipalities in Tirschenreuth. At BL, municipality-specific seropositivity ranged

from 1 % [95%-CI 0.18-5.45] to 22.62 % [95%-CI 14.49-33.52]. At FU1 compared to BL (July to November 2020), new seropositivity was negligible. At FU2 compared to FU1 (November 2020 to April 2021), new seropositivity ranged from 3.31% [based on registered cases] to 15.95% [95%-CI 14.49-33.52] (**Supplementary Table 8**). The total proportion of individuals infected until FU2 (% ever seropositive) ranged from 8.17 % [95%-CI 3.69-17.12] to 34.07 % [95%-CI 22.96-47.27] depending on the respective municipality (**Supplementary Table 7**)

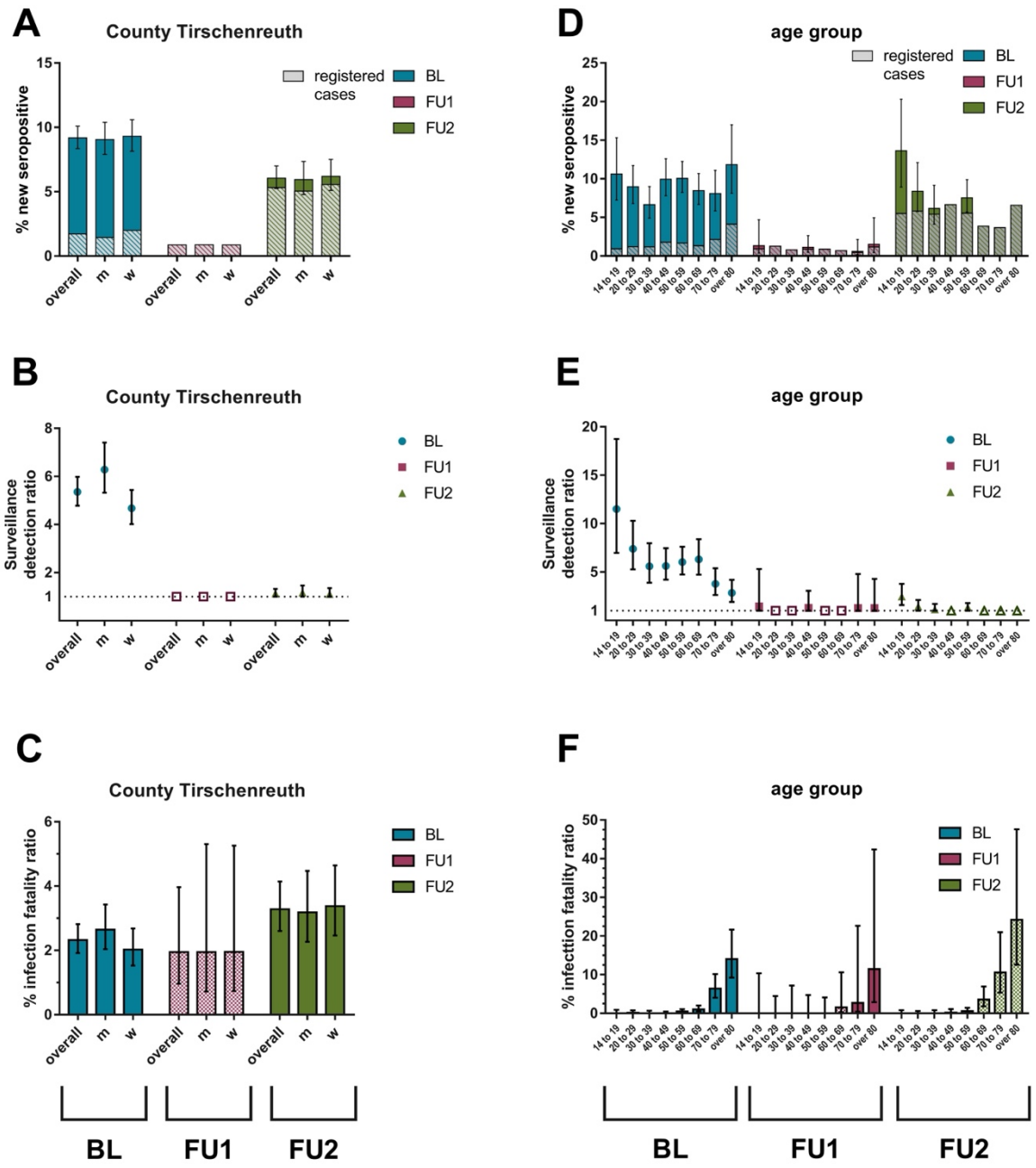

Figure 14 Standardized (N-based) new seropositivity, surveillance detection ratio (SDR), and infection fatality ratio (IFR) for Baseline (BL), Follow up 1 (FU1) and Follow up 2 (FU2). Shown are new seropositivity (based on N-antibodies) (%) and new registered case incidence (%), the surveillance detection ratio (SDR) and infection fatality ratio (IFR) (%) in the county population overall (A-C) and by age-groups (D-F). Non-solid coloring of symbols or bars (B, C, E, F) represents derived estimates from registered cases rather than serology, when registered cases exceeded the number of expected infections in the county based on serology. Error bars represent 95% confidence intervals (95%-CI, A, D) or 95% credibility intervals (B, C and E, F), respectively.

5.4.4.5 Development of SDR and IFR across the observation periods

The German testing strategy at the beginning of the pandemic was limited in terms of test availability and logistics and therefore focused mainly on identifying symptomatic infections and contact tracing. This regime was reflected in our BL results, yielding an overall SDR of 5.35 (95%-CI 4.78-5.99), with higher SDR in the younger population (e.g. 13.64, 95%-CI 8.92-20.30, for 14 to 19-year-old) and lower SDR in the elderly (e.g. 2.84, 95%-CI 1.90-4.20, for the 80+) (**Figure 14B**; **Supplementary Table 5**).

Our calculated SDRs for FU1 or FU2 were - for some age groups - below unity. In these instances, the SDR was set to 1.0. For the observation period between BL and FU1, we observed an SDR of 1.44 [95%-CI 1-5.31] for the 14-19 years old, which was substantially lower than for the period until BL, 1.27 [95%-CI 1.90-4.20] for the 80+ and close to unity in other age-groups (**Figure 14**, indicated by non-solid coloring/gray). For the observation period between FU1 and FU2, we found an SDR overall of 1.14 (95%-CI 1.00-1.32) meaning that most infections in Tirschenreuth were detected and registered by health authorities. Regarding the age-dependent SDR, most age-groups showed a factor around 1 with the elderly population (80+) showing a lower and the young population showing slightly higher factors (e.g. 2.48, 95%-CI 1.59-3.77, for the 14-19 years old) (**Figure 14 B, E**; **Supplementary Table 5** and **Supplementary Table 6**).

To further investigate the low SDRs in certain strata, especially at FU1, we conducted a sensitivity analysis: in the main analysis we accounted for misclassification in the antibody tests during estimation of the number of new seropositives. The registered infections may also be affected by misclassification, as they may include individuals who were not infected at the time of testing but were registered as a SARS-CoV-2 case due to a false-positive PCR test result. Such false-positive cases could bias the SDR towards too low values (or even below 1). False-positive PCR tests might play a particularly large role in times of low incidence and large amounts of performed tests (e.g., screening tests among symptom-free persons). To examine the potential magnitude of such a bias, we approximated the total number of performed PCR tests in the county based on the fraction of individuals with self-reported PCR tested in our cohort (BL 12%, BL-FU1 27% and FU1-FU2 46%). We assumed, as a worst-case scenario, a sensitivity of 95 % and a specificity of 99.5 % for general PCR-testing, derived the fraction of "false-positive infections" among the registered cases (3% until BL, 17% BL-FU1 and 4% FU1-FU2) and corrected the registered cases accordingly. Finally, we calculated SDRs based on our serology data and the corrected registered cases. For BL only a minor increase from 5.35 to 5.51 was observed for overall SDR with slight variations in different age groups. In contrast, the correction had a larger impact at FU 1 increasing SDR from 0.82 to 0.99. Nevertheless, our SDR estimates were still below unity for several age-groups. The change in the FU2 estimate was smaller again, with an overall increase in the SDR from 1.14 to 1.19 (**Supplementary Table 9**). In conclusion, this sensitivity analysis revealed a potential for a non-negligible impact of "false positive" registered cases during low incidence times. On the other

hand, it couldn't solely explain the finding of SDRs below unity in our cohort, which can most probably be attributed to selection bias in certain age groups.

IFRs for the 3rd observation period were increased compared to IFR in the first or 2nd observation period (i.e. pre-pandemic until BL): while in BL (spring 2020), we found an overall IFR of 2.32 % (95%-CI 1.92-2.82), the overall IFR dropped between BL and FU1 to 1.95 % (95%-CI 0.96-3.97), but increased between FU1 and FU2 to 3.28 % (95%-CI 2.60-4.14), clearly above BL levels (**Figure 14C**). There was no substantial difference in IFR between men and women.

We found a distinct age-pattern in IFRs that was similar for all three observation periods: the IFR was increased in the 50-70 years old, highest in the very old (70+), and near 0 in the younger population (<40 years old) (**Figure 14C, F**; **Supplementary Table 5** and **Supplementary Table 6**). The increased IFR in the third observation period compared to the 1st was due to higher IFR in the 50–70-year-old and the very old, not due higher IFR in the young. However, the IFR for higher age-groups in the 3rd observation period was, in fact, the CFR, since the number of expected infected in the county based on serology from this cohort was lower than the number of registered cases.

5.4.4.6 Contribution of senior care homes to overall N-antibody seropositivity, SDR and IFR across the observation periods

Senior care home residents make up for 1.4% of the county population and form a special group in terms of vulnerability to COVID-19. They contributed for almost 50 % of COVID-19 related deaths in individuals 70+ years of age in spring 2020. Despite the offer of a home visit by the study team, participation rate of senior care home residents was low, rendering the calculation of estimates specific to this group unfeasible. As an approximation, we calculated standardized new seropositivity, SDR and IFRs separately for municipalities with and for municipalities without a senior care home. New seropositivity was comparable for all three intervals, BL, BL to FU and FU1 to FU2, respectively. However, at BL, the SDR was 4.66 (95%-CI 4.08-5.32) for municipalities with senior care homes and 8.1 (95%-CI 6.53-10.03) for municipalities without. In contrast, for FU1 and FU2, the SDR dropped down to approximately 1 (min. 1.0 max. 1.19) with no notable differences between municipalities with or without senior care homes. While remarkably higher IFRs were found for municipalities with senior care homes (3.3%; 95-% CI 2.46-3.74) vs municipalities without senior care homes (0.72%; 95%-CI 0.41-1.27) at BL, those differences dwindled in winter 2020/spring 2021 (period between FU1-FU2) with 3.43% (95%-CI 2.63-4.49) for municipalities with and 2.90% (95%-CI 1.84-4.59%) without senior care homes (**Figure 15A-C**; **Supplementary Table 10**).

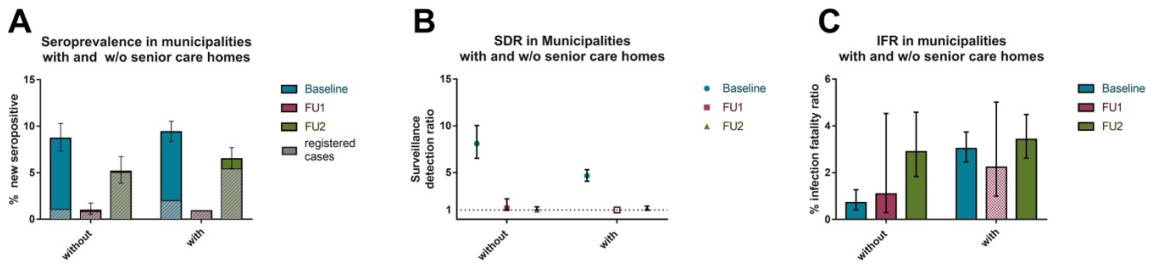

Figure 15 New N-antibody seropositivity, surveillance detection ratio (SDR), and infection fatality ratios (IFR) with or without senior care homes (SCH). Shown are (A) new seropositive (based on N-antibodies) (%), (B) SDR (closed symbols: based on serology data; open symbols: based on registered cases) and (C) IFR (%, nonsolid color: based on registered cases) for municipalities with and without senior care homes. Where the expected number of infected in the county based on serology in the cohort was lower than registered cases, the case fatality ratio was used as best approximation of fatality. Error bars represent Wilson 95% confidence intervals (95%-CI) for seroprevalence and 95% Bayesian credibility intervals for SDR and fatality ratio, respectively.

5.4.4.7 Vaccination

By the end of 2020, different SARS-CoV-2 vaccines received conditional market approval by the EMEA and were shortly after rolled out as part of the national vaccination campaign[37,40,43]. Reflected by 6.06 % newly N-antibody seropositives between November 2020 and April 2021 (FU2 compared to FU1), the Tirschenreuth county was once again among the counties in Germany most affected by the quickly spreading SARS-CoV-2 alpha variant. The most affected counties in Germany / Bavaria received extra vaccine doses to accelerate their vaccination campaign.

By combining both N-protein and S-protein based serological tests, together with our questionnaire information on vaccination status, we were able to distinguish infected from vaccinated individuals. Among the 1859 participants in FU2 without report of any received vaccination and successful S- and N-test, 20.19% were N- and S-protein seropositive and thus had experienced a SARS-CoV-2 infection. 1.61% among the non-vaccinated were only S-seropositive, lacking evidence for N-seropositivity (**Table 12**). This may be attributable to loss of N-specific antibodies, false-negative anti-N-tests, or wrong self-report of vaccination status in the questionnaire.

Table 12 Antibody response in vaccinated (self reported) and infected study participants. For the 3351 individuals with a valid questionnaire result for vaccination at FU2, we determined S- and N-antibody seropositivity. Indicated are % (#) of S antibody positive and % (#) N antibody positive among unvaccinated and vaccinated at FU2 (April 2021, based on self-report via questionnaire). We determined the impact of 1 versus 2 vaccinations and also the time interval from vaccination to blood drawl (< versus ≥ 14 days after vaccination).

Vaccination[1]- and Serostatus	N+S antibody positive % (#)	only S antibody positive % (#)	S seropositive % (#)	S antibody negative % (#)
Not vaccinated, n= 1859	20.17 (375)	1.61 (30)	21.79 (405)	78.21 (1454)
vaccinated (all), n= 1492	9.18 (137)	63.47 (947)	72.65 (1084)	27.35 (408)
1x vaccinated (<14d), n= 448	8.48 (38)	14.73 (66)	23.21 (104)	76.79 (344)
1x vaccinated (>14d), n= 711	10.69 (76)	81.43 (579)	92.12 (655)	7.88 (56)
2x vaccinated (<14d), n= 8	25 (2)	75 (6)	100 (8)	0 (0)
2x vaccinated (>14d), n= 306	6.21 (19)	93.46 (286)	99.67 (305)	0.33 (1)
No of vaccinations unknown n= 19	10.5 (2)	52.6 (10)	63.2 (12)	36.8 (7)

[1] according to questionnaire. For n=23 individuals either vaccine or serostatus couldn't be determined and they were therefore excluded from the analysis

Among the 3351 participants at FU2 with valid antibody tests for S and N as well as valid questionnaire information regarding vaccination, 44.3% (n=1492) reported to have been vaccinated at least once. Of these, 63.47% (n=947) were positive for S-specific antibodies and negative for N-specific antibodies. Adding the 137 (9.18%) vaccinated and infected individuals (N and S seropositive) to the 947 (63.47%) vaccinated S-seroconverters, we noticed 27.35 % (n=408) vaccinated individuals who scored S antibody negative at the time of the blood draw. We therefore divided the vaccinated into 4 subgroups (once or twice vaccinated, for ≥ or <14 days) assuming that seroconversion is completed 14 days after vaccination. This subgroup analysis revealed 92.12% seroconversion ≥14 days after the 1st vaccination, even rising to 99.67 % 14 days after the second vaccination. Most vaccinated but seronegative individuals (n= 344) were found among the one times vaccinated, who provided blood <14 days after vaccination (**Table 12**).

Although (immune) correlates of protection from SARS-CoV-2 infection or severe disease remain a widely discussed topic, we computed standardized overall S-based seroprevalence within the county of Tirschenreuth. The overall S-based seroprevalence at that time (FU2) was 45.79% (95%-CI 44.11-47.47). Of note, the vaccinated at that time already contributed 30.53% (95%-CI 29.00-32.10). We

found no differences between sexes, neither in the vaccinated nor in the naturally infected population, as well as in the combined overall population (**Figure 16A**, **Supplementary Table 11**).

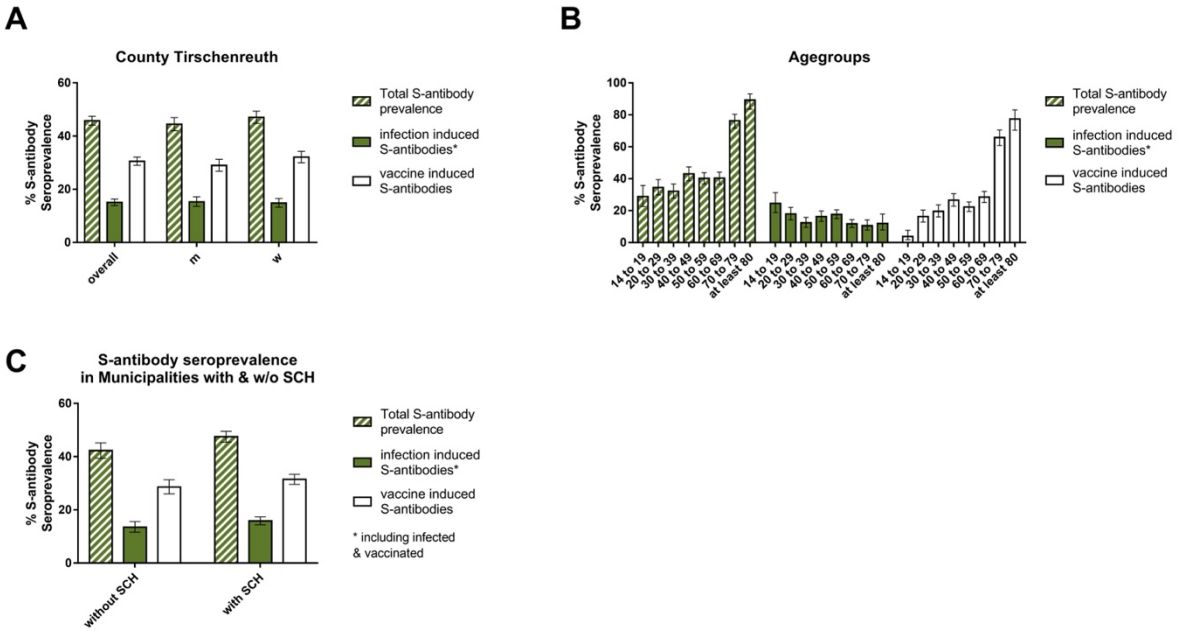

Figure 16 S-specific antibody seroprevalence at FU2. Shown is the standardized S antibody seroprevalence at FU2 (i) counting all S-antibody positive individuals (total prevalence), (ii) counting S-positives that were also N-positive (infection induced antibodies, including vaccinated and unvaccinated individuals) or (iii) counting S-positives that were N-negative (i.e. uninfected but vaccinated individuals), in the overall population of Tirschenreuth (A), by age-groups (B) and for municipalities with or without senior care homes (C).

Natural S-seropositivity was similar across most age-groups, with a slight trend towards higher S-seropositivity in the younger population. In contrast, vaccine elicited S-antibody seroprevalence revealed a clear increase by higher age, in line with the German vaccine prioritization program assigning a higher priority to the elderly at the start of the roll-out. Thus, vaccine elicited S-seropositivity within the under 20 year old population was very low (3.8 %; 95%-CI 1.83-7.73) raising up to 77.0 % (95%-CI 70.34-83.11) in the 80+ year olds at the time of FU2, April 2021. Overall S-antibody prevalence reached up to 89.23 % (95%-CI 83.54-93.12) in the over 80 years old, when infected (non-vaccinated) individuals were also considered, dropping to about 40 % in the 40-69 year old population and dropping further for the younger age groups. Slightly higher natural infection as well as vaccine elicited S-specific seroprevalence was found for municipalities with senior care homes (**Figure 16B** and **C**, **Supplementary Table 11**).

5.4.5 Discussion

Most longitudinal studies including some nation-wide surveys conducted in several European countries or China[32,305–307,325] repeated "cross-sectional analyses" using different panels of individuals, which hampers the comparison over time and may lead to undetected selection bias. In contrast, longitudinal population-based "follow-up analysis" allows for a careful analysis of dropouts and potential selection bias.

Herein, we conducted a longitudinal population-based study following more than 3300 individuals from the Tirschenreuth county with repeated serology. By this, our serology data captured the SARS-CoV-2 infection occurrence for more than one year since the start of the pandemic and the dynamic over time. Our standardized new seropositivity in each of the three observation periods of 9.2%, 0.9% and 6.1% reflected clearly the high incidence period in the Tirschenreuth county in spring 2020, the low incidence period in summer 2021 and the new surge of infections in autumn/winter 2020/21, respectively, resulting in more than 15% ever seropositives in April 2021. The SDR of about 5 in spring 2020 decreased to unity afterwards, indicating excellent detection of infections owed to massive testing. We still observed a high IFR of > 3% for the 2nd/3rd wave comparable to the 2.3 % in the 1st wave. This was again mostly owed to high infection-related mortality in the old aged, but our results indicated a reduced contribution of deaths in senior care homes when compared to the 1st wave.

Our data document the substantially higher infection occurrence in the Tirschenreuth county compared to other regions in Germany: seroprevalence estimated in November 2020 of at 1.8% in Munich (KoCo19[309,326]), 1.3%-2.8% in 7 different regions in Germany in the MuSPAD study[307], or 1.7% by a nation-wide survey (RKI-SOEP[327]) compared to 9.2% in the Tirschenreuth county. In the MuSPAD study, 4.1% to 13.1% seroprevalence was observed for spring 2021 assessments compared to the 6.5% total seroprevalence estimated in July 2021 in Munich[328,329] and 15.4% ever seropositives in Tirschenreuth after the combined 2nd / 3rd wave in April 2021. Despite major differences in the design of these studies, it is fair to conclude that (i) the dynamics of virus spread differs by regions and (ii) the Tirschenreuth population was hit particularly hard both by the 1st and also by the combined 2nd and 3rd wave, in line with national surveillance data in this county (RKI)[330].

Of particular relevance is our finding of about 4% of the originally seropositive participants turning seronegative in the reassessment five months later – both when comparing November 2020 to July 2020 and April 2021 to November 2020. This provides a remarkable consistency of seroconversion from positive to negative regardless of the respective time period under study and a particular strength of our repeated assessments. Although wrong test results (either false positive at preceding time point or false negative 5 months later) may contribute to the observed changes in serostatus, the loss of N-specific antibodies is the most probable cause[331].

The decrease in SDR from about 5 in the spring 2020 wave to values approaching 1 for the summer/autumn 2020 and winter/spring 2020/21 observation periods underscore the effectiveness of the testing strategy in that county. We observed in several strata of the data from the two observation periods after the baseline survey an even higher number of registered SAR-CoV-2 cases in the county than expected seropositives projected from serology testing in our sample, meaning that the SDR is paradoxically lower than 1 in these strata. In a sensitivity analysis we checked whether this underestimation resulted from false-positive PCR tests which may have inflated the number of registered cases. The results showed that false-positive PCR tests influenced the SDR, especially in the low incidence period during summer/autumn 2020, but had no decisive impact that could explain the underestimation fully. A more plausible explanation is that we must acknowledge some selection bias in our population sample that occurred despite high, though not 100%, participation of randomly drawn subjects. The reasons for the selection bias may be manifold. While we accounted for COVID-19 related deaths often unaccounted for in serology studies, hospitalized infected subjects who are non-participants in the study may contribute to this undercapturing of infected individuals. A more risky behavior towards protecting against infections may be inversely related to participation in a serology – or any health-related – population study. Such differences between participants and non-participants cannot be adjusted for by standardizing for age, sex, and municipality. The high response rate in our study limited, however, the magnitude of the bias. We have not used the raw estimates of seropositives in those strata with SDR < 1, we have instead imputed the number of registered cases for subsequent calculations to further reduce the effect of selection bias on our results. SDRs reported in other German studies like SaarCoPS, MuSPAD and KoCo19 ranged from 2.5 to 4.5 and generally decreased in winter/spring 2020/2021 to 1.3 and 2.9[307,315,328,330]. However, the previously published studies did not capture a high infection wave in spring 2020 with limited testing available and therefore could not document the change in surveillance detection over time, as achieved in our study here.

Our observation of an IFR of 3.3% for the 2nd/3rd infection wave versus 2.3% for the 1st wave documents the continued menace of the SARS-Cov-2 infection until a time where the vaccination roll-out was just getting started. The underestimation of the number of SARS-CoV-2 infections in our sample discussed above leads to some overestimation of the IFR. In all instances, where the CFR was lower than the serology-based IFR, we used strata specific CFRs as a better estimate for fatality, which is an upper bound of the fatality estimate. Despite our full efforts to account for bias where possible, some overestimation of the IFR might have remained.

The overall higher estimate of 3.3% IFR in the winter/spring 2020/21 infection wave compared with the 2.3% estimated for the spring 2020 wave is thus to be interpreted with caution. This is also within statistical uncertainty bounds. Nevertheless, an increased IFR over time - before the vaccination roll-

out - would be in line with the introduction of the SARS-CoV-2 alpha variant in December 2020/ January 2021, which was shown to be linked to increased illness and mortality as compared to SARS-CoV2 (wt and D414G)[48,300,332].

In our study, we have offered home visits also to senior care home residents and other immobile individuals, to make every possible attempt to capture the full population, also the particularly vulnerable. This might be one reason for IFRs, which seem to be overall higher compared to those reported for other areas in Germany. While SaarCoPS with 2.1% reports an overall IFR close to our baseline result[315], MuSPAD for example reports an IFR of 1.3 % across all age groups ranging between 0.3% (lowest; Magdeburg, 11/2020) and 2.4% (highest; Freiburg, 08/2020).The relationship of IFRs during 1st wave and 2nd/3rd wave did not follow a consistent pattern and was higher either for the 1st or the 2nd/3rd wave, dependent on the investigated region, respectively.

Noteworthy was our observation of a reduced impact on fatality from Tirschenreuth county municipalities with senior care homes. These municipalities accounted for a large part of the overall IFR in spring 2020 (IFR of 3.2 % with and 0.7 % w/o senior care homes), but not anymore in winter/spring 2020/21 (IFR of 3.1 % with and 2.6 % w/o). This suggests that senior care homes were not prominent drivers of infection fatality during the 2nd and 3rd wave any more.

Consistent with previous reports[304,333], and also in line with our BL analysis, the proportion of elderly is key for estimated IFRs. IFRs determined for the different age groups at FU2 increased from 0.6 % to 3.5 %, 10.6% and 24.2 % for the 50-59, the 60-69, the 70-79 and the 80+ years old participants, respectively. Trends to higher IFRs at FU2 as compared to the BL analysis were again within statistical uncertainty bounds and may also represent an overestimate for the reasons discussed above. Our age-group specific IFR estimates are in general agreement with several pre-vaccination metaanalysis reporting an exponential relationship between age and IFR for COVID-19[304,333]. Substantial heterogeneity was found in the IFR by age, location, and time, respectively. Age-specific IFR estimates increased through ages 30 years (0.05%), 60 years (1%) and 90 years (20.3%). Global IFR estimates including all ages are lower at 0.3% in January 2021[333], as is the proportion of high aged individuals compared to Germany.

We also found an exceptionally high early response to the vaccination campaign in the elderly in the Tirschenreuth county, leading (together with previous infections) to an S-antibody seroprevalence of 76.3% and 89.2% in the 70-79 years old or > 80 years old population, respectively, until April 2021. Unfortunately, no real vaccination tracking was applied in Germany. Nevertheless, estimates of 20 % overall (basic) immunization rate in Germany in the beginning of June 2021[334] support our findings of a higher, but realistic, overall immunization rate of 30.5 % for the Tirschenreuth population at that time.

Among the strengths of our study are the population-based, prospective cohort design and the large number of participants across the various age-groups combined with high retention of study subjects over the complete follow-up period. This design allowed us to systematically describe the evolution of seroprevalence in our population over time. More specifically, we were able to describe the frequency of newly emerging seropositivity and the loss of existing antibodies, rather than just providing information on seroprevalence at specific time points.

In our study, we observed an association between prior serostatus and willingness to participate in further assessments; seropositive study participants were more likely to participate in the further assessments. A reason for this could be the disclosure of test results to study participants, which in principle could also be waived. However, we think that such disclosure can act as an important incentive for study participation and - at times when no vaccination was available - has been perceived as obligation for ethical reasons. By performing the sequential estimation of seroprevalence at each time point, we can avoid bias due to this differential response. In our case, the (unstandardized) cross-sectional estimate of overall seroprevalence was, e.g., 15.69 % in FU2, while the estimate from the sequential approach was 14.09 %. Magnitude of the bias of the cross-sectional estimate depends on the degree of differential response due to knowledge of the serostatus at previous time points. In case of a seroprevalence study with prospective cohort design and disclosure of antibody test results at intermediate study time points we recommend to focus on cumulative incidence of (new) seropositivity at each study time point to characterize infection dynamics and use the sequential approach when interested in seroprevalence at specific study time points.

We also acknowledge some limitations, that might reflect general challenges of seroprevalence studies. While seroprevalence studies are superior to registered infection data to estimate cumulative infections by the detectability of asymptomatic infections, selection bias in the beginning as well as differential attrition at follow-up are important to consider when interpreting results. Our drop-out analyses identified lower attrition among individuals having been seropositive at baseline. This might have derived from the fact, that study participants were informed about their serostatus and seropositives might have been more curious to participate further in line with previous reports of enrichment of previously tested positive individuals among NAKO participants[335]. We were able to account for this by the sequential assessment of period-specific incidence rather than comparing directly computed total seropositivity at each assessment. The observation of lower number of serology-based expected than registered infected individuals and its consequences is duly noted above. Overall, seroprevalence studies and derived SDRs and IFR are important to help judge the pandemic dynamic, particularly when applied longitudinally, but our in-depth analyses also highlights some underlying challenges.

5.4.6 Conclusions

Our population-based, prospective cohort design and the large number of participants across the various age-groups combined with high retention of study subjects over the complete follow-up period allowed us to systematically describe the evolution of seroprevalence, SDR and IFR in our population over time. Along these lines, decreased underreporting of infections highlights the success of massively increased testing in the population. A persistent high IFR particularly among the old aged was documented for the combined 2nd and 3rd infection wave in winter/spring 2020/21 before the vaccination roll-out. Though elderly were still at highest mortality risk, we provide evidence that senior care homes were no longer the dominant key determinants of infection fatality during the 2nd and 3rd wave. High vaccination rates especially in individuals aged 70+ were noticed suggesting good compliance of this risk group in that county with the implemented vaccination campaign.

5.4.7 Appendix & Declarations

Author Contributions: Conceptualization, K.Ü. and R.W.; methodology, S.E., D.P., F.G., A.B.P.; validation, S.E, D.P., S.W. ; formal analysis, F.G., S.W., A.B.P., I.M.H., O.G.; investigation D.P., S.E., R.B., S.B., P.S., A.K.,K.K.,A.S., K.J.S. and H.-H.N.; resources, H.S., I.M.H., O.G.,K.Ü., R.W.; data curation, S.E., S.B., F.G., M.B., M.K., K.Ü., R.W.; writing—original draft preparation, S.E., R.W.; writing—review and editing, K.Ü., O.G., F.G., I.M.H.; visualization, S.E., R.W.; supervision, K.Ü.,O.G., H.K., I.M.H., R.W.; project administration and funding acquisition R.W. and K.Ü. All authors have read and agreed to the published version of the manuscript.

Funding: This work was supported by the Bavarian States Ministry of Science and Arts (TiKoCo-19 and ForCovid, StMWK; grant to R.W. and K.Ü.) as well as by the National Research Network of the University Medicine (NUM; applied surveillance and testing; B-FAST) to KÜ and RW. The funders had no role in study design, data collection and analysis, decision to publish, or preparation of the manuscript.

Institutional Review Board Statement: The TiKoCo-19 study was approved by the Ethics Committee of the University of Regensburg, Germany (vote 20-1867-101) and adopted by the Ethics Committee of the University of Erlangen (vote 248_20 Bc). The study complies with the 1964 Helsinki Declaration and its later amendments. All participants provided written informed consent.

Informed Consent Statement: Informed consent was obtained from all subjects involved in the study.

Data Availability Statement: All authors declare that data and materials will be made available according to the guidelines of the journal.

Acknowledgments: We are particularly grateful to all the study participants. We would like to thank the office staff and numerous students of the University of Regensburg and the University Erlangen as well as the employees of the Bavarian Red Cross, the members of the civil protection, the county office,

and the public health office of county Tirschenreuth, respectively, for their tremendous support. We are also grateful to Christine Wolff from wECARE and Jakob Niggel from MaganaMed for providing questionnaires and the database for the study.

Conflicts of Interest: The authors declare that no competing interests or conflicts of interest exist. The authors have no financial or proprietary interests in any material discussed in this article.

5.4.8 Supplementary Materials

Supplementary Materials: The following are also available online at www.mdpi.com/article/10.3390/v14061168/s1

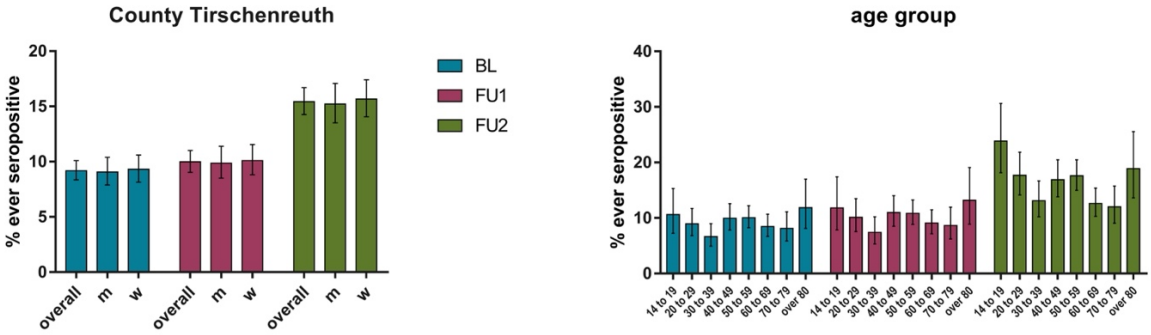

Supplemental Figure 6 Standardized ever seropositives (N-based) overall and by age groups until Baseline (BL), Follow up 1 (FU1) and Follow up 2 (FU2)

Supplementary Table 3 (Supplement to Table 9) Participant characteristics and dropout analysis. Shown are, as indicated, median and IQR or percentage and number of individuals for the given characteristic for analyzable participants and dropouts at BL, FU1, and FU2. P-values test for difference in the characteristics between analyzable participants and dropouts.

Variable	BL	FU1 participant	FU1 dropout	FU1 p-value	FU2 participant	FU2 dropout	FU2 p-value
Age median (min, max, IQR)	52.0 (14.0, 102.0, 35.0-64.0) [n=4181]	53.0 (14.0, 102.0, 37.0-64.0) [n=3513]	42.0 (14.0, 93.0, 29.0-58.0) [n=668]	<0.001	53.0 (14.0, 102.0, 37.0-64.0) [n=3374]	44.0 (14.0, 91.0, 30.0-59.0) [n=807]	<0.001
Age 14-20 % (n)	5.4 (225) [n=4181]	5.0 (176) [n=3513]	7.3 (49) [n=668]	0.019	5.2 (177) [n=3374]	5.9 (48) [n=807]	0.48
Age 20-49 % (n)	40.8 (1707) [n=4181]	38.3 (1345) [n=3513]	54.2 (362) [n=668]	<0.001	38.1 (1284) [n=3374]	52.4 (423) [n=807]	<0.001
Age 50-69 % (n)	38.8 (1624) [n=4181]	41.2 (1449) [n=3513]	26.2 (175) [n=668]	<0.001	41.2 (1389) [n=3374]	29.1 (235) [n=807]	<0.001
Age 70+ % (n)	14.9 (625) [n=4181]	15.5 (543) [n=3513]	12.3 (82) [n=668]	0.04	15.5 (524) [n=3374]	12.5 (101) [n=807]	0.035
Female % (n)	51.6 (2158) [n=4181]	53.0 (1861) [n=3513]	44.5 (297) [n=668]	<0.001	53.7 (1813) [n=3374]	42.8 (345) [n=807]	<0.001
BMI median (min, max, IQR)	26.6 (13.9, 62.1, 23.7-30.4) [n=4134]	26.6 (13.9, 62.1, 23.7-30.3) [n=3474]	26.8 (16.0, 56.5, 23.9-30.4) [n=660]	0.396	26.6 (13.9, 62.1, 23.7-30.4) [n=3339]	26.3 (16.0, 56.5, 23.7-30.1) [n=795]	0.556
Disease							
autoimmune % (n)	7.1 (289) [n=4081]	7.3 (250) [n=3435]	6.0 (39) [n=646]	0.296	7.4 (243) [n=3300]	5.9 (46) [n=781]	0.172
cancer % (n)	4.9 (202) [n=4081]	5.2 (178) [n=3435]	3.7 (24) [n=646]	0.139	5.0 (164) [n=3300]	4.9 (38) [n=781]	0.977
diabetes % (n)	7.6 (312) [n=4081]	7.5 (259) [n=3435]	8.2 (53) [n=646]	0.615	7.4 (245) [n=3300]	8.6 (67) [n=781]	0.309
cardiovascular % (n)	9.9 (402) [n=4081]	9.6 (331) [n=3435]	11.0 (71) [n=646]	0.323	9.5 (314) [n=3300]	11.3 (88) [n=781]	0.158
none % (n)	75.8 (3093) [n=4081]	75.6 (2596) [n=3435]	76.9 (497) [n=646]	0.49	76.0 (2507) [n=3300]	75.0 (586) [n=781]	0.614
Education							

years median (min, max, IQR)	11.0 (6.0, 22.0, 10.0-14.0) [n=4085]	11.0 (6.0, 22.0, 10.0-13.0) [n=3433]	11.0 (6.0, 21.0, 10.0-14.0) [n=652]	0.406	11.0 (6.0, 22.0, 10.0-14.0) [n=3301]	11.0 (6.0, 21.0, 10.0-14.0) [n=784]	0.365
high % (n)	30.0 (1225) [n=4085]	29.5 (1013) [n=3433]	32.5 (212) [n=652]	0.136	29.8 (985) [n=3301]	30.6 (240) [n=784]	0.703
antibody status							
N-antibody positive at BL % (n)	8.9 (374) [n=4181]	10.0 (351) [n=3513]	3.4 (23) [n=668]	<0.001	10.3 (349) [n=3374]	3.1 (25) [n=807]	<0.001

Supplementary Table 4 (Supplement to Table 10). Crude seroprevalence among analyzed participants and changes over time. The number of total and newly seropositive and newly seronegative participants for N or S protein specific antibodies at baseline (June 2020), at FU1 (November 2020), and at FU2 (April 2021) also shown is the percentage of the according participants group.

Time of analysis	Analyzable participants #		Newly N antibody positive % (#)1	Newly N antibody negative % (#)1	Seropositive as sum	Ever seropositive
participant age		Participants# previously pos/neg				
Baseline	**4181**	**0/4181**	**8.95 (374)**	**(n/a)**		
14 to 19	225	0/225	10.67 (24)	(n/a)		
20 to 29	523	0/523	8.99 (47)			
30 to 39	583	0/583	6.69 (39)			
40 to 49	601	0/601	9.98 (60)			
50 to 59	875	0/875	10.06 (88)			
60 to 69	749	0/749	8.41 (63)			
70 to 79	420	0/420	7.62 (32)			
over 80	205	0/205	10.24 (21)			
FU1[1]	**3513**	**351/3162**	**0.66 (21)**	**3.70 (13)**	**9.22**	**9.55**
14 to 19	176	24/152	1.32 (2)	4.17 (1)	11.40	11.84
20 to 29	400	42/358	0.84 (3)	2.38 (1)	9.54	9.75
30 to 39	447	37/410	0.00 (0)	8.11 (3)	6.15	6.69
40 to 49	498	56/442	1.13 (5)	5.36 (3)	10.47	11
50 to 59	766	81/685	0.73 (5)	1.23 (1)	10.59	10.71
60 to 69	683	61/622	0.32 (2)	3.28 (2)	8.43	8.71
70 to 79	373	32/341	0.59 (2)	6.25 (2)	7.68	8.16
over 80	170	18/152	1.32 (2)	0.00 (0)	11.42	11.42
FU2[2]	**3177**	**349/2828**	**5.80 (164)**	**4.30 (15)**	**14.09**	**14.80**
14 to 19	164	24/140	13.57 (19)	4.17 (1)	22.95	23.81
20 to 29	340	41/299	8.36 (25)	4.88 (2)	16.63	17.30
30 to 39	390	32/358	6.15 (22)	12.5 (4)	11.15	12.42
40 to 49	454	57/397	5.79 (23)	8.77 (5)	14.74	16.16
50 to 59	700	83/617	7.46 (46)	2.41 (2)	17.00	17.37
60 to 69	629	60/569	3.51 (20)	1.67 (1)	11.51	11.91
70 to 79	348	32/316	2.53 (8)	0.00 (0)	10.02	10.49
over 80	142	20/132	0.76 (1)	0.00 (0)	12.1	12.1

Supplementary Table 5(supplement to Figure 14). Standardized (N-based) seroprevalence, surveillance detection ratio (SDR), and infection fatality ratios (IFR) overall and by age groups for Baseline (BL), Follow up 1 (BL to FU1) and Follow up 2 (FU1 to FU2). Shown are the population at risk in the general Tirschenreuth population and the analyzed cohort as numbers and percentage of the overall group. Further shown are standardized and corrected seroprevalence (based on N-antibodies) (%), the surveillance detection ratio (SDR) and infection fatality ratio (%) in the overall county population, the indicated sexes and the indicated age groups. Further given are the 95% Wilson confidence intervals (95%-CI) or 95% Bayesian credibility intervals, respectively. The CI is marked as [reg.] for seroprevalence and SDR, when case prevalence based on registered infections exceeded standardized seroprevalence. In those cases SDR was set to 1.0 and registered case numbers were used for further calculations.

Sub group	Population at risk Tirschenreuth #; [%]			Population at risk Cohort #; [%]			standardized new seropositive %; [95%-CI]			SDR ratio; [95% CI]			IFR %; [95%-CI]		
	BL	FU1	FU2	BL	FU1	FU2	BL	FU1	FU2	BL	FU1	FU2	BL	FU1	FU2
Overall	64643; [100]	58709; [100]	58288; [100]	4181; [100]	3162; [100]	2828; [100]	9.18; [8.34 - 10.09]	0.87; [reg.]	6.06; [5.24 - 7.00]	5.35; [4.78 - 5.99]	1.00; [reg.]	1.14; [1.00 - 1.32]	2.32; [1.92 - 2.82]	1.95; [0.96 - 3.97]	3.28; [2.60 - 4.14]
m	32239; [49.87]	29318; [49.94]	29105; [49.93]	2023; [48.39]	1488; [47.06]	1304; [46.11]	9.06; [7.89 - 10.39]	0.88; [reg.]	5.94; [4.78 - 7.35]	6.29; [5.32 - 7.41]	1.00; [reg.]	1.17; [1.00 - 1.46]	2.64; [2.04 - 3.43]	1.95; [0.72 - 5.31]	3.18; [2.27 - 4.47]
w	32404; [50.13]	29392; [50.06]	29183; [50.07]	2158; [51.61]	1674; [52.94]	1524; [53.89]	9.30; [8.14 - 10.59]	0.87; [reg.]	6.19; [5.09 - 7.51]	4.68; [4.02 - 5.44]	1.00; [reg.]	1.11; [1.00 - 1.36]	2.02; [1.53 - 2.68]	1.95; [0.74 - 5.26]	3.38; [2.46 - 4.65]
age group															
14 to 19	3994; [6.18]	3570; [6.08]	3522; [6.04]	225; [5.38]	152; [4.81]	140; [4.95]	10.62; [7.24 - 15.33]	1.33; [0.37 - 4.69]	13.64; [8.92 - 20.30]	11.51; [6.97 - 18.75]	1.44; [1.00 - 5.31]	2.48; [1.59 - 3.77]	0.00; [0.00 - 0.90]	0.00; [0.00 - 10.36]	0.00; [0.00 - 0.80]
20 to 29	8146; [12.60]	7416; [12.63]	7354; [12.62]	523; [12.51]	358; [11.32]	299; [10.57]	8.96; [6.80 - 11.72]	1.28; [reg.]	8.39; [5.76 - 12.09]	7.39; [5.27 - 10.30]	1.00; [reg.]	1.44; [1.00 - 2.10]	0.14; [0.03 - 0.78]	0.00; [0.00 - 4.49]	0.00; [0.00 - 0.62]
30 to 39	8430; [13.04]	7869; [13.40]	7869; [13.50]	583; [13.94]	410; [12.97]	358; [12.66]	6.65; [4.90 - 8.98]	0.80; [reg.]	6.16; [4.11 - 9.15]	5.58; [3.90 - 7.97]	1.00; [reg.]	1.14; [1.00 - 1.70]	0.00; [0.00 - 0.67]	0.00; [0.00 - 7.17]	0.00; [0.00 - 0.79]
40 to 49	8782; [13.59]	7909; [13.47]	7819; [13.41]	601; [14.37]	442; [13.98]	397; [14.04]	9.94; [7.80 - 12.59]	1.14; [0.49 - 2.63]	6.65; [reg.]	5.62; [4.21 - 7.45]	1.29; [1.00 - 3.06]	1.00; [reg.]	0.00; [0.00 - 0.43]	0.00; [0.00 - 4.71]	0.19; [0.04 - 1.12]
50 to 59	12813; [19.82]	11524; [19.63]	11440; [19.63]	875; [20.93]	685; [21.66]	617; [21.82]	10.06; [8.24 - 12.23]	0.89; [reg.]	7.53; [5.70 - 9.88]	6.02; [4.74 - 7.61]	1.00; [reg.]	1.36; [1.02 - 1.80]	0.47; [0.21 - 1.04]	0.00; [0.00 - 4.08]	0.58; [0.25 - 1.42]
60 to 69	10412; [16.11]	9531; [16.23]	9501; [16.3]	749; [17.91]	622; [19.67]	569; [20.12]	8.46; [6.67 - 10.67]	0.69; [reg.]	3.86; [reg.]	6.30; [4.73 - 8.39]	1.00; [reg.]	1.00; [reg.]	1.03; [0.53 - 2.04]	1.52; [0.28 - 10.61]	3.54; [1.81 - 6.95]
70 to 79	6772; [10.48]	6224; [10.60]	6186; [10.61]	420; [10.05]	341; [10.78]	316; [11.17]	8.10; [5.85 - 11.10]	0.60; [0.17 - 2.13]	3.67; [reg.]	3.78; [2.62 - 5.39]	1.28; [1.00 - 4.79]	1.00; [reg.]	6.38; [4.04 - 10.16]	2.69; [0.40 - 22.63]	10.57; [5.37 - 20.96]
at least 80	5294; [8.19]	4667; [7.95]	4597; [7.89]	205; [4.90]	152; [4.81]	132; [4.67]	11.84; [8.11 - 16.99]	1.50; [0.44 - 4.95]	6.57; [reg.]	2.84; [1.90 - 4.20]	1.27; [1.00 - 4.29]	1.00; [reg.]	14.04; [9.23 - 21.63]	11.43; [2.90 - 42.39]	24.17; [12.55 - 47.61]

Supplementary Table 6 (supplement to Figure 14, part 2). Numbers of registered SARS-CoV-2 infections and related death case in the county Tirschenreuths. Given are the general population of Tirschenreuth as of the census 2019 (14 years and older) as well as registered deaths andSARS-CoV-2 infections for BL, the period beween BL and FU1 (FU1) and the period between FU1 and FU2 (FU2). Numbers are shown for the overall county population as well as the indicated age groups, sexes and municipalities.

	Tirschenreuth	**Registered deaths #**			**Registered infections #**		
	population #	**BL**	**FU1**	**FU2**	**BL**	**FU1**	**FU2**
overall	64643	138	10	116	1109	513	3100
age group							
14 to 19	3994	0	0	0	37	33	194
20 to 29	8146	1	0	0	99	95	428
30 to 39	8430	0	0	0	101	63	427
40 to 49	8782	0	0	1	156	70	520
50 to 59	12813	6	0	5	214	102	635
60 to 69	10412	9	1	13	139	66	367
70 to 79	6772	35	1	24	145	29	227
over 80	5294	87	8	73	218	55	302
sex							
m	32239	77	5	55	464	257	1473
w	32404	61	5	61	645	256	1627
municipality							
Bad Neualbenreuth	1186	0	0	5	10	4	55
Brand	1025	0	0	1	5	2	65
Bärnau	2795	2	0	4	45	33	117
Ebnath	1710	0	0	0	3	7	52
Erbendorf	4476	21	0	6	93	22	187
Falkenberg	822	0	0	2	11	3	38
Friedenfels	1103	1	1	1	19	2	53
Fuchsmühl	1387	8	0	0	54	5	59
Immenreuth	1600	0	0	2	1	17	132
Kastl	1208	1	0	0	5	10	50
Kemnath	4773	7	0	4	30	11	307
Konnersreuth	1501	9	0	3	60	14	58
Krummennaab	1299	2	0	0	34	8	36
Kulmain	1928	0	0	2	4	19	93
Leonberg	870	2	0	2	12	6	37
Mitterteich	5899	21	0	17	172	60	191
Mähring	1560	4	0	4	31	17	64
Neusorg	1810	2	1	4	17	16	77
Pechbrunn	1173	0	0	1	20	8	30
Plößberg	2835	15	0	1	85	21	151
Pullenreuth	1500	1	0	2	7	7	78
Reuth b.Erbendorf	994	0	1	2	16	12	50
Tirschenreuth	7807	15	5	30	145	80	516
Waldershof	3869	12	2	5	51	42	176
Waldsassen	5862	8	0	9	103	65	293
Wiesau	3651	7	0	9	75	22	135
Senior care homes							
without senior care home	20773	13	2	28	223	155	950
with senior care home	43870	125	8	88	885	358	2150

Supplementary Table 7 (Supplement to Supplemental Figure 6) Standardized % "ever seropositives" for the indicated intervals and subgroups

	standardized ever seropositive %; [CI]		
	until BL	**until FU1**	**until FU2**
Overall	9.18; [8.34-10.09]	9.97; [9.03-11.01]	15.43; [14.25-16.69]
m	9.06; [7.89-10.39]	9.86; [8.51-11.39]	15.21; [13.51-17.08]
w	9.30; [8.14-10.59]	10.09; [8.80-11.54]	15.65; [14.05-17.40]
Age group			
14 to 19	10.62; [7.24-15.33]	11.81; [7.84-17.41]	23.84; [18.16-30.63]
20 to 29	8.96; [6.80-11.72]	10.13; [7.54-13.47]	17.67; [14.14-21.86]
30 to 39	6.65; [4.90-8.98]	7.40; [5.32-10.21]	13.11; [10.22-16.67]
40 to 49	9.94; [7.80-12.59]	10.97; [8.52-14.02]	16.89; [13.83-20.47]
50 to 59	10.06; [8.24-12.23]	10.86; [8.85-13.26]	17.57; [14.99-20.48]
60 to 69	8.46; [6.67-10.67]	9.09; [7.16-11.48]	12.60; [10.27-15.37]
70 to 79	8.10; [5.85-11.10]	8.65; [6.20-11.94]	12.00; [9.04-15.76]
at least 80	11.84; [8.11-16.99]	13.17; [8.89-19.07]	18.87; [13.62-25.55]
Municipality			
Bad Neualbenreuth	7.65; [3.77-14.88]	7.98; [3.73-16.29]	14.07; [8.09-23.34]
Brand	5.16; [1.78-14.02]	5.35; [1.73-15.34]	14.00; [6.95-26.19]
Bärnau	9.51; [6.06-14.63]	12.25; [8.02-18.28]	16.44; [11.35-23.22]
Ebnath	6.25; [2.47-14.91]	8.20; [3.38-18.58]	11.24; [5.24-22.48]
Erbendorf	8.22; [5.47-12.19]	8.72; [5.63-13.26]	13.08; [9.12-18.41]
Falkenberg	2.73; [0.76-9.37]	4.40; [1.46-12.50]	11.71; [5.83-22.12]
Friedenfels	5.99; [2.62-13.13]	6.17; [2.52-14.32]	10.97; [5.56-20.50]
Fuchsmühl	14.61; [8.69-23.52]	14.97; [8.52-24.96]	19.85; [12.01-31.01]
Immenreuth	1.00; [0.18-5.45]	2.06; [0.52-7.85]	10.22; [5.27-18.91]
Kastl	2.52; [0.71-8.52]	3.34; [1.02-10.39]	8.17; [3.69-17.12]
Kemnath	1.88; [0.83-4.17]	2.11; [0.93-4.71]	10.90; [7.49-15.60]
Konnersreuth	12.73; [7.72-20.28]	13.66; [8.28-21.70]	18.24; [11.71-27.29]
Krummennaab	12.26; [6.86-20.96]	13.76; [7.60-23.64]	16.77; [9.69-27.46]
Kulmain	5.22; [2.57-10.34]	6.21; [2.94-12.62]	10.98; [6.24-18.61]
Leonberg	20.88; [12.95-31.87]	21.57; [12.99-33.62]	34.07; [22.96-47.27]
Mitterteich	19.03; [15.38-23.30]	20.05; [16.01-24.80]	25.07; [20.53-30.23]
Mähring	18.32; [12.14-26.71]	19.41; [12.74-28.44]	23.46; [15.97-33.07]
Neusorg	7.09; [3.81-12.81]	8.16; [4.29-14.99]	12.42; [7.28-20.39]
Pechbrunn	12.71; [6.87-22.33]	15.98; [9.06-26.65]	21.89; [12.94-34.57]
Plößberg	7.06; [4.27-11.46]	7.80; [4.57-13.02]	13.13; [8.94-18.87]
Pullenreuth	3.78; [1.50-9.21]	4.25; [1.58-10.92]	9.43; [4.74-17.87]
Reuth b.Erbendorf	22.62; [14.49-33.52]	23.82; [15.06-35.55]	32.83; [22.29-45.42]
Tirschenreuth	10.64; [8.32-13.51]	11.86; [9.22-15.12]	18.47; [15.18-22.27]
Waldershof	3.80; [1.92-7.40]	4.89; [2.54-9.21]	11.63; [7.57-17.46]
Waldsassen	9.04; [6.47-12.48]	10.14; [7.21-14.09]	15.91; [12.11-20.61]
Wiesau	8.62; [5.64-12.97]	9.79; [6.28-14.94]	16.14; [11.51-22.18]
Senior care homes			
without senior care home	8.71; [7.34-10.31]	9.59; [8.04-11.41]	14.25; [12.32-16.42]
with senior care home	9.40; [8.37-10.54]	10.22; [9.06-11.51]	16.05; [14.60-17.62]

Supplementary Table 8 Standardized (N-based) period seroprevalence by municipality at Baseline (BL), at FU1 (period between BL and FU1) and FU2 (period between FU1 and FU2). Shown are the population at risk in the general Tirschenreuth population and the analyzed cohort as absolute numbers and percentages of the according group. Further shown is standardized and corrected seroprevalence (based on N-antibodies) (%) in the indicated municipalities with the 95% Wilson confidence intervals (95%-CI). The CI is marked as [registered] for seroprevalence, when case prevalence exceeded seoprevalence, as SDR was then set to 1.0 and registered cases were used for all calculations.

Subgroup	**Population at risk Tirschenreuth #; [%]**			**Population at risk Cohort #; [%]**			**new seropositive %; [95%-CI]**		
Municipality	**BL**	**FU1**	**FU2**	**BL**	**FU1**	**FU2**	**BL**	**FU1**	**FU2**
Bad Neualbenreuth	1186; [1.83]	1095; [1.87]	1095; [1.88]	93; [2.22]	69; [2.18]	66; [2.33]	7.65; [3.77 - 14.88]	0.37; [registered]	6.61; [2.70 - 15.30]
Brand	1025; [1.59]	972; [1.66]	972; [1.67]	59; [1.41]	47; [1.49]	45; [1.59]	5.16; [1.78 - 14.02]	0.21; [registered]	9.14; [3.66 - 21.05]
Bärnau	2795; [4.32]	2529; [4.31]	2453; [4.21]	183; [4.38]	141; [4.46]	123; [4.35]	9.51; [6.06 - 14.63]	3.03; [1.22 - 7.33]	4.77; [registered]
Ebnath	1710; [2.65]	1603; [2.73]	1570; [2.69]	65; [1.55]	51; [1.61]	49; [1.73]	6.25; [2.47 - 14.91]	2.09; [0.39 - 10.50]	3.31; [registered]
Erbendorf	4476; [6.92]	4108; [7.00]	4108; [7.05]	262; [6.27]	195; [6.17]	175; [6.19]	8.22; [5.47 - 12.19]	0.54; [registered]	4.78; [2.48 - 9.03]
Falkenberg	822; [1.27]	800; [1.36]	786; [1.35]	74; [1.77]	62; [1.96]	55; [1.94]	2.73; [0.76 - 9.37]	1.71; [0.32 - 8.74]	7.64; [3.08 - 17.74]
Friedenfels	1103; [1.71]	1037; [1.77]	1036; [1.78]	86; [2.06]	67; [2.12]	63; [2.23]	5.99; [2.62 - 13.13]	0.19; [registered]	5.12; [registered]
Fuchsmühl	1387; [2.15]	1184; [2.02]	1184; [2.03]	87; [2.08]	62; [1.96]	53; [1.87]	14.61; [8.69 - 23.52]	0.42; [registered]	5.75; [1.99 - 15.49]
Immenreuth	1600; [2.48]	1584; [2.70]	1584; [2.72]	100; [2.39]	83; [2.62]	75; [2.65]	1.00; [0.18 - 5.45]	1.07; [registered]	8.33; [registered]
Kastl	1208; [1.87]	1178; [2.01]	1178; [2.02]	83; [1.99]	70; [2.21]	61; [2.16]	2.52; [0.71 - 8.52]	0.85; [registered]	4.99; [1.72 - 13.59]
Kemnath	4773; [7.38]	4683; [7.98]	4683; [8.03]	291; [6.96]	251; [7.94]	217; [7.67]	1.88; [0.83 - 4.17]	0.23; [registered]	8.99; [5.86 - 13.54]
Konnersreuth	1501; [2.32]	1310; [2.23]	1310; [2.25]	109; [2.61]	88; [2.78]	80; [2.83]	12.73; [7.72 - 20.28]	1.07; [registered]	5.30; [2.14 - 12.57]
Krummennaab	1299; [2.01]	1140; [1.94]	1120; [1.92]	84; [2.01]	62; [1.96]	58; [2.05]	12.26; [6.86 - 20.96]	1.71; [0.32 - 8.74]	3.49; [0.97 - 11.79]
Kulmain	1928; [2.98]	1827; [3.11]	1827; [3.13]	136; [3.25]	96; [3.04]	82; [2.9]	5.22; [2.57 - 10.34]	1.04; [registered]	5.09; [registered]
Leonberg	870; [1.35]	688; [1.17]	688; [1.18]	69; [1.65]	46; [1.45]	39; [1.38]	20.88; [12.95 - 31.87]	0.87; [registered]	15.95; [7.62 - 30.38]

Mitterteich	5899; [9.13]	4777; [8.14]	4716; [8.09]	376; [8.99]	252; [7.97]	223; [7.89]	19.03; [15.38 - 23.30]	1.26; [0.44 - 3.54]	6.28; [3.78 - 10.26]
Mähring	1560; [2.41]	1274; [2.17]	1274; [2.19]	107; [2.56]	78; [2.47]	72; [2.55]	18.32; [12.14 - 26.71]	1.33; [registered]	5.02; [registered]
Neusorg	1810; [2.8]	1682; [2.86]	1662; [2.85]	131; [3.13]	96; [3.04]	81; [2.86]	7.09; [3.81 - 12.81]	1.16; [0.22 - 5.85]	4.63; [registered]
Pechbrunn	1173; [1.81]	1024; [1.74]	986; [1.69]	72; [1.72]	57; [1.8]	44; [1.56]	12.71; [6.87 - 22.33]	3.75; [1.07 - 12.26]	7.03; [2.46 - 18.50]
Plößberg	2835; [4.39]	2635; [4.49]	2616; [4.49]	202; [4.83]	149; [4.71]	138; [4.88]	7.06; [4.27 - 11.46]	0.80; [registered]	5.77; [registered]
Pullenreuth	1500; [2.32]	1443; [2.46]	1443; [2.48]	109; [2.61]	80; [2.53]	71; [2.51]	3.78; [1.50 - 9.21]	0.49; [registered]	5.40; [registered]
Reuth b.Erbendorf	994; [1.54]	769; [1.31]	768; [1.32]	72; [1.72]	49; [1.55]	44; [1.56]	22.62; [14.49 - 33.52]	1.56; [registered]	11.82; [5.24 - 24.53]
Tirschenreuth	7807; [12.08]	6976; [11.88]	6881; [11.81]	545; [13.04]	409; [12.93]	374; [13.22]	10.64; [8.32 - 13.51]	1.36; [0.61 - 3.02]	7.50; [registered]
Waldershof	3869; [5.99]	3722; [6.34]	3720; [6.38]	203; [4.86]	165; [5.22]	146; [5.16]	3.80; [1.92 - 7.40]	1.13; [registered]	7.09; [3.94 - 12.45]
Waldsassen	5862; [9.07]	5332; [9.08]	5332; [9.15]	354; [8.47]	271; [8.57]	244; [8.63]	9.04; [6.47 - 12.48]	1.22; [registered]	6.41; [3.96 - 10.21]
Wiesau	3651; [5.65]	3336; [5.68]	3294; [5.65]	229; [5.48]	166; [5.25]	150; [5.30]	8.62; [5.64 - 12.97]	1.27; [0.36 - 4.39]	7.05; [3.93 - 12.30]

Supplementary Table 9 Sensitivity analysis of our SDR estimates for Baseline (BL) Follow up 1 (FU1) and Follow up 2 (FU2), calculated with an assumed (lower bound) specificity of 99.5% for PCR testing and thus registered cases at health authorities. Missing a better estimate, the total number of tests in the county was derived from the fraction tested within our cohort and standardized to the whole population.

	SURVEILLANCE DETECTION RATIO-SENSITIVITY ANALYSIS		
SUBGROUP	**BL**	**FU1**	**FU2**
	sens, [prev; % change]	sens, [prev; % change]	sens, [prev; % change]
OVERALL	5.51, [5.35, 3.07]	0.99, [0.82, 20.42]	1.19, [1.14, 4.17]
M	6.49, [6.3, 3.11]	1.00, [0.83, 20.66]	1.22, [1.17, 4.17]
W	4.81, [4.67, 3.04]	0.98, [0.81, 20.75]	1.16, [1.11, 4.16]
14 TO 19	11.79, [11.47, 2.78]	1.76, [1.44, 22.22]	2.58, [2.48, 4.3]
20 TO 29	7.6, [7.37, 3.13]	0.79, [0.65, 20.25]	1.5, [1.44, 4.14]
30 TO 39	5.72, [5.55, 3.06]	N/A, [N/A, 0]	1.18, [1.14, 4.15]
40 TO 49	5.78, [5.6, 3.31]	1.55, [1.29, 20.69]	0.91, [0.88, 4.21]
50 TO 59	6.2, [6.02, 2.88]	0.99, [0.82, 20]	1.41, [1.36, 4.1]
60 TO 69	6.52, [6.34, 2.96]	0.55, [0.46, 20]	0.99, [0.95, 4.26]
70 TO 79	3.89, [3.78, 2.84]	1.55, [1.28, 20.83]	0.83, [0.79, 4.13]
AT LEAST 80	2.97, [2.88, 3.32]	1.56, [1.27, 22.22]	0.37, [0.35, 4.14]

Supplementary Table 10 (Supplement to Figure 15) Standardized (N-based) Seroprevalence, SDR and IFR in municipalities with and w/o SCH at Baseline (BL), at FU1 (period between BL and FU1) and FU2 (period between FU1 and FU2). Shown are the population at risk in the general Tirschenreuth population and the analyzed cohort as absolute numbers and percentages of the according group. Further shown is standardized and corrected seroprevalence (based on N-antibodies) (%) in the indicated municipalities with the 95% Wilson confidence intervals (95%-CI) as well as SDR and IFR with 95% Bayesian credibility intervals. The CI is marked as [reg.] for seroprevalence and SDR, when case prevalence exceeded seoprevalence, as SDR was then set to 1.0 and registered cases were used for all calculations.

Subgroup	**Population at risk Tirschenreuth #; [%]**			**Population at risk Cohort #; [%]**			**new seropositive %; [95%-CI]**			**SDR #; [95%-CI]**			**IFR %; [95%-CI]**		
	BL	**FU1**	**FU2**	**BL**	**FU1**	**FU2**	**BL**	**FU1**	**FU2**	**BL**	**FU1**	**FU2**	**BL**	**FU1**	**FU2**
without senior care home	20773; [32.13]	18964; [32.30]	18780; [32.22]	1392; [33.29]	1058; [33.46]	947; [33.49]	8.71; [7.34 – 10.31]	0.97; [0.53 – 1.76]	5.15; [3.91 – 6.74]	8.10; [6.53 – 10.03]	1.18; [1.00 – 2.19]	1.02; [1.00 – 1.34]	0.72; [0.41 – 1.27]	1.09; [0.29 – 4.53]	2.90; [1.84 – 4.59]
with senior care home	43870; [67.87]	39746; [67.70]	39508; [67.78]	2789; [66.71]	2104; [66.54]	1881; [66.51]	9.40; [8.37 – 10.54]	0.90; [reg.]	6.50; [5.47 – 7.70]	4.66; [4.08 – 5.32]	1.00; [reg.]	1.19; [1.00 – 1.42]	3.03; [2.46 – 3.74]	2.23; [1.00 – 5.02]	3.43; [2.63 – 4.49]

Supplementary Table 11 (Supplement to Figure 16) Standardized (S-based) period seroprevalence at Baseline (BL), at FU1 (period between BL and FU1) and FU2 (period between FU1 and FU2). Shown are the population at risk in the general Tirschenreuth population and the analyzed cohort as absolute numbers as well as absolute numbers off all S-antibody positive, S&N positive and only S positive participants. Further shown is standardized and corrected seroprevalence (based on S-antibodies) (%) in the indicated groups with the 95% Wilson confidence intervals (95%-CI).

Subgroup	population at risk # County [# Cohort]	S-antibody positive # total [# S&N, # only S]	Standardized total S positive % [CI]	Standardized S&N positive % [CI]	Standardized only S positive % [CI]
overall	64379 [3371]	1503 [515, 988]	45.79 [44.11-47.47]	15.06 [13.89-16.31]	30.53 [29.00-32.10]
sex					
m	32102 [1559]	674 [242, 432]	44.48 [42.03-46.96]	15.29 [13.59-17.16]	28.96 [26.76-31.26]
w	32277 [1812]	829 [273, 556]	47.08 [44.79-49.39]	14.83 [13.27-16.54]	32.09 [29.98-34.28]
age group					
14 to 19	3994 [177]	51 [44, 7]	28.77 [22.60-35.83]	24.50 [18.75-31.33]	3.80 [1.83-7.73]
20 to 29	8145 [374]	129 [68, 61]	34.47 [29.84-39.43]	17.87 [14.32-22.07]	16.29 [12.90-20.38]
30 to 39	8430 [420]	135 [53, 82]	32.11 [27.83-36.72]	12.34 [9.53-15.83]	19.54 [16.03-23.60]
40 to 49	8781 [488]	210 [81, 129]	43.06 [38.74-47.49]	16.29 [13.28-19.83]	26.53 [22.81-30.62]
50 to 59	12802 [737]	296 [132, 164]	40.18 [36.70-43.76]	17.60 [15.02-20.51]	22.30 [19.45-25.45]
60 to 69	10389 [652]	263 [78, 185]	40.35 [36.65-44.16]	11.69 [9.44-14.38]	28.49 [25.16-32.08]
70 to 79	6712 [360]	274 [39, 235]	76.32 [71.66-80.41]	10.57 [7.80-14.17]	65.82 [60.77-70.53]
over 80	5126 [163]	145 [20, 125]	89.23 [83.54-93.12]	11.99 [7.86-17.87]	77.35 [70.34-83.11]
senior care homes					
without SCH	20730 [1114]	459 [155, 304]	42.25 [39.39-45.18]	13.49 [11.61-15.62]	28.58 [26.00-31.30]
with SCH	43649 [2257]	1044 [360, 684]	47.46 [45.41-49.53]	15.81 [14.36-17.37]	31.45 [29.57-33.40]

5.5 Manuscript 4: ”Comparative Immunogenicity of COVID-19 Vaccines in a Population-Based Cohort Study with SARS-CoV-2-Infected and Uninfected Participants”

5.5.1 Abstract

To assess vaccine immunogenicity in non-infected and previously infected individuals in a real-world scenario, SARS-CoV-2 antibody responses were determined during follow-up 2 (April 2021) of the population-based Tirschenreuth COVID-19 cohort study comprising 3378 inhabitants of the Tirschenreuth county aged 14 years or older. Seronegative participants vaccinated once with Vaxzevria, Comirnaty, or Spikevax had median neutralizing antibody titers ranging from ID50 = 25 to 75. Individuals with two immunizations with Comirnaty or Spikevax had higher median ID50s (of 253 and 554, respectively). Regression analysis indicated that both increased age and increased time since vaccination independently decreased RBD binding and neutralizing antibody levels. Unvaccinated participants with detectable N-antibodies at baseline (June 2020) revealed a median ID50 of 72 at the April 2021 follow-up. Previously infected participants that received one dose of Vaxzevria or Comirnaty had median ID50 to 929 and 2502, respectively. Individuals with a second dose of Comirnaty given in a three-week interval after the first dose did not have higher median antibody levels than individuals with one dose. Prior infection also primed for high systemic IgA levels in response to one dose of Comirnaty that exceeded IgA levels observed after two doses of Comirnaty in previously uninfected participants. Neutralizing antibody levels targeting the spike protein of Beta and Delta variants were diminished compared to the wild type in vaccinated and infected participants.

5.5.2 Introduction

Currently, there are four widely used COVID-19 vaccines in Europe and their immunogenicity has been assessed during clinical development[37,40,43] and post-marketing follow-up studies[38,336–338]. Different study populations, assays, and time points of analysis hinder direct comparisons between the different vaccines. Investigations on the immune responses after mix-and-match regimens also included conventional homologous immunizations enabling comparisons between different vaccines, but are limited to time points of analyses immediately after the second immunization and particular study populations younger than 60 years of age[339–342]. We therefore determined antibody responses to different vaccines in a population-based cohort under real-world conditions. The cohort was established in June 2020 to assess seroprevalence for SARS-CoV-2 antibodies in the county of Tirschenreuth[201], which was one of the hardest-hit regions in Germany early during the pandemic. The 4201 participants were aged 14 years and older and were representative of the county’s population[201]. Two follow-up surveys including serum sampling and a questionnaire on the participants’ SARS-CoV-2 infection and vaccination history were performed in November 2020 and April 2021 with 3546 and 3391 participants, respectively. Seroprevalence data from the November 2020 and April 2021 sampling

revealed a cumulative N-antibody seropositivity of 8.93% and 13.30%, respectively (Einhauser et al., manuscript in preparation[343]). Since the vaccination roll-out in Germany started at the end of December 2020, the April 2021 samples allowed to assess the antibody responses after vaccination and to compare them to those induced by infection or immunization after infection. Dependence of the antibody responses on the age of vaccinees and on the time since the second immunization were also of interest considering the current need for booster immunizations.

5.5.3 Material and Methods

5.5.3.1 Cohort

The cohort at baseline was described thoroughly in Wagner et al. 2021. In brief, 6540 of 6608 randomly selected inhabitants of Tirschenreuth aged 14 years or older were invited to participate in the TiKoCo study in June 2020. Overall, 4203 individuals participated between 28 June and 13 July 2020 by giving 5.7 mL blood and filling out a questionnaire, yielding a net response of 64.26%, with a higher response among the age group 20–74 years compared to those 14–19 years or 75+ years of age and slight differences amongst the 26 local municipalities. The 4203 participants included 48.3% men; age ranged from 14 to 102 years (refer to Table 1 in Wagner et al. [201] for more detailed information). Of the 4203 participants at baseline, 3534 successfully participated in the first follow-up between 16 November and 27 November 2020, while 3378 participated in the second follow-up (between 19 April and 30 April 2021), yielding a follow-up response of 84.1 and 80.4%, respectively. Overall, 3196 participants took part in all three rounds of investigation, leading to a full participation rate of 76.0%. (Einhauser et al. manuscript in preparation[343]). For vaccination, self-reports on vaccination status, type of vaccine, and date of vaccination were obtained by questionnaire at T3. Age at baseline was determined by data from population registries and the time since vaccination was determined from the time between follow-up 2 and the reported date of vaccination.

The TiKoCo study was approved by the Ethics Committee of the University of Regensburg, Germany (vote 20-1867-101) and adopted by the Ethics Committee of the University of Erlangen (vote 248_20 Bc). The study complies with the 1964 Helsinki declaration and its later amendments. All participants provided written informed consent.

5.5.3.2 Antibody Assays

Participants with prior SARS-CoV-2 infection were identified by the detection of antibodies to nucleoprotein N. The Elecsys Anti-SARS-CoV-2 N test (Roche Diagnostics GmbH, Mannheim, Germany)[276] detecting all classes of immunoglobulins directed to the nucleoprotein N was operated on the COBAS pro e 801 module according to the manufacturer's recommendations. Cutoff values were chosen as specified by the manufacturer. Participants without detectable levels of N antibodies at all study time points were considered uninfected and assigned the N antibody status T0. Participants

seropositive for N antibodies at baseline (June 2020) were assigned the N-antibody status T1. T3 participants were seronegative at baseline and at the follow-up 1 (November 2020) but converted to detectable N antibody levels at follow-up 2 (April 2021).

To assess protective antibody responses after infection and immunization, four different assays were performed: (i) The Elecsys Anti-SARS-CoV-2 S test (Roche Diagnostics GmbH, Mannheim, Germany)[277] detecting complete Ig directed to spike (S) protein receptor-binding domain (RBD) was operated on the COBAS pro e 801 module according to the manufacturer's recommendations. Cutoff values were chosen as specified by the manufacturer. According to information provided by Roche[277,322], 1 U/mL (Elecsys) corresponds to 1 BAU/mL (WHO standard). (ii) Our validated in-house ELISA detecting IgA antibody responses to the SARS-CoV-2 spike protein's receptor-binding domain (RBD) was performed as described earlier[260]. (iii) The neutralization assay using the Vesicular Stomatitis Virus (VSV -Δ G*FLuc) pseudotyped with wt-SARS-CoV-2-Spike-ΔER was performed as described earlier[322]. In brief, an inoculum of 25,000 ffu was neutralized with a 2-fold serum dilution series for 1 h, and luciferase activity was determined 20 h post infection of HEK293T-ACE2 + -cells using BrightGlo (Promega Corp, Madison, WI, USA). iv) The capacity of antisera to neutralize different VoCs was determined using a lentiviral pseudotype assay. As described previously[344,345], lentiviral vector particles expressing luciferase and pseudotyped with the spike protein of the different VOCs were produced on HEK 293T cells (ECACC 12022001). The neutralization activity of serial dilutions of sera was analyzed on a HEK293T cell line overexpressing-ACE2 48 h after infection[346]. The cells were exposed to a lentiviral pseudotype dose resulting in 2.5–10 × 104 RLU/s in the absence of serum. The 50% inhibitory dilution (ID50) of the sera was calculated with Prism 9 GraphPad (San Diego, CA, USA).

5.5.3.3 Statistical Analysis

We compared antibody responses in the different vaccine groups and groups of participants with different infection statuses by non-parametric tests. For each research question regarding two groups of independent individuals, we applied a Mann–Whitney test. For questions regarding more than two groups of independent individuals, a Kruskal–Wallis test for the overall group comparison was performed just followed by a Mann–Whitney test for pairwise comparisons. Significance was judged at 0.05, except for pairwise tests implying multiple testing where a Bonferroni-corrected level of 0.05 divided by the number of tests was applied. For comparisons including the same individuals comparing different measurements, we applied the Wilcoxon rank-sum test. These analyses were performed with Prism 9 GraphPad.

5.5.3.4 Regression Analysis

We used generalized additive regression to jointly investigate the association of quantitative antibody levels with time after vaccination and age (measured at baseline) among study participants vaccinated

twice with Comirnaty. We estimated a separate model for RBD binding and neutralizing antibodies (ID50). For each, we modeled the quantitative antibody levels in a Gaussian model with log-link (assumption of a conditional log-normal distribution for the quantitative antibodies) and estimated non-linear associations with the mean using a thin plate regression spline per covariate. Smoothing parameter selection was based on restricted maximum likelihood (REML). To investigate the possibility of differing trajectories of antibody decrease with time for individuals of varying age, we also estimated a bivariate spline-surface and compared model fit based on the explained deviance. We illustrated the model results by inspecting the estimated (non-linear) associations and visualizing the predicted antibody levels over the range of observed times after vaccination (time between second vaccination and blood drawn at the second follow-up, 14–100 days) for an age of 30, 55, or 80 years, respectively. The models were estimated using the mgcv-package in R [347,348].

For comparisons of proportions, two-sided Fisher's exact tests were performed by an online tool at https://www.langsrud.com/stat/fisher.htm (accessed on 21/12/2021). p-values were judged at Bonferroni-corrected significance level when multiple testing was implied.

5.5.4 Results

5.5.4.1 Antibody Responses Induced by the Various Vaccines among Previously Infected Individuals

The antibody response after infection with SARS-CoV-2 was determined as a benchmark for the immunogenicity of vaccines. In sera from the April 2021 visit (T3), we evaluated the neutralizing and the spike protein RBD binding antibody levels (Roche Elecsys Anti-SARS-CoV-2 S test) after infection in individuals that were unvaccinated as well as in individuals that were vaccinated.

First, we compared the sub-cohort of unvaccinated participants that were N-antibody positive already at the June 2020 visit (T1, time to blood drawn at T3 > 9 months, n = 227) with the sub-cohort of unvaccinated participants that seroconverted for N antibodies between the November 2020 (T2) and the April 2021 visit (T3, n = 164). This recent seroconverter group had lower RBD binding antibody levels but higher neutralizing antibody levels than the sub-cohort that had been infected at least 9 months before blood sampling (T3 versus T1) (**Figure 17A,B**; RBD median = 73 versus 171; ID50 median = 140 versus 72). Of note, participants of the sub-cohort infected >9 months ago may include a small percent-age of individuals reinfected within the last 9 months before blood drawn at T3.

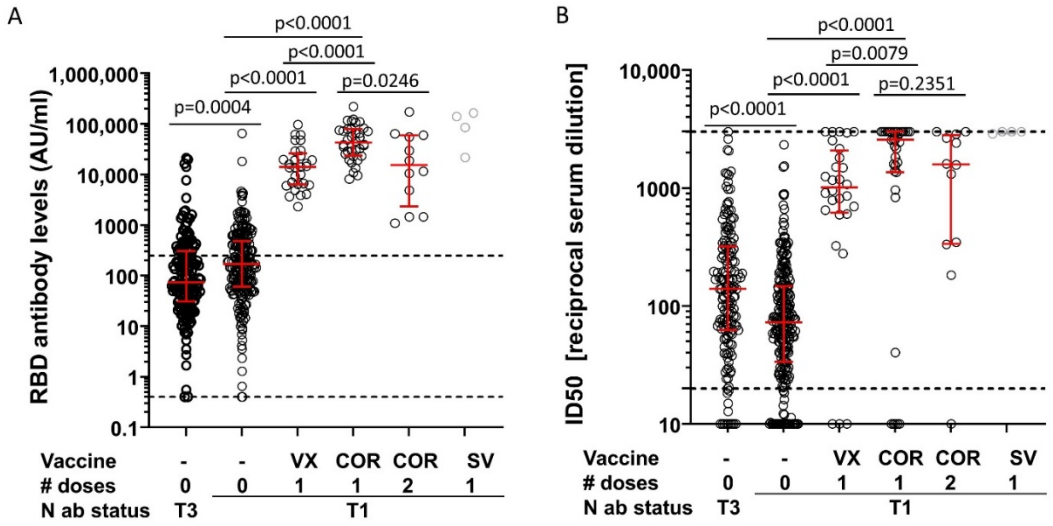

Figure 17 Antibody responses in infected participants. Shown are antibody levels to the receptor-binding domain (RBD) of the S protein (Roche Elecsys Anti-SARS-CoV-2 S test; arbitrary units AU) (A) and neutralizing antibody levels (ID50) (B) in seropositive participants receiving the indicated number of doses of Vaxzevria (VX), Comirnaty (COR), or SpikeVax (SV). Median and interquartile range are indicated by red bars. The Kruskal–Wallis test including all five groups with more than six participants indicated significant differences for the RBD and neutralizing antibody levels ($p < 0.0001$ for both, judged at 5% significance level). Pairwise comparisons were performed to (i) analyze a potential waning of immune responses after infection (0 dose T3 vs 0 dose T1), (ii) determine and compare the effect of one dose of Vaxzevria and Corminaty (0 dose T1 vs 1 dose VX vs 1 dose COR) and (iii) explore the effect of a second dose of Cormirnaty (1 dose COR vs 2 dose COR). p-values of these pairwise group comparisons with the Mann–Whitney test are shown (judged for significance at a Bonferroni-corrected level of 0.05/5 = 0.01 to account for 5 tests). N antibody (ab) status: T1: participants that were N-antibody positive already at the June 2020 visit; T3: participants negative for N antibodies at the June and November 2020 visits, but positive at the April 2021 visit. Dashed lines in (A) mark the upper and lower limits of the linear range of the assay, the dashed line in (B) mark the upper and lower limits of detection.

Supplementary Table **12**A,B provide number of participants, basic demographic characteristics and the median time interval between the last immunization and blood sampling. # doses indicates the number of applied doses.

Second, to assess antibody response after vaccination in previously infected participants, we restricted the analysis to participants that were N-antibody positive at the June 2020 visit (T1), since this excluded the possibility that participants were immunized prior to a SARS-CoV-2 infection. The RBD and neutralizing antibody levels were then compared between those that were not vaccinated and those receiving one vaccination with Vaxzevria or Comirnaty. Demographic characteristics for the different sub-cohorts, sample size by group, and median time between last immunization and blood sampling are summarized in

Supplementary Table 12**A,B**. Clearly, a single immunization with Vaxzevria or Comirnaty strongly enhanced the median RBD antibody levels even above the upper limit of the linear range of the assay[277] (**Figure 17A**). Median neutralizing antibody levels also increased more than 10-fold in previously infected participants receiving one vaccination with Comirnaty or one vaccination with Vaxzevria (**Figure 17B**). Overall, Vaxzevria appeared to be inferior in boosting RBD binding and neutralizing

antibody titers as compared to Comirnaty, but time since vaccination was longer for Vaxzevria and lower levels are potentially explained by antibody decline (

Supplementary Table 12**A,B**).

Third, to evaluate a potential beneficial effect of two doses of Comirnaty in previously infected participants, the antibody levels were compared between participants receiving a single dose of Comirnaty and those receiving a second Comirnaty immunization; second doses were given at a median time interval of 21 days (IQR: 21–21.5) after the first. Although limited by a small number of participants in the group receiving two doses of Comirnaty, individuals with a second dose did not have higher median antibody levels than individuals with one dose; in fact, lower median values were observed. However, these differences were not statistically significant when accounting for multiple testing and potentially due to individuals with two doses being older and vaccinated longer ago (

Supplementary Table 12**A,B**).

5.5.4.2 Antibody Responses Induced by the Various Vaccines among Previously Uninfected Individuals

In participants without prior SARS-CoV-2 infection (N-antibody negative at T1, T3, and if tested T2), median RBD antibody levels after one vaccination with Comirnaty, Vaxzevria, or Spikevax were at least two orders of magnitude lower (**Figure 18A**) than after one immunization in previously SARS-CoV-2-infected participants (**Figure 17A**). Median neutralizing antibodies were also at least one order of magnitude lower (**Figure 17B** and **Figure 18B**). Even after two immunizations of uninfected participants with Comirnaty of Spikevax, median RBD antibody levels and neutralizing antibody levels were lower than those observed in infected participants after a single immunization with the respective mRNA vaccines (**Figure** 17 and **Figure 18**).

With respect to potential differences in the immunogenicity of the different vaccines, we first compared RBD and neutralizing antibody levels after a single immunization. Spikevax induced significantly higher antibody levels than Comirnaty and Vaxzevria (**Figure 18A,B**). Pairwise comparison of Vaxzevria and Comirnaty revealed slightly higher median neutralizing antibody levels after Comirnaty immunization (**Figure 18B**), while no difference was observed for median RBD antibody levels (**Figure 18A**). Of note, individuals with one Spikevax immunization are younger than the group of individuals receiving one dose of Corminaty (median age 56 versus 68 years; **Supplementary Table 13**) and time since vaccination was slightly shorter compared to one VX group individuals (22 versus 34 days; **Supplementary Table 13**).

Second, we compared individuals vaccinated twice with individuals vaccinated once with the respective vaccine. Individuals with two immunizations with Comirnaty and Spikevax had substantially higher median RBD and neutralizing antibody levels than individuals with one immunization with the respective vaccine type (**Figure 18 A, B**; Mann–Whitney test $p < 0.0001$ for both).

Third, median RBD binding antibody levels were also significantly higher after two Spikevax immunizations than after two doses of Comirnaty (Mann–Whitney p < 0.0001, **Figure 18A**). However, the difference in the median neutralizing antibody levels between the two groups did not reach statistical significance (Mann–Whitney p = 0.0501, **Figure 18B**); age and time since vaccination were similar for this group comparison (**Supplementary Table 13**).

Due to the longer time interval recommended between the two Vaxzevria immunizations, only a limited number of samples were available for two doses of Vaxzevria at the T3 assessment of this cohort.

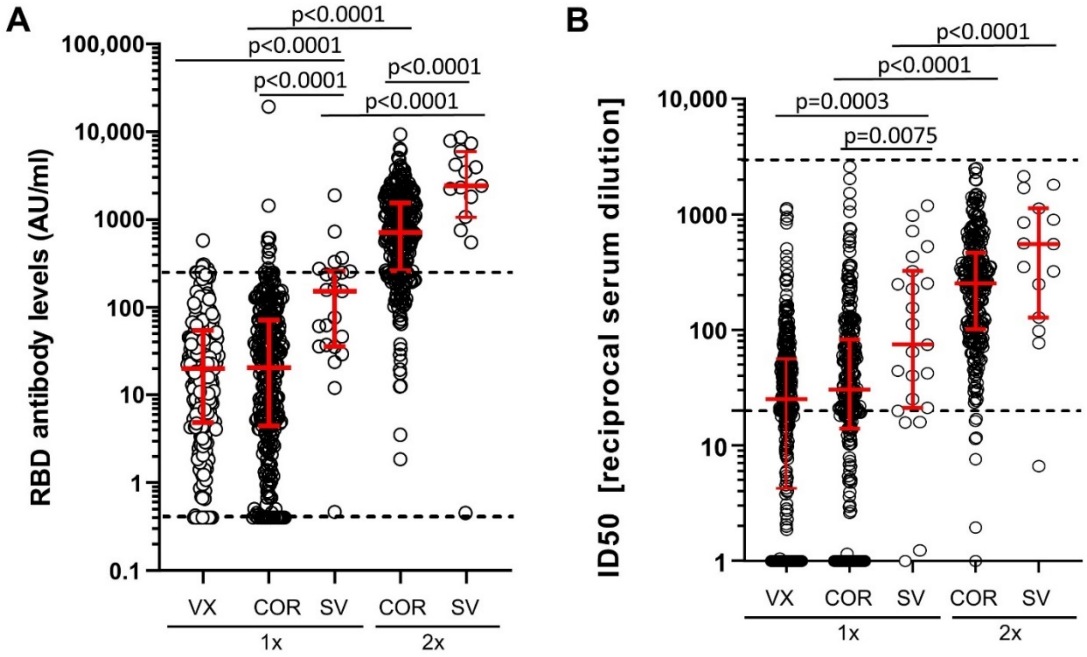

Figure 18 RBD binding and neutralizing antibodies in uninfected participants after vaccination. (A) Binding antibody levels to RBD (arbitrary units, AU) and (B) neutralizing antibodies (ID50) in N-antibody seronegative participants vaccinated once (1×) or twice (2×) with Vaxzevria (VX), Comirnaty (COR), or Spikevax (SV). The Kruskal–Wallis test including all five groups indicated significant differences for the RBD and neutralizing antibody levels ((A) p < 0.0001, (B) p < 0.0001, judged at 5% significance level). Pairwise comparisons were performed to (i) compare antibody response to one vaccination between vaccine types (COR vs. VX, SV vs. VX, SV vs. COR), (ii) compare two versus one vaccination (COR-2x vs. COR-1x, SV-2x vs. SV-1x) and (iii) compare two vaccinations of different vaccine types (SV-2x vs. COR-2x). p-values of these pairwise group comparisons with the Mann–Whitney test are shown (judged for significance at a Bonferroni-corrected level of 0.05/6 = 0.008 to account for 6 tests). Dashed lines mark the upper and lower limits of the linear range of the assay.

To better understand the variability of measured antibody levels between individuals, we analyzed the impact of age and time since vaccination on RBD binding and virus neutralizing antibody levels (**Supplementary Table 13A,B**). For this, we focused on individuals vaccinated with Comirnaty. First, we evaluated the relationship between age and time since vaccination and found a distinct pattern (**Supplemental Figure 7**): (i) early on, vaccinated individuals included younger and older age (time since vaccination 50–100 days), (ii) followed by an interim interval where almost exclusively older individuals were vaccinated (30–50 days, 75+ years of age), and (iii) for the period most closely to blood drawn,

vaccinated individuals again included all ages. This pattern can bias univariate association estimates of antibodies and age and time since vaccination which prompted us to apply multiple regression analysis allowing for non-linear associations (generalized additive models).

Multiple regression revealed significant associations of both age and time since vaccination with measured RBD binding antibodies and neutralization titers (**Figure 19 A,B;** $p < 0.0001$ for age and time for both antibody levels). We found a close-to-linear decrease in antibody levels on a log-scale by increasing age and increasing time after the vaccination (**Supplemental Figure 8**). We also investigated the possibility of a varying functional form for the decrease in antibodies by time since vaccination with changing age based on a bivariate spline surface. We found no evidence for such interaction of the covariates (explained deviance spline surface vs. spline per covariate: 22.3% vs. 23% for RBD binding antibodies and 27.2% vs. 28.3% for neutralizing antibodies). We therefore present results with non-linear effects per covariate. These results indicate that both increased age and increased time since vaccination have an independent decreasing effect on antibody levels.

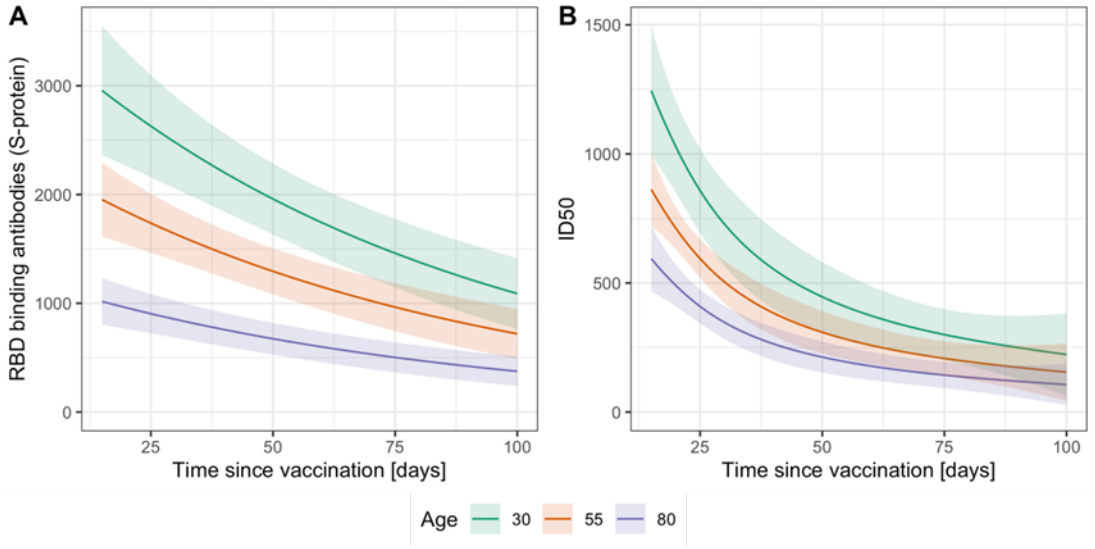

Figure 19 Model-based RBD binding and neutralization antibody levels related to age and time since vaccination. We applied a generalized additive model with assumed log-normal distribution of the antibody levels and non-linear associations with age and time since vaccination on the cross-sectional data from T3. On the example of individuals vaccinated twice with COV, we show predicted levels of (A) RBD binding antibodies (arbitrary units AU/mL) and (B) neutralizing antibodies (ID50) for the age of 30, 55, and 80 years and over the observed range of days since second vaccination (n = 272 and 269, respectively). Shaded regions indicate approximate 95%-prediction intervals (Prediction ± 2×SE).

5.5.4.3 Breadth of Neutralization after Natural Infection or Vaccination

To determine the breadth of the neutralizing activity after SARS-CoV-2 infection or vaccination, we used a lentiviral pseudotype neutralization assay against the D614G wildtype virus as well as against the Alpha, Beta, and Delta variants of concern (VOC). For this, we selected four random samples of participants (in each, 50% women): one group of participants with SARS-CoV-2 infection and no vaccination (n = 30, seropositive at T1, T2, or T3), and 3 groups of uninfected participants vaccinated with 2 doses of Comirnaty (30 participants each by age-groups 18–59, 60–79, 80+ years). In total, the

four different neutralizing antibody levels (50% inhibitory dose against WT, Alpha, Beta, and Delta) were evaluated in 120 participants based on blood samples from April 2021.

Among the 30 infected participants, median ID50 values against VOCs were lower compared to wild type (**Figure 20A**). This was particularly pronounced for Beta and Delta (Wilcoxon test $p < 0.01$). However, a large proportion of individuals were below the lower limit of detection: median ID50 against wildtype was 74 (40% below detection level); median levels for VOCs were below the lower detection limit at 20 (**Figure 20A**), which indicated that less than 50% of participants had detectable levels of neutralizing antibodies against any VOCs in this pseudotype neutralization assay (**Figure 20A**).

Among each of the three groups of vaccinated individuals without infection (n = 30 each, **Figure 20B–D**), median ID50 values were lower for VOCs compared to wild type, particularly for Beta and Delta (Wilcoxon test $p < 0.01$).

When comparing the three groups of vaccinated individuals across the different age groups, we found a general tendency of lower ID50 values for older individuals (80+ years) compared to younger for all VOCs. This is in line with the findings of lower RBD binding or neutralizing antibodies from the previous chapter; some of these differences can also be due to differences in time since vaccination as highlighted above.

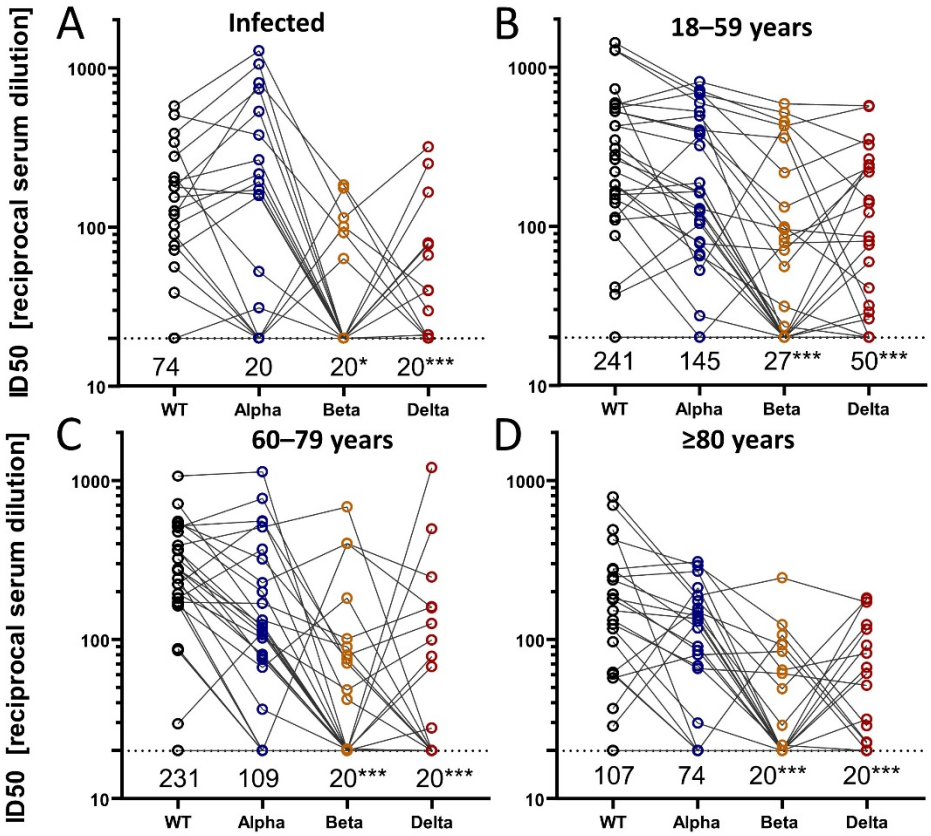

Figure 20 Breadth of neutralization after infection or vaccination. We randomly selected four groups of participants totaling n = 120 (30 infected and unvaccinated (A), 90 vaccinated twice with Comirnaty from three age groups (B–D)). The neutralization activity was determined in a lentiviral pseudotype assay using the spike proteins of wild type (D614G) SARS-CoV-2 and the indicated VOCs. Shown are the reciprocal of the 50% inhibitory dilution (ID50) of each serum sample by WT or VOCs. Person-specific measurements for WT and VOCs are connected by gray lines. Dashed black lines indicate the lower limit of detection (ID50 = 20) and median ID50 values per group are stated below this line. We conducted paired tests (Wilcoxon rank-sum test) com-paring VOCs with WT and indicate significant differences in the medians by *, *** for p-values of <0.01 and <0.0001, respectively.

5.5.4.4 IgA Response

To further explore potential differences in the antibody responses to infection without and with vaccination, IgA-specific antibody responses against RBD were also determined in samples collected in April 2021 using our in-house RBD ELISA. Unvaccinated participants that were N-antibody seropositive in June 2020 and those that seroconverted for N antibodies between November 2020 and April 2021 (recently infected) were predominantly IgA negative (**Figure 21**). Most participants that were N-antibody seronegative at all three study time points and vaccinated once with Vaxzevria or once or twice with Comirnaty did not develop detectable IgA antibody levels to the RBD, either (**Figure 21**). However, after one or two immunizations with Spikevax, more than half of the vaccinees had detectable levels of IgA antibodies to RBD. Interestingly, participants that were already N-antibody seropositive in June 2020 (infection >9 months ago) and subsequently immunized once with any of the COVID-19 vaccines showed elevated IgA levels for all vaccine types (**Figure 21**, **Supplementary Table 14** and **Supplementary Table 15**).

When comparing the percentage of IgA positives of uninfected individuals vaccinated twice with COR to one-time vaccinated individuals with infection >9 months ago (39.9% and 100%, respectively), we found a significant difference (exact Fisher's test p < 10−20, **Supplementary Table 14**). This indicates that a prior SARS-CoV-2 infection primes for stronger IgA responses than one immunization with Comirnaty, which is in line with previous work[349].

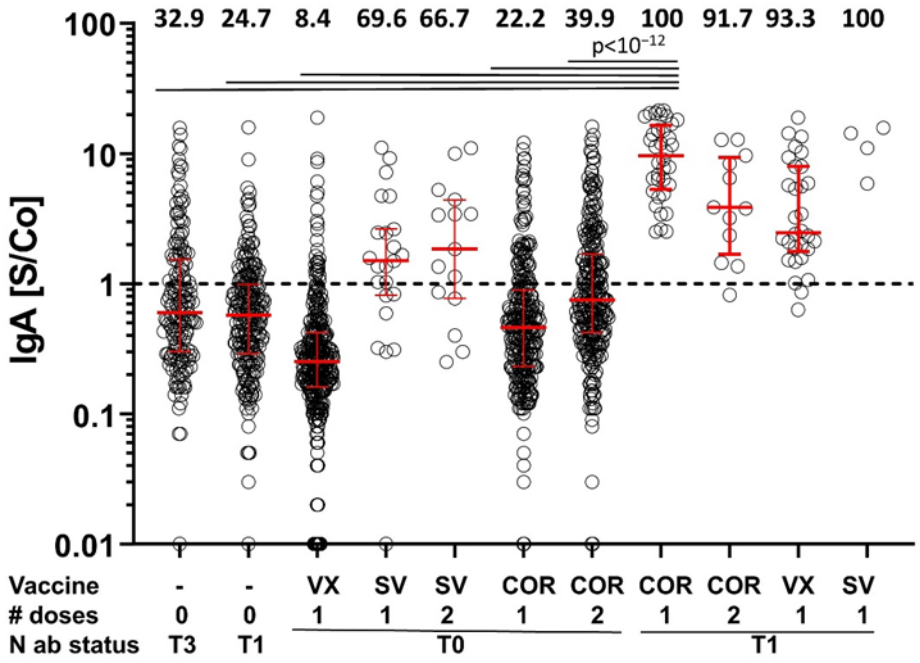

Figure 21 IgA antibody levels. Shown are IgA signal to cut-off ratios (S/Co) for serum samples from the indicated groups of participants. Numbers on top of the graph give the percentage of IgA-positive participants of each group. Fisher's exact tests were used for pairwise comparison of all groups without correcting for multiple testing (see Supplementary Table 16) and judged at Bonferroni-corrected significance of 0.05/55 = 9.09 × 10−4. For clarity reasons, highly significant differences (p < 10−12) between groups are only shown for comparisons of participants that were N-antibody (ab) seropositive at the June 2020 time point (N ab status: T1) and vaccinated once with Comirnaty (COR). T3: participants negative for N antibodies at the June and November 2020 visits, but positive at the April 2021 visit. N ab status: T0: participants seronegative for N antibodies at all study time points analyzed. VX: Vaxzevria; SV: Spikevax; The dashed line separates IgA seropositive from seronegative samples. Supplementary Table 16, Supplementary Table 17 and Supplementary Table 18 provide p-values of all pairwise comparisons as well as number of participants, basic demographic characteristics and the median time interval between the last immunization and blood sampling. # doses indicates the number of applied doses.

5.5.5 Discussion

Early on, binding and neutralizing antibody levels have been proposed as correlates of protection after vaccination with COVID-19 vaccines[180]. Recently, Gilbert et al. indeed observed a correlation of RBD binding /neutralizing antibody levels four weeks after the second Spikevax immunization with vaccine efficacy during a 100 day period after the second immunization[42]. Although proof that this correlation can be extended to other vaccines or antibody levels determined at later time points after

immunization is lacking, recommendations on immunization practices have partially been based on immunogenicity data, since efficacy or effectiveness data were not available.

The need for national booster immunization campaigns has been widely discussed during summer 2021 and weighted against prioritization of available vaccine doses for resource-poor settings in which primary immunization is still lacking behind. Tailored recommendations for booster immunizations limited to particular age groups or less effective vaccines may help to reconcile these divergent requests. Herein, we could show a significant decrease in antibody levels dependent on both age and time since vaccination, rationalizing a prioritization scheme based on age for 3rd vaccinations. The latter becomes particularly important with the emergence of Omicron, for which a close to 40-fold decrease in in vitro neutralization in sera even from recently fully vaccinated individuals has been reported[350]. Interestingly, a total of three antigen exposures by either infection or vaccination induced better neutralizing activity against all variants of concern[351]. However, further booster immunizations for all or particular age groups may become necessary as waning protection has also been observed after the 1st booster immunization[352]. Expanded booster campaigns should be accompanied by the quest to expand global manufacturing capacities and timely adoption of vaccine antigens.

The extent of antibody levels after infection compared to vaccination and a combination is still a current debate. For vaccinated individuals, we document an independent relationship of declining antibody response by older age and longer time since vaccination. Furthermore, the changing recommendations of different vaccines for different age groups provide a relationship of time since vaccination and age to vaccine type. These aspects render group comparisons inherently complex, between different vaccines as well as between vaccination and infection. Nevertheless, our data show substantially higher RBD binding and neutralizing antibody responses to a single vaccination after infection compared to a single vaccination without infection. It was reported that vaccination provided better protection from COVID-19 than a past infection[353,354]. However, two other publications indicate that protection from (re-)infection with the Delta variant after a first SARS-CoV-2 infection may be stronger than the protection conferred by two Comirnaty immunizations[355,356]. These data are supported by findings from Wang and colleagues reporting that, in the absence of vaccination, antibody reactivity to the receptor-binding domain (RBD) of SARS-CoV-2, neutralizing activity, and the number of RBD-specific memory B cells remain relatively stable between 6 and 12 months after infection[357]. Further evidence suggests that vaccination following natural infection increases all components of the humoral response and yields serum neutralizing activities against variants of concern (VOC)[358–360]. However, additional studies are needed to draw firm conclusions on the degree and duration of protection from reinfection after a first SARS-CoV-2 infection.

The analysis of serum IgA levels after SARS-CoV-2 infection combined with vaccination reveals for the first time that SARS-CoV-2 infection primes for a stronger IgA response after a single immunization with any of the three COVID-19 vaccines, than either two vaccinations in previously uninfected participants or a SARS-CoV-2 infection by itself. The higher proportion of IgA positives in infected individuals after one immunization parallels the increased effectiveness observed after a single dose of Comirnaty in previously infected individuals. However, it remains to be determined whether IgA levels are indeed a good correlate of protection in individuals vaccinated after a previous SARS-CoV-2 infection.

As reported previously, we also observed reduced immunogenicity of Comirnaty in the elderly consistent with the evidence for a higher risk for breakthrough infections in this age group and the quest for a booster vaccination[361]. Comparisons of differential effectiveness by different vaccines need to take age and time since vaccination into account. We did not observe a significant difference in S antibody responses after two doses of Comirnaty between male and female participants of our study. However, an indepth analysis is still needed to adjust for age and time since vaccination.

Importantly, we document the decline in neutralization antibodies for the Beta and Delta VOCs across all age groups for vaccinated as well as infected individuals. This highlights the relevance of VOCs in future handling of the pandemic.

5.5.6 Conclusions

In conclusion, we found that RBD binding and neutralizing antibody levels after two mRNA immunizations of previously uninfected individuals are higher than those raised by SARS-CoV-2 infection, but lower than titers raised by SARS-CoV-2 infection combined with one vaccination. Furthermore, we found a clear dependency of vaccine-elicited antibodies on age and time since vaccination. Finally, we could show increased IgA responses for previously infected and vaccinated participants in comparison to infection or vaccination by itself.

5.5.7 Appendix & Declarations

Author Contributions: Conceptualization, K.Ü. and R.W.; methodology, D.P., S.E., R.B. and M.T.; validation, D.P., S.E., S.B., K.Ü. and R.W.; formal analysis, S.B., K.Ü., B.A., F.G. and I.M.H.; investigation, D.P., S.E., M.S., R.B., A.S.P., S.B. and H.-H.N.; resources, R.W., A.G., I.M.H. and K.Ü.; data curation, S.E., S.B., R.W. and K.Ü.; writing—original draft preparation, K.Ü. and R.W.; writing—review and editing, S.E., D.P. F.G., I.M.H., M.T. and P.S.; visualization, K.Ü. and S.B.; supervision, R.W. and K.Ü.; project administration and funding acquisition R.W. and K.Ü. All authors have read and agreed to the published version of the manuscript.

Funding: This work was supported by the Bavarian States Ministry of Science and Arts (TiKoCo-19 and ForCovid, StMWK; grant to R.W. and K.Ü.) as well as by the National Research Network of the

University Medicine (NUM; applied surveillance and testing; B-FAST) to KÜ and RW. The funders had no role in study design, data collection and analysis, decision to publish, or preparation of the manuscript.

Institutional Review Board Statement: The TiKoCo-19 study was approved by the Ethics Committee of the University of Regensburg, Germany (vote 20-1867-101) and adopted by the Ethics Committee of the University of Erlangen (vote 248_20 Bc). The study complies with the 1964 Helsinki Declaration and its later amendments. All participants provided written informed consent.

Informed Consent Statement: Informed consent was obtained from all subjects involved in the study.

Data Availability Statement: All authors declare that data and materials will be made available according to the guidelines of the journal.

Acknowledgments: We are particularly grateful to all the study participants. We would like to thank the office staff and numerous students of the University of Regensburg and the University Erlangen as well as the employees of the Bavarian Red Cross, the members of the civil protection, the county office, and the public health office of county Tirschenreuth, respectively, for their tremendous support. We would also like to thank J. Kimpel, Institute of Virology, Medical University, Innsbruck (AU), for providing the ACE-2 overexpressing HEK293T cell line. We are also grateful to Christine Wolff from wECARE and Jakob Niggel from MaganaMed for providing questionnaires and the database for the study.

Conflicts of Interest: The authors declare that no competing interests or conflicts of interest exist. The authors have no financial or proprietary interests in any material discussed in this article.

5.5.8 Supplementary Materials

The following are also available online https://www.mdpi.com/article/10.3390/vaccines10020324/s1

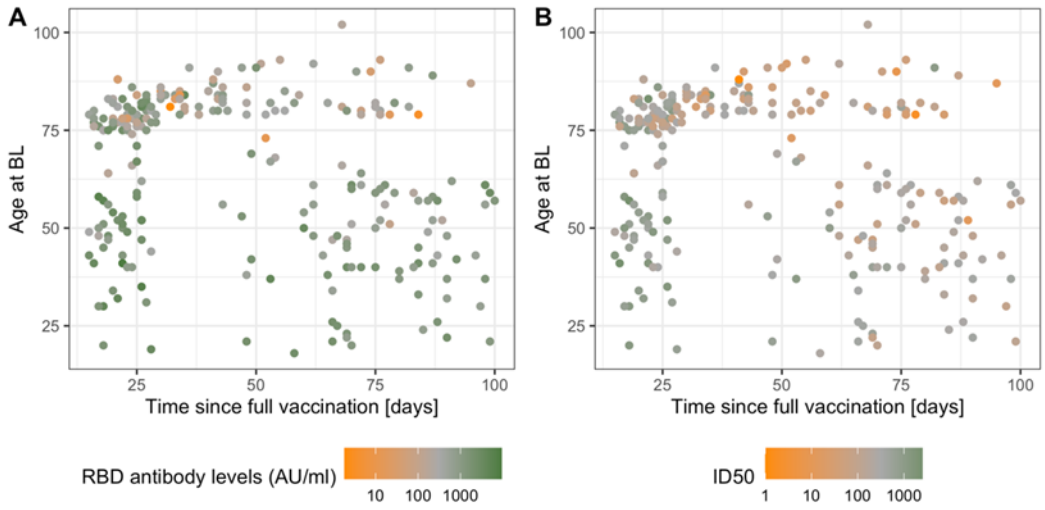

Supplemental Figure 7 Scatterplot of the observed time since full vaccination and age of participants in the subset of individuals that were vaccinated twice with the Comirnaty vaccine at least 14 days before blood draw. Panel A shows the measured RBD binding antibody levels of the 272 individuals, panel B the measured ID50 levels of 269 individuals in color.

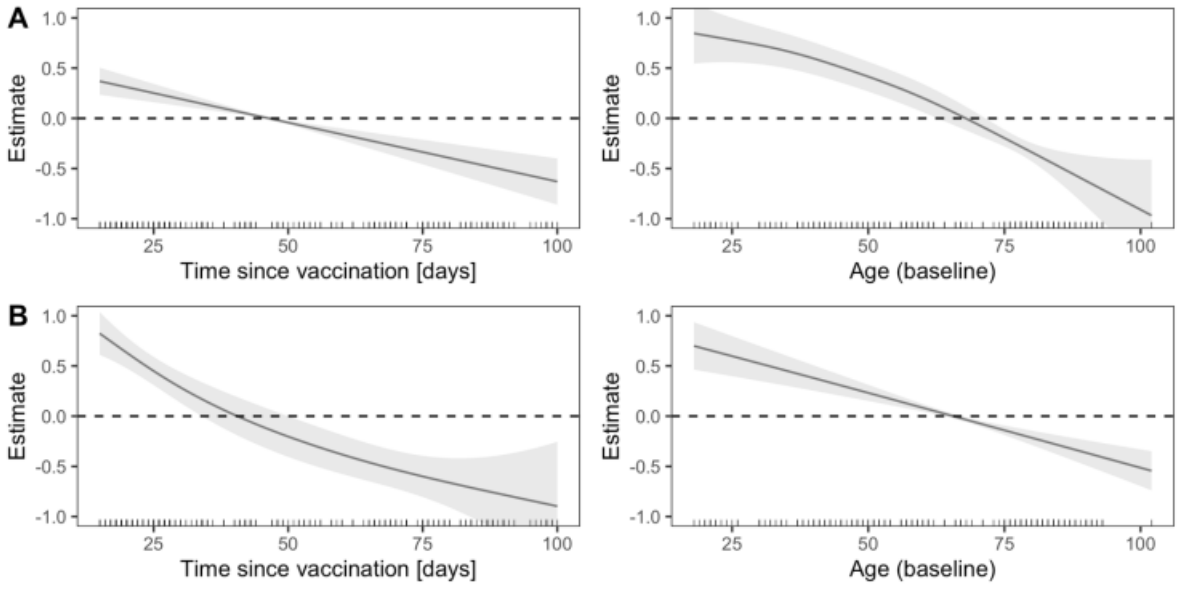

Supplemental Figure 8 Estimated non-linear associations of time since vaccination and age at BL with RBD binding antibody levels (Panel A) and neutralizing antibodies (ID 50, Panel B). Shown the estimated non-linear effects and 95%-confidence intervals.

Supplementary Table 12 Composition of study population: Infected unvaccinated versus infected and vaccinated individuals tested for Spike-RBD binding antibodies. (Supplement to Figure 17A)

N ab status	T3	T1				
Doses, vaccine	0	0	1, VX	1, COR	1, SV	2, COR
N	164	227	30	36	4	12
Sex, female / male	90/74	121/106	17/13	15/21	0/4	10/2
AU/ml, median (IQR)	73 (31-303)	171 (60.8-474)	14185 (6471-23234)	42967 (25114-57335)	114049 (70011-148592)	15324 (4053-56841)
Age in years, median (IQR)	46 (28-56)	49 (31.5-58)	63.5 (46.75-73.5)	66.5 (50-68.25)	65.5 (48-75,25)	56.5 (48-78,5)
Days since last immunization Median (IQR)	n.a.	n.a.	44 (27.75-52.75)	23 (17-29.5)	26,5 (24-27)	54 (24.75-78.75)

Supplementary Table 13 Composition of study population: Infected unvaccinated versus infected and vaccinated individuals tested for neutralization (Supplement to Figure 17B)

N ab status	T3	T1				
Doses, vaccine	0	0	1, VX	1, COR	1, SV	2, COR
N	164	226	28	36	4	12
Sex, female / male	90/74	120/106	15/13	15/21	0/4	10/2
ID50, median (IQR)	140 (63-313)	72 (34-146)	1013 (639-1898)	2558 (1377-3001)	3001 (2971.75-3001)	1591 (343-2712)
Age in years, median (IQR)	46 (28-56)	49 (31.25-57.75)	63.5 (48.25-74.5)	66.5 (50-68.25)	65.5 (48-75.25)	56.5 (48-78.5)
Days since last immunization Median (IQR)	n.a.	n.a.	45 (29.25-53)	23 (17-29.5)	26,5 (24-27)	54 (24.75-78.75)

Supplementary Table 14 Composition of study population: non-infected individuals immunized with different vaccines, tested for Spike-RBD binding antibodies (Supplement to Figure 18A)

Doses	1 immunization			2 immunizations	
Vaccine	VX	COR	SV	COR	SV
N=	321	287	23	271	15
Sex, female / male	179/142	135/152	12/11	163/108	10/5
AU/ml, median (IQR)	20 (4.9-53.5)	20.4 (4.4-71.1)	152 (36.3-251)	713 (262-1524)	2416 (1433-5067)
Age in years, median (IQR)	57 (45-71)	68 (57-71)	56 (48-68,5)	76 (50-81)	76 (55.5-83)
Days since last immunization Median (IQR)	34 (25-48)	21 (18-25)	22 (19.5-26)	38 (23.5-69.5)	48 (25-70.5)

Supplementary Table 15 Composition of study population: non-infected individuals immunized with different vaccines, tested for neutralizing antibodies (Supplement to Figure 18B)

Doses	1 immunization			2 immunizations	
Vaccine	VX	COR	SV	COR	SV
N=	319	285	23	268	15
Sex, female / male	178/141	133/152	12/11	160/108	10/5
ID50, median (IQR)	25.3 (4.3-55.8)	30.3 (14.1-81.8)	74.9 (23.2-288)	253 (103-463)	554 (188-1016)
Age in years, median (IQR)	57 (45-70.5)	68 (57-71)	56 (48-68,5)	76 (50-81)	76 (55.5-83)
Days since last immunization Median (IQR)	34 (25-48)	21 (18-25)	22 (19.5-26)	39 (23-70)	48 (25-70.5)

Supplementary Table 16 P-values of pairwise comparisons with two-sided Fisher´s exact test (Supplement for Figure 21).

	0, T1	1, VX, T0	1, SV, T0	2, SV, T0	1,COR, T0	2,COR, T0	1,COR, T1	2,COR T1	1, VX, T1
0, T3	0.087	$<10^{-10}$	0.001	0.021	0.014	0.154	$<10^{-14}$	$<10^{-4}$	$<10^{-9}$
0, T1		$<10^{-6}$	$<10^{-4}$	0.001	0.465	$<10^{-3}$	$<10^{-18}$	$<10^{-5}$	$<10^{-12}$
1, VX, T0			$<10^{-10}$	$<10^{-6}$	$<10^{-5}$	$<10^{-19}$	$<10^{-31}$	$<10^{-9}$	$<10^{-23}$
1, SV, T0				1	$<10^{-5}$	0.008	$<10^{-3}$	0.216	0.031
2, SV, T0					$<10^{-3}$	0.057	0.001	0.182	0.032
1,COR, T0						$<10^{-5}$	$<10^{-20}$	$<10^{-5}$	$<10^{-14}$
2,COR, T0							$<10^{-12}$	$<10^{-3}$	$<10^{-7}$
1,COR, T1								0.250	0.203
2,COR T1									1

T1, T3, VX, SV, COR as in Figure legend 5. T0: participants seronegative for N antibodies at all study time points.

Supplementary Table 17 part 1. Composition of study population: IgA Spike-RBD binding antibodies in infected and vaccinated individuals (Supplement for Figure 21)

N ab status	T3	T1	N antibody negative				
Doses, vaccine	0	0	1, VX	1, SV	2, SV	1, COR	2, COR
N	164	227	323	23	15	288	271
Sex, female / male	90/74	121/106	180/143	12/11	10/5	135/153	163/108
# IgA [S/Co] >1 / # IgA [S/Co] ≤1	54/110	56/171	27/296	16/7	10/5	64/228	108/163
IgA [S/Co] median (IQR)	0.60 (0.30-1.54)	0.57 (0.29-0.98)	0.25 (0.16-0.42)	1.50 (0.82-2.55)	1.85 (0.81-3.93)	0.46 (0.24-0.88)	0.75 (0.42-1.65)
Age in years, median (IQR)	46 (28-56)	49 (31.5-58)	57 (45-71)	56 (48-68,5)	76 (55.5-83)	68 (57-71)	76 (50-81)
Days since last immunization Median (IQR)	n.a.	n.a.	34 (25-48)	22 (19.5-26)	48 (25-70.5)	21 (18-25)	38 (23.5-69.5)

Supplementary Table 18 part 2. Composition of study population: IgA Spike-RBD binding antibodies in infected and vaccinated individuals (Supplement Figure 21)

N ab status	T1			
Doses, vaccine	1, COR	2, COR	1, VX	1, SV
N	36	12	30	4
Sex, female / male	15/21	10/2	17/13	0/4
# IgA [S/Co] >1 / # IgA [S/Co] ≤1	36/0	11/1	28/2	0/4
IgA [S/Co] median (IQR)	9.62 (5.61-14.3)	3.83 (2.13-8.69)	2.47 (1.85-7.44)	12.6 (9.72-14.6)
Age in years, median (IQR)	66.5 (50-68.25)	56.5 (48-78,5)	63.5 (46.75-73.5)	65.5 (48-75,25)
Days since last immunization Median (IQR)	23 (17-29.5)	54 (24.75-78.75)	44 (27.75-52.75)	26,5 (24-27)

5.6 Manuscript 5: "Longitudinal effects of SARS-CoV-2 breakthrough infection on imprinting of neutralizing antibody responses"

5.6.1 Abstract

The impact of the infecting SARS-CoV-2 variant of concern (VOC) and the vaccination status was determined on the magnitude, breadth, and durability of the neutralizing antibody (nAb) profile in a longitudinal multicenter cohort study. 173 vaccinated and 56 non-vaccinated individuals were enrolled after SARS-CoV-2 Alpha, Delta, or Omicron infection and visited four times within 6 months. Magnitude-breadth-analysis showed enhanced neutralization capacity in vaccinated individuals against WT, Alpha, Delta, Omicron BA.1, BA.2, BA.5 and BQ.1.1 VOCs. Longitudinal analysis revealed sustained neutralization magnitude-breadth after antigenically distant Delta or Omicron breakthrough infection (BTI), with triple-vaccinated individuals showing significantly elevated titers and improved breadth. Antigenic mapping and antibody landscaping revealed initial boosting of vaccine-induced WT-specific responses after BTI, a delayed shift in neutralization towards infecting VOCs at peak responses and an immune imprinted bias towards dominating WT immunity in the long-term. Despite that bias, random-forest and neural-network machine-learning models confirmed a sustained shift of the immune-profiles following BTI.

5.6.2 Introduction

The appearance of new SARS-CoV-2 immune escape variants remained an ongoing threat and resulted in high numbers of vaccine breakthrough infections (BTI) over the last 2 years[362].

Multiple risk factors for a BTI[363] - such as time after vaccination, age, previous disease, vaccine type, and circulating VOC - have been identified in various studies[364,365], including a waning of vaccine-elicited antibodies against SARS-CoV-2 infection over time[316,366]. Furthermore, the rapid emergence and global spread of Alpha, Delta, and Omicron VOCs impressively demonstrated that neither prior infection nor vaccination efficiently protected from infection with new VOCs[367].

Regarding heterologous vaccine booster immunizations[316], combinations of vaccination and infection ("hybrid immunity")[368], especially breakthrough infection (BTI), or repeated infection with different VOCs[369], questions were raised whether immune imprinting[370] might be relevant in cases of preexisting immunity. This phenomenon, also known for other respiratory viruses such as the influenza virus, might limit broadening of immune responses following repeated exposure to variants of the same antigen[162,371–373].

Since serum neutralization capacity was identified as a key correlate of protection from COVID-19[42,180,291], the impact of prior vaccination on neutralizing antibody responses (nAb) following SARS-CoV-2 infection with different VOCs is of high importance[374–376].

Accordingly, based on a cohort of 229 subjects with documented vaccination, infection, and clinical history, this longitudinal study aims to elucidate the interplay of prior vaccination and BTI with different SARS-CoV-2 VOCs on the kinetic, magnitude, breadth, and durability of neutralizing antibody responses compared to infection in unvaccinated individuals. Using antigenic mapping and neutralization landscaping as advanced bioinformatic tools, this study will also provide insight into the potential impact of vaccine-induced immune imprinting on neutralization capacity following BTI.

5.6.3 Material and Methods

5.6.3.1 Sampling

Blood samples of individuals from a prospective longitudinal multicenter cohort study (CoVaKo) of acute SARS-CoV-2 BTIs and non-BTIs were analyzed. Study centers were the respective University Hospitals in Erlangen, Regensburg, Augsburg, Würzburg, and Munich (TUM and LMU), all located in Bavaria, Germany. The study design is described in Prelog *et al*. [377].

In brief, samples of 56 non-vaccinated and 173 vaccinated individuals with a newly diagnosed SARS-CoV-2 infection were collected between April 2021 and April 2022 for Alpha (n=32), Delta (n=134) infections and between January and August 2022 for Omicron infections (n=63). vaccinated individuals received at least two vaccinations with wildtype-based mRNA vaccines (BNT162b2, Comirnaty, BioNTech/Pfizer and mRNA-1273, Spikevax, Moderna (n=155)) or vector-based vaccines (AZD1222, Vaxzevria, AstraZeneca and JNJ-78436735, Jcovden; Janssen-Cilag/Johnson&Johnson (n=8)) or a combination of vector and mRNA-based vaccines (n=10) (**Table 13, Supplementary Table 19**).

The first study visit took part within 14 days after the first positive SARS-CoV-2 RT-qPCR test (day 1, visit V1) and included a VOC-specific PCR for determining the SARS-CoV-2 VOC. Follow-up visits were carried out on day 8±1 (V2), day 15±1 (V3), day 22±2 (V4) and between 4-6 months (V5) after the initial visit, respectively. As V3 was an optional visit according to the study protocol, which was only carried out in a minority of individuals, this study visit was not included in this analysis. The participant sex data was collected by conversational self-reporting to a medical professional, thus, any reporting of gender instead of sex can be excluded.

Written informed consent was provided by all study participants, the study was approved by the Ethics Committee of the Friedrich-Alexander-University Erlangen-Nürnberg, Germany (vote 46_21 B) and adopted by the local ethics committees of all other study centers. The study complies with the 1964 Declaration of Helsinki and its later amendments.

5.6.3.2 Pseudotype neutralization assay

The capacity of sera to neutralize different SARS-CoV-2 variants was determined using a lentiviral pseudotype assay, as described previously[378].

In brief, an inoculum of 2.5*10^5 rlu/384-well of lentiviral particles expressing luciferase and pseudotyped with SARS-CoV-2 spike protein was neutralized with a 2-fold serum dilution series for 1 h. Luciferase activity was determined 48 h post-infection of HEK293T-ACE2 + -cells using BrightGlo (Promega Corp, Madison, WI, USA). The 50% inhibitory dilution (ID50) of the sera was calculated using GraphPad Prism 8 (San Diego, CA, USA) after normalizing to noninfected and infected cells and curve fitting with the algorithm “log(inhibitor) vs. normalized response”. Neutralizing antibody titers were determined against the variants WT/D614G, Alpha (B.1.1.7), Delta (B.1.617.2), Omicron BA.1, BA.2, BA.5 and BQ.1.1 (for V5).

5.6.3.3 Magnitude-breadth analysis

As both, magnitude (nAb titer) and breadth (percentage of VOCs neutralized) of serum neutralization are important criteria for the evaluation of humoral immunity, we utilized the concept of magnitude-breadth curves, as described early for the analysis of humoral HIV immunity [379–381]. In brief, for each serum and time point, a Kaplan-Meier style curve was calculated using the neutralization data against all tested variants. Curves were calculated with “50% neutralization of one variant” defined as the “event of interest” and the “time-to-event” representing the 50% inhibitory concentration (IC50) for that variant. Thus, yielding a curve representing the magnitude of the immune response on the x-axis and the breadth, represented by the percentage of variants neutralized, on the y-axis. Magnitude-breadth curves for each group were calculated as the sum of individual curves divided by the number of individuals in the group. In addition, areas under the curve (AUC) were calculated for each magnitude breath curve, which facilitates the comparison of neutralization magnitude-breadth results between the different groups and visits.

5.6.3.4 Antigenic Cartography

Antigenic maps and antibody landscapes were calculated in R[348] as previously described by others [382–384]. In brief, antigenic cartography quantifies and visualizes neutralization data. It uses a two-dimensional antigenic map to represent the difference in log2 titers between antiserum S and antigens A and B. Modified multidimensional scaling arranges the points on the map to match the target distances from the neutralization data. The resulting map shows the antigenic distance, with distances between antigens and antisera inversely related to log2 titers. Antigenic maps were computed using the Racmacs package[385]. Maps were constructed with 1000 optimizations, setting the minimum column basis parameter to "none". Map bootstrap was performed by randomly resampling the dataset with replacement 1000 times, calculating new maps with those samples and reoptimizing each map

100 times, as further specified in the racmacs package reference. Finally, a blob representing one standard deviation of the antigen position was calculated from the resulting bootstrap positions.

Antibody landscapes were generated by adding a third dimension to the antigenic map represented by the geometric mean titers to each variant and subsequently fitting a cone-shaped object. Landscapes were calculated using the ablandscapes package by Sam Wilks[386]. Further packages used were: tidyverse, meantiter, r3js, htmlwidgets, webshot 2, grid, gridExtra, and patchwork.

5.6.3.5 Regression Analysis

After explorative Spearman correlation, generalized additive regression in R was used to jointly investigate the association of quantitative nAb levels against the BTI variant (IC50) with time after vaccination until BTI and breakthrough variant among vaccinated study participants. Separate models were calculated for the different visits. Smoothing terms were calculated using a thin plate regression spline basis, with automatic selection of the effective degrees of freedom. We illustrated the model results by inspecting the estimated (non-linear) associations and visualizing the predicted antibody levels over the range of observed times after the last vaccination until alpha, delta, and omicron infected, respectively. The models were estimated using the mgcv-package in R[347].

5.6.3.6 Adjustment to studycenter effects and varying days of the visit

To adjust the neutralization data for study center effects and varying visit days, a Tobit model was selected as the most suitable approach due to the upper and lower censoring of the neutralization data. Biologically, different directions and strengths of visit day effects are expected at different time points (e.g., increasing titers over time at visit 1 vs. waning titers at visit 5). Therefore, according to the principle of parsimony, separate (simpler) models were calculated for each visit opposed to one large but complex model accounting for those effects. To avoid overadjustment in the later visits, the day of the visit was scaled to the mean day of the current visit for each visit.

To ensure robustness, we chose a more stringent model using the larger groups of vaccinated and unvaccinated individuals, rather than the smaller groups also stratified by infection or breakthrough variant. This approach minimizes the risk of fitting bias due to single outliers in the smaller groups. For study center effects, center 5 (University Hospital Regensburg), which provided the most participants, was used as the baseline. Thus, all models were calculated with neutralization titers dependent on the neutralized virus variant, the number of days between the first positive PCR test and the current visit, vaccination status, study centers, and interaction effects between the visit day and vaccination status. Finally, all neutralization values were corrected for study center effects, visit day effects, and the interaction effects of visit day and vaccination status, specific to each visit.

Finally, adjustment of neutralization values was performed utilizing the tobit-models' effects as linear effects and applying post-adjustment censoring to the adjusted values to still comply with the experimental upper and lower bound of 1 and 2561.

5.6.3.7 Machine Learning models

Random forest models with 500 trees as well as neural networks were utilized to predict the infecting variant (Alpha, Delta, Omicron) of either vaccinated or unvaccinated individuals from their neutralization titers (IC50) against all tested VOCs. Thus utilizing models with the titers against D614G, Alpha, Delta, BA1, BA2 and BA5 as features and virus (Alpha, Delta, Omicron) as a target on data filtered by vaccination status and visit. Data was split in half into training and testing data by random sampling of the single groups. To avoid learning bias from different group sizes we used a method inspired by bootstrapping with monte-carlo simulation. In brief, the amount of learning data was increased by random but group stratified resampling from the available training datasets to gain a total of 999 equally fractioned training datasets. To avoid overlearning from the resampling process, additional noise was introduced in all resampled values while keeping the overall neutralization profile. Single values were randomly drawn from a generated normal distribution of 50 values with a mean of the original value and a standard deviation of 10% of the original value. As a compromise of avoiding bias and improving accuracy, a brute-force approach was used: 100 models were calculated on the generated training data set and checked for predictive accuracy using the respective test dataset. After keeping the best model, novel datasets were generated as described above and utilized to calculate 100 new models. This process was looped 100 times finally reporting the mean metrics of all 100 models calculated on the different datasets. Separate models were calculated for the vaccinated and unvaccinated subgroups as well as for the different visits. For neural networks, hyperparameter selection (3 to 5 neurons in the first, 0 to 3 neurons in the second hidden layer) was performed by calculating 10 models of each possible configuration, using the dataset for vaccinated individuals at visit 4, the visit with the assumed highest effect and the lowest chance of bias. The simplest configuration resulting in the best mean accuracy was chosen. Finally, shallow neural networks with 5 neurons in one hidden layer, using a maximum of 109 gradient steps for adjusting the weights of the network and a threshold of 0.1 for the partial derivatives of the error function to stop learning. Networks were trained for 100 independent datasets, generated as described above, finally reporting the mean accuracy of all models. Models were calculated in R using the randomForest and neuralnet packages.

5.6.3.8 Statistical analysis

For intergroup comparison, we used Kruskal-Wallis tests combined with post-hoc Dunn's-corrected multiple comparison tests, while we used Friedman tests with Bonferroni-corrected post-hoc Wilcoxon

testing for longitudinal/paired comparisons (e.g. visits). Two vs. three times vaccinated groups were compared using a Mann-Whitney U test. Individuals with Adenovirus/Vector vaccination were compared to individuals with mRNA vaccination using Mann-Whitney-U tests. The proportion of current smokers, defined by self-reported cigarette smoking, and sex distribution for individual groups was evaluated using Fisher's exact tests. Age differences between groups as well as the days between vaccination and infection were assessed using the aforementioned Kruskal-Wallis-tests. Differences between magnitude-breadth curves were assessed by log-rank-tests, while differences between the AUCs were assessed by Kruskal-Wallis tests combined with post-hoc Dunn's-corrected multiple comparison tests.

5.6.3.9 Multivariate analysis

For multivariate analysis we utilized PERMANOVA models with post hoc pairwise comparison, due to the non-normality of censored neutralization data. As some possible influencing variables like number of vaccines, vaccine type/vector vaccine or days_since_vax were non applicable for unvaccinated individuals, and missing values are unsupported by the method, two models were calculated. Modelling neutralization distances at the four visits as a function of age, gender, smoking status, virus to be neutralized, infection variant for the unvaccinated individuals, adding in the aforementioned vaccination specific variables for the vaccinated individuals. To adjust post-hoc comparison, we utilized a tobit-model to retrieve residuals of neutralization as a function of visit, age, gender, smoking status, virus to be neutralized. Additionally, for vaccinated individuals including number of vaccines, vaccine type/vector vaccine and days_since_vax. Here, infection variant was not included as it ought to be post-hoc analyzed. Afterwards, we performed pairwise PERMANOVA on the distance matrix of residuals.

5.6.3.10 Software

Statistical analysis was performed using SPSS Statistics (version 29.0.0.0(241), IBM Corp. Released 2021. IBM SPSS Statistics for Windows, Version 28.0. Armonk, NY, USA), GraphPad Prism 8 for Windows (version 8.0.1, GraphPad Software, San Diego, CA, USA) or R (version 4.2.3, R core team, Vienna, Austria) in RStudio (2023.12.0 Build 369, RStudio Team, Boston MA, USA).

5.6.3.11 Data and Code availability

A github repository containing the dataset and all the code is available on github via https://github.com/rwagnerlab/Einhauseretal2024_imprinting_neutralizing_antibodies/

5.6.4 Results

5.6.4.1 Descriptive analysis of the study cohort

In total, 229 individuals (173 BTIs and 56 non-BTIs) were included (**Table 13**). The majority of the two-times and the three-times vaccinated individuals received the BNT162b2mRNA (BioNTech/Pfizer) vaccine (n=104, 83.2% and n=36, 75.0%, respectively) (**Supplementary Table 19**). The vaccinated group comprised of individuals with a median age of 39 years (IQR 29-49), 57.8% (n=100) being women and 14.5% (n=25) current smokers whilst the unvaccinated group included individuals with a median age of 32 years (IQR 28-47), a female share of 62.5% (n=35) and 14.3% (n=8) current smokers. Comparing variant-stratified vaccinated and unvaccinated groups, no significant differences in age (p=0.443), sex (p=0.481), or smoking status (p= 0.670) composition could be found. The median interval in days from the last vaccination was 76±32, 95±55, and 108±46 days for Alpha, Delta, and Omicron BTIs, respectively. Comparing those intervals, we found significant differences between Alpha and Omicron BTIs (p=0.002). Previous infection was excluded by N-antibody measurements, health authority data and self-reporting as described in Prelog et [377].

Table 13 Demographic characteristics of the study cohort Including the numbers of participants for the respective subgroups, as well as age, sex, smoking status, vaccination status and days between last vaccination and study inclusion (days after vax, "-" means undeterminable due to no vaccination received). Abbreviations: number (n), interquartile range (IQR).

Vaccination Status	Vaccinated	Unvaccinated	Vaccinated	Unvaccinated	Vaccinated	Unvaccinated	All	All	All	Total	Vaccinated	Unvaccinated
Infection with	Alpha	Alpha	Delta	Delta	Omicron	Omicron	Alpha	Delta	Omicron	Total	Total	Total
n	24	8	94	40	55	8	32	134	63	229	173	56
Age (median)	40	35.5	38.5	31.5	38	30	39.5	37.5	34	38	39	31.5
Age (IQR)	34 - 46.3	30.8 - 42.8	29 - 50.8	27 - 46.5	28.5 - 45.5	29 - 37.5	32.8 - 46.3	28 - 49	29 - 45.5	29 - 48	29 - 49	28 - 46.5
Female n	18	6	53	25	29	4	24	78	33	135	100	35
Female %	75	75	56.4	62.5	52.7	50	75	58.2	52.4	59	57.8	62.5
Days after vax (median)	76	-	95	-	108	-	76	95	108	95	95	-
Days after vax (IQR)	61.8 - 81.8	-	56.3 - 134.5	-	85 - 140	-	61.8 - 87.8	56.3 - 134.5	83.5 - 140	65 - 132.6	65 - 133	-
Current smoking n	5	1	15	6	5	1	6	21	6	33	25	8
Smoking %	20.8	12.5	16	15	9.1	12.5	18.8	15.7	9.5	14.4	14.5	14.3

5.6.4.2 Adjustment for follow up time and studycenter effects

As this study was comprised of individuals sampled in multiple study centers at varying time points for each visit, bias/effects from both, study centers or follow up time could not be excluded. On top, biologically, different effects (e.g. raising titers with time after the initial infection, waning titers at the long-term visit) were to be expected from follow up time for the different visits. Thus, all neutralization data was adjusted for those effects utilizing four tobit models, one for each visit. Combining the

predictions of the single models for the whole dataset, overall variance accounted for by the models was 0.69. The models identified several significant influences of all, studycenters (2 and 4 at visit 1; 2,3 and 4 at visit 2; 2 and 4 at visit 4; 1,3 and 4 at visit 5), follow up time (visit 1 and visit 4) and interaction of vaccination status and follow up time at visit 5, justifying the adjustment. Effect strength and direction were, as biologically expected, varying at the different visits the splitting of the models to the different visits (**Supplemental Figure 9**).

5.6.4.3 Neutralization assays of Alpha/Delta/Omicron-infected groups

The samples of vaccinated and unvaccinated participants of the Alpha-, Delta- and Omicron-infected groups were analyzed for their neutralizing antibodies against the WT/D614G and the VOCs Alpha, Delta, Omicron BA.1, BA.2, and BA.5 at four timepoints (V1, V2, V4, V5; see **Figure 22**), and additionally against the VOCs BQ1.1, XBB.1.5 and JN.1 at V5 (**Supplemental Figure 10**).

In general, for infections with the SARS-CoV-2 Delta and Omicron VOC, a higher median neutralization capacity was found for vaccinated individuals compared to the unvaccinated groups at all visits, regardless of which pseudotype variant (PV) was used in the neutralization assay. Nevertheless, a high nAb titer was found for unvaccinated individuals tested against their infecting variant. Noteworthy, Omicron infection in unvaccinated individuals resulted in overall low nAbs against all tested PV variants except for the last visit, where omicron-specific nAbs started to increase. Consequently, individuals with Omicron BTI did benefit most from prior vaccination regarding their nAb response.

Additionally, sera at V5 (140 d, IQR 133-150 d after infection) were analyzed for their neutralization capacity against the Omicron variant BQ.1.1, XBB.1.5 and JN.1 (Supplemental Figure 10). Differences were analyzed by Kruskal-Wallis tests with post-hoc Dunn's tests. The highest BQ.1.1 nAb titers were found in individuals with Omicron infection history, whilst median IC50s were comparable in vaccinated and unvaccinated individuals. BQ1.1 nAb titers in the Omicron infected were significantly higher than those determined in the Alpha and Delta infected individuals, regardless of vaccination status, respectively (p-values denoted in the figure). NAb titers were lowest after infection and BTI with the alpha VOC. Only in the Delta-infected group, vaccinated individuals showed higher nAb titers against BQ.1.1. in comparison to unvaccinated individuals (p=0.0001). Moving to the more recent variants XBB.1.5. and JN.1 a similar pattern was revealed, though with notably lower overall response revealing a loss of differences between the vaccinated and unvaccinated individuals with omicron infection history. Regarding vaccinated individuals: while for BQ.1.1 a significantly increased titer was found for omicron BTI compared to Delta BTI ($p < 0.05$) and Alpha BTI ($p < 0.001$), XBB.1.5 neutralization reached significance only for Delta BTI ($p < 0.001$). Regarding JN.1 neutralization significance was lost for both Alpha and Delta BTI.

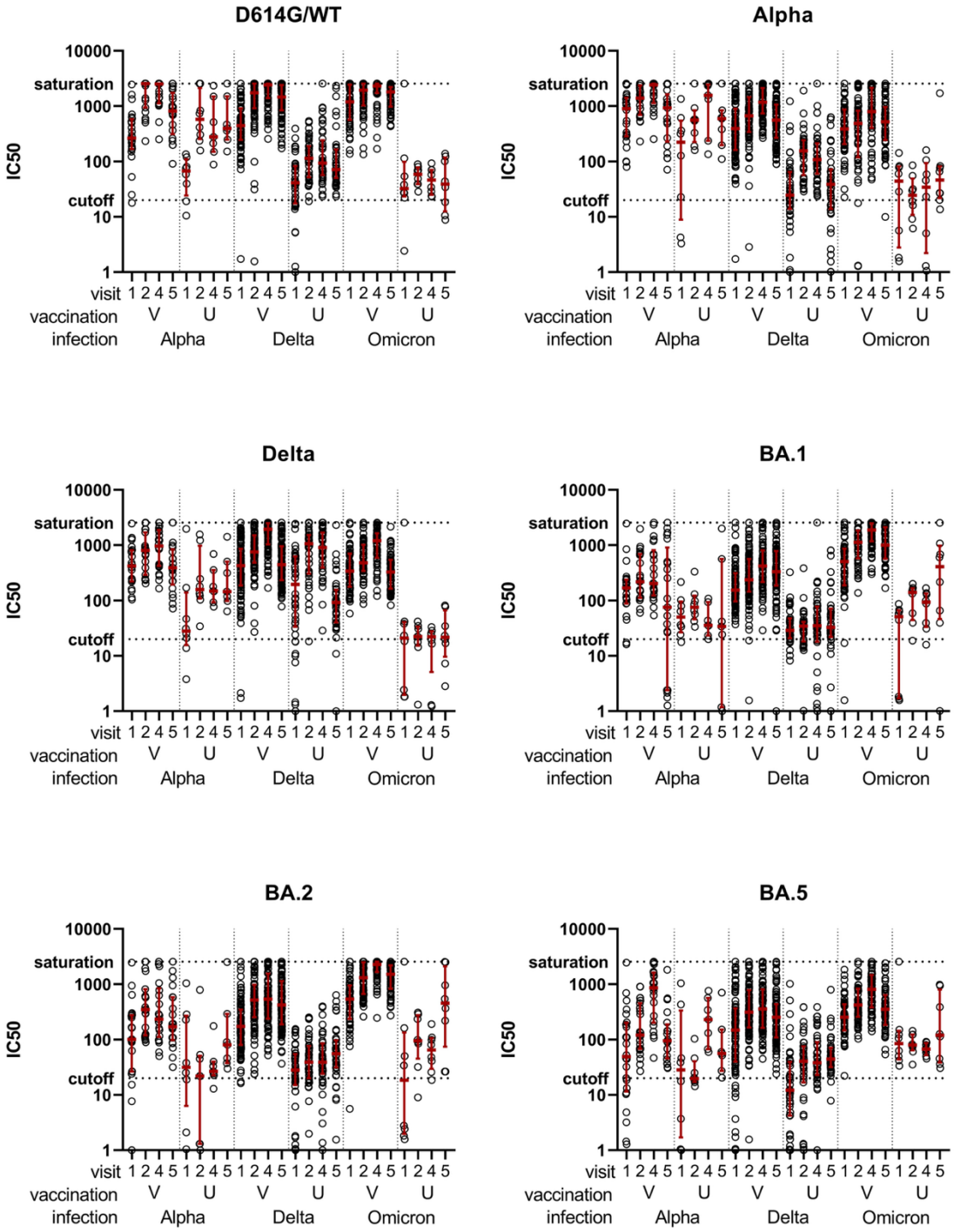

Figure 22 Neutralization assays against different SARS-CoV-2 variants for vaccinated and unvaccinated Alpha, Delta and Omicron infected study groups. Neutralizing antibody responses of vaccinated (V) and unvaccinated (U) individuals at visit 1, 2, 4 and 5 after infection with Alpha (A), Delta(D) or Omicron (O) (as indicated on the x-axis). Shown are the dilution factors for 50 % Inhibitory concentration (IC50) for WT/D614G, Alpha, Delta, Omicron BA.1, Omicron BA.2 and Omicron BA.5 spike, as indicated by the individual graph titles. The assay cut-off (IC50 = 20) as well as saturation (IC50 = 2560) are indicated by dashed lines. Median and interquartile ranges are indicated by the red horizontal line and whiskers.

Furthermore, we determined the variant-specific neutralization profiles normalized to the infecting variant for each group (**Supplemental Figure 11**). Distinct neutralization profiles were found for Alpha, Delta, or Omicron infected individuals peaking for the infecting VOC, respectively. The vaccinated groups revealed an additional maximum for WT/D614G corresponding to the vaccine-encoded antigen (**Supplemental Figure 11A-C**).

5.6.4.4 Effects of booster vaccination, adenoviral-vector vaccination and time between vaccination and BTI

An important covariate to be considered is the number of vaccinations. Therefore, we utilized our vaccinated Omicron group, the only one where individuals received either 2 or 3 vaccinations (**Supplementary Table 19**). Noteworthy, whereas no significant differences in neutralization capacity could be found for all variants during V1 – V4, the triple-vaccinated individuals revealed (significantly) higher IC50 titers for the VOCs Alpha ($p<0.05$), Delta ($p =0.055$), BA.1 ($p<0.05$) and BA.2 ($p<0.05$) at V5 compared to the double-vaccinated group (**Supplemental Figure 12**).

We further analyzed the impact of adenoviral vector-based vaccines in comparison to vast majority of participants who received only mRNA-based vaccines. Due to the heterogeneity of vaccination regimens (see **Supplementary Table 19**) in combination with low numbers of participants, all participants who received any vector-based vaccine (Janssen or Astra-Zeneca) at any point in their vaccination history (first, second, third or multiple) were pooled as the “vector-vaccinated group” (n = 18). To evaluate on general effects, neutralization titers against all variants were pooled as overall neutralization. Here, no significant differences between individuals in the vector-vaccinated group and individuals without any vector vaccination were found at any visit (**Supplemental Figure 13A**). Regarding variant and visit specific effects (**Supplemental Figure 13B**) we found significantly increased titers in the vector-vaccinated group at visit 5 against D614G and Alpha ($p = 0.042$ & $p = 0.048$).

Additionally, the effects of the time intervals between vaccination and BTI on the nAb response towards the infecting variant were investigated. Spearman correlation revealed significant but poor correlation only for V2 and V5 ($p = 0.030$, $rho = 0.165$ and $p = 0.002$, $rho = 0.238$, respectively). Subsequent nonlinear regression models exhibited non-significant or insufficient fits for all visits. Overall, only a maximum of 9.39% of the individual IC50 deviance could be explained by the best model (for visit 5). Breakthrough variant stratified analysis of did not reveal any significant smooths. (**Supplemental Figure 14**)

5.6.4.5 Magnitude-breadth analysis of Alpha-/Delta-/Omicron-infected groups

To explore and visualize differences in the magnitude and breadth of neutralizing antibodies responses, infection variant and vaccination-status stratified (U = unvaccinated, V= vaccinated; A = Alpha infection, D = Delta infection, O = Omicron infection) magnitude-breadth curves were calculated for the study visits V1, V2, V4 and V5 (**Figure 23A-D**). The corresponding AUCs were determined based on the nAb titers against WT/D614G, Alpha, Delta, Omicron BA.1, BA.2, and BA.5, respectively (**Figure 23E**).

In line with the analysis of single variant neutralization, vaccinated groups revealed consistently higher magnitude-breadth than unvaccinated groups between visits V1 and V4. (**Figure 23A-C, E**). While the unvaccinated groups showed very low magnitude-breadth profiles at V1, higher and comparable magnitude-breadth was observed in all vaccinated groups (**Figure 23A, E**). Whereas the magnitude breadth profiles of all unvaccinated groups remained at overall low levels (V2-V4) (Friedman test V1-V4 p(UA)= 0,6529, p(UD)<0.0001, p(UO)= 0,1993), a significant increase was found for all vaccinated groups, respectively (Friedman test V1-V4 p(VA)<0.0001, p(VD)<0.0001, p(VO)<0.0001) (**Figure 23B, C, E**). At visit 1, significantly increased magnitude-breadth was found for vaccinated omicron infected compared to vaccinated individuals with delta BTI (Kruskal-Wallis with Dunn's $p < 0.01$) yet not for alpha BTI (Kruskal-Wallis with Dunn's $p = 0.184$). Else, until V4 no significant variant-specific differences in magnitude-breadth levels were observed neither in the vaccinated nor the unvaccinated groups (**Figure 23E**).

In contrast, the long-term visit V5 revealed significant differences (Kruskal-Wallis V5 p<0.0001) between variant stratified groups. Alpha BTIs lost neutralization magnitude and breadth (Friedman-Dunn's p(VA V4 vs . VA V5)<0.0001) and yielded significantly lower AUCs compared to Omicron BTIs (Kruskal-Wallis Dunn's p(VA V5 vs. VO V5)<0.05), dropping down to the unvaccinated groups level (**Figure 23D, E**). Though magnitude-breadth profiles for Delta and Omicron BTIs also significantly decreased compared to V4 (Friedman Dunn's p(VD V4 vs. V5)<0.0001; p(VO V4 vs. V5)<0.0001), the magnitude-breadth AUC remained significantly higher compared to unvaccinated groups. At V5, Omicron BTIs showed though not significant compared to Delta BTI, the highest median neutralization magnitude-breadth AUC of all groups (Kruskal-Wallis Dunn's p(VO vs. VD =0.156), p(VA vs VO <0.05)), which was also seen when including neutralization data for Omicron BQ.1.1 (**Figure 23F**).

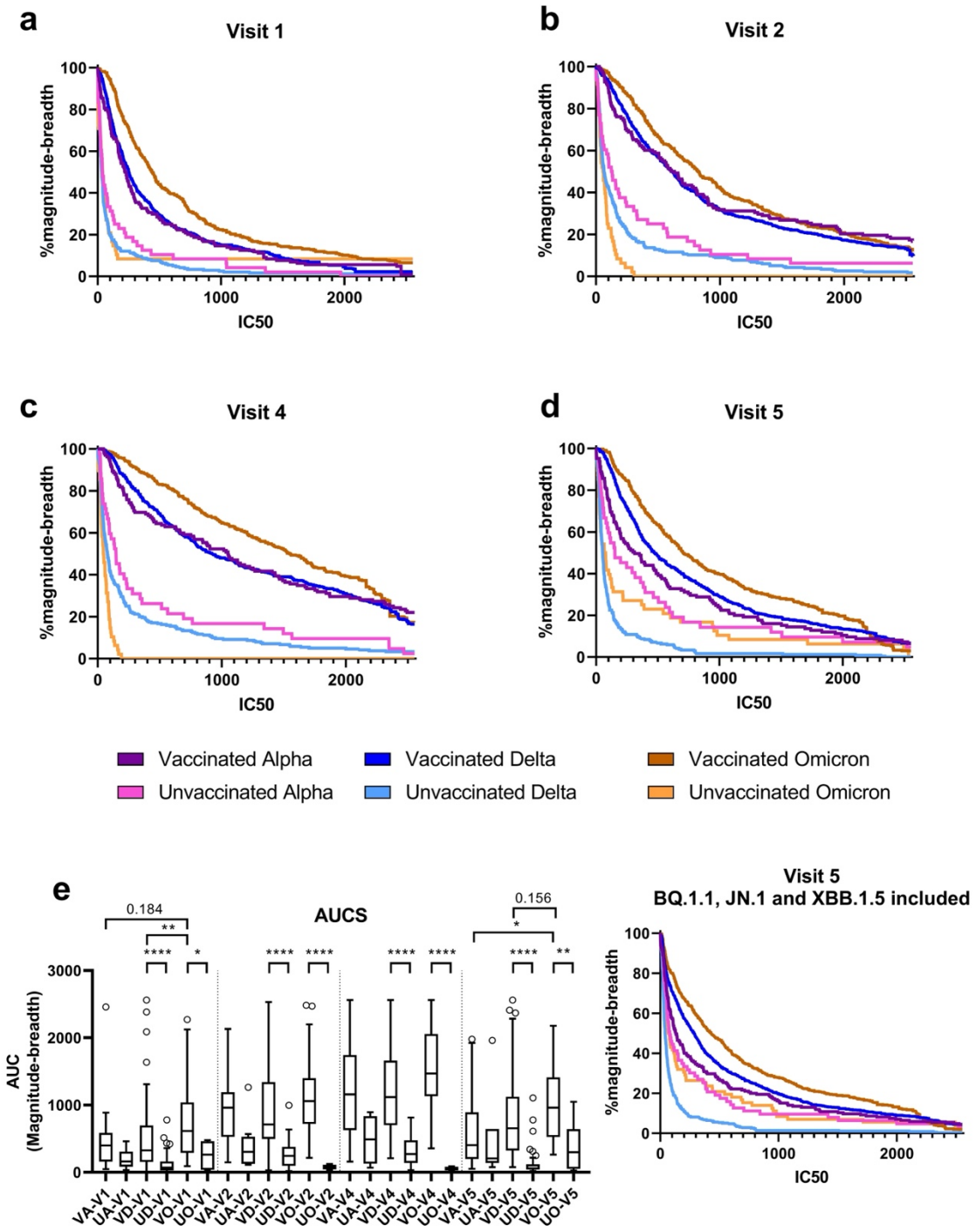

Figure 23 Magnitude-breadth analysis for all study groups at the different visits. Magnitude-breadth curves of the vaccinated & Alpha infected (VA), unvaccinated Alpha infected (UA), vaccinated & Delta infected (VD), unvaccinated Delta infected (UD), vaccinated & Omicron infected (VO) and unvaccinated Omicron infected (UO) groups at visit 1 (V1), visit 2 (V2), visit 4 (V4) and visit 5 (V5) (A-D). E Magnitude-breadth curves at V5 with the variant BQ.1.1 included in the analysis. F Calculated Areas under the curve (AUC) of the magnitude-breadth curves in A-D for each infection variant-vaccination status combination sorted by visits. AUCs were analyzed by Kruskal-Wallis test and significance levels were adjusted by Dunn's correction for multiple tests. Statistically significant differences are indicated by p values (* p<0.05, ** p<0.005, *** p <0.001, **** p<0.0001).

To provide an additional layer of comparison, log-rank tests were performed to compare the overall magnitude breadth curves (**Supplemental Figure 15**), confirming our AUC-based comparison of curves. At visit 1-4, significantly higher magnitude breadth was found for all vaccinated groups compared to the unvaccinated groups (all $p < 0.0001$). At visit 1, Omicron BTI exhibited even higher initial magnitude breadth than Delta or Alpha BTI (both $p < 0.0001$). At visit 2 and 4, significantly reduced magnitude breadth was found for Omicron infection without vaccination compared to Alpha or Delta infection (all $p < 0.0021$). As opposed to comparing AUCs, Omicron BTI elicited a significantly higher magnitude breadth compared to Delta BTI (visit 2 $p = 0.0144$, visit 4 $p = 0.0135$). At visit 5, Omicron BTI still exhibited a significantly higher magnitude breadth than Delta BTI ($p = 0.0459$) and Alpha BTI ($p = 0.0017$), while Delta BTI exhibited a significantly increased magnitude breadth compared to Alpha BTI ($p = 0.0459$). Surprisingly, magnitude breadth of Omicron infected without a vaccination increased at visit 5 to similar levels as Alpha infection, leaving delta infection in the last place (p Alpha vs Delta < 0.0001, p Omicron vs Delta = 0.0062).

Noteworthy, a subgroup analysis of the two- versus three-time-vaccinated individuals with Omicron BTI (**Supplemental Figure 16A-E**) at V5 revealed that the magnitude breadth level of triple-vaccinated individuals remained significantly higher in comparison to 2x vaccinated individuals (p(O3xV vs. O2xV)=0.0384) on the level of the previously analyzed vaccinated Omicron BTI group (**Supplemental Figure 16D, E**). The 2x vaccinated individuals with Omicron BTI dropped to levels similar to those of 2x vaccinated individuals with Delta BTI. Similar to the previous analysis, no significant differences regarding magnitude and breath were found in 2x or 3x vaccinated between V1 and V4 (**Supplemental Figure 16A-C, E**).

5.6.4.6 Multivariate analysis

Multivariate analysis was conducted using separate PERMANOVA models for individuals with vaccination as well as individuals without vaccination, this enabled inclusion of vaccine-specific variables such as days between vaccination and infection, number of vaccinations, and if the individual received any vector vaccine. Those were included on top of sex/gender, age, smoking status, neutralized variant, and infection variant as used for modeling individuals without vaccination.

For vaccinated individuals, we found significant impact of age ($p = 0.001$), number of vaccinations ($p = 0.009$), time between vaccination and infection ($p = 0.001$), virus to be neutralized ($p = 0.001$), and the infection variant ($p = 0.001$) on neutralization. Post-hoc pairwise PERMANOVA testing adjusted for all aforementioned variables utilizing tobit models identified significant differences between Omicron and Delta BTI ($p = 0.006$) as well as Omicron and Alpha BTI ($p = 0.015$) but no differences between Delta and Alpha BTI ($p = 0.158$).

Similarly, significant impact of the infection variant ($p = 0.001$) and virus to be neutralized ($p = 0.001$) was found for individuals without vaccination before infection. In contrast to vaccinated individuals, age did not have an impact in unvaccinated individuals ($p = 0.978$) but a significant impact was found for smoking ($p = 0.005$). Adjusted post-hoc pairwise PERMANOVA testing revealed significant differences between all cross-compared groups: Delta, Omicron and Alpha infection (all $p = 0.003$)

5.6.4.7 Antigenic mapping and antibody landscapes

Subsequently, we used our neutralization data to construct antigenic maps, visualizing the antigenic relationship of the tested viruses and antibody responses elicited in the different groups, for all study time points (**Figure 24**). The mapped distances between VOCs and the relative placement of the individual antisera, respectively, correspond to the antigenic relationship and indicate the profile of the antibody response for the respective groups at the indicated time points (V1-5).

At early convalescence (V1-V2), the sera of the vaccinated groups cluster mainly around the vaccine-matched WT/D614G strain, regardless of the infecting VOC. This suggests that vaccine-primed nAb specificities are extended in the first place. Beginning at V2 and towards the peak of the neutralizing antibody responses at V4, the sera of the vaccinated groups shift with time towards the respective infecting variant (e.g. sera from Alpha BTI shifting towards the Alpha variant). Interestingly, in the long-term (V5) the sera from all BTI groups revoked and shifted back towards the vaccine-matched WT/D614G strain (**Figure 24**).

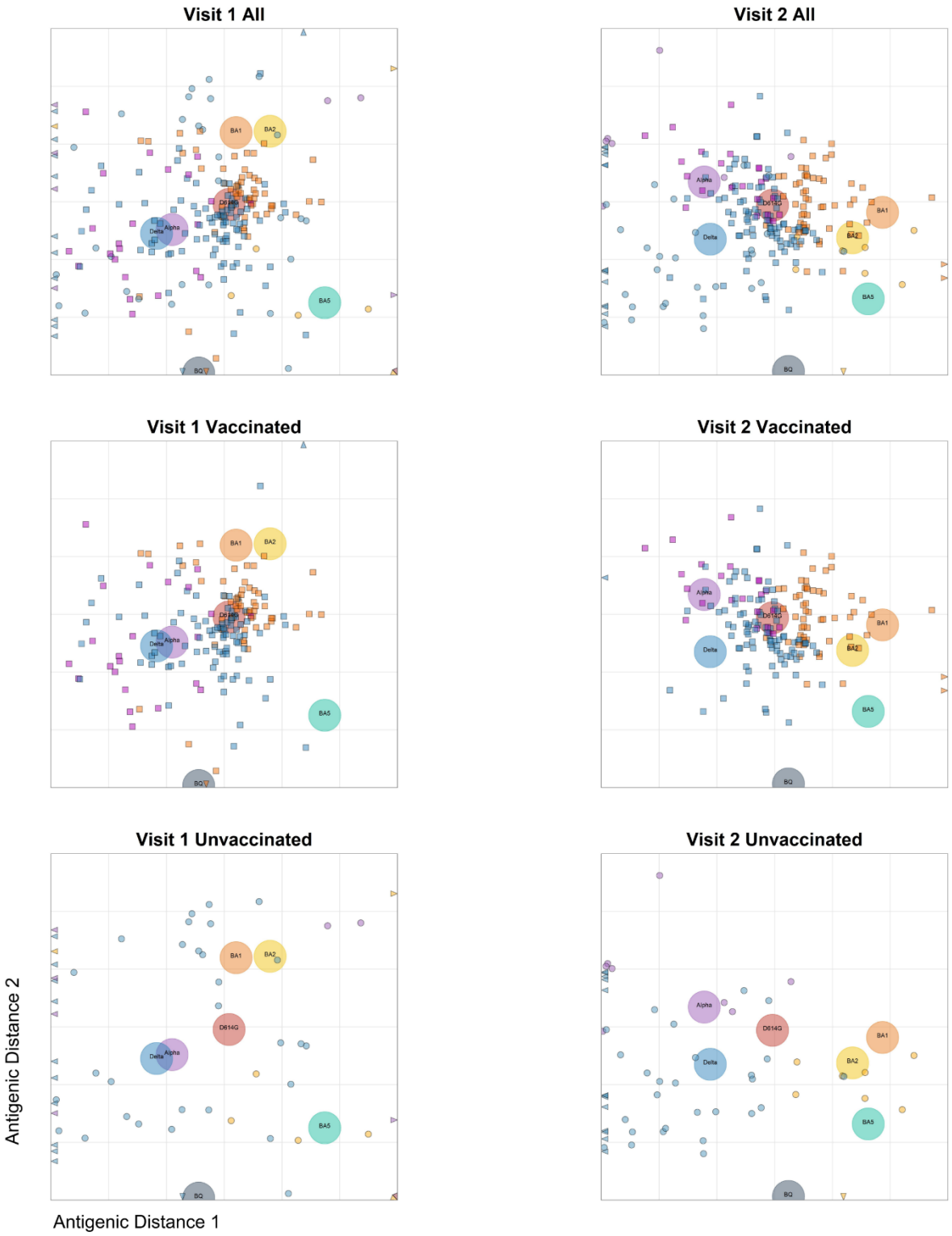
Visit 1 All
Visit 2 All
Visit 1 Vaccinated
Visit 2 Vaccinated
Visit 1 Unvaccinated
Visit 2 Unvaccinated
Antigenic Distance 2
Antigenic Distance 1
BA1
BA2
BA5
BQ
Alpha
Delta
D614G

Figure 24 Antigenic maps for SARS-CoV-2 variants. Antigenic maps for four different study time points (V1, V2, V4 and V5) based on sera of vaccinated and unvaccinated participants with Alpha, Delta or Omicron infections. The SARS-CoV-2 variants are shown as big colored circles on the map Wuhan/D614G (red), Alpha (purple), Delta (blue), Omicron BA.1 (orange), BA.2 (yellow), BA.5 (green) and BQ.1.1. (grey) and respective individual sera are indicated as small squares (vaccinated) or small circles (unvaccinated) in purple, blue and orange for Alpha, Delta or Omicron infections, respectively. The y- and x-axes of the map both represent antigenic distance. Each grid square (1 antigenic unit) represents a 2-fold change in neutralization titer. Row one are maps including all sera, while row two and three show only the sera of vaccinated or unvaccinated individuals, as indicated.

In contrast, the sera from unvaccinated individuals were initially more widely distributed at V1, mainly due to initially very low neutralization titers, but at the later visits increasingly clustered around the infecting variant, most pronounced at peak neutralizing responses at V4. At V5, the localizations of the unvaccinated sera dispersed again, likely due to the lower overall neutralization titers (**Figure 24, Figure 22**). Bootstrapping and calculation of confidence intervals confirmed the localization of virus variants on the map, while the highest insecurity was found for BQ.1.1 at V1, and the highest confidence levels were achieved at V4 (**Supplemental Figure 17**).

Finally, antibody landscaping complemented antigenic mapping by the addition of quantitative neutralization information. Confirming our magnitude-breadth analysis, we found an increased and broadened response in vaccinated versus unvaccinated individuals at V1-V4 (**Figure 25**). Similar shapes and magnitudes were calculated for the vaccinated groups at V1 and V2. In contrast, obvious differences amongst the vaccinated groups were revealed at peak response (V4). This is particularly evident comparing the tilt of the Omicron BTI group displaying a peak at the map's BA.1/2 cluster with the Delta infected individuals peaking at the map's Alpha/Delta cluster (**Figure 25**). This was true for both, the two times and three times vaccinated after Omicron BTI (**Supplemental Figure 18**). At V5 tilting reverted back towards a peak at the WT/D614G strain, leaving similar landscapes for both, Delta and Omicron BTI. Additionally, sustained neutralization magnitude and breadth were found after Omicron or Delta BTI, while Alpha BTI reverted back towards the levels of unvaccinated groups (**Figure 25**).

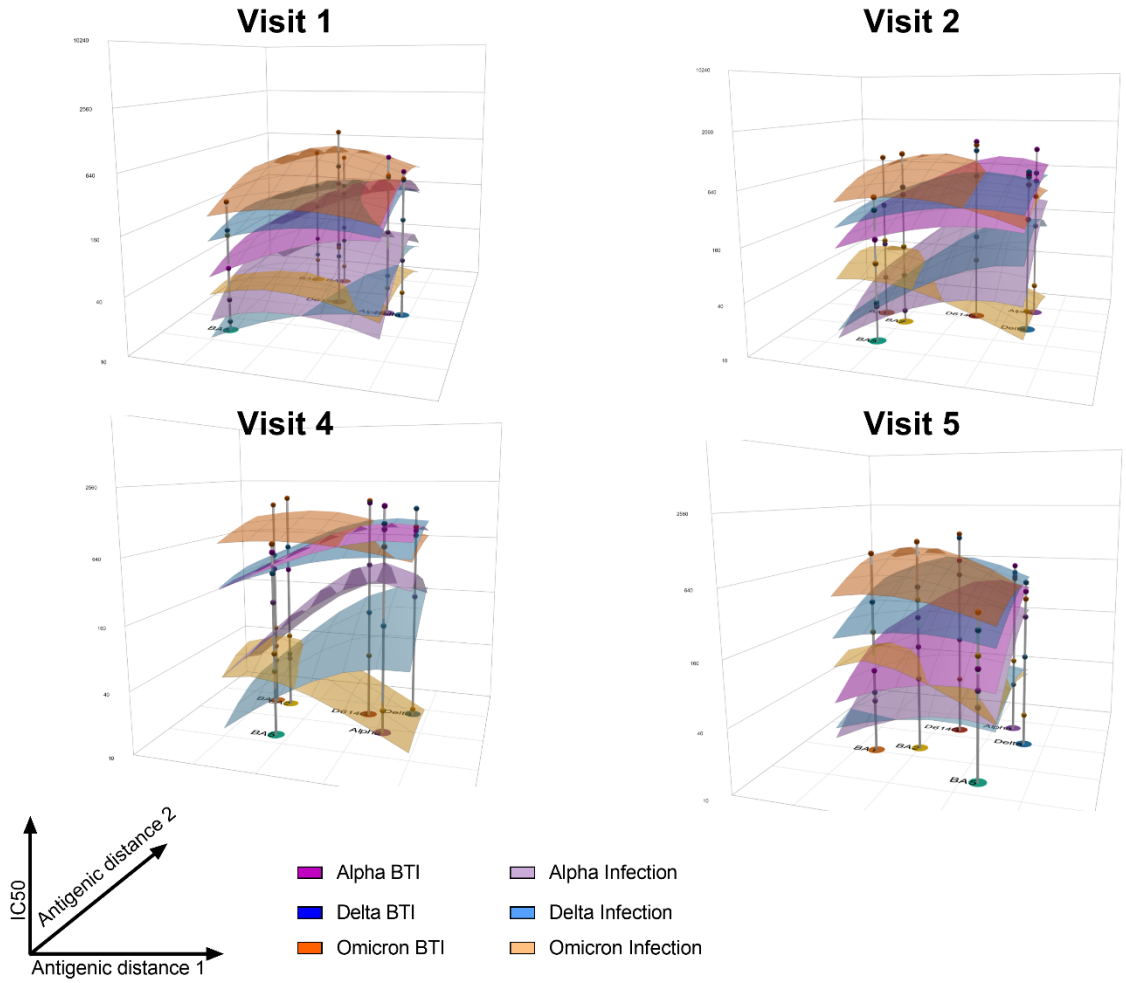

Figure 25 Antibody landscapes for each study group. Colored surfaces show the fitted geometric mean titer (GMT) antibody landscapes for the different study groups vaccinated & Alpha infected (dark purple), unvaccinated Alpha infected (light purple), vaccinated & Delta infected (dark blue), unvaccinated Delta infected (light blue), vaccinated & Omicron infected (dark yellow) and unvaccinated Omicron infected (light yellow). While the base x-y plane corresponds to the antigenic map shown in Figure 24, gray impulses show the height of the GMT for specific SARS-CoV-2 variants. The vertical z-axis in each plot corresponds to the GMT on the log2 scale, each two-fold increment is marked, starting from a titer of 20at the map surface. The antibody landscapes for visit 1 can be seen in the upper left panel, visit 2 in the upper right panel, visit 4 in the lower left panel and visit 5 in the lower right panel.

5.6.4.8 Machine Learning models to predict infecting VOC from neutralization profiles

To confirm expansion of the nAb profile towards the break-through infecting variant, random-forest models were trained to predict the infecting VOC (Alpha, Delta, Omicron) from the neutralization profile in break-through infected or infected individuals. Reported are mean accuracies and errors of 100 models trained and tested on independently generated datasets. Out-of-bag error was at 4.38% for the vaccinated at V4 and below 1.1 % for all other conditions, showing solid training for all models (**Figure 26A**).

In unvaccinated individuals, model accuracy increased from 72.5 % (visit 1) to 87.8 and 87.1 % for V2 and V4, respectively, staying at a high level of 78.7 % for the long-term visit (V5). Similarly, model accuracy in vaccinated individuals started with 71.3 % (V1), increased to 76.1 % (V2), peaked at V4 (77.3 %) and slightly decreased towards the long-term V5 (75.3 %). Model accuracies for the break-through infected were slightly reduced compared to the unvaccinated group. However, overall prediction of the infecting variant was still reliable in all BTI models, especially at V4. This provides additional proof, of a strong shift in overall immune profiles following BTI - despite prior vaccination (**Figure 26B**).

Consistently lowest variant-specific accuracy (25 - 70%) was found for Alpha BTI throughout all visits, slightly increasing towards visit 2 and 4 . For Delta and Omicron, increased accuracies were found for V2 and V4, staying high at the long-term V5, similar to the general model accuracy. Highest accuracies were achieved for omicron BTI . A similar pattern was found for the unvaccinated and infected. (**Figure 26C & D**).

Random forest results were independently verified by training neural networks as exemplarily shown in **Figure 26E**, achieving accuracies of 51.8, 57.6, 61.9 and 61.1 % for the breakthrough infected individuals and 72.6, 85.7, 84.7 and 79.7 % in the infected individuals for the respective visits (**Figure 26F**).

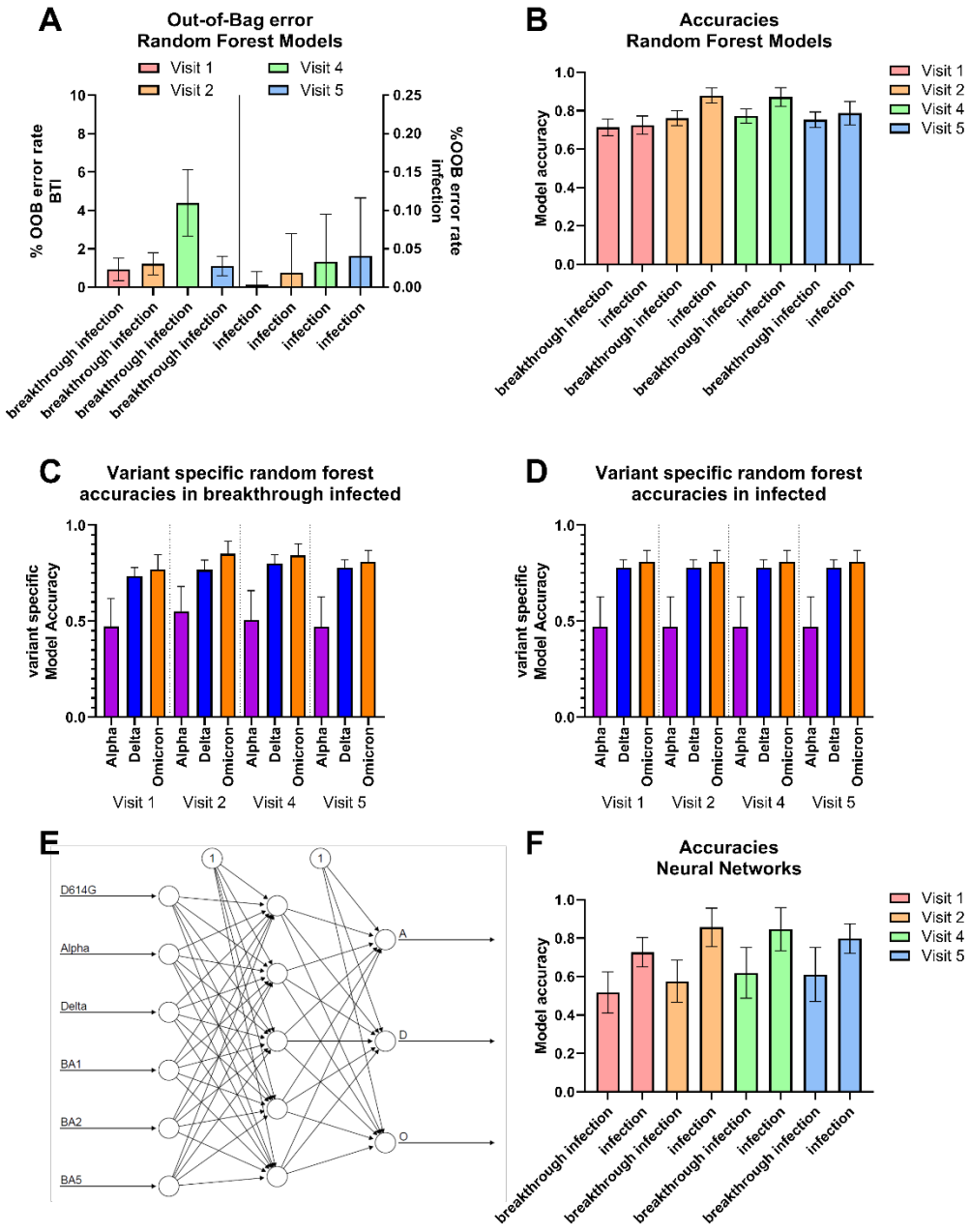

Figure 26 Machine Learning model accuracy and error rates. A Out of bag error rate of random forest models for the vaccinated, breakthrough infected and unvaccinated, infected groups at the visits 1,2,4 and 5. B Random forest model accuracies for the vaccinated and breakthrough infected or unvaccinated and infected groups at the visits 1,2,4 and 5 on an independent test dataset. C Variant-specific accuracy in vaccinated and breakthrough infected individuals for visit 1,2,4 and 5 D Variant-specific accuracy in unvaccinated and infected individuals for visit 1,2,4 and 5. E Exemplary neuron configuration of the neural networks used. With 6 input neurons, one hidden layer of 5 neurons and three output neurons giving the probability for A (Alpha), D (Delta) and O (Omicicron) infection. F Neural network model accuracies for the vaccinated and breakthrough infected or unvaccinated and infected groups at the visits 1,2,4 and 5 on independent test datasets.

5.6.5 Discussion

Our study demonstrated that hybrid immunity, i.e. the immune response acquired by vaccination and subsequent BTI is superior to infection-induced immunity alone in terms of magnitude, breadth, and durability of the neutralizing immune response. Yet, an antigenically closely related immune response of limited magnitude and breadth, may still be superior against a newly emerging VOC, compared to an antigenically distant immune response of high magnitude and breadth. The highest magnitude and breadth were observed in BTIs with the VOCs Delta and Omicron, which are antigenically most distant to the vaccine-encoded wildtype-based SARS-CoV-2 spike. Nonetheless, even those groups lost their long term response against novel and far distant variants like XBB1.5. and JN.1, whereas Omicron infection without prior vaccination revealed a significantly higher response against those far distant Omicron descendants as compared to delta infection. Noteworthy, a third vaccination, although based on the original SARS-CoV-2 wildtype spike, significantly improved the long-term magnitude-breadth profile, while we didn't find any impact of a vector vaccine history. Antigenic mapping indicated specific neutralizing antibody profiles elicited by BTI or non-BTI, which evolved differently depending on the infecting SARS-CoV-2 VOC. Noteworthy this analysis provided evidence of initial immune imprinting by vaccination prior to BTI with any of the VOC. Finally, antigenic landscaping highlighted the impact of a third vaccination and helped to quantitatively refine our finding of a long-term bias towards immunity against the vaccine antigen.

Whereas the majority of previous studies on BTI are either based on smaller numbers of participants or lacking long-term follow-up data[387–389], our prospective and longitudinal multicenter study design comprised 229 participants, who were observed for a period of 4-6 months. A Kaplan-Meier function was introduced to quantify and combine neutralization against multiple SARS-CoV-2 VOCs (magnitude-breadth) at different time points. Our data confirm and expand previous findings showing that VOC BTIs enlarge the functional neutralization footprint of wild-type based COVID-19 vaccines[390,391].

Previous studies have found differences in individuals vaccinated with mRNA based vaccines compared to individuals receiving a combination of Adenoviral and mRNA based vaccines, leveled out by a third vaccination[392]. Our data suggest that those differences get largely leveled out by breakthrough infection, though increased titers against D614G and Alpha hint towards a slightly increased durability. However, regarding the heterogenicity and size of the vector-vaccinated group within this study-collective, those results should not be over-interpreted. A different cohort, designed around this research topic would be needed to provide more reliable insights.

Previous data have shown[390], that short- or long-time intervals between vaccination and subsequent BTI impede or enlarge neutralizing antibody levels, respectively. Our data added evidence, that enlarged intervals barely influenced short-term nAb responses against the infecting VOC but had some positive impact on the long-term outcome of the neutralization capacity.

Furthermore, a third vaccination was demonstrated to have long-term benefit neutralization magnitude and breadth[393–395], even for more recent VOC such as BQ.1.1. Noteworthy, also the antigenic distance between the spike antigen presented with the BTI and the spike variant (WT/D614G) delivered by the vaccine significantly impacts the magnitude-breadth profile of hybrid immunity[387–389,396]. In particular, our longitudinal analysis demonstrates that the long-term neutralization magnitude-breadth persisted at higher levels in Delta or Omicron BTI if compared to Alpha BTIs, which are antigenically most related to the COVID-19 vaccine. This suggests that a durable nAb response with a high magnitude-breadth is preferentially induced by exposure to antigenically more distant Delta or Omicron variants. Nonetheless, even those groups lost their long-term response against novel and far distant variants like XBB1.5. and JN.1, whereas Omicron infection without prior vaccination showed similar response against those far distant Omicron descendants compared to vaccination and Omicron BTI.

Using antigenic cartography, initially developed to evaluate the quality of neutralizing antibody responses against multiple influenza variants[397], the analysis of sera from unvaccinated infected individuals confirmed distinct antigenic clusters, formed dependent on the antigenic relationship of the analyzed SARS-CoV-2 variants[383,398–400]. Additionally, we found different antibody profiles depending on vaccination history and the infecting VOC. Noteworthy, the longitudinal evolution of antigenic maps in BTIs suggests an initial boost of the vaccine-primed wildtype-directed nAb response followed by a broadening of nAb responses towards the infecting variant with time. At the long-term visit, a subsequent contraction of the nAbs towards wild-type-specific nABs dominating could be observed.

This effect might be explained by either de-novo stimulation of naïve B-cells or, alternatively, by affinity maturation and/or expansion of already primed memory B-cells. Recent evidence based on antibody depletion studies and longitudinal BCR sequencing convincingly suggests boosting and expansion of imprinted B-cell specificities as the most probable explanation for the observed broadening of neutralization capacity[401,402]. This pattern hints towards a phenomenon referred to as “immune imprinting”, which has previously been found for other viruses such as influenza[372]. Our data would also be compatible with a de novo priming of VOC-specific neutralizing B cell responses, peaking at V4, but vanishing faster as WT specific neutralization due to lack of expansion and affinity maturation. As evidenced recently, more sustained responses to the new and antigenically distant infecting variant could be achieved by repeated contact eventually overcoming immune imprinting[403]. Both interpretations would be in agreement with our quantitative analysis highlighting that neutralization magnitude-breadth improved with antigenic distance of the VOC causing the BTI to the vaccine antigen. Further implications of those phenomenons are effectively illustrated with our data of an increased immune response towards novel Omicron descendents such as BQ.1.1, XBB.1.5. and JN.1[404]

in individuals with Omicron infection but no vaccination history. Emphasizing, that a lower overall breadth, but imprinted with an antigenically closer antigen may still be beneficial over a high overall breadth but imprinted with a distant antigen.

Finally, antibody landscaping[399] affirmed and expanded our magnitude-breadth analysis by resolving the contribution of VOC specific neutralization. This was especially relevant comparing Omicron and Delta BTI, which yielded different slopes and directions in their fitted landscapes, especially when the three times vaccinated individuals were excluded. Subsequent reversion towards similar peaks and slopes after Delta or Omicron BTI regarding long-term nAb response provide further confirmation for the observed long-term bias towards WT SARS-CoV-2 neutralization. Random forest models and neural networks reliably predicted the infecting and, noteworthy, also the breakthrough infecting VOC from the neutralization profiles, including at the long term V5. This independently confirmed a sustained shift of the neutralization profile towards the breakthrough infecting VOC, despite prior vaccination and immune imprinting. Of note, multiple potential risks can be associated with machine learning-based data analysis, possibly resulting in biased results[405]. We tried to minimize bias derived from sample imbalance by resampling and counteract potential bias from overfitting, by introducing noise into resampled values. Looking at the different variant-specific accuracies, a consistently lower Alpha accuracy implied, that those measures might positively influence but still not fully equalize the bias derived from small and imbalanced groups. This expresses the need for larger cohorts or even combined databases of multiple cohorts to yield more refined models. To minimize the impact of this potential bias and still allow careful interpretation, we reported mean accuracies of 100 independent models on 100 independently drawn datasets. Another relevant consideration is the neural network's lower predictive accuracy, despite the neural networks' theoretical advantages in modeling complex, non-linear relationships. This highlights their potential underperformance in smaller datasets, once again underscoring the necessity of larger datasets and maybe necessary inclusion of additional variables for more refined models. Nevertheless, we think our work provides a solid proof of concept for the usability of such models in answering arising questions of the field.

Our study also has some limitations. Due to the lack of pre-infection samples and analytical reference points, we could not exactly determine the impact of preexisting immunity. Furthermore, the comparably low number of individuals in the unvaccinated Alpha and Omicron groups could impact comparisons between non-BTIs and BTIs, respectively. Nevertheless, the results shown align with the results obtained for comparing Delta infection with and without prior vaccination. Another possible source of bias might derive from cohort differences, in specific, significantly increased prevalence regarding preexisting disease in individuals with vaccination compared to unvaccinated individuals. However, no significant differences were found regarding immune-related disease[377]. Furthermore, despite random and multicenter recruitment of acutely infected individuals with and without prior

vaccination reported by health authorities, we cannot fully exclude potential sampling bias e.g. due to individuals avoiding official SARS-CoV-2 testing to evade strict quarantine regulations or other confounding effects.

In conclusion, our prospective and longitudinal multicenter cohort study revealed that neutralization capacity, breadth, and durability did benefit from the number of vaccinations and antigenic distance between the infecting VOC and the WT spike delivered via the vaccine. Antigenic mapping, antibody landscaping, and machine learning models affirmed distinct immune profiles, shaped based on the infecting VOC and time after BTI. Our longitudinal study design proved an immune imprinted initial boost of vaccine-specific neutralization and a delayed shift towards the infecting VOC at peak response, while the long-term neutralization was contracted towards the vaccine antigen.

5.6.6 Appendix & Declarations

Members of the CoVaKo study group

Prof. Dr. Helmut Messmann, Dr. Andre Fuchs, Dr. Alanna Ebigbo, Dr. Christoph Römmele, Maximilian Ullrich, Marie Freitag, Prof. Dr. Claudia Traidl-Hoffmann, Mehmet Goekkaya, Aline Metz, Corinna Holetschek, Prof. Dr. Avidan Neumann, Elisabeth Kling, Prof. Dr. Reinhard Hoffmann, Mihail Pruteanu, PD Dr. Thomas Wibmer, Dr. Susanne Rost, Prof. Dr. Klaus Überla, Dr. Philipp Steininger, Dr. Monika Wytopil, Stephanie Beileke, Dr. Sandra Müller-Schmucker, Dr. Klaus Korn, Tamara Hastreiter, Kirsten Fraedrich, Debora Obergfäll, Dr. Frank Neumann, Dr. Claudia Kuhn, Dr. Katja Günther, Dr. Elke Friedrich, Prof. Dr. Michael Hoelscher, PD Dr. Andreas Wieser, PD Dr. Christof Geldmacher, Christian Janke, Michael Plank, Jessica Guggenbühl, Christina Reinkemeyer, Ivan Noreña, Dr. Noemi Castelletti, Dr. Raquel Rubio Acero, M. I.M. Ahmed, Paulina Diepers, Tabea M. Eser, Anna Fuchs, Olga Baranov, Bernadette Bauer, Danni Wang, Ivana Paunovic, Prof. Dr. Ulrike Protzer, Samuel D. Jeske, Catharina Christa, Kathrin Tinnefeld, Martin Vu, Annika Willmann, Dr. Hedwig Roggendorf, Dr. Nina Körber, Dr. Tanja Bauer, PD Dr. Sabine Gleich, Prof. Dr. Ralf Wagner, Dr. Claudia Asam, Sebastian Einhauser, Manuela Weps, Antonia Senninger, Dr. George Carnell, Prof. Jonathan Luke Heeney, Antonia Ebner, Maria José de Schultz, Cedric Rajes, Aya Al Wafai, David Brenner, Laura Sicheneder, Melanie Berr, Anja Schütz, Dr. Stilla Bauernfeind, Dr. Andreas Hiergeist, Prof. Dr. Dr. André Gessner, Prof. Dr. Barbara Schmidt, Dr. Hans-Helmut Niller, Dr. Jürgen Wenzel, Daniela Biermeier, Dr. Benedikt Lampl, Ulrich Rothe, Dr. Ute Gleißner, Dr. Susanne Brückner, Michaela Treml, Holger Schedl, Dr. Beate Biermaier, Markus Achatz, Dr. Daniela Hierhammer, Johanna Englhardt, Werner Scheidl, Dr. Sivaji Jeyaraman, Dr. Barbara Schutt, Prof. Dr. Johannes Liese, Prof. Dr. Martina Prelog, PD Dr. Giovanni Almanzar, Valeria Schwägerl, Dr. Julia Bley, Tim Vogt, Kimia Kousha, Lars Ziegler, Astrid Stein, Franziska Förg, Dr. med. Johann Löw, Barbara Finkenberg, Dennis Pollak, Alexander Zamzow, Dr. Nicole Eberbach, Lara Balkie, Tanja Kretzschmann, Matthias Gehrig, Matthias Bandorf, Kilian Keck, Dr. Jan Allmanritter, Shahid

Rafique, Mona Finster, Dr. med. Ingo Baumgart, Sabine Heumüller-Klug, Hans-Jürgen Koglin, Prof. Dr. Olaf Gefeller, Dr. Christine Gall, Prof. Dr. Annette B. Pfahlberg, Isabelle Kaiser Prof. Dr. Jörg Scheidt, Johannes Drescher, Yannic Siebenhaar, Dr. Florian Wogenstein, Dr. Dirk Reinel, Prof. Dr. Beatrix Weber, Fabian Zarzitzky, Prof. Dr. Bernhard Liebl, Prof. Dr. Caroline Herr, Dr. Katharina Katz, Prof. Dr. Dr. Andreas Sing and Dr. Alexandra Dangel

Funding

This work was funded by the Bavarian State Ministry of Science and the Arts for the CoVaKo study and the ForCovid project. The funder had no influence on the study design, data analysis or data interpretation.

Contributors

Conceptualization: R.W., K.Ü., P.S.; Methodology: S.E., R.W., Participant recruitment and study visits: S.D.J., C.A., A.F., M.W., S.B., C.J., C.C., A.Wil., M.V., M.We., B.M.J.L., V.S., B.L., P.S.; Laboratory investigations: S.E., A.S., D.P.; Statistical analysis: S.E., B.A., R.W. Visualization: S.E., C.A., P.S.; Resources: M.P., H.M., U.P., J.L., M.H., R.W., K.Ü.; Writing (original draft): S.E., C.A., R.W.; Writing (review and editing): all authors; Supervision: M.P., H.M., U.P., J.L., M.H., R.W., K.Ü., P.S.; Project administration: K.Ü., P.S.; Funding acquisition: H.M., U.P., J.L., M.H., R.W., K.Ü.; All authors have read and agreed to the published version of the manuscript.

Acknowledgments

We are particularly grateful to all study participants. We would like to thank the heads and employees of the Bavarian Health and Food Safety Authority and the public health offices of Augsburg, Bad Kissingen, Erlangen-Höchstadt, Forchheim, Fürth, Kelheim, Kitzingen, Main-Spessart, Munich, Neumarkt, Nuremberg, Regensburg, Schwandorf, Schweinfurt, Straubing, Tirschenreuth and Würzburg for their tremendous support.

Data Sharing Statement

Data and source-code can be accessed on github in the public repository: rwagnerlab/Einhauseretal2024_imprinting_neutralizing_antibodies/

Conflict of Interest / Disclosures

M.P. receives honoraria for scientific talks from Abbvie, BioNTech, Chugai-Roche, GSK, Esanum, Janssen, Novartis, Moderna, MSD, Pfizer, Sanofi, and SOBI, for consultant tasks from Abbvie, BioNTech, GSK, Janssen, Novartis, and Pfizer, travel scholarships from Chugai-Roche, GSK, Novartis, and Pfizer and support for investigator-initiated research from Baxter, Chugai-Roche, Galapagos, GSK, MSD, Moderna, Novartis, Pfizer and SOBI. U.P. received personal fees from Abbott, Abbvie, Arbutus, Gilead, GSK, J&J, MSD, Roche, Sanofi, Sobi, and Vaccitech. U.P. is co-founder, share-holder and board member of SCG Cell Therapy Inc.

5.6.7 Supplementary Materials

Supplementary Table 19 Vaccination schemes of study cohorts. Including the numbers of participants of the different breakthrough groups for the respective vaccination schemes. Abbreviations: A, vaccine Vaxzevria, AstraZeneca, AZD1222; B, vaccine Comirnaty, BioNTech/Pfizer, BNT162b2; M, Spikevax, Moderna, mRNA-1273; J, Jcovden former COVID-19 Vaccine Janssen, Janssen-Cilag/Johnson&Johnson, JNJ-78436735.

Variant of infection	Number of vaccinations	A - A	A - B	B - B	B - M	M - B	M - M	J- B	A-A-B	A-B-B	A-M-B	B-B-B	B-B-M	M-M-B	M-M-M
Alpha	2	1	1	19	1	1	1	-	-	-	-	-	-	-	-
Delta	2	6	3	81	-	1	3	-	-	-	-	-	-	-	-
Omicron	2	1	-	4	-	-	-	2	-	-	-	-	-	-	-
Omicron	3	-	-	-	-	-	-	-	1	2	1	36	6	1	1

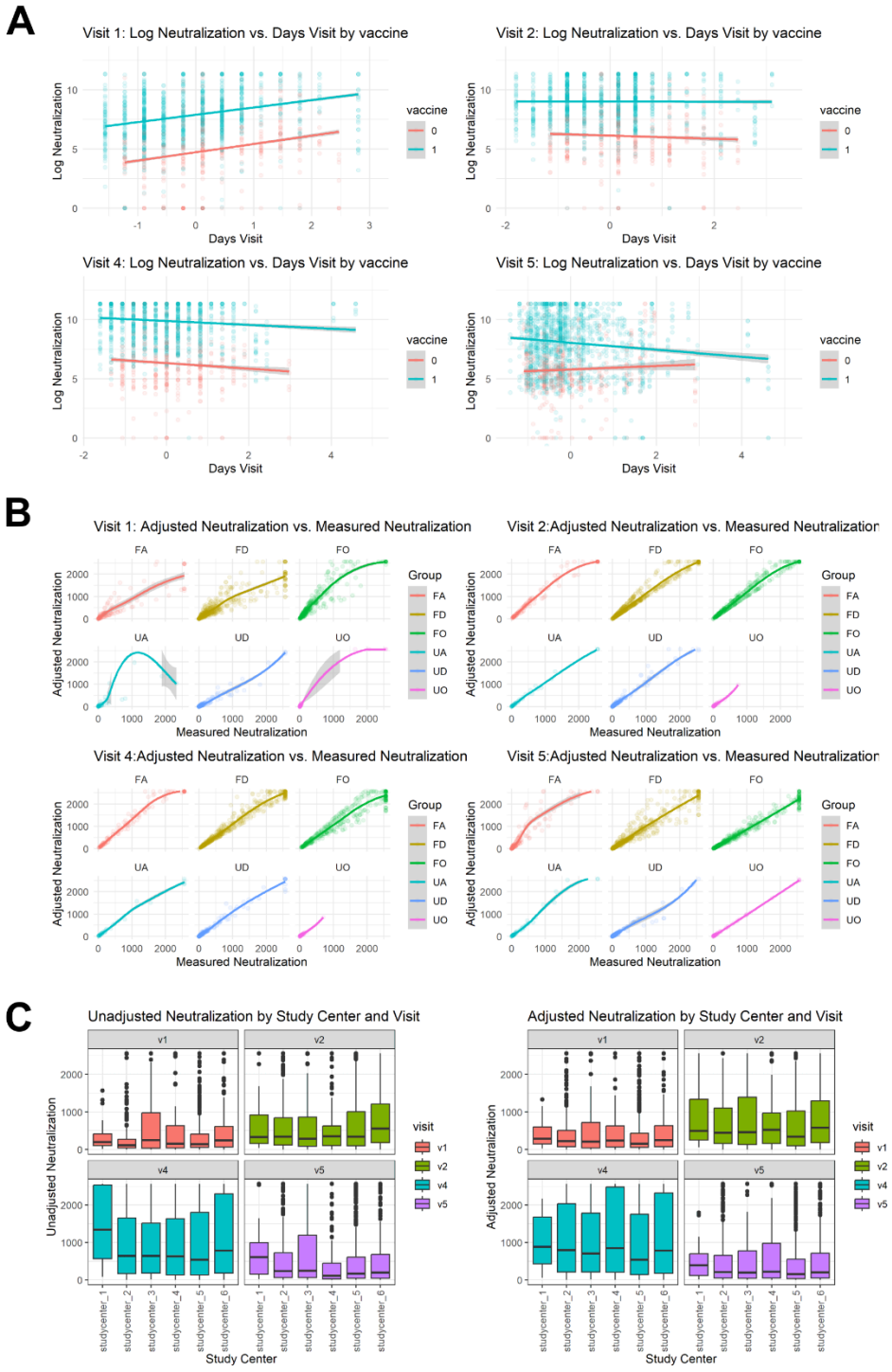

Supplemental Figure 9 Adjustment for follow up time and studycenter effects. Tobit models for every visit were utilized to adjust the neutralization data for follow up time (scaled to mean) and studycenter effects with center 5 as reference. A Visualization of assumed linear follow-up time effects by vaccination status (0 = no vaccination, 1 = vaccinated) and visit. B Visualization of the adjustment for each visit and within the different groups analyzed later (FA = Vaccinated Alpha BTI, FD = Vaccinated Delta BTI, FO = Vaccinated Omicron BTI, UA = Unvaccinated Alpha Infection, UD = Unvaccinated Delta Infection, UO = Unvaccinated Omicron infection). Shown are adjusted values on thy y axis and unadjusted values on the X axis with loess regression to visualize trends. C Visualization of studycenter stratified nAb titers and studycenter adjustment, shown are median titers for each visit by studycenter. The left panel shows unadjusted values, the right panel the adjusted values.

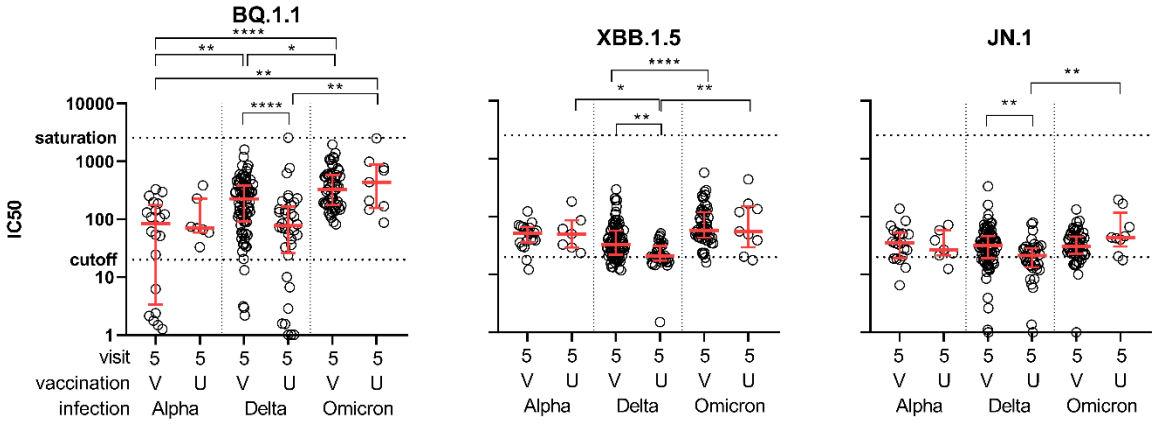

Supplemental Figure 10 Neutralization assays against the SARS-CoV-2 variant BQ.1.1 for vaccinated and unvaccinated Alpha, Delta and Omicron infected study groups at visit 5. Antibody responses of vaccinated (V) and unvaccinated (U) individuals at visit 5 after infection with Alpha, Delta or Omicron (as indicated on the x-axis). Serum dilution factors needed to reach 50% inhibitory concentration (IC50) for Omicron BQ.1.1. The assay cut-off (IC50 = 20) as well as saturation (IC50 = 2560) are indicated by dashed lines. Median and interquartile ranges are indicated in blue. Differences between vaccinated and unvaccinated were analyzed by Mann-Whitney test, statistically significant differences are indicated by p values (** p<0.005). Differences between infection variant groups were analyzed by Kruskal-Wallis tests with post-hoc Dunn's corrected multiple comparisons tests, statistically significant differences are indicated by p values (* p<0.05,** p<0.005, *** p<0.001, **** p<0.0001)

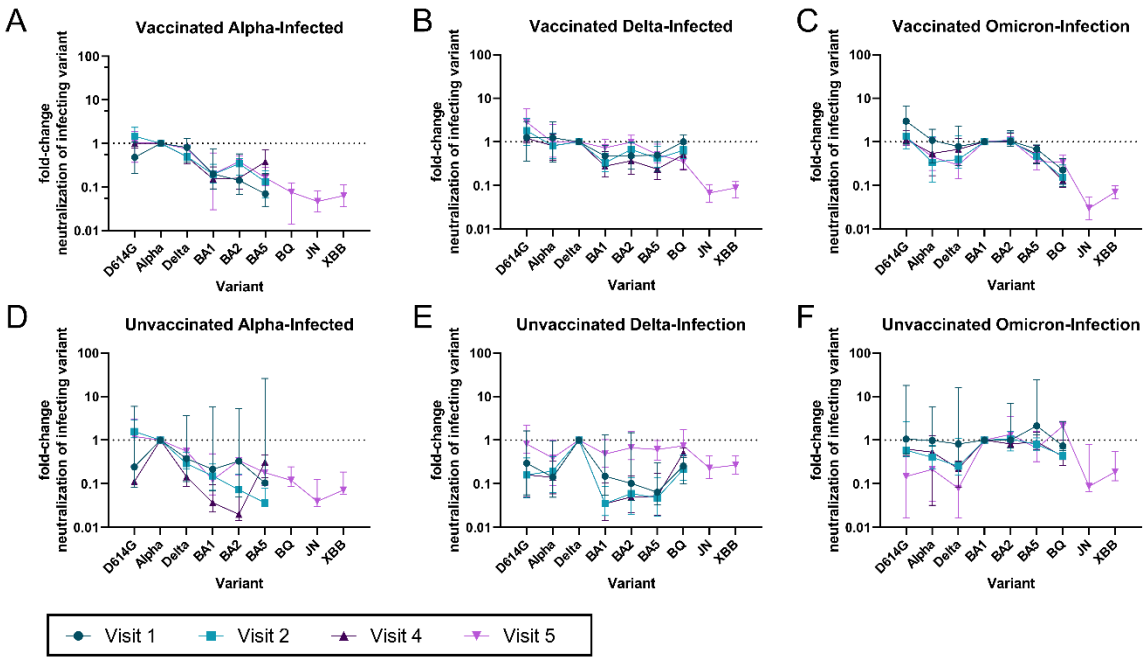

Supplemental Figure 11 Estimates of fold-change compared to the homologous variant. Comparison of median fold differences for all measured SARS-CoV-2 variants relative to the titers against the variant of infection : Alpha panel A (vaccinated) and D (unvaccinated), Delta panel B (vaccinated) and E (unvaccinated), Omicron panel C (vaccinated) and F (unvaccinated). Visits 1, 2, 4 and 5 are shown simultaneous in each panel. Points show the median estimate for the fold-change difference while lines show the interquartile range for the estimate.

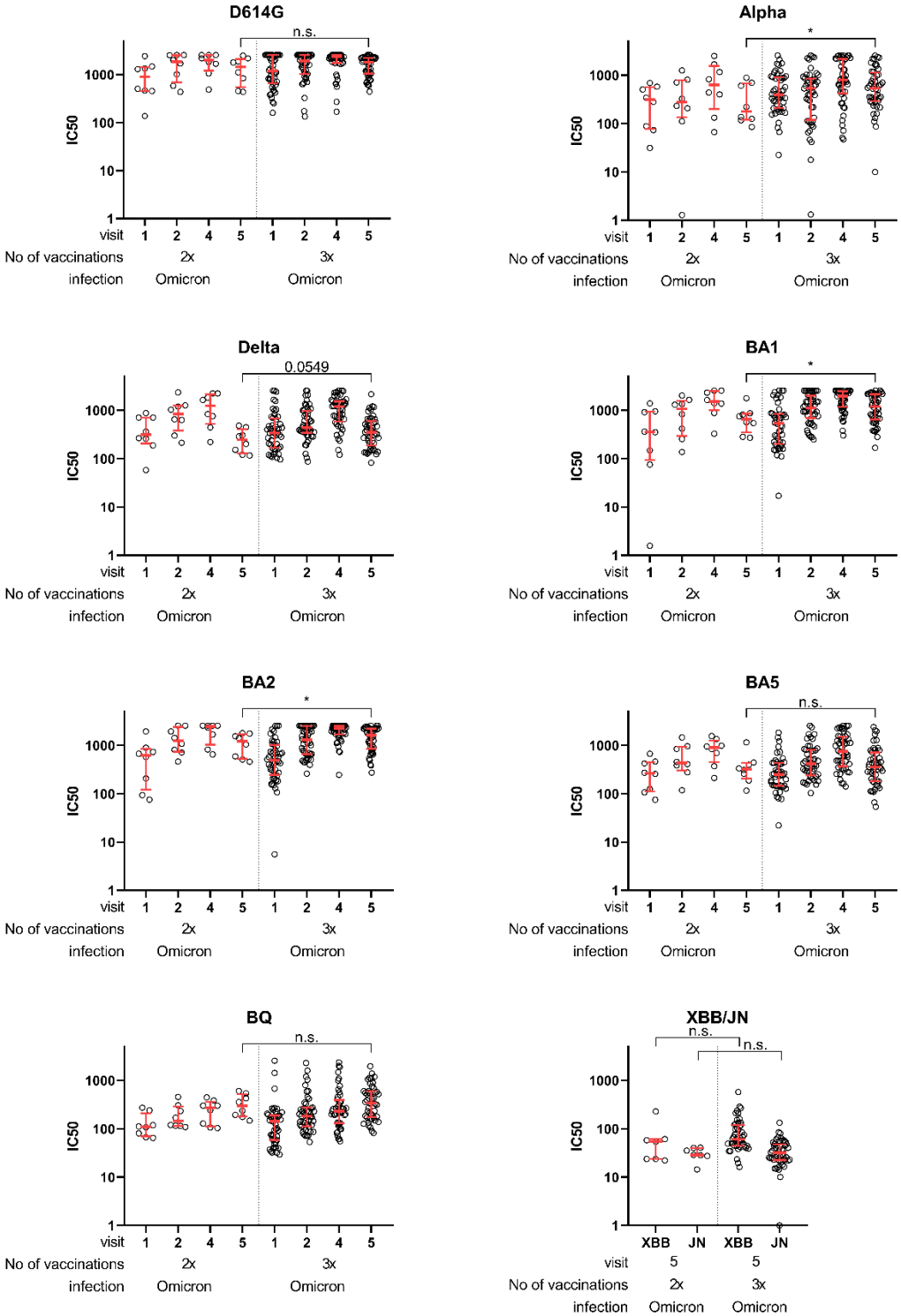

Supplemental Figure 12 Comparison of neutralization assays against different SARS-CoV-2 variants for double- and triple-vaccinated Omicron groups. Antibody responses of double vaccinated (2V) and triple vaccinated (3V) individuals at visit 1, 2, 4 and 5 after infection with Alpha, Delta or Omicron (as indicated on the x-axis). Shown are the dilution factors for 50 % Inhibitory concentration (IC50) for WT/D614G, Alpha, Delta, Omicron BA.1, Omicron BA.2 and Omicron BA.5 spike, as indicated by the individual graph titles. The assay cut-off (IC50 = 20) as well as saturation (IC50 = 2560) are indicated by dashed lines. Median and interquartile ranges are indicated in blue. Data were analyzed by Mann-Whitney test, statistically significant differences are indicated by p values (* $p<0.05$, ** $p<0.005$).

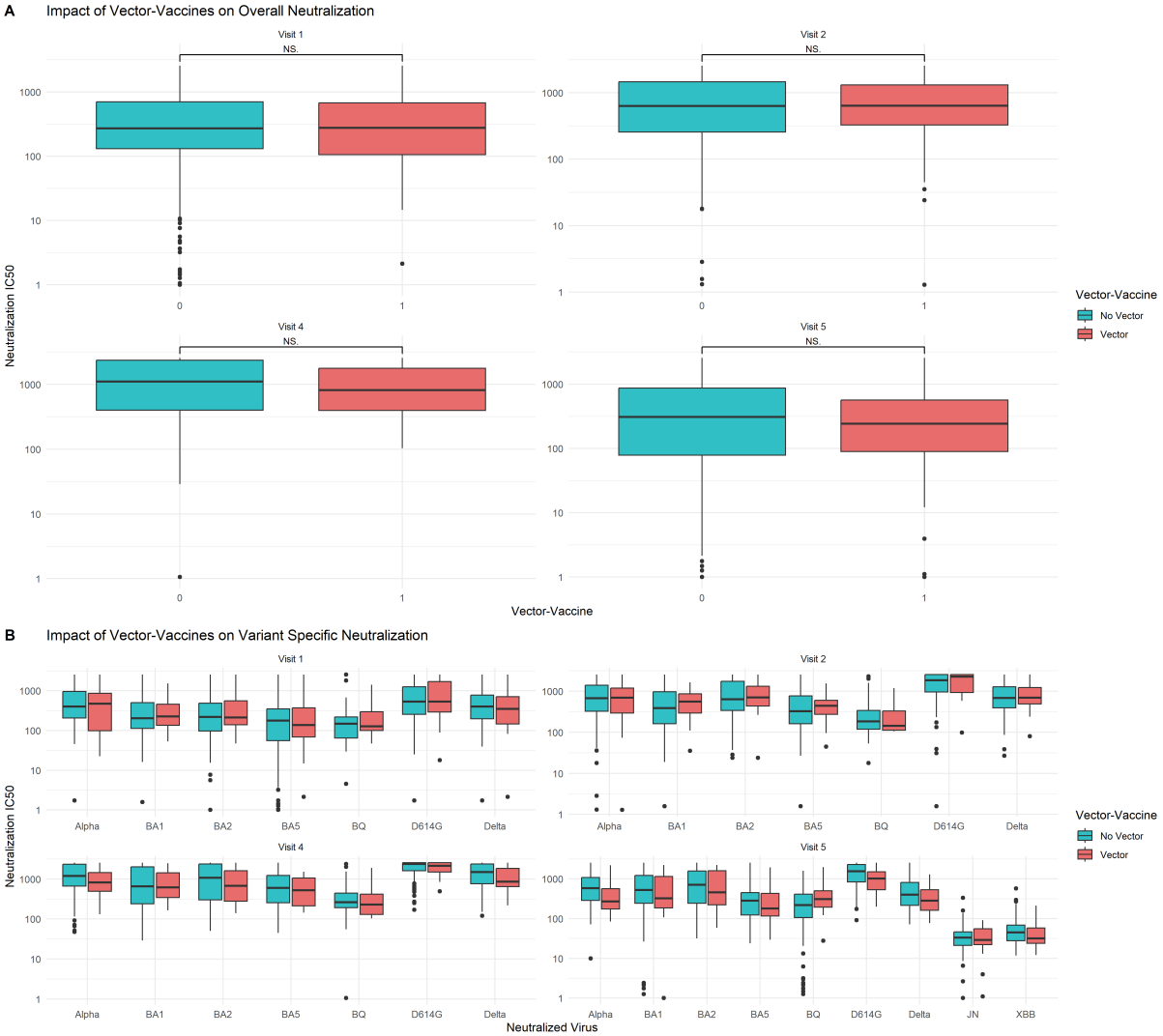

Supplemental Figure 13 Comparison of neutralization in adenoviral vector- or mRNA vaccinated individuals. A Shown are pooled nAb titers against all tested variants (D614G, Alpha, Delta, BA1, BA2, BA5) in either individuals who received an adenoviral vaccination at any point (n = 18) or in individuals who only received mRNA vaccines, for the different visits. Data were analyzed by Mann-Whitney test, statistically significant differences are indicated by p values (* p<0.05, ** p<0.005) B Shown are variant specific nAb titers at four different visits in either individuals who received an adenoviral vaccination at any point (n = 18) or in individuals who only received mRNA vaccines. Data were analyzed by Mann-Whitney test, statistically significant differences are indicated by p values (* p<0.05, ** p<0.005).

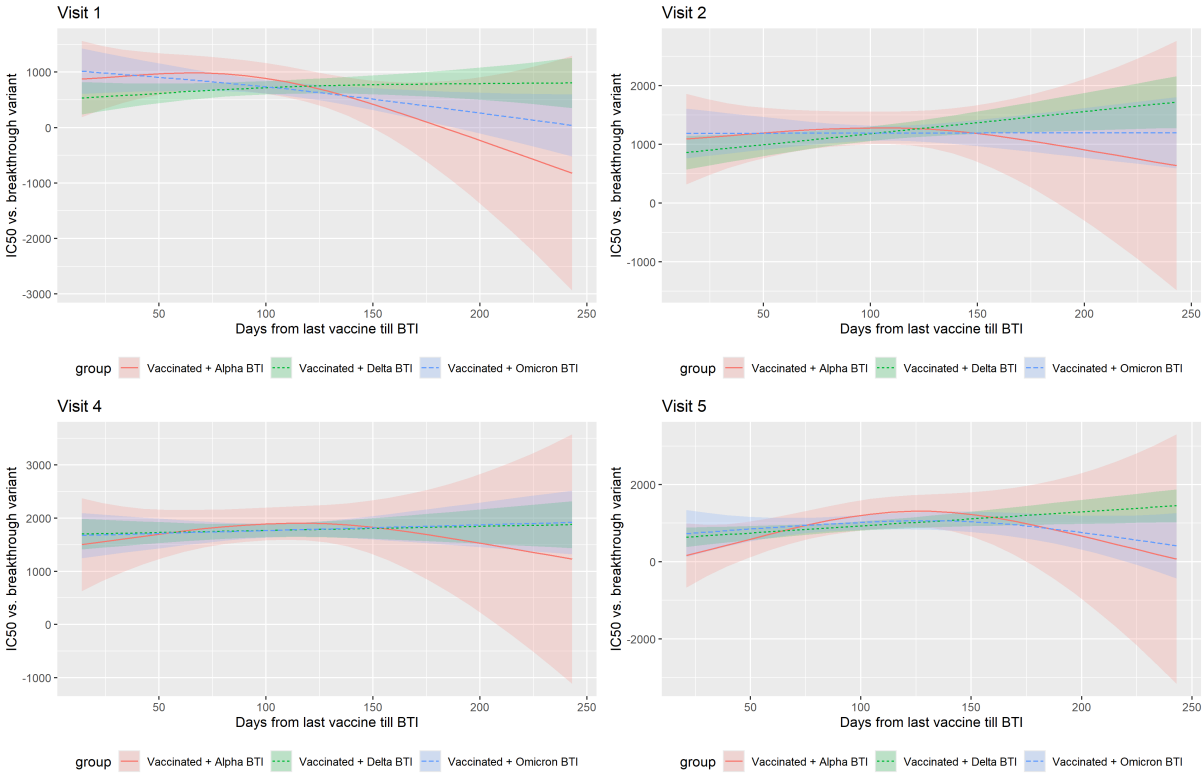

Supplemental Figure 14 Non-linear association of time intervals between vaccination and BTI on the nAb response (IC50) towards the infecting variant. Generalized additive model smooths based on thin plate regression splines, with automatic selection of the effective degrees of freedom, for alpha (red), delta (green) and omicron (blue) BTI. Shown are separate models for Visit 1, Visit 2, Visit 4 and Visit 5. Shaded regions indicate approximate 95%-prediction intervals (Prediction ± 2×SE).

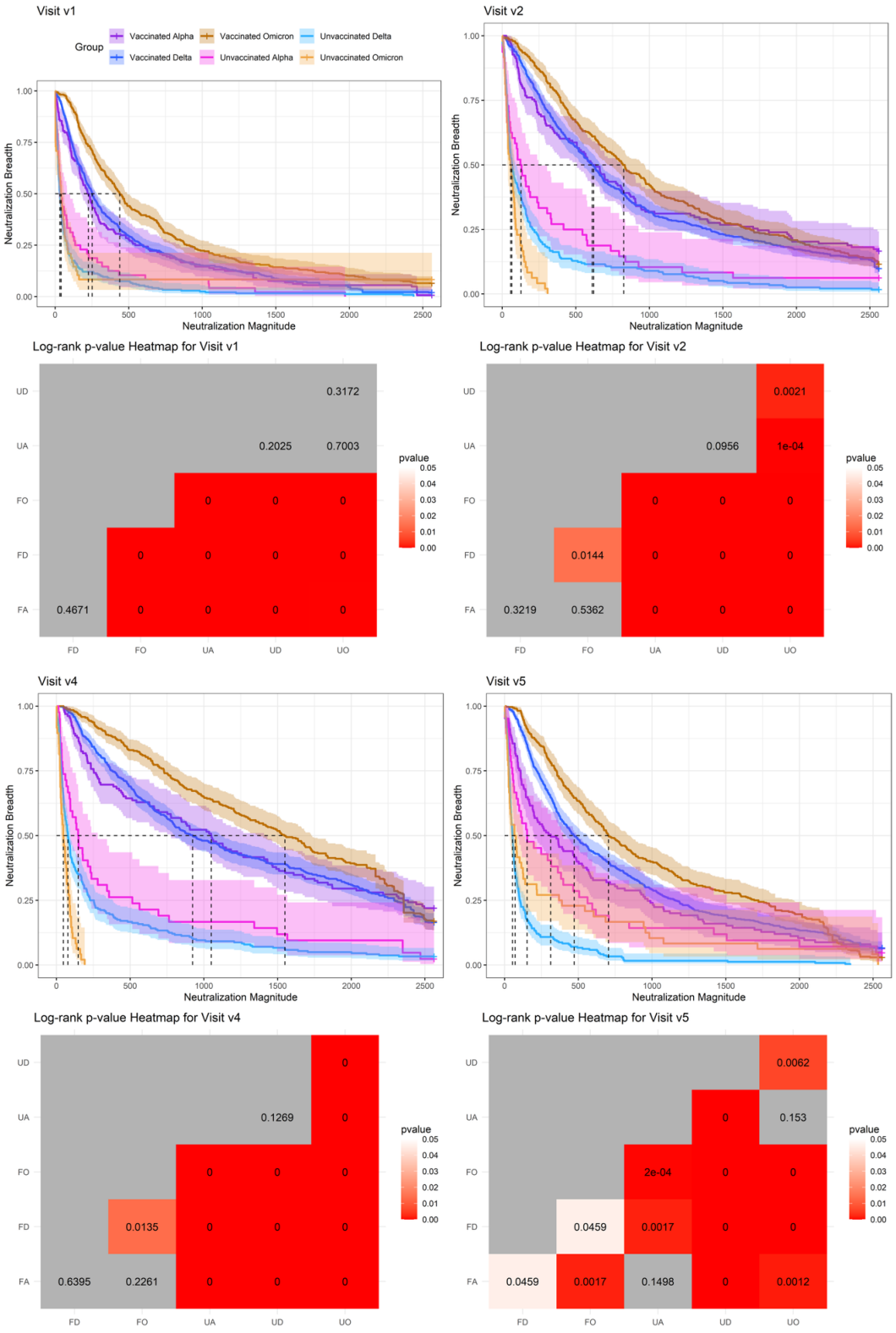

Supplemental Figure 15 Magnitude breadth curves with confidence 95% confidence intervals and log-rank tests as alternative comparison method. Shown are the four panels (one for each visit) with magnitude breadth curves color coded for the different groups (Purple = Alpha BTI, Darkblue = Delta BTI, brown = Omicron BTI and pink = Alpha infection, lightblue = Delta infection, orange = Omicron infection). Below are the results of the log rank tests for comparison of all groups (FA = Alpha BTI, FD = Delta BTI, FO = Omicron BTI and UA = Alpha infection, UD = Delta infection, UO = Omicron infection), plotted as a heatmap (grey = not significant, white to red = significant, 0 denotes a pvalue < 0.0001) for each visit.

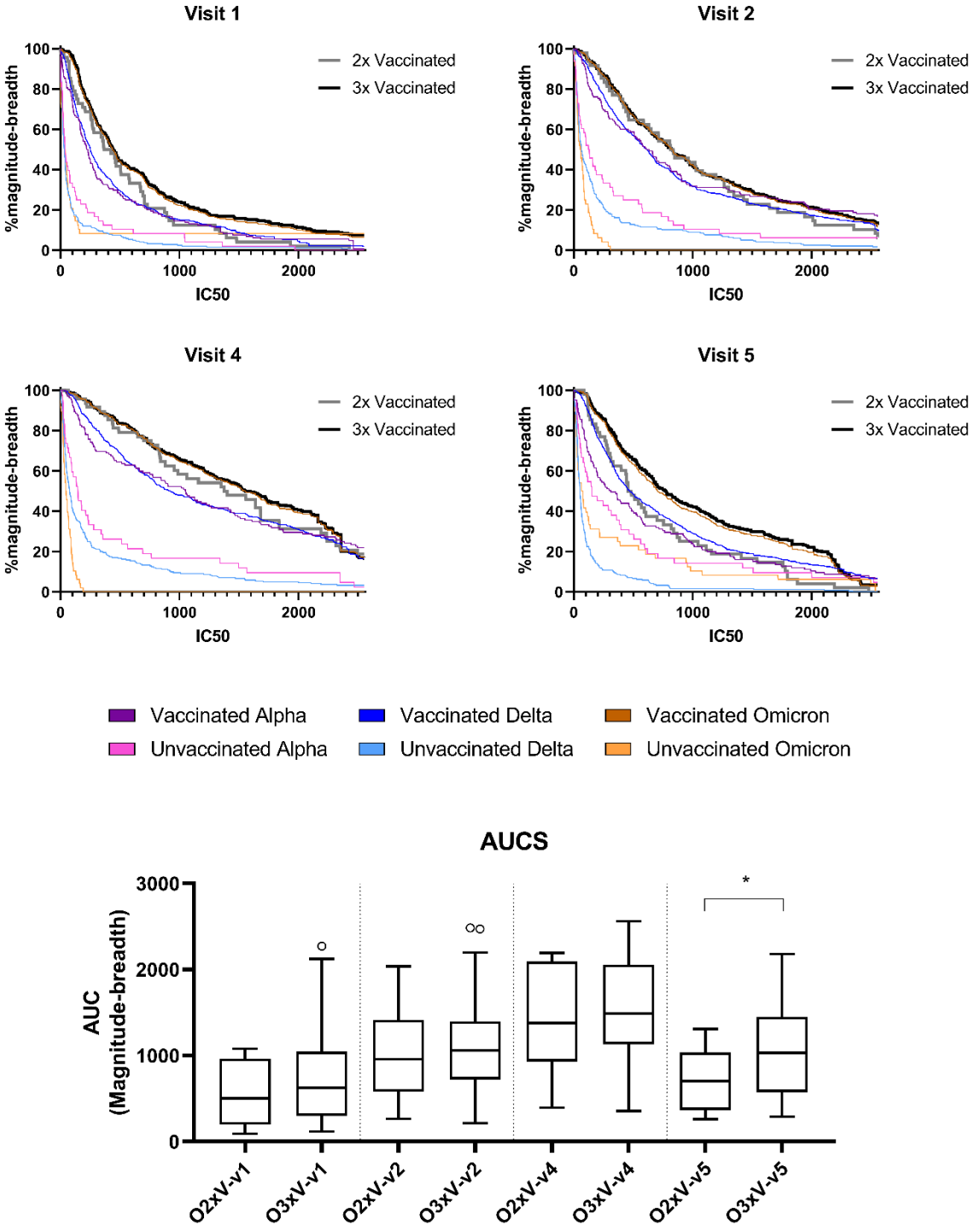

Supplemental Figure 16 Comparison of magnitude-breadth analysis between double- and triple-vaccinated Omicron groups. To the magnitude breadth curves of Figure 23 the curves for double- (O2xV) and triple-(O3xV) vaccinated & Omicron infected subgroups are added at visit 1 (V1), visit 2 (V2), visit 4 (V4) and visit 5 (V5) (A-D). E, Area under the curve (AUC) for the double- and triple-vaccinated & Omicron infected groups are calculated and compared at V1, V2, V4 and V5. Data were analyzed by Mann-Whitney test, statistically significant differences are indicated by p values (* p<0.05, ** p<0.005, *** p <0.001).

Supplemental Figure 17 Assessing the effect of the uncertainty in variant reactivity for the antigenic maps using bootstrapping. Antigenic maps for four different study time points (V1, V2, V4 and V5, as indicated) based on sera of vaccinated and unvaccinated participants with Alpha, Delta or Omicron infections. The SARS-CoV-2 variants are shown as big colored circles on the map WT/D614G (red), Alpha (purple), Delta (blue), Omicron BA.1 (orange), BA.2 (yellow), BA.5 (green) and BQ.1.1. (grey) Individual sera are not shown. The x- and y-axes of the map both represent antigenic distance. Each grid square (1 antigenic unit) represents a 2-fold change in neutralization titer. 1,000 resampling bootstrap repeats were performed with 100 optimizations per repeat. at all visits. Each colored region indicates the area in which 68% (one standard deviation) of the positional variation of variant.

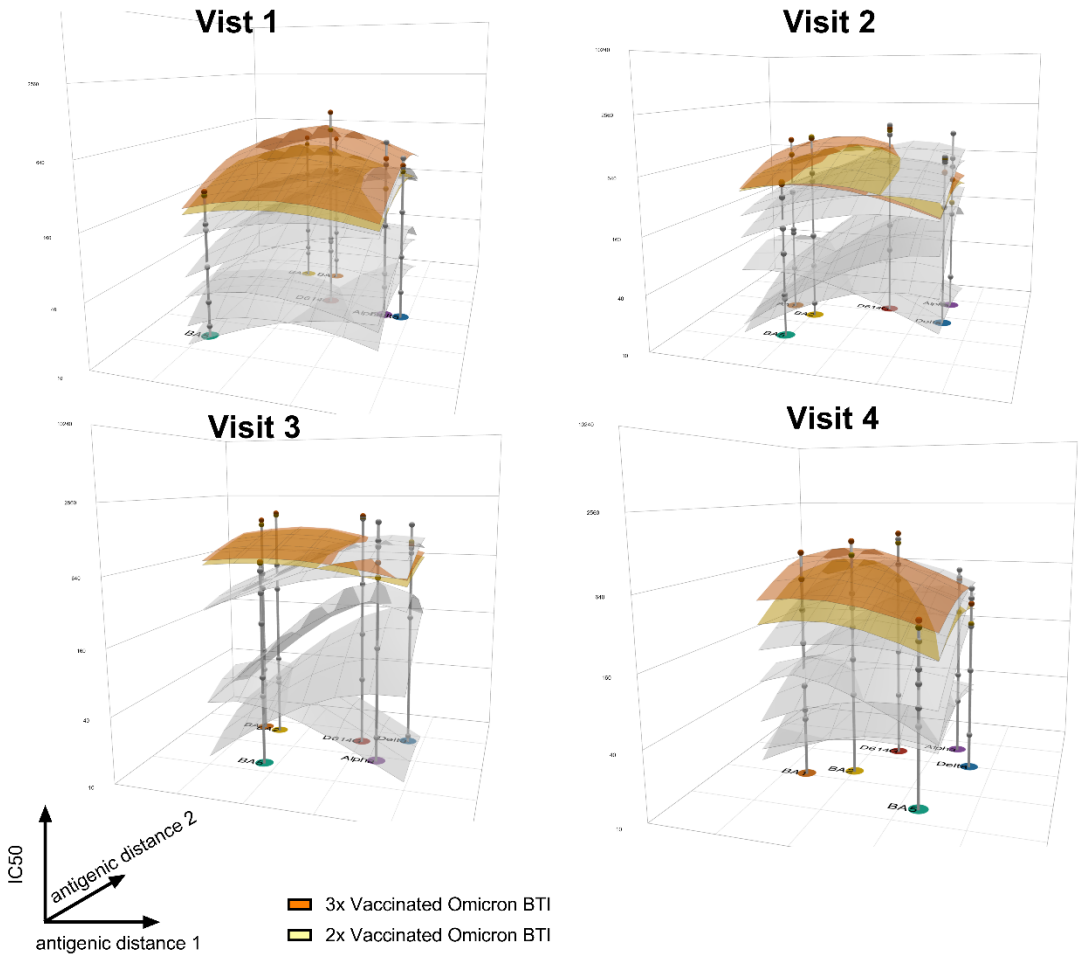

Supplemental Figure 18 Antibody landscapes for Omicron double-vaccinated versus triple-vaccinated cases. Colored surfaces show the fitted geometric mean titer (GMT) antibody landscapes for the different study groups vaccinated & Alpha infected (dark purple), unvaccinated Alpha infected (light purple), vaccinated & Delta infected (dark blue), unvaccinated Delta infected (light blue), triple vaccinated & Omicron infected (dark yellow), double vaccinated & Omicron infected (red) and unvaccinated Omicron infected (light yellow). While the base x-y plane corresponds to the antigenic map shown in Figure 24, gray impulses show the height of the GMT for specific SARS-CoV-2 variants. The vertical z-axis in each plot corresponds to the GMT on the log2 scale, each two-fold increment is marked, starting from a titer of 20 at the map surface. The antibody landscapes for visit 1 can be seen in the upper left panel, visit 2 in the upper right panel, visit 4 in the lower left panel and visit 5 in the lower right panel.

6 Summary of Findings

6.1 Test Development and Benchmarking

Serological **SARS-CoV-2 antibody tests** are routinely applied in diagnostics and seroepidemiological studies. In this thesis, a variety of commonly used serological tests, namely the Roche Cobas S-RBD and N total Ig tests, a S-RBD ELISA specific for IgG, IgA or IgM and the YHLO IFlash N&S total Ig assay, as well as Latent Class analysis based combinations of those tests, were qualitatively and quantitatively benchmarked against each other and a VSV-based SARS-CoV-2 pseudovirus neutralization assay using a subgroup of the TiCoKo19 study cohort (n = 856). The commercial Cobas S and N tests revealed a nearly ideal dichotomous agreement with Cohens $\kappa = 0.96$. Also, YHLO and IgG ELISA showed high agreements with each other and the Cobas test with $\kappa > 0.87$, while IgA and IgM ELISA showed generally poor agreement ($\kappa < 0.22$). Various Latent class analysis models revealed a good concordance with dichotomized neutralization ($\kappa > 0.92$), yet the models could not surpass the Cobas S single test. Additionally, **spectrum bias effects** could be demonstrated comparing the population-based full sub-cohort with a defined subgroup of individuals with absolutely no or strong neutralization titers. Here, the Roche S test showed nearly no bias ($\Delta\kappa = 0.025$), while slight effects were apparent for the Roche N test ($\Delta\kappa = 0.056$) and medium bias effects were revealed ($\Delta\kappa \sim 0.1$) for YHLO and ELISA. Finally, quantitative analysis assigned the highest correlation (Pearson R = 0.66) with neutralization to the IgG RBD ELISA. (see 5.3 Manuscript 2: “Spectrum Bias and Individual Strengths of SARS-CoV-2 Serological Tests-A Population-Based Evaluation”)

To explore **alternative readouts**, a novel VSV pseudovirus readout based on ECIS (electric cell-substrate impedance sensing) was investigated and compared to classical VSV pseudovirus-based GFP readout as a proof of concept. Virus induced CPE could be dose dependently detected for viral concentrations (MOI = 1 up to MOI = 5) already 5-10 h post infection. This enabled neutralization assays using either a monoclonal VSV-G antibody against VSV-G pseudotypes or human sera against VSV-SARS-CoV-2-Spike pseudotypes. Comparison of fluorescence and impedance-based readout correlated highly significant with a Spearman r = 0.87 for titration experiments and a Spearman r = 0.91 for neutralization experiments. (see 9.1.16 “Appendix Manuscript 16: Impedance-based monitoring of titration and neutralization assays with VSV-G and SARS-CoV-2-spike pseudoviruses”)

Additionally, **novel test formats** were explored in the form of Sulforhodamine-B filled and SARS-CoV-2 RBD decorated liposomes competing with antibodies for Ace2 binding, either in a high-throughput format (HT) or a point-of-care (POC) lateral flow format. This enabled determination of EC50 values

and comparison to an established lentiviral pseudotype neutralization assay for monoclonal SARS-CoV-2 antibodies and for a selection of 20 positive and 10 negative human Sera. The comparisons resulted in a 100 % specificity, sensitivities of 80 (HT) and 50 % (POC) and a correlation of Spearman r = 0.85 (HT) and r = 0.75 (POC), emphasizing the potential of the novel format. (see 9.1.9 “Appendix Manuscript 9: Liposome-based high-throughput and point-of-care assays toward the quick, simple, and sensitive detection of neutralizing antibodies against SARS-CoV-2 in patient sera”)

Finally, production conditions and readout cell lines were optimized for a variety of human CoVs using a **lentiviral pseudotype** system. Here, SARS-CoV-1, multiple SARS-CoV-2 VOCs, and HCoV-NL63 efficiently transduced HEK293T/17 cells expressing ACE2 and TMPRSS2. HCoV-229E and MERS-CoV preferred HUH7 cells. ACE2 and TMPRSS2 co-expression enhanced ACE2-dependent entry, and TMPRSS2 alone rendered HEK293T/17 cells permissive to HCoV-HKU1 and HCoV-OC43. Additionally, pseudotypes including other viral proteins such as SARS-CoV-2 E and M, and HE proteins were successfully produced. (see 9.1.4 “Appendix Manuscript 4: Coronavirus Pseudotypes for All Circulating Human Coronaviruses for Quantification of Cross-Neutralizing Antibody Responses”)

6.2 General Epidemiology

In early 2020, many epidemiological cohorts, such as the “Tirschenreuth Kohorte Covid 19” (TiKoCo) and “Coronavirusinfektionen bei Kindern in Bayern” (CoKiBa), “UK healthcareworkers & immunodeficient cohort” and many more, were introduced to research general or specific epidemiological properties during the SARS-CoV-2 pandemic.

The **population-based TiKoCo study** analyzed 4203 participants, sampled from the Tirschenreuth population aged ≥14 years, for SARS-CoV-2 antibodies via three antibody tests and subsequent latent class analysis and investigated symptoms and other characteristics with a questionnaire. This resulted in a standardized seroprevalence of 8.6 % and an underreporting factor of 5. Higher seroprevalence was observed among medical workers and a lower seroprevalence among current smokers, indicating potential behavioral or biological factors. The most abundant symptoms included taste- and olfactory problems and fever, yet a variety of other symptoms was reported more frequently among seropositive individuals, with only 12.9 % completely asymptomatic infections. Though no age trends were found for standardized seroprevalence, undetected infections were far more common in younger individuals than the elderly. The overall infection fatality ratio (IFR) was 2.5 % but dropped to 1.4 % when excluding senior care home residents, who accounted for 45 % of COVID-19-related deaths. IFRs increased sharply with age, starting at <0.5 % in under 60-year-olds, reaching 13.2 % in those aged 70 and above. (see 9.1.2 “Appendix Manuscript 2: Estimates and Determinants of SARS-Cov-2

Seroprevalence and Infection Fatality Ratio Using Latent Class Analysis: The Population-Based Tirschenreuth Study in the Hardest-Hit German County in Spring 2020")

In the following, 3546 participants were analyzed at FU1 (Follow up 1, November 2020) and 3391 at FU2 (Follow up 2, April 2021) to research the t**ime trends in seropositivity, surveillance detection ratio** (= underreporting factor, SDR), **infection fatality** and the now introduced vaccination campaign. Reanalyzed for only N-seropositivity the new baseline seroprevalence was 9.2 % with minor new infections between BL and FU1 (0.9%) but 6.1 % new N-seropositives between FU1 and FU2 (total ever seropositives at FU2: 15.4 %). During that time, the surveillance detection ratio decreased to 1.1 at FU2, meaning nearly every infection got detected by surveillance at the second follow up. Though, by trend, IFRs consistently increased for all age groups at FU2, no significant changes were found towards baseline. However, the increased baseline IFR in municipalities with senior-care-homes (3.0 % vs. 0.7 %) leveled out due to an increase in IFR in municipalities without a senior-care-home (3.4 % vs. 2.9 %). (see 5.4 Manuscript 3: "Time Trend in SARS-CoV-2 Seropositivity, Surveillance Detection- and Infection Fatality Ratio until Spring 2021 in the Tirschenreuth County-Results from a Population-Based Longitudinal Study in Germany").

The **increased seroprevalence in medical personnel** (Odds Ratio 1.41-3.17) persisted at all time points. Yet, these findings were not reflected in PCR testing data, possibly owed to increased testing frequency of medical personnel, skewing the ratio of positive tests. Additionally, the **decreased seroprevalence in smokers** (Odds Ratio 0.40-0.56) held true for all three time points. Here, neither differences in antibody responses (N and S) nor antibody durability were found after infection or vaccination. Finally, lower infection probability of current smokers was persistently reflected in the proportion of positive PCR tests at all time points. (see 9.1.8 "Appendix Manuscript 8: Higher Infection Risk among Health Care Workers and Lower Risk among Smokers Persistent across SARS-CoV-2 Waves-Longitudinal Results from the Population-Based TiKoCo Seroprevalence Study")

On top, infection derived anti-SARS-CoV-2 **antibody durability** of 211 seropositive but unvaccinated individuals was assessed by 8 binding, 4 avidity and a neutralization assay for one year post infection. Both, neutralizing and binding antibodies significantly declined over time, with a stronger decline in men, while S-specific avidity increased over time. Higher antibody levels in the elderly, disappeared when adjusted for disease severity (see 9.1.13 "Appendix Manuscript 13: Population-based study of the durability of humoral immunity after SARS-CoV-2 infection").

Exploring the **role of children** in the early pandemic (Spring 2020), a cross-sectional cohort of 2832 Bavarian children aged 1-17 years was analyzed for symptoms, disease severity, S and N specific binding antibodies as well as neutralizing antibody response. 162 (5.6 %) children showed detectable binding antibodies, with 60 % thereof showing high levels, however, a subgroup analysis of PCR results revealed no seroconversion for 30 % of children, hinting towards a high number of undetected cases. Additionally, neutralizing antibodies could only be detected for 135 children. Though only a quarter of seroconverted children were completely asymptomatic, symptoms were mostly unspecific and less prevalent than in the seronegative control group, leaving only loss of smell and taste as significantly specific symptoms (see Manuscript 1: "Symptoms, SARS-CoV-2 antibodies and neutralization capacity in a cross sectional population of German children").

A **meta genome analysis**, of 219692 cases and over 3 million controls, merging data from multiple studies enabled to map genes to pathways that are involved in viral entry, airway defense and immune system response. 51 distinct genome-wide significant loci were identified, including Type I interferon pathway genes as well as *TMPRSS* and *MUC5B* loci mapped to disease severity (see 9.1.11 "Appendix Manuscript 11: A second update on mapping the human genetic architecture of COVID-19").

Finally, with the end of 2020, several **vaccines** got approved in Germany and a vaccination campaign was started including risk group prioritization. Within the **TiKoCo study population** at FU2, 44.3 % (n=1492) had been vaccinated at least once, with higher rates of up to 77.0 % vaccine elicited S-seropositivity in the over 80 years old population and lower rates in the younger age-groups. Though only 63.5 % of the vaccinated population were positive for S-specific antibodies, this effect could be attributed to the time between vaccination and blood drawl, raising up to 99.67 % seroconversion 14 days post second vaccination (see 5.4 Manuscript 3: "Time Trend in SARS-CoV-2 Seropositivity, Surveillance Detection- and Infection Fatality Ratio until Spring 2021 in the Tirschenreuth County-Results from a Population-Based Longitudinal Study in Germany").

6.3 Vaccine Immunogenicity and Reactogenicity

Deeper analysis of the TiKoCo cohort regarding **immunogenicity of COVID-19 vaccination** and infection revealed low nAb titers after a single vaccination, raising up to median ID50s of 550 post two Moderna mRNA vaccinations. Though only low nAb titers (ID50 of 72) were found post infection, the combination of infection with a single dose of vaccination (often described as "hybrid immunity") resulted in high titers of 929 or 2502 (for BioNtech or Moderna vaccination). Both, RBD binding and neutralizing antibody levels significantly decreased with increased age and increased time since

vaccination. VOC specific neutralization assays revealed lower titers for Beta and Delta within all age groups and immunization backgrounds. Finally, significantly higher IgA levels were found in hybrid immunity compared to vaccination or infection alone. (see 5.5 Manuscript 4: ”Comparative Immunogenicity of COVID-19 Vaccines in a Population-Based Cohort Study with SARS-CoV-2-Infected and Uninfected Participants”)

Looking at a cross-sectional cohort of UK **health care workers** (n = 142) and **immunodeficient patients** (n = 107), neutralizing antibody titers were measured against the vaccine strain (WT/B.1) as well as three VOCs (Alpha/B1.1.7, Beta/B.1.351, Gamma/B1.1.248/P1). Among immunodeficient patients, only 5 % showed detectable nAbs to B.1.1.7 and only 3 % to B.1.351, with overall titers fivefold lower than in health-care workers. In health-care workers without prior SARS-CoV-2 infection, detectable nAb responses were found in 45% (B.1), 37% (B.1.1.7), and only 10% (B.1.351 and P.1), whereas those with prior infection had significantly higher response rates and titers to all strains. (see 9.1.3 “Appendix Manuscript 3: Paucity and discordance of neutralising antibody responses to SARS-CoV-2 VOCs in vaccinated immunodeficient patients and health-care workers in the UK”)

Additionally, the connections between **adverse reaction from two vaccinations and immune response** were investigated. Out of 735 vaccinated health care workers, 38 participants with severe adverse reactions were matched by age and sex with participants with minor side effects and humoral as well as T-cell-mediated immune response was analyzed. Here, men with severe adverse reactions had significantly higher (1.5-fold) RBD IgG binding antibody titers, as well as significantly increased neutralizing antibody titers, while T-cell mediated immune response was not influenced by reactogenicity. However, no differences were found in women. (see 9.1.5 “Appendix Manuscript 5: Association between Reactogenicity and Immunogenicity after Vaccination with BNT162b2”) A follow-up visit around the 3rd vaccination, in 65 of the matched participants, revealed sustained effects of increased binding and neutralization capacity in men with severe side effects. However, post 3rd vaccination, no more differences in binding antibodies, neutralising antibodies or T-cell response were detectable dependent in vaccine side effects, neither for women nor men (see 9.1.7”Appendix Manuscript 7: Association between Adverse Reactions and Humoral Immune Response No Longer Detectable after BNT162b2 Booster Vaccination”).

6.4 Breakthrough Infection, Immune Imprinting and Correlates of Protection

Despite vaccination, people were still getting SARS-CoV-2 infections, in this case often called **vaccine breakthrough infection** (BTI), emphasizing the need to determine actual correlates of protection. At the same time, the emergence of VOCs, especially omicron, brought attention to VOC-specific increased BTI frequency, variant specific immunity and potential **immune imprinting**.

To determine **neutralization hierarchy of SARS-CoV-2 variants**, convalescent sera of, non-vaccinated but previously infected ICU patients (n=38) and HCW (n=23), were analysed for neutralizing antibodies using WHO standards. Neutralisation was significantly reduced for variants P.1 and B.1.351 (over 8-fold), while variants like B.1.1.7 and B.1.1.298 showed only modest reductions. ICU patients exhibited stronger neutralising responses than HCWs across all variants, in line with higher COVID-19 disease severity being strongly correlated with nAb-titers. At the same time, individuals with a low disease severity did not reach 50 % protective titers (54 IU/ml) (see 9.1.6 “Appendix Manuscript 6: Neutralisation Hierarchy of SARS-CoV-2 Variants of Concern Using Standardised, Quantitative Neutralisation Assays Reveals a Correlation With Disease Severity; Towards Deciphering Protective Antibody Thresholds”).

To gain deeper insights into **correlates of protection**, antibody and T-cell response dynamics were investigated during vaccination schemes and after BTI. Both, spike-specific T-cell frequencies and peak nAb titers against multiple variants significantly increased after each immunization, with notably lower titers against omicron derived VOCs. Subsequent omicron BTI broadened virus-specific T-cell responses to other viral proteins and increased neutralization magnitude and breadth, especially omicron specific nAbs. Survival analysis and mathematical modeling taking infection risk into account identified significant protective effects for nAb IC50s against BA5 > 400, with a higher risk reduction dependent on higher titers. (see 9.1.15 “Appendix Manuscript 15: Evolution of protective SARS-CoV-2-specific B and T cell responses upon vaccination and Omicron breakthrough infection”)

To further explore **effects of VOC stratified breakthrough infection**, 212 vaccinated individuals and 88 nonvaccinated individuals, (breakthrough-)infected with Alpha or Delta were longitudinally analyzed for **symptoms and immune response**. Vaccination significantly decreased symptom load with reduced risk of fever, cough, dysgeusia, dizziness and nausea. At the same time, vaccinated individuals showed significantly higher anti-S IgG avidity as well as a higher VOC specific nAb response (see 9.1.14 ”Appendix Manuscript 14: Clinical and immunological benefits of full primary COVID-19 vaccination in

individuals with SARS-CoV-2 breakthrough infections: A prospective cohort study in non-hospitalized adults")

Finally, **immune imprinting effects** were assessed longitudinally in 173 vaccinated and 56 non-vaccinated individuals after SARS-CoV-2 Alpha, Delta or Omicron (breakthrough) infection. Measuring neutralizing antibodies against D614G, Alpha, Delta, BA.1, BA.2, BA.5, BQ.1.1, XBB.1.5 and JN.1 allowed for detailed immune profiles using magnitude breadth (MB) analysis and antigenic cartography. BTI with a more distant VOC (Delta or Omicron) resulted in an increased and more sustained MB, with even more increased breadth in triple vaccinated individuals. Antigenic mapping revealed an initial boosting of vaccine directed antibody response, followed by a shift in immune profile towards the breakthrough VOC but an immune imprinted long-term bias towards the vaccine antigen. Both, the MB findings as well as the antigenic mapping's findings could be validated by antigenic landscaping. Finally, random forest models and neural networks could consistently and accurately assign the infection variant from immune profiles, even at the long term visit, identifying a sustained shift in immunity, despite a vaccine antigen bias (see 5.6 Manuscript 5: "Longitudinal effects of SARS-CoV-2 breakthrough infection on imprinting of neutralizing antibody responses").

6.5 Vaccine Design

Regarding the development of **SARS-CoV-2 vaccines**, different **SARS-CoV-2 spike (S) protein designs**, focusing on versions stabilized in the closed conformation by Furin cleavage site modification and 986 KV mutation, were evaluated in mice. Here, all constructs elicited strong T-cell responses as well as potent and durable neutralizing antibody responses against B.1 (WT), B.1.351(Beta) and P.1(Gamma), while the GSAS-PP modified variant elicited the highest durability and strongest VOC specific response (see 9.1.1 "Appendix Manuscript 1: SARS-CoV-2 Spike Protein Stabilized in the Closed State Induces Potent Neutralizing Responses").

In another approach, the **non-neutralizing RBD epitopes were glycan masked** to enhance generation of neutralizing epitopes in a DNA and MVA based vaccine design in mice. Though a solely DNA based vaccine regime yielded no benefits in terms of binding or neutralizing antibodies, a combination of DNA and MVA vaccination resulted a higher binding and neutralizing antibody response with increased breadth against multiple VOCs , compared to the same vaccination strategy with a wildtype RBD based vaccine (see 9.1.10 "Appendix Manuscript 10: Glycan masking of a non-neutralising epitope enhances neutralising antibodies targeting the RBD of SARS-CoV-2 and its variants").

Another approach utilized a **computational method** to generate **immune-optimized and structurally engineered antigens** as a pan-Sarbecovirus RBD-based vaccine design. A prime-boost vaccination regimen with an AZD1222 prime and either DNA or MVA boost using the designed T2_17 antigen, successfully elicited a broad neutralizing antibody response against distant sarbecoviruses such as RaTG13, WIV16 and SARS-CoV-1 as well as multiple SARS-CoV-2 VOCs. Challengend K18/huACE2 mice were protected against SARS-CoV-2 WT as well as the Delta variant (see 9.1.12 “Appendix Manuscript 12: A computationally designed antigen eliciting broad humoral responses against SARS-CoV-2 and related sarbecoviruses”).

Finally, an updated version of **computationally designed antigens**, using an **epitope consensus-based approach** of WT, Alpha, Beta, Gamma, Delta and Omicron BA.1 was evaluated for immunogenicity in K18-ACE2-mice. After 3 DNA and one MVA immunization, mice elicited a broad nAb response against all tested variants. Even neutralization against novel Omicron variants like XBB.1.5, not included in the vaccine design, was significantly improved compared to only WT based vaccination. Additionally, two mRNA based vaccinations with the designed antigens revealed enhanced overall nAb breadth of antigen designs, though specific immunity (e.g. against BA.1, BA.2) was inferior to autologous or antigenically close vaccination with a BA.1 antigen (see 9.1.17 “Appendix Manuscript 17: Computationally designed Spike antigens induce neutralising responses against the breadth of SARS-COV-2 variants”).

7 General Discussion

7.1 Benchmarks of Serological Testing

Within this thesis, several widely used **serological assays were benchmarked** for their performance regarding indirect detection of neutralizing antibodies. Though the Roche ELECSYS N and S tests showed the highest dichotomous concordance, a S-RBD ELISA showed the highest correlation with nAb levels. Additionally, novel test formats and concepts based on liposomes or impedance-based readouts have been introduced to the research community, though not yet fully applicable in real diagnostics. Finally, the widely used lentiviral pseudotype system was adapted to novel SARS-CoV-2 VOCs and other Coronaviruses.

The high **test performance** of the Roche Elecsys assays is in line with previous studies[406], though those didn't benchmark against neutralization, but only detected infection. Nonetheless, despite the manufacturer's claims[277], the CLIA-based format doesn't allow for accurate quantitative readouts regarding neutralizing antibodies, rendering the results ineffective for studying correlates of protection and quantitative immunity after infection or vaccination.

It should be noted that the **pseudoviral systems**, either lentiviral or VSV-based, themselves only provide a surrogate to SARS-CoV-2 real virus-based neutralization, but the safer pseudoviral alternatives are widely accepted in the field while providing excellent correlations[209,407–409]. Yet, current pseudoviral systems still require biosafety level one or two handling, making them rather unfeasible for high-throughput measurements or everyday diagnostics.

Here, **ELISA-based formats**, though inferior in accuracy, provide a solid, quantitative correlation for neutralization, either pseudovirus-based or real virus-based[260]. Additionally, quantitative correlation could be further improved by using full Spike ELISA[260] or ACE2-inhibition[410,411] ELISA formats as neutralization surrogates. Those established assay formats could potentially be further improved by the herein developed liposome-based ACE-2 inhibition assay, mimicking the surface of actual viruses during binding inhibition and thereby accounting for avidity effects, which are, by design, biased in the currently used ELISA-based format. Avidity effects reflect antibody maturation post infection or vaccination[412,413] and might gain more attention in the field with increasing immune imprinting effects and novel variants[370,403,414].

Additionally, novel **impedance-based readout options** were introduced for the VSV-based pseudoviral assay, enabling a faster and time-resolved readout compared to the currently utilized luciferase or GFP-based options. Another advantage of impedance-based options would be massive parallelization, permitting readouts of hundreds of plates at the same time. Though both novel formats already

provide a promising base, both require additional benchmarking to get a better idea of assay accuracy and correlation with nAb titers.

Finally, most currently approved diagnostic SARS-CoV-2 assay formats rely on the wild-type antigen[415] for readout, whereas multiple studies have shown drastically decreasing **neutralization efficacy against newly emerging variants** like Delta or Omicron subtypes[383,416,417]. Thus, with the introduction of VOCs into the epidemiological situation, a solid understanding of variant-specific immunity[49,233,389] is essential to study immune responses with different exposure backgrounds and understand correlates of protection against infection. Here, only real virus isolates or pseudotyping can provide a sufficiently fast and up-to-date readout option, compared to diagnostic serological testing. Despite the indisputable superior robustness of real SARS-CoV-2 isolates[418], pseudotyping provides a faster adaptability and the option for broader immune-profile studies, as some isolates as e.g., Seasonal CoVs, MERS, SARS-CoV-1, or specific SARS-CoV-2 subvariants, might be hard to come by in certain areas[419].

7.2 Seroepidemiological Studies during the SARS-CoV-2 Pandemic

The TiKoCo and CoKiBa studies enabled the estimation of important **epidemiological factors and time trends** such as seroprevalence, surveillance detection ratio, infection fatality ratio, symptoms, risk factors, and response to the vaccination.

The **TiKoCo study** identified 5 times more infections than initially reported based on PCR data (underreporting factor/SDR), resulting in a total standardized seroprevalence of 8.6 % and an infection fatality of 2.5 %, of which a large portion could be attributed to senior care homes. Longitudinal analysis revealed nearly no new infections until the first follow-up, but 6.1% new N-seropositives at follow-up two. At the same time, SDR dropped to 1.1, while infection fatality ratio increased, non-significantly, to 3.3% with a dwindling effect of senior care homes. Though no age-specific differences in seroprevalence could be identified, SDR was higher in the younger population, while IFR strongly increased with age. Medical workers showed consistently higher seroprevalence, while current smokers revealed a dose-dependent decreased risk of infection.

Cross-sectional **seroprevalence in children** younger than 14 years was estimated at 5.6% and thus lower than for grown-ups, though comparison with PCR data suggested an underestimation of true seroprevalence caused by missing seroconversion for appx. 30% of children. Symptoms for both grown-ups and children included loss of taste and smell as well as fever, whereas symptom load increased with age and children showed a higher frequency of asymptomatic infection.

Comparing multiple **seroprevalence studies in Germany and Europe** at the beginning of 2020, the TiKoCo study's seroprevalence findings fit well into the stark local differences, ranging from 1.6 % in Munich[420] up to 15.5 % seropositivity in the German carnival hotspot Heinsberg[311] and even 42 % in the ski region Ischgl[421], Austria. Off note, apart from those hotspots, nationwide studies like RKI-SOEP estimated the general seroprevalence in Germany much lower at 1.7 %[422], comparable with Munich. Other European studies found similar but higher ranges, starting from 4.9 % and 5 % in France and Spain, up to 10.8 % seropositivity in Geneva, Italy[31,423,424].

The **longitudinal** analysis of low new **seropositivity** in summer 2020 and another wave of infections in autumn/winter 2021 is well reflected in the KoCo19 study increasing from 1.6 % seropositivity in summer 2020 to 14.5 % in summer 2021, and in line with results of the nationwide German MuSPAD study, reporting a strong increase in nationwide seropositivity from 1.3–2.8 % in summer 2020 to 4.1–13.1 % in spring 2021[307,420]. Furthermore, most studies confirmed that reported cases vastly undercounted true infections in 2020, though also prone to **local differences**. For example, in Ischgl only 16.3 % of infections were identified, in Heinsberg 20 %, and in Munich appx. 50 %. Also, the larger German multicenter "MuSPAD" study found similar longitudinal surveillance detection ratios ranging from 2.2–5.1 in the early pandemic, shrinking down to 1.3–2.9 during later visits.[307,311,420,421]

Regarding **infection fatality**, the TiKoCo study found notably higher infection fatality rates ranging from 2.5 % to 3.3 %, compared to 0.37 % in Gangelt and 0.27 % in Ischgl, closer to early WHO global case fatality reports of 3.4 %[425]. Later meta-analysis, including 61 seroprevalence studies in multiple countries, inferred IFRs between 0 and 1.6 %[426], which is still notably lower compared to TiKoCo findings. These discrepancies were likely caused by different **age structures** in the examined populations[304], as well as a large proportion of senior care home infections within Tirschenreuth. Analysis excluding senior care homes in the TiKoCo study resulted in more comparable IFRs of 1.4 % or <0.5 % in individuals aged below 60 years. Additionally, CFRs and most probably also IFRs were drastically decreasing with time, vaccination, and for novel variants, as shown in a retrospective analysis between 2020 and 2023[427]. Given those implications of age and risk group-dependent IFR, combined with different infection dynamics in certain professions or areas, as well as later influences from variants and vaccination, it's fair to conclude that simple standardization might not be sufficient for accurate general estimation of IFR, and more complex models are needed to ensure generalizability of findings[428].

Overall, those findings emphasize both the **advantages and** use cases as well as the **critiques** and downfalls of such **seroepidemiological studies**. Especially in the early pandemic, without any proper PCR and POC testing surveillance structure in place, such seroepidemiological studies could expand the understanding of the infection dynamics. Additionally, estimates of key variables could be sharpened, symptoms and risk factors could be identified, surveillance strategies could be evaluated, and decisions for proper countermeasures could be supported by data.

Yet, the classic seroepidemiological studies could only provide a snapshot in time and geographical area, with often low generalizability of the data. Especially later in the pandemic, the **epidemiological dynamics changed rapidly**, with novel emerging VOCs[49,429], changing vaccination strategies[430], lifted or implemented countermeasures[431], rendering results of rather sturdily designed epidemiological studies outdated before publication. The scientific community in parts reacted by publication of an increased number of preprints or preliminary results, which arguably impacted research quality negatively due to missing or insufficient peer review[432,433].

A **welcome development**, however, was the establishment of larger research consortia involving multiple study centers[434–436], as well as the creation of openly accessible data hubs[437–439]. These collaborative efforts facilitated the pooling of data across regions and timeframes, thereby improving the robustness, comparability, and timeliness of epidemiological analyses. Moreover, such infrastructures promoted transparency, reproducibility, and interdisciplinary collaboration, all of which are essential for addressing the complex and evolving challenges posed by the pandemic[440].
Despite the limitations of seroepidemiological studies in capturing real-time dynamics, their **structured design** and use of biological endpoints offer essential insights that effectively complement other surveillance approaches. Moreover, the findings and lessons learned from these studies may inform and enhance the design of public health responses in future outbreak scenarios[441]. Furthermore, seroepidemiological studies have proven particularly valuable for addressing specific research questions, such as the durability of antibody responses, population-level vaccine effectiveness, and the comparative impact of different vaccination strategies, as will be discussed in the following.

7.3 Antibody Durability, Vaccine Efficacy and Immune Imprinting

This thesis could highlight the **dynamic nature of SARS-CoV-2 antibody responses** following infection, vaccination or combinations thereof. After natural infection, antibody levels and neutralization capacity declined over time, though the quality of antibodies, particularly spike-specific avidity, continued to improve. Vaccination resulted in significantly larger antibody responses than infection alone, yet vaccinated individuals with prior infection exhibited even higher neutralizing titers than those vaccinated without previous exposure. **Breakthrough infections** with variants like Delta or Omicron further enhanced magnitude and breadth of the neutralizing antibody response, though long-term responses remained biased toward the original vaccine strain. Additionally, neutralizing antibodies could be proven to be a significant **correlate of protection**, especially nAbs against the at that time circulating variant. Finally, machine learning could prove useful in identification of the previous infection VOC from current **immune profiles**, on the one hand proofing sustained changes in immune responses, on the other hand providing novel tools for epidemiological studies. Overall, these findings suggest that while immunity wanes quantitatively, qualitative improvements and variant exposure contribute to the evolution of a robust and cross-reactive protection.

The observed **waning of infection induced antibody levels** is in line with other reports, who also noted a decline in titers over time while observing improvements in antibody affinity and memory B cell maturation[287,442]. Similarly, the enhancement of antibody responses following vaccination, especially in individuals with prior infection is nowadays well documented in the literature and commonly referred to as "**hybrid immunity**"[351,443,444]. Apart from differences in peak response, the type of immunization also strongly impacts nAb kinetics, with mRNA resulting in strong but short-lived responses and natural infection or adenoviral vector immunization resulting in weaker but more durable responses[444]. Here, hybrid immunity, with an infection either before or post vaccination, seems to combine those advantages resulting in a stronger and more durable response[396]. However, acquiring hybrid immunity through natural **SARS-CoV-2 infection** entails significant health risks, including severe acute illness[445], long-term complications[446] such as cardiovascular disease or Long COVID[55]. Therefore, repeated vaccination represents the safer and more controlled strategy to achieve comparable immune protection[171], especially as heterologous “mix and match” approaches with different available vaccine platforms demonstrated similar effects on magnitude and durability[447].

Despite multiple studies showing solid **protection from severe disease** and at least a lower risk of infection after vaccination or previous infection[448,449], there is still ongoing debate about how to achieve sterile immunity[450]. Within this thesis, neutralizing antibody cutoffs providing a significant

hazard reduction regarding breakthrough infection could be determined, supporting previous claims of a relationship between neutralizing activity and protection from (symptomatic) infection[180], ultimately supporting nAb titers a correlate of protection[179,451]. However, true sterile immunity might be not only dependent on absolute nAb titers, but more on their location, as some studies suggested mucosal immunity as the driving force in interrupting transmission[452–454]. Here, multiple approaches of intranasal immunization could show promising results in animals towards enhancing sterile mucosal immunity[455–457].

The **emergence of SARS-CoV-2 VOCs**, especially the Omicron lineage, reshaped the discussion on immunity, as the efficacy of previously existing neutralizing antibodies dwindled[49,458–460], but was quickly followed by the introduction of adjusted, Omicron specific vaccines[461]. Concurrently, the emergence of novel antigens sparked discussion about **immune imprinting** effects[370,462] previously known for influenza[165,463].

In line with previous findings, this thesis could demonstrate a boost in both **magnitude and breadth** of neutralizing antibodies following breakthrough infections with variants such as Delta or Omicron[458,464]. On top of that, our longitudinal study design allowed for the identification of a persisting long-term bias towards the vaccine antigen after the initial boost, expanding the results of previous studies on the effects of booster vaccination[465]. This continued bias toward the ancestral strain, despite exposure to newer variants by infection or vaccination, strongly suggests **persistent imprinting** or "original antigenic sin" effects, which should be considered in vaccination strategies[414]. Additionally, there is convincing evidence, that no novel B-Cells get primed after secondary e.g. Omicron contact, to support the observed imprinting effects on a cellular basis[402].

In contrast, the application of **machine learning** to infer previous infection history from immune profiles suggests a durable change in antibody profiles, despite imprinting effects. These observations are supported by reports of the possibility to “override” an imprinted wildtype response by repeated exposure to Omicron XBB antigens[403]. More research is needed to determine whether this “overriding” is driven by evolution and maturation of existing responses, if there exists a defined antigenic distance at which novel B-Cell priming could still be possible, or if it’s the sheer number of immunization events.

Apart from pure scientific curiosity, it further needs to be discussed how to **translate** those insights **into vaccination scheme recommendations**. Since all current circulating variants are descendants of the Omicron lineage, one simple and straightforward option would be to abandon wildtype vaccine antigens and switch any new primary immunization to the currently circulating variant, as suggested

by Yisimayi *et al*.[403] However, previous research in vaccinology often suggested ancestral antigen designs as a possible option to achieve a broad immunity in "universal" or "pan-clade" vaccines[466–468]. Here, the wildtype antigen as a "true natural ancestor" might provide a better base to protect against future SARS-CoV-2 variants from other lineages than Omicron or even other potentially emerging novel CoVs (e.g., "SARS-CoV-3"). Another option would be to sequentially vaccinate with a designed series of antigenically distinct and distant antigens might broaden responses[469].

In the case of **already imprinted responses**, be it from vaccination or infection, one option would be to specifically mask preexisting highly immunogenic epitopes on **novel antigens**, to target immunity on desired novel epitopes, similar to the glycan masking as presented within this thesis. Another option would be to use existing strategies from other fields, like germline targeting from HIV vaccination designs[470,471], to guide B-cell evolution to the currently circulating antigens instead of trying to override existing responses by numerously repeated vaccination.

Overall, SARS-CoV-2 vaccination with whichever type or scheme, still provides solid **protection** against severe disease with efficacy >90 %[449,472] and reduces the risk of Long COVID (HR 0.55)[473], especially when refreshed regularly or in combination with a previous infection[474]. Hence, it provides a safe option of risk reduction[171], in risk groups like the elderly population, as well as in the non-risk-group grown-up population, and maybe even for children regarding multi-inflammatory syndrome[475].

8 Conclusion and Outlook

8.1 Conclusion

Since the emergence of SARS-CoV-2 in 2019, the world has witnessed intense research on all aspects of SARS-CoV-2 and endured high numbers of infections, deaths, restrictions and uncertainty. Therein, this thesis aimed to shed light on multiple facets of SARS-CoV-2 diagnostics, antibody dynamics, vaccine responses, and vaccine design.

In the early phase of the pandemic, the urgent need for reliable **diagnostic tools** led to a rapid expansion of available serological assays. More recently supplemented with novel liposome-based assay formats and an impedance-based readout as introduced here. Through systematic benchmarking, this work demonstrated solid performance of multiple widely used serological assays. Here the Roche Cobas S-RBD total Ig assay consistently outperformed others, offering high diagnostic accuracy and robustness across populations. Still a simple ELISA provided the best quantitative correlation with neutralization. Additionally, the evaluation revealed spectrum biases, with a varying extent in different assays, important to consider in other or future studies.

Building on these diagnostic benchmarks, the **population-based TiKoCo19 cohort** enabled a deep and nuanced understanding of SARS-CoV-2 infection dynamics and immune durability over time. Seroprevalence data from multiple time points revealed substantial under detection of infections during the early waves of the pandemic, particularly among younger individuals who were less likely to be tested. These findings highlighted the limitations of (early) case-based surveillance in capturing the true extent of viral spread. Moreover, the **infection fatality rates** derived from serological data were strongly age-dependent and considerably influenced by outbreaks in senior care homes. As the pandemic progressed, improvements in testing infrastructure were reflected in a more accurate case detection, though concurrent increases in population-immunity and improved protective measures were not (yet) reflected in lower infection fatality or less risk for health care workers, respectively.

Longitudinal follow-up within the cohort provided further insights into the **persistence and determinants of humoral immunity**. Here, antibody titers following natural infection showed a gradual decline over time. Notably, sex and disease severity emerged as significant modifiers of antibody durability, with more robust and sustained responses observed in individuals who had experienced more severe disease and in male participants, underscoring the importance of accounting for demographic and clinical heterogeneity in both serological and epidemiological interpretation.

Furthermore, this thesis explored how immunity evolved after vaccination. While **vaccine-induced antibody responses** varied by regimen and recipient characteristics, including age and immunocompetence, hybrid immunity arising from the combination of infection and vaccination, consistently yielded higher antibody levels and broader cross-variant neutralization. These effects were seen across multiple settings and remained detectable even among immunocompromised individuals. Interestingly, reactogenicity after base immunization was associated with stronger humoral responses in men, suggesting a potential link between innate immune activation and adaptive outcomes. Longitudinal study design enabled confirmation of neutralizing antibody titers as a correlate of protection, with determination of variant-specific cutoff levels for hazard reduction.

As the virus evolved, it became important to evaluate **immune profiles and antigenic landscapes**. Breakthrough infections with variants of concern not only boosted immunity but also provided insight into **immune imprinting effects**. Here, antigenic mapping revealed, that prior vaccine-induced immunity biased the post-infection antibody profiles, though the breakthrough variant reshaped breadth and specificity during peak response. Despite this bias, machine learning analyses could proof sustained shifts in immune profiles following breakthrough infection.

Altogether, these findings underscore the value of integrating laboratory assay development, epidemiological surveillance, and immunological profiling to inform public health strategies. They highlight the challenges of diagnostic bias, the dynamic nature of protection, and the need to anticipate the effects of immune imprinting in a changing viral landscape.

8.2 Outlook

As the SARS-CoV-2 pandemic **transitions into an endemic**, future research must address emerging questions about the durability of hybrid immunity, the impact of repeated exposures through vaccination and or reinfection, and the evolving role of novel variants combined with variant-adjusted vaccines. Population-based cohorts like the TiKoCo19 cohort remain essential for monitoring disease dynamics over time and may be integrated into larger cluster studies to overcome geographical limitations. Additionally, wastewater surveillance enables quick and easy identification of novel outbreaks, hotspots or even novel VOCs.

After the current vaccine generation, **second-generation vaccines** should implement knowledge on immune imprinting effects and provide strategies to bypass or maybe even exploit those effects. Current and novel strategies should investigate pan-sarbecovirus or pan-CoV vaccines utilizing consensus or ancestor designs, variant-specific or germline targeting sequential immunizations or multivalent approaches. Successful approaches could then be combined with intranasal application to induce sufficient mucosal immunity, to finally enable a broad and sterile immunity[476,477].

Another challenge will be the exploration and treatment of **long and post COVID**, posing a growing challenge to public health and economics. Recent studies have highlighted that approximately 8-30 % of working-age adults reported experiencing long COVID[478], leading to elevated risks of unemployment, financial difficulties, and mental health issues. Research into long COVID is still ongoing, with studies exploring various underlying mechanisms such as immune dysfunction, viral persistence, and autoimmunity. However, the absence of validated biomarkers complicates diagnosis and research, highlighting the need for further studies to understand the condition’s pathophysiology and to develop effective treatments.

9 Appendix

9.1 Appendix Publication Abstracts

Due to the number of co-authored manuscripts, only the abstracts are shown within this thesis. The full publications can be accessed online using the DOIs provided in B) B) Appendix publications.

9.1.1 Appendix Manuscript 1: SARS-CoV-2 Spike Protein Stabilized in the Closed State Induces Potent Neutralizing Responses

Authors: Carnell GW, Ciazynska KA, Wells DA, Xiong X, Aguinam ET, McLaughlin SH, Mallery D, Ebrahimi S, Ceron-Gutierrez L, Asbach B, **Einhauser S**, Wagner R, James LC, Doffinger R, Heeney JL, Briggs JAG

Published on 12th of **July 2021 in Journal of Virology**

DOI: 10.1128/JVI.00203-21

The majority of SARS-CoV-2 vaccines in use or advanced development are based on the viral spike protein (S) as their immunogen. S is present on virions as prefusion trimers in which the receptor binding domain (RBD) is stochastically open or closed. Neutralizing antibodies have been described against both open and closed conformations. The long-term success of vaccination strategies depends upon inducing antibodies that provide long-lasting broad immunity against evolving SARS-CoV-2 strains. Here, we have assessed the results of immunization in a mouse model using an S protein trimer stabilized in the closed state to prevent full exposure of the receptor binding site and therefore interaction with the receptor. We compared this with other modified S protein constructs, including representatives used in current vaccines. We found that all trimeric S proteins induced a T cell response and long-lived, strongly neutralizing antibody responses against 2019 SARS-CoV-2 and variants of concern P.1 and B.1.351. Notably, the protein binding properties of sera induced by the closed spike differed from those induced by standard S protein constructs. Closed S proteins induced more potent neutralizing responses than expected based on the degree to which they inhibit interactions between the RBD and ACE2. These observations suggest that closed spikes recruit different, but equally potent, immune responses than open spikes and that this is likely to include neutralizing antibodies against conformational epitopes present in the closed conformation. We suggest that closed spikes, together with their improved stability and storage properties, may be a valuable component of refined, next-generation vaccines.

IMPORTANCE: Vaccines in use against SARS-CoV-2 induce immune responses against the spike protein. There is intense interest in whether the antibody response induced by vaccines will be robust against new variants, as well as in next-generation vaccines for use in previously infected or immunized individuals. We assessed the use as an immunogen of a spike protein engineered to be conformationally stabilized in the closed state where the receptor binding site is occluded. Despite

occlusion of the receptor binding site, the spike induces potently neutralizing sera against multiple SARS-CoV-2 variants. Antibodies are raised against a different pattern of epitopes to those induced by other spike constructs, preferring conformational epitopes present in the closed conformation. Closed spikes, or mRNA vaccines based on their sequence, can be a valuable component of next-generation vaccines.

9.1.2 Appendix Manuscript 2: Estimates and Determinants of SARS-Cov-2 Seroprevalence and Infection Fatality Ratio Using Latent Class Analysis: The Population-Based Tirschenreuth Study in the Hardest-Hit German County in Spring 2020

Authors: Ralf Wagner*, David Peterhoff†, Stephanie Beileke†, Felix Günther†, Melanie Berr, **Sebastian Einhauser**, Anja Schütz, Hans Helmut Niller, Philipp Steininger, Antje Knöll, Matthias Tenbusch, Clara Maier, Klaus Korn, Klaus J. Stark, André Gessner, Ralph Burkhardt, Michael Kabesch, Holger Schedl, Helmut Küchenhoff, Annette B. Pfahlberg, Iris M. Heid†, Olaf Gefeller†, and Klaus Überla*

Published on 10th **June 2021 in Viruses**.

DOI: 10.3390/v13061118

SARS-CoV-2 infection fatality ratios (IFR) remain controversially discussed with implications for political measures. The German county of Tirschenreuth suffered a severe SARS-CoV-2 outbreak in spring 2020, with particularly high case fatality ratio (CFR). To estimate seroprevalence, underreported infections, and IFR for the Tirschenreuth population aged ≥14 years in June/July 2020, we conducted a population-based study including home visits for the elderly, and analyzed 4203 participants for SARS-CoV-2 antibodies via three antibody tests. Latent class analysis yielded 8.6% standardized county-wide seroprevalence, a factor of underreported infections of 5.0, and 2.5% overall IFR. Seroprevalence was two-fold higher among medical workers and one third among current smokers with similar proportions of registered infections. While seroprevalence did not show an age-trend, the factor of underreported infections was 12.2 in the young versus 1.7 for ≥85-year-old. Age-specific IFRs were <0.5% below 60 years of age, 1.0% for age 60–69, and 13.2% for age 70+. Senior care homes accounted for 45% of COVID-19-related deaths, reflected by an IFR of 7.5% among individuals aged 70+ and an overall IFR of 1.4% when excluding senior care home residents from our computation. Our data underscore senior care home infections as key determinant of IFR additionally to age, insufficient targeted testing in the young, and the need for further investigations on behavioral or molecular causes of the fewer infections among current smokers.

9.1.3 Appendix Manuscript 3: Paucity and discordance of neutralising antibody responses to SARS-CoV-2 VOCs in vaccinated immunodeficient patients and health-care workers in the UK

Authors: Nadesalingam A, Cantoni D, Wells DA, Aguinam ET, Ferrari M, Smith P, Chan A, Carnell G, Ohlendorf L, **Einhauser S**, George C, Wagner R, Temperton N, Castillo-Olivares J, Baxendale H, Heeney JL; HICC consortium.

Published in **September 2021 in The Lancet Microbe**.

Doi: 10.1016/S2666-5247(21)00157-9

No published abstract available. Own abstract below:

As of mid-2021, widespread yet incomplete COVID-19 vaccination in the UK coincided with the emergence of SARS-CoV-2 Variants of Concern (VOCs), raising concerns about vaccine effectiveness, especially in immunocompromised populations. This single-centre, cross-sectional study assessed neutralising antibody (NAb) responses to the original B.1 vaccine strain and three major VOCs (B.1.1.7, B.1.351, and P.1) in 142 vaccinated healthcare workers and 107 immunodeficient outpatients following one dose of either BNT162b2 (Pfizer–BioNTech) or ChAdOx1 nCoV-19 (Oxford–AstraZeneca). Results showed low or undetectable NAb titres in most immunodeficient individuals and reduced NAb responses in healthcare workers without prior SARS-CoV-2 infection. In contrast, prior infection significantly boosted NAb titres post-vaccination across all strains. These findings underscore the vulnerability of immunocompromised individuals and healthcare workers with low NAbs to infection and transmission of VOCs. The study highlights the need for continued surveillance of immune responses, especially in high-risk groups, and supports tailored booster strategies to address emerging variants and maintain vaccine efficacy.

9.1.4 Appendix Manuscript 4: Coronavirus Pseudotypes for All Circulating Human Coronaviruses for Quantification of Cross-Neutralizing Antibody Responses

Authors: Sampson AT, Heeney J, Cantoni D, Ferrari M, Sans MS, George C, Di Genova C, Mayora Neto M, **Einhauser S**, Asbach B, Wagner R, Baxendale H, Temperton N, Carnell G

Published on 10th of **August 2021 in Viruses**

DOI: 10.3390/v13081579

The novel coronavirus SARS-CoV-2 is the seventh identified human coronavirus. Understanding the extent of pre-existing immunity induced by seropositivity to endemic seasonal coronaviruses and the impact of cross-reactivity on COVID-19 disease progression remains a key research question in immunity to SARS-CoV-2 and the immunopathology of COVID-2019 disease. This paper describes a panel of lentiviral pseudotypes bearing the spike (S) proteins for each of the seven human coronaviruses (HCoVs), generated under similar conditions optimized for high titre production allowing a high-throughput investigation of antibody neutralization breadth. Optimal production conditions and most readily available permissive target cell lines were determined for spike-mediated entry by each HCoV pseudotype: SARS-CoV-1, SARS-CoV-2 and HCoV-NL63 best transduced HEK293T/17 cells transfected with ACE2 and TMPRSS2, HCoV-229E and MERS-CoV preferentially entered HUH7 cells, and CHO cells were most permissive for the seasonal betacoronavirus HCoV-HKU1. Entry of ACE2 using pseudotypes was enhanced by ACE2 and TMPRSS2 expression in target cells, whilst TMPRSS2 transfection rendered HEK293T/17 cells permissive for HCoV-HKU1 and HCoV-OC43 entry. Additionally, pseudotype viruses were produced bearing additional coronavirus surface proteins, including the SARS-CoV-2 Envelope (E) and Membrane (M) proteins and HCoV-OC43/HCoV-HKU1 Haemagglutinin-Esterase (HE) proteins. This panel of lentiviral pseudotypes provides a safe, rapidly quantifiable and high-throughput tool for serological comparison of pan-coronavirus neutralizing responses; this can be used to elucidate antibody dynamics against individual coronaviruses and the effects of antibody cross-reactivity on clinical outcome following natural infection or vaccination.

9.1.5 Appendix Manuscript 5: Association between Reactogenicity and Immunogenicity after Vaccination with BNT162b2

Authors: Bauernfeind S, Salzberger B, Hitzenbichler F, Scigala K, **Einhauser S**, Wagner R, Gessner A, Koestler J, Peterhoff D.

Published on 27th of **September 2021 in Vaccines**

DOI: 10.3390/vaccines9101089

It is not clear whether there is an association between adverse reactions and immune response after vaccination. Seven hundred and thirty-five vaccinees from our University Medical Center vaccination clinic provided information about sex, age and adverse reactions after first and second vaccination with BNT162b2. Adverse reactions were categorized into three groups: no or minor on the injection side, moderate (not further classified) and severe—defined as any symptom(s) resulting in sick leave. We chose 38 vaccinees with the most severe adverse reactions and compared their humoral and T-cell-mediated immune responses after second vaccination with those of 38 sex and age matched controls without or only minor injection-side related adverse reactions. Severe acute respiratory syndrome coronavirus 2 (SARS-CoV-2) anti-receptor binding domain (RBD) IgG titers were detectable in all participants (median 5528; range 958–26,285). Men with severe adverse reactions had 1.5-fold higher median SARS-CoV-2 RBD IgG titers compared to men without adverse reactions (median 7406 versus 4793; $p < 0.001$). Similarly; neutralization activity was significantly higher in men with severe adverse reactions (half maximal inhibitory concentrations (IC_{50}) median 769 versus 485; $p < 0.001$). Reactogenicity did not influence humoral immune response in women nor T-cell-mediated immune response in any sex. To conclude; adverse reactions after vaccination with BNT162b2 do influence humoral immune response yet only in men and are not a prerequisite for a robust antibody response.

9.1.6 Appendix Manuscript 6: Neutralisation Hierarchy of SARS-CoV-2 Variants of Concern Using Standardised, Quantitative Neutralisation Assays Reveals a Correlation With Disease Severity; Towards Deciphering Protective Antibody Thresholds

Authors: Cantoni D, Mayora-Neto M, Nadesalingam A, Wells DA, Carnell GW, Ohlendorf L, Ferrari M, Palmer P, Chan ACY, Smith P, Bentley EM, **Einhauser S**, Wagner R, Page M, Raddi G, Baxendale H, Castillo-Olivares J, Heeney J, Temperton N.

Published on 7th of **March 2022 in Frontiers of Immunology**

DOI: 10.3389/fimmu.2022.773982

The rise of SARS-CoV-2 variants has made the pursuit to define correlates of protection more troublesome, despite the availability of the World Health Organisation (WHO) International Standard for anti-SARS-CoV-2 Immunoglobulin sera, a key reagent used to standardise laboratory findings into an international unitage. Using pseudotyped virus, we examine the capacity of convalescent sera, from a well-defined cohort of healthcare workers (HCW) and Patients infected during the first wave from a national critical care centre in the UK to neutralise B.1.1.298, variants of interest (VOI) B.1.617.1 (Kappa), and four VOCs, B.1.1.7 (Alpha), B.1.351 (Beta), P.1 (Gamma) and B.1.617.2 (Delta), including the B.1.617.2 K417N, informally known as Delta Plus. We utilised the WHO International Standard for anti-SARS-CoV-2 Immunoglobulin to report neutralisation antibody levels in International Units per mL. Our data demonstrate a significant reduction in the ability of first wave convalescent sera to neutralise the VOCs. Patients and HCWs with more severe COVID-19 were found to have higher antibody titres and to neutralise the VOCs more effectively than individuals with milder symptoms. Using an estimated threshold for 50% protection, 54 IU/mL, we found most asymptomatic and mild cases did not produce titres above this threshold.

9.1.7 Appendix Manuscript 7: Association between Adverse Reactions and Humoral Immune Response No Longer Detectable after BNT162b2 Booster Vaccination

Authors: Bauernfeind S, **Einhauser S**, Tydykov L, Mader AL, Salzberger B, Hitzenbichler F, Mohr A, Burkhardt R, Wagner R, Peterhoff D

Published on 25th of **September 2022 in Vaccines**

DOI: 10.3390/vaccines10101608

In a previous study, we described a highly significant association between reactogenicity and SARS-CoV-2 RBD IgG titers and wild-type neutralization capacity in males after basic vaccination with BNT162b2. The objective of this study was to assess whether this benefit was long lasting and also evident after BNT162b2 booster vaccination. Reactogenicity was classified into three groups: no or minor injection site symptoms, moderate (not further classified) and severe adverse reactions (defined as any symptom(s) resulting in sick leave). We initially compared 76 non-immunocompromised individuals who reported either no or minor injection site symptoms or severe adverse reactions after second vaccination. In total, 65 of them took part in another blood sampling and 47 were evaluated after booster vaccination. 26 weeks after second vaccination, men who reported severe adverse reactions after second vaccination had 1.7-fold higher SARS-CoV-2 RBD IgG titers ($p = 0.025$) and a 2.5-fold better neutralization capacity ($p = 0.006$) than men with no or only minor injection site symptoms. Again, no association was found in women. Reactogenicity of BNT162b2 booster vaccination was different from second vaccination according to our classification and was no longer associated with SARS-CoV-2 RBD IgG titers or wild-type neutralization capacity. To conclude, after BNT162b2 basic vaccination, the association between reactogenicity and humoral immune response in men persisted over time but was no longer detectable after BNT162b2 booster vaccination.

9.1.8 Appendix Manuscript 8: Higher Infection Risk among Health Care Workers and Lower Risk among Smokers Persistent across SARS-CoV-2 Waves-Longitudinal Results from the Population-Based TiKoCo Seroprevalence Study

Authors: Günther F, **Einhauser S**, Peterhoff D, Wiegrebe S, Niller HH, Beileke S, Steininger P, Burkhardt R, Küchenhoff H, Gefeller O, Überla K, Heid IM, Wagner R.

Published on 17th of **December 2022 in International Journal of Environmental Research and Public Health**

DOI: 10.3390/ijerph192416996

SARS-CoV-2 seroprevalence was reported as substantially increased in medical personnel and decreased in smokers after the first wave in spring 2020, including in our population-based Tirschenreuth Study (TiKoCo). However, it is unclear whether these associations were limited to the early pandemic and whether the decrease in smokers was due to reduced infection or antibody response. We evaluated the association of occupation and smoking with period-specific seropositivity: for the first wave until July 2020 (baseline, BL), the low infection period in summer (follow-up 1, FU1, November 2020), and the second/third wave (FU2, April 2021). We measured binding antibodies directed to SARS-CoV-2 nucleoprotein (N), viral spike protein (S), and neutralizing antibodies at BL, FU1, and FU2. Previous infection, vaccination, smoking, and occupation were assessed by questionnaires. The 4181 participants (3513/3374 at FU1/FU2) included 6.5% medical personnel and 20.4% current smokers. At all three timepoints, new seropositivity was higher in medical personnel with ORs = 1.99 (95%-CI = 1.36-2.93), 1.41 (0.29-6.80), and 3.17 (1.92-5.24) at BL, FU1, and FU2, respectively, and nearly halved among current smokers with ORs = 0.47 (95%-CI = 0.33-0.66), 0.40 (0.09-1.81), and 0.56 (0.33-0.94). Current smokers compared to never-smokers had similar antibody levels after infection or vaccination and reduced odds of a positive SARS-CoV-2 result among tested. Our data suggest that decreased seroprevalence among smokers results from fewer infections rather than reduced antibody response. The persistently higher infection risk of medical staff across infection waves, despite improved means of protection over time, underscores the burden for health care personnel.

9.1.9 Appendix Manuscript 9: Liposome-based high-throughput and point-of-care assays toward the quick, simple, and sensitive detection of neutralizing antibodies against SARS-CoV-2 in patient sera

Authors: Streif S, Neckermann P, Spitzenberg C, Weiss K, Hoecherl K, Kulikowski K, Hahner S, Noelting C, **Einhauser S**, Peterhoff D, Asam C, Wagner R, Baeumner AJ.

Published in **March 2023 in Analytical and Bioanalytical Chemistry**

DOI: 10.1007/s00216-023-04548-3

The emergence of severe acute respiratory syndrome-related coronavirus 2 (SARS-CoV-2) in 2019 caused an increased interest in neutralizing antibody tests to determine the immune status of the population. Standard live-virus-based neutralization assays such as plaque-reduction assays or pseudovirus neutralization tests cannot be adapted to the point-of-care (POC). Accordingly, tests quantifying competitive binding inhibition of the angiotensin-converting enzyme 2 (ACE2) receptor to the receptor-binding domain (RBD) of SARS-CoV-2 by neutralizing antibodies have been developed. Here, we present a new platform using sulforhodamine B encapsulating liposomes decorated with RBD as foundation for the development of both a fluorescent, highly feasible high-throughput (HTS) and a POC-ready neutralizing antibody assay. RBD-conjugated liposomes are incubated with serum and subsequently immobilized in an ACE2-coated plate or mixed with biotinylated ACE2 and used in test strip with streptavidin test line, respectively. Polyclonal neutralizing human antibodies were shown to cause complete binding inhibition, while S309 and CR3022 human monoclonal antibodies only caused partial inhibition, proving the functionality of the assay. Both formats, the HTS and POC assay, were then tested using 20 sera containing varying titers of neutralizing antibodies, and a control panel of sera including prepandemic sera and reconvalescent sera from respiratory infections other than SARS-CoV-2. Both assays correlated well with a standard pseudovirus neutralization test ($r = 0.847$ for HTS and $r = 0.614$ for POC format). Furthermore, excellent correlation ($r = 0.868$) between HTS and POC formats was observed. The flexibility afforded by liposomes as signaling agents using different dyes and sizes can hence be utilized in the future for a broad range of multianalyte neutralizing antibody diagnostics.

9.1.10 Appendix Manuscript 10: Glycan masking of a non-neutralising epitope enhances neutralising antibodies targeting the RBD of SARS-CoV-2 and its variants

Authors: Carnell GW, Billmeier M, Vishwanath S, Suau Sans M, Wein H, George CL, Neckermann P, Del Rosario JMM, Sampson AT, **Einhauser S**, Aguinam ET, Ferrari M, Tonks P, Nadesalingam A, Schütz A, Huang CQ, Wells DA, Paloniemi M, Jordan I, Cantoni D, Peterhoff D, Asbach B, Sandig V, Temperton N, Kinsley R, Wagner R, Heeney JL

Published on 23rd of **February 2023 in Frontiers of Immunology**

DOI: 10.3389/fimmu.2023.1118523

The accelerated development of the first generation COVID-19 vaccines has saved millions of lives, and potentially more from the long-term sequelae of SARS-CoV-2 infection. The most successful vaccine candidates have used the full-length SARS-CoV-2 spike protein as an immunogen. As expected of RNA viruses, new variants have evolved and quickly replaced the original wild-type SARS-CoV-2, leading to escape from natural infection or vaccine induced immunity provided by the original SARS-CoV-2 spike sequence. Next generation vaccines that confer specific and targeted immunity to broadly neutralising epitopes on the SARS-CoV-2 spike protein against different variants of concern (VOC) offer an advance on current booster shots of previously used vaccines. Here, we present a targeted approach to elicit antibodies that neutralise both the ancestral SARS-CoV-2, and the VOCs, by introducing a specific glycosylation site on a non-neutralising epitope of the RBD. The addition of a specific glycosylation site in the RBD based vaccine candidate focused the immune response towards other broadly neutralising epitopes on the RBD. We further observed enhanced cross-neutralisation and cross-binding using a DNA-MVA CR19 prime-boost regime, thus demonstrating the superiority of the glycan engineered RBD vaccine candidate across two platforms and a promising candidate as a broad variant booster vaccine.

9.1.11 Appendix Manuscript 11: A second update on mapping the human genetic architecture of COVID-19

Authors: COVID-19 Host Genetics Initiative

Published on 6th of **September 2023 in Nature**

DOI: 10.1038/s41586-023-06355-3

No Abstract published, Summary below:

In summary, we have substantially expanded the current knowledge of host genetics for COVID-19 susceptibility and severity by further doubling the case numbers from the previous data release and identifying 28 additional loci. The increased number of loci enables us to map genes to pathways that are involved in viral entry, airway defence and immune system response. Notably, we observed

severity loci mapped to type I interferon pathway, while susceptibility loci mapped to viral entry and airway defence pathways, with notable exceptions for severity-classified *TMPRSS* and *MUC5B* loci. Further investigation of how such susceptibility and severity loci map to different pathways would provide mechanistic insights into the human genetic architecture of COVID-19.

9.1.12 Appendix Manuscript 12: A computationally designed antigen eliciting broad humoral responses against SARS-CoV-2 and related sarbecoviruses

Authors: Vishwanath S, Carnell GW, Ferrari M, Asbach B, Billmeier M, George C, Sans MS, Nadesalingam A, Huang CQ, Paloniemi M, Stewart H, Chan A, Wells DA, Neckermann P, Peterhoff D, **Einhauser S**, Cantoni D, Neto MM, Jordan I, Sandig V, Tonks P, Temperton N, Frost S, Sohr K, Ballesteros MTL, Arbabi F, Geiger J, Dohmen C, Plank C, Kinsley R, Wagner R, Heeney JL

Published on 25th of **September 2023 in Nature Biomedical Engineering**

DOI: 10.1038/s41551-023-01094-2

The threat of spillovers of coronaviruses associated with the severe acute respiratory syndrome (SARS) from animals to humans necessitates vaccines that offer broader protection from sarbecoviruses. By leveraging a viral-genome-informed computational method for selecting immune-optimized and structurally engineered antigens, here we show that a single antigen based on the receptor binding domain of the spike protein of sarbecoviruses elicits broad humoral responses against SARS-CoV-1, SARS-CoV-2, WIV16 and RaTG13 in mice, rabbits and guinea pigs. When administered as a DNA immunogen or by a vector based on a modified vaccinia virus Ankara, the optimized antigen induced vaccine protection from the Delta variant of SARS-CoV-2 in mice genetically engineered to express angiotensin-converting enzyme 2 and primed by a viral-vector vaccine (AZD1222) against SARS-CoV-2. A vaccine formulation incorporating mRNA coding for the optimized antigen further validated its broad immunogenicity. Vaccines that elicit broad immune responses across subgroups of coronaviruses may counteract the threat of zoonotic spillovers of betacoronaviruses.

9.1.13 Appendix Manuscript 13: Population-based study of the durability of humoral immunity after SARS-CoV-2 infection

Authors: Peterhoff D, Wiegrebe S, **Einhauser S**, Patt AJ, Beileke S, Günther F, Steininger P, Niller HH, Burkhardt R, Küchenhoff H, Gefeller O, Überla K, Heid IM, Wagner R.

Published on 5th of **October 2023 in Frontiers of Immunology**

DOI: 10.3389/fimmu.2023.1242536

SARS-CoV-2 antibody quantity and quality are key markers of humoral immunity. However, there is substantial uncertainty about their durability. We investigated levels and temporal change of SARS-CoV-2 antibody quantity and quality. We analyzed sera (8 binding, 4 avidity assays for spike-(S-)protein and nucleocapsid-(N-)protein; neutralization) from 211 seropositive unvaccinated participants, from the population-based longitudinal TiKoCo study, at three time points within one year after infection with the ancestral SARS-CoV-2 virus. We found a significant decline of neutralization titers and binding

antibody levels in most assays (linear mixed regression model, $p<0.01$). S-specific serum avidity increased markedly over time, in contrast to N-specific. Binding antibody levels were higher in older versus younger participants - a difference that disappeared for the asymptomatic-infected. We found stronger antibody decline in men versus women and lower binding and avidity levels in current versus never-smokers. Our comprehensive longitudinal analyses across 13 antibody assays suggest decreased neutralization-based protection and prolonged affinity maturation within one year after infection.

9.1.14 Appendix Manuscript 14: Clinical and immunological benefits of full primary COVID-19 vaccination in individuals with SARS-CoV-2 breakthrough infections: A prospective cohort study in non-hospitalized adults

Authors: Prelog M, Jeske SD, Asam C, Fuchs A, Wieser A, Gall C, Wytopil M, Mueller-Schmucker SM, Beileke S, Goekkaya M, Kling E, Geldmacher C, Rubio-Acero R, Plank M, Christa C, Willmann A, Vu M, **Einhauser S**, Weps M, Lampl BMJ, Almanzar G, Kousha K, Schwägerl V, Liebl B, Weber B, Drescher J, Scheidt J, Gefeller O, Messmann H, Protzer U, Liese J, Hoelscher M, Wagner R, Überla K, Steininger P; CoVaKo Study Group.

Published in **November 2023 in Journal of Clinical Virology**

DOI: 10.1016/j.jcv.2023.105622

Background: SARS-CoV-2 variants of concern (VOC) may result in breakthrough infections (BTIs) in vaccinated individuals. The aim of this study was to investigate the effects of full primary (two-dose) COVID-19 vaccination with wild-type-based SARS-CoV-2 vaccines on symptoms and immunogenicity of SARS-CoV-2 VOC BTIs.

Methods: In a longitudinal multicenter controlled cohort study in Bavaria, Germany, COVID-19 vaccinated and unvaccinated non-hospitalized individuals were prospectively enrolled within 14 days of a PCR-confirmed SARS-CoV-2 infection. Individuals were visited weekly up to 4 times, performing a structured record of medical data and viral load assessment. SARS-CoV-2-specific antibody response was characterized by anti-spike-(S)- and anti-nucleocapsid-(N)-antibody concentrations, anti-S-IgG avidity and neutralization capacity.

Results: A total of 300 individuals (212 BTIs, 88 non-BTIs) were included with VOC Alpha or Delta SARS-CoV-2 infections. Full primary COVID-19 vaccination provided a significant effectiveness against five symptoms (relative risk reduction): fever (33 %), cough (21 %), dysgeusia (22 %), dizziness (52 %) and nausea/vomiting (48 %). Full primary vaccinated individuals showed significantly higher 50 % inhibitory concentration (IC_{50}) values against the infecting VOC compared to unvaccinated individuals at week 1 (269 vs. 56, respectively), and weeks 5-7 (1,917 vs. 932, respectively) with significantly higher relative anti-S-IgG avidity (78% vs. 27 % at week 4, respectively).

Conclusions: Full primary COVID-19 vaccination reduced symptom frequencies in non-hospitalized individuals with BTIs and elicited a more rapid and longer lasting neutralization capacity against the infecting VOC compared to unvaccinated individuals. These results support the recommendation to offer at least full primary vaccination to all adults to reduce disease severity caused by immune escape-variants.

9.1.15 Appendix Manuscript 15: Evolution of protective SARS-CoV-2-specific B and T cell responses upon vaccination and Omicron breakthrough infection

Authors: Ahmed MIM, **Einhauser S**, Peiter C, Senninger A, Baranov O, Eser TM, Huth M, Olbrich L, Castelletti N, Rubio-Acero R, Carnell G, Heeney J, Kroidl I, Held K, Wieser A, Janke C, Hoelscher M, Hasenauer J, Wagner R, Geldmacher C; KoCo19/ORCHESTRA working group.

Published on 21st of **June 2024 in iScience**

DOI: 10.1016/j.isci.2024.110138

Severe acute respiratory syndrome coronavirus 2 (SARS-CoV-2) Omicron breakthrough infection (BTI) induced better protection than triple vaccination. To address the underlying immunological mechanisms, we studied antibody and T cell response dynamics during vaccination and after BTI. Each vaccination significantly increased peak neutralization titers with simultaneous increases in circulating spike-specific T cell frequencies. Neutralization titers significantly associated with a reduced hazard rate for SARS-CoV-2 infection. Yet, 97% of triple vaccinees became SARS-CoV-2 infected. BTI further boosted neutralization magnitude and breadth, broadened virus-specific T cell responses to non-vaccine-encoded antigens,and protected with an efficiency of 88% from further infections by December 2022. This effect was then assessed by utilizing mathematical modeling, which accounted for time-dependent infection risk, the antibody, and T cell concentration at any time point after BTI. Our findings suggest that cross-variant protective hybrid immunity induced by vaccination and BTI was an important contributor to the reduced virus transmission observed in Bavaria in late 2022 and thereafter.

9.1.16 Appendix Manuscript 16: Impedance-based monitoring of titration and neutralization assays with VSV-G and SARS-CoV-2-spike pseudoviruses

Authors: Anne-Kathrin Mildner, Sebastian Einhauser, Stefanie Michaelis, Klara Rogalla v. Bieberstein, Ralf Wagner, Joachim Wegener.

Published on 27th **August 2024 in Applied Research**.

DOI: 10.1002/appl.202400097.

Since cell-based virus neutralization assays are still the gold standard to assess a patient's immune protection against a given virus, they are of utmost importance for serodiagnosis, convalescent plasma therapy, and vaccine development. Monitoring the emergence and characteristics of neutralizing antibodies in an outbreak situation, confirming neutralizing antibodies as correlates of protection from infection and testing vaccine-induced potency of neutralizing antibody responses, quests for automated, fast, and parallel neutralization assays. We developed an impedance-based sensor

platform (electric cell-substrate impedance sensing, ECIS) providing time-resolved monitoring of the host cell response to viral pseudotypes. For validation, the impedance assay was compared with state-of-the-art quantification of virus-induced reporter protein expression as an independent indicator of virus infection and neutralization. Vesicular stomatitis virus (VSV) derived pseudoviruses encoding the green fluorescent protein (GFP) as reporter and the autologous G protein (VSV-G) for the initial binding to the host cell membrane were used for monitoring of HEK293T cell infection and neutralization with both, impedance and optical readout. Virus-induced cytopathic effects (CPE) were detectable for low pseudotype concentrations (multiplicity of infection 1) in time-resolved impedance profiles as soon as 5–10 h after infection in a concentration-dependent manner. Neutralization efficacy of α-VSV-G antibodies was determined from impedance time courses and IC_{50} values compared favorably with fluorescence measurements of virus-borne GFP expression. Sera of convalescent COVID-19 patients were tested successfully for SARS-CoV-2 neutralizing antibodies by incubating VSV, pseudotyped with the SARS-CoV-2 spike protein, with different sera before host cell exposure and impedance recordings. In summary: (i) ECIS monitoring was successfully applied to detect virus-mediated cell infection and neutralization; (ii) Impedance-based monitoring allows reducing the assay time to 5–10 h; and (iii) the platform is easily adapted to other virus-based diseases and scalable to high-throughput.

9.1.17 Appendix Manuscript 17: Computationally designed Spike antigens induce neutralising responses against the breadth of SARS-COV-2 variants

Authors: Vishwanath S, Carnell GW, Billmeier M, Ohlendorf L, Neckermann P, Asbach B, George C, Sans MS, Chan A, Olivier J, Nadesalingam A, **Einhauser S**, Temperton N, Cantoni D, Grove J, Jordan I, Sandig V, Tonks P, Geiger J, Dohmen C, Mummert V, Samuel AR, Plank C, Kinsley R, Wagner R, Heeney JL.
Published on 9th **September 2024 in NPJ Vaccines**.
DOI: 10.1038/s41541-024-00950-9

Updates of SARS-CoV-2 vaccines are required to generate immunity in the population against constantly evolving SARS-CoV-2 variants of concerns (VOCs). Here we describe three novel in-silico designed spike-based antigens capable of inducing neutralising antibodies across a spectrum of SARS-CoV-2 VOCs. Three sets of antigens utilising pre-Delta (T2_32), and post-Gamma sequence data (T2_35 and T2_36) were designed. T2_32 elicited superior neutralising responses against VOCs compared to the Wuhan-1 spike antigen in DNA prime-boost immunisation regime in guinea pigs. Heterologous boosting with the attenuated poxvirus - Modified vaccinia Ankara expressing T2_32 induced broader neutralising immune responses in all primed animals. T2_32, T2_35 and T2_36 elicited broader neutralising capacity compared to the Omicron BA.1 spike antigen administered by mRNA immunisation in mice. These findings demonstrate the utility of structure-informed computationally

derived modifications of spike-based antigens for inducing broad immune responses covering more than 2 years of evolved SARS-CoV-2 variants.

9.2 List of Abbreviations

bAbs	Binding antibodies	Ig	immunoglobulin
BL	Baseline	LLM	Large language model (e.g. ChatGPT, Google Gemini)
bnAbs	Broadly neutralizing antibodies	log	Logarithm
BTI	Breakthrough infection	MB	Magnitude & Breadth
CI	Confidence/Credibility Intervall	MERS	Middle Easter Respiratory Syndrome
CoV	Coronavirus	MOI	Multiplicity of infection
COVID	Coronavirus Disease	nAbs	Neutralizing Antibodies
CPE	Cytopathic effect	NN	Neural Network
EC50	50% effective concentration	NPV/ PPV	Negative/positive predictive value
ECIS	Electric cell impedance sensing	OR	Odds Ratio
FU	Follow Up	PV	Pseudovirus
GFP	Green fluorescent protein	RF	RandomForest
HCW	Health Care worker	SARS	Severe Acute Respiratory Syndrome
HIV	Human Immunodeficiency Virus	SD	Standard Deviation
HR	Hazard ratio	SDR	Surveillance Detection Ratio
IC50/ID50	50% inhibitory concentration/dilution	VOC	Variant of Concern
ICU	Intensive care unit	VOI	Variant of Interest
IFR	Infection Fatality Ratio	VSV	Vesicular Stomatitis Virus

10 References

1. Tyrrell, D. A. J. & Bynoe, M. L. Cultivation of a Novel Type of Common-cold Virus in Organ Cultures. *Br. Med. J.* **1**, 1467–1470 (1965).
2. Monto, A. S., Cowling, B. J. & Peiris, J. S. M. Coronaviruses: The Common Cold, SARS, and MERS. in *Viral Infections of Humans* 1–53 (Springer, New York, NY, 2024). doi:10.1007/978-1-4939-9544-8_67-1.
3. DocCheck, M. bei. Coronavirus. *DocCheck Flexikon* https://flexikon.doccheck.com/de/Coronavirus.
4. 'Wir waren immun-naiv': Was fünf Jahre später über SARS-CoV-2 bekannt ist. *ZDFheute* https://www.zdfheute.de/wissen/corona-coronavirus-sars-cov-2-fuenf-jahre-100.html (2025).
5. Zhou, Z., Qiu, Y. & Ge, X. The taxonomy, host range and pathogenicity of coronaviruses and other viruses in the Nidovirales order. *Anim. Dis.* **1**, 5 (2021).
6. International Committee on Taxonomy of Viruses (ICTV). https://talk.ictvonline.org/taxonomy/.
7. Cui, J., Li, F. & Shi, Z.-L. Origin and evolution of pathogenic coronaviruses. *Nat. Rev. Microbiol.* **17**, 181–192 (2019).
8. Liu, D. X., Liang, J. Q. & Fung, T. S. Human Coronavirus-229E, -OC43, -NL63, and -HKU1 (Coronaviridae). *Encycl. Virol.* 428–440 (2021) doi:10.1016/B978-0-12-809633-8.21501-X.
9. Zhou, H. *et al.* A Review of SARS-CoV2: Compared With SARS-CoV and MERS-CoV. *Front. Med.* **8**, (2021).
10. Rabaan, A. A. *et al.* An updated review on pathogenic coronaviruses (CoVs) amid the emergence of SARS-CoV-2 variants: A look into the repercussions and possible solutions. *J. Infect. Public Health* **16**, 1870–1883 (2023).
11. Rabaan, A. A. *et al.* SARS-CoV-2, SARS-CoV, and MERS-COV: A comparative overview. *Infez. Med.* **28**, 174–184 (2020).
12. Berche, P. The enigma of the 1889 Russian flu pandemic: A coronavirus? *Presse Medicale Paris Fr. 1983* **51**, 104111 (2022).
13. Stadler, K. *et al.* SARS — beginning to understand a new virus. *Nat. Rev. Microbiol.* **1**, 209–218 (2003).
14. Cherry, J. D. & Krogstad, P. SARS: The First Pandemic of the 21st Century. *Pediatr. Res.* **56**, 1–5 (2004).
15. Xu, R.-H. *et al.* Epidemiologic Clues to SARS Origin in China. *Emerg. Infect. Dis.* **10**, 1030–1037 (2004).
16. Wang, L.-F. & Eaton, B. T. Bats, Civets and the Emergence of SARS. *Wildl. Emerg. Zoonotic Dis. Biol. Circumst. Consequences Cross-Species Transm.* **315**, 325–344 (2007).
17. Shi, Z. & Hu, Z. A review of studies on animal reservoirs of the SARS coronavirus. *Virus Res.* **133**, 74–87 (2008).
18. Ramadan, N. & Shaib, H. Middle East respiratory syndrome coronavirus (MERS-CoV): A review. *Germs* **9**, 35–42 (2019).
19. Mobaraki, K. & Ahmadzadeh, J. Current epidemiological status of Middle East respiratory syndrome coronavirus in the world from 1.1.2017 to 17.1.2018: A cross-sectional study. *BMC Infect. Dis.* **19**, (2019).
20. Han, H.-J., Yu, H. & Yu, X.-J. Evidence for zoonotic origins of Middle East respiratory syndrome coronavirus. *J. Gen. Virol.* **97**, 274–280 (2016).

21. Hoang, T. & Anh, T. T. T. Treatment Options for Severe Acute Respiratory Syndrome, Middle East Respiratory Syndrome, and Coronavirus Disease 2019: a Review of Clinical Evidence. *Infect. Chemother.* **52**, 317–334 (2020).
22. Zhu, N. *et al.* A novel coronavirus from patients with pneumonia in China, 2019. *N. Engl. J. Med.* **382**, 727–733 (2020).
23. CDC. CDC Museum COVID-19 Timeline. *Centers for Disease Control and Prevention* https://www.cdc.gov/museum/timeline/covid19.html (2024).
24. Naming the coronavirus disease (COVID-19) and the virus that causes it. https://www.who.int/emergencies/diseases/novel-coronavirus-2019/technical-guidance/naming-the-coronavirus-disease-(covid-2019)-and-the-virus-that-causes-it.
25. Cucinotta, D. & Vanelli, M. WHO Declares COVID-19 a Pandemic. *Acta Bio Medica Atenei Parm.* **91**, 157–160 (2020).
26. COVID-19 pandemic - Germany. https://global-monitoring.com/gm/page/events/epidemic-0001937.eP207vO5rIwe.html?lang=en.
27. COVID-19 cases | WHO COVID-19 dashboard. *datadot* https://data.who.int/dashboards/covid19/deaths.
28. Koch-Institut, R. SARS-CoV-2 Infektionen in Deutschland. Zenodo (2025).
29. Seroepidemiological Studies in Germany. https://www.rki.de/EN/Topics/Infectious-diseases/Acute-respiratory-infections/COVID-19/seroepidemiological-studies/AKS_Map.html.
30. Bergeri, I. *et al.* Global SARS-CoV-2 seroprevalence from January 2020 to April 2022: A systematic review and meta-analysis of standardized population-based studies. *PLOS Med.* **19**, e1004107 (2022).
31. Pollán, M. *et al.* Prevalence of SARS-CoV-2 in Spain (ENE-COVID): a nationwide, population-based seroepidemiological study. *The Lancet* **396**, 535–544 (2020).
32. Espenhain, L. *et al.* Prevalence of SARS-CoV-2 antibodies in Denmark: nationwide, population-based seroepidemiological study. *Eur. J. Epidemiol.* **36**, 715–725 (2021).
33. Bajema, K. L. *et al.* Estimated SARS-CoV-2 Seroprevalence in the US as of September 2020. *JAMA Intern. Med.* **181**, 450–460 (2021).
34. Remdesivir bei COVID-19 - Empfehlungen zum sachgerechten Einsatz. https://www.rki.de/DE/Themen/Infektionskrankheiten/Biologische-Gefahren/STAKOB/Handlungshinweise/Stellungnahme-Covid-19_Remdesivir.html.
35. Blair, H. A. Remdesivir: A Review in COVID-19. *Drugs* **83**, 1215–1237 (2023).
36. Copin, R. *et al.* The monoclonal antibody combination REGEN-COV protects against SARS-CoV-2 mutational escape in preclinical and human studies. *Cell* **184**, 3949-3961.e11 (2021).
37. Polack, F. P. *et al.* Safety and Efficacy of the BNT162b2 mRNA Covid-19 Vaccine. *N. Engl. J. Med.* **383**, 2603–2615 (2020).
38. Thomas, S. J. *et al.* Safety and Efficacy of the BNT162b2 mRNA Covid-19 Vaccine through 6 Months. *N. Engl. J. Med.* **385**, 1761–1773 (2021).
39. Voysey, M. *et al.* Safety and efficacy of the ChAdOx1 nCoV-19 vaccine (AZD1222) against SARS-CoV-2: an interim analysis of four randomised controlled trials in Brazil, South Africa, and the UK. *The Lancet* **397**, 99–111 (2021).
40. Voysey, M. *et al.* Single-dose administration and the influence of the timing of the booster dose on immunogenicity and efficacy of ChAdOx1 nCoV-19 (AZD1222) vaccine: a pooled analysis of four randomised trials. *The Lancet* **397**, 881–891 (2021).
41. Knoll, M. D. & Wonodi, C. Oxford–AstraZeneca COVID-19 vaccine efficacy. *The Lancet* **397**, 72–74 (2021).

42. Gilbert, P. B. *et al.* Immune correlates analysis of the mRNA-1273 COVID-19 vaccine efficacy clinical trial. *Science* **375**, 43–50 (2022).
43. Baden, L. R. *et al.* Efficacy and Safety of the mRNA-1273 SARS-CoV-2 Vaccine. *N. Engl. J. Med.* **384**, 403–416 (2021).
44. COVID-19 Vaccines with WHO Emergency Use Listing | WHO - Prequalification of Medical Products (IVDs, Medicines, Vaccines and Immunization Devices, Vector Control). https://extranet.who.int/prequal/vaccines/covid-19-vaccines-who-emergency-use-listing.
45. Ghazy, R. M. *et al.* Efficacy and Effectiveness of SARS-CoV-2 Vaccines: A Systematic Review and Meta-Analysis. *Vaccines* **10**, 350 (2022).
46. SARS-CoV-2 variants of concern as of 28 May 2025. https://www.ecdc.europa.eu/en/covid-19/variants-concern (2021).
47. Domingo, P. & Benito, N. de. Alpha variant SARS-CoV-2 infection: How it all starts. *eBioMedicine* **74**, (2021).
48. Davies, N. G. *et al.* Estimated transmissibility and impact of SARS-CoV-2 lineage B.1.1.7 in England. *Science* **372**, eabg3055 (2021).
49. Carabelli, A. M. *et al.* SARS-CoV-2 variant biology: immune escape, transmission and fitness. *Nat. Rev. Microbiol.* **21**, 162–177 (2023).
50. COVID-19 vaccines | WHO COVID-19 dashboard. *datadot* https://data.who.int/dashboards/covid19/vaccines.
51. WHO chief declares end to COVID-19 as a global health emergency | UN News. https://news.un.org/en/story/2023/05/1136367 (2023).
52. COVID-19 cases | WHO COVID-19 dashboard. *datadot* https://data.who.int/dashboards/covid19/deaths.
53. Gesundheit, B. für. Infektionsradar. https://infektionsradar.gesund.bund.de/de/covid/abwasser.
54. CDC. SARS-CoV-2 Variant XEC Increases as KP.3.1.1 Slows. *National Center for Immunization and Respiratory Diseases* https://www.cdc.gov/ncird/whats-new/sars-cov-2-variant-xec-increases-as-kp-3-1-1-slows.html (2025).
55. Davis, H. E., McCorkell, L., Vogel, J. M. & Topol, E. J. Long COVID: major findings, mechanisms and recommendations. *Nat. Rev. Microbiol.* **21**, 133–146 (2023).
56. Ely, E. W., Brown, L. M. & Fineberg, H. V. Long Covid Defined. *N. Engl. J. Med.* **391**, 1746–1753 (2024).
57. Steiner, S. *et al.* SARS-CoV-2 biology and host interactions. *Nat. Rev. Microbiol.* **22**, 206–225 (2024).
58. Yao, H. *et al.* Molecular Architecture of the SARS-CoV-2 Virus. *Cell* **183**, 730-738.e13 (2020).
59. Naqvi, A. A. T. *et al.* Insights into SARS-CoV-2 genome, structure, evolution, pathogenesis and therapies: Structural genomics approach. *Biochim. Biophys. Acta Mol. Basis Dis.* **1866**, 165878 (2020).
60. Arya, R. *et al.* Structural insights into SARS-CoV-2 proteins. *J. Mol. Biol.* **433**, 166725 (2021).
61. Helmy, Y. A. *et al.* The COVID-19 Pandemic: A Comprehensive Review of Taxonomy, Genetics, Epidemiology, Diagnosis, Treatment, and Control. *J. Clin. Med.* **9**, 1225 (2020).
62. Justo Arevalo, S. *et al.* What do we know about the function of SARS-CoV-2 proteins? *Front. Immunol.* **14**, 1249607 (2023).
63. Baddock, H. T. *et al.* Characterization of the SARS-CoV-2 ExoN (nsp14ExoN–nsp10) complex: implications for its role in viral genome stability and inhibitor identification. *Nucleic Acids Res.* **50**, 1484–1500 (2022).
64. Sanjuán, R., Nebot, M. R., Chirico, N., Mansky, L. M. & Belshaw, R. Viral Mutation Rates. *J. Virol.* **84**, 9733–9748 (2010).

65. Bai, C., Zhong, Q. & Gao, G. F. Overview of SARS-CoV-2 genome-encoded proteins. *Sci. China Life Sci.* **65**, 280–294 (2022).
66. Wang, Q. *et al.* Structural and Functional Basis of SARS-CoV-2 Entry by Using Human ACE2. *Cell* **181**, 894-904.e9 (2020).
67. Huang, Y., Yang, C., Xu, X., Xu, W. & Liu, S. Structural and functional properties of SARS-CoV-2 spike protein: potential antivirus drug development for COVID-19. *Acta Pharmacol. Sin.* **41**, 1141–1149 (2020).
68. Glowacka, I. *et al.* Evidence that TMPRSS2 Activates the Severe Acute Respiratory Syndrome Coronavirus Spike Protein for Membrane Fusion and Reduces Viral Control by the Humoral Immune Response ▿ . *J. Virol.* **85**, 4122–4134 (2011).
69. Boluda, S. *et al.* Golgi localization of SARS-CoV-2 spike protein and interaction with furin in cerebral COVID-19 microangiopathy: a clue to the central nervous system involvement? *Free Neuropathol.* **4**, 1.
70. Yu, J. *et al.* Deletion of the SARS-CoV-2 Spike Cytoplasmic Tail Increases Infectivity in Pseudovirus Neutralization Assays. *J. Virol.* **95**, 10.1128/jvi.00044-21 (2021).
71. Dey, D. *et al.* A single C-terminal residue controls SARS-CoV-2 spike trafficking and incorporation into VLPs. *Nat. Commun.* **14**, 8358 (2023).
72. Hoffmann, M. *et al.* SARS-CoV-2 Cell Entry Depends on ACE2 and TMPRSS2 and Is Blocked by a Clinically Proven Protease Inhibitor. *Cell* **181**, 271-280.e8 (2020).
73. Hoffmann, M., Kleine-Weber, H. & Pöhlmann, S. A Multibasic Cleavage Site in the Spike Protein of SARS-CoV-2 Is Essential for Infection of Human Lung Cells. *Mol. Cell* **78**, 779-784.e5 (2020).
74. Li, F. Structure, Function, and Evolution of Coronavirus Spike Proteins. *Annu. Rev. Virol.* **3**, 237–261 (2016).
75. Jackson, C. B., Farzan, M., Chen, B. & Choe, H. Mechanisms of SARS-CoV-2 entry into cells. *Nat. Rev. Mol. Cell Biol.* **23**, 3–20 (2022).
76. Akıl, C., Xu, J., Shen, J. & Zhang, P. Unveiling the structural spectrum of SARS-CoV-2 fusion by in situ cryo-ET. *Nat. Commun.* **16**, 5150 (2025).
77. Shang, J. *et al.* Cell entry mechanisms of SARS-CoV-2. *Proc. Natl. Acad. Sci.* **117**, 11727–11734 (2020).
78. Singh, P. *et al.* SARS-CoV-2 spike fusion peptide trans interaction with phosphatidylserine lipid triggers membrane fusion for viral entry. *mBio* **15**, e01077-24 (2024).
79. Doms, R. W. & Moore, J. P. HIV-1 Membrane Fusion. *J. Cell Biol.* **151**, f9–f14 (2000).
80. Xia, X. Domains and Functions of Spike Protein in SARS-Cov-2 in the Context of Vaccine Design. *Viruses* **13**, 109 (2021).
81. Hsieh, C.-L. *et al.* Structure-based design of prefusion-stabilized SARS-CoV-2 spikes. *Science* **369**, 1501–1505 (2020).
82. Xiaojie, S., Yu, L., lei, Y., Guang, Y. & Min, Q. Neutralizing antibodies targeting SARS-CoV-2 spike protein. *Stem Cell Res.* **50**, 102125 (2021).
83. López-Cortés, G. I. *et al.* The Spike Protein of SARS-CoV-2 Is Adapting Because of Selective Pressures. *Vaccines* **10**, 864 (2022).
84. Escalera, A. *et al.* Mutations in SARS-CoV-2 variants of concern link to increased spike cleavage and virus transmission. *Cell Host Microbe* **30**, 373-387.e7 (2022).
85. Castillo, G. *et al.* Molecular mechanisms of human coronavirus NL63 infection and replication. *Virus Res.* **327**, 199078 (2023).

86. Li, W. *et al.* Receptor and viral determinants of SARS-coronavirus adaptation to human ACE2. *EMBO J.* **24**, 1634–1643 (2005).
87. Wang, Q. *et al.* Structural and Functional Basis of SARS-CoV-2 Entry by Using Human ACE2. *Cell* **181**, 894-904.e9 (2020).
88. Lambert, D. W. *et al.* Tumor necrosis factor-alpha convertase (ADAM17) mediates regulated ectodomain shedding of the severe-acute respiratory syndrome-coronavirus (SARS-CoV) receptor, angiotensin-converting enzyme-2 (ACE2). *J. Biol. Chem.* **280**, 30113–30119 (2005).
89. Heurich, A. *et al.* TMPRSS2 and ADAM17 cleave ACE2 differentially and only proteolysis by TMPRSS2 augments entry driven by the severe acute respiratory syndrome coronavirus spike protein. *J. Virol.* **88**, 1293–1307 (2014).
90. Samavati, L. & Uhal, B. D. ACE2, Much More Than Just a Receptor for SARS-COV-2. *Front. Cell. Infect. Microbiol.* **10**, 317 (2020).
91. Oudit, G. Y., Wang, K., Viveiros, A., Kellner, M. J. & Penninger, J. M. Angiotensin-converting enzyme 2—at the heart of the COVID-19 pandemic. *Cell* **186**, 906–922 (2023).
92. Laghlam, D., Jozwiak, M. & Nguyen, L. S. Renin-Angiotensin-Aldosterone System and Immunomodulation: A State-of-the-Art Review. *Cells* **10**, 1767 (2021).
93. Nabah, Y. N. A. *et al.* Angiotensin II Induces Neutrophil Accumulation In Vivo Through Generation and Release of CXC Chemokines. *Circulation* **110**, 3581–3586 (2004).
94. Lim, S., Zhang, M. & Chang, T. L. ACE2-Independent Alternative Receptors for SARS-CoV-2. *Viruses* **14**, 2535 (2022).
95. Cantuti-Castelvetri, L. *et al.* Neuropilin-1 facilitates SARS-CoV-2 cell entry and infectivity. *Science* **370**, 856–860 (2020).
96. Gudowska-Sawczuk, M. & Mroczko, B. The Role of Neuropilin-1 (NRP-1) in SARS-CoV-2 Infection: Review. *J. Clin. Med.* **10**, 2772 (2021).
97. Mayi, B. S. *et al.* The role of Neuropilin-1 in COVID-19. *PLOS Pathog.* **17**, e1009153 (2021).
98. Nakanishi, T., Fujita, Y. & Yamashita, T. Neuropilin-1-mediated pruning of corticospinal tract fibers is required for motor recovery after spinal cord injury. *Cell Death Dis.* **10**, 67 (2019).
99. Nguyen, H. L., Hieu, H. K., Nguyen, T. Q., Nhung, N. T. A. & Li, M. S. Neuropilin-1 Protein May Serve as a Receptor for SARS-CoV-2 Infection: Evidence from Molecular Dynamics Simulations. *J. Phys. Chem. B* **128**, 7141–7147 (2024).
100. Daly, J. L. *et al.* Neuropilin-1 is a host factor for SARS-CoV-2 infection. *Science* eabd3072 (2020) doi:10.1126/science.abd3072.
101. WHO. updated_working_definitions_17-08-2023. https://www.who.int/docs/default-source/coronaviruse/annex1_updated_working_definitions_17-08-2023.pdf.
102. CoVariants. https://covariants.org/.
103. Plante, J. A. *et al.* Spike mutation D614G alters SARS-CoV-2 fitness. *Nature* **592**, 116–121 (2021).
104. Yurkovetskiy, L. *et al.* Structural and Functional Analysis of the D614G SARS-CoV-2 Spike Protein Variant. *Cell* **183**, 739-751.e8 (2020).
105. Arora, P., Pöhlmann, S. & Hoffmann, M. Mutation D614G increases SARS-CoV-2 transmission. *Signal Transduct. Target. Ther.* **6**, 101 (2021).
106. Korber, B. *et al.* Tracking Changes in SARS-CoV-2 Spike: Evidence that D614G Increases Infectivity of the COVID-19 Virus. *Cell* **182**, 812-827.e19 (2020).
107. Kidd, M. *et al.* S-Variant SARS-CoV-2 Lineage B1.1.7 Is Associated With Significantly Higher Viral Load in Samples Tested by TaqPath Polymerase Chain Reaction. *J. Infect. Dis.* **223**, 1666–1670 (2021).

108. Galloway, S. E. Emergence of SARS-CoV-2 B.1.1.7 Lineage — United States, December 29, 2020–January 12, 2021. *MMWR Morb. Mortal. Wkly. Rep.* **70**, (2021).
109. Rambaut, A. *et al.* A dynamic nomenclature proposal for SARS-CoV-2 lineages to assist genomic epidemiology. *Nat. Microbiol.* **5**, 1403–1407 (2020).
110. Pascall, D. J. *et al.* The SARS-CoV-2 Alpha variant was associated with increased clinical severity of COVID-19 in Scotland: A genomics-based retrospective cohort analysis. *PLOS ONE* **18**, e0284187 (2023).
111. Fernández, J. *et al.* Neutralization of alpha, gamma, and D614G SARS-CoV-2 variants by CoronaVac vaccine-induced antibodies. *J. Med. Virol.* **94**, 399–403 (2022).
112. Tian, F. *et al.* N501Y mutation of spike protein in SARS-CoV-2 strengthens its binding to receptor ACE2. *eLife* **10**, e69091 (2021).
113. Zhang, L. *et al.* Furin cleavage of the SARS-CoV-2 spike is modulated by O-glycosylation. *Proc. Natl. Acad. Sci.* **118**, e2109905118 (2021).
114. Lista, M. J. *et al.* The P681H Mutation in the Spike Glycoprotein of the Alpha Variant of SARS-CoV-2 Escapes IFITM Restriction and Is Necessary for Type I Interferon Resistance. *J. Virol.* **96**, e01250-22 (2022).
115. Meng, B. *et al.* Recurrent emergence of SARS-CoV-2 spike deletion H69/V70 and its role in the Alpha variant B.1.1.7. *Cell Rep.* **35**, 109292 (2021).
116. CoVariants: 20I (Alpha, V1). https://covariants.org/variants/20I.Alpha.V1.
117. Jangra, S. *et al.* SARS-CoV-2 spike E484K mutation reduces antibody neutralisation. *Lancet Microbe* **2**, e283–e284 (2021).
118. Wu, L. *et al.* Exploring the immune evasion of SARS-CoV-2 variant harboring E484K by molecular dynamics simulations. *Brief. Bioinform.* **23**, bbab383 (2022).
119. Preliminary genomic characterisation of an emergent SARS-CoV-2 lineage in the UK defined by a novel set of spike mutations - SARS-CoV-2 coronavirus / nCoV-2019 Genomic Epidemiology. *Virological* https://virological.org/t/preliminary-genomic-characterisation-of-an-emergent-sars-cov-2-lineage-in-the-uk-defined-by-a-novel-set-of-spike-mutations/563 (2020).
120. Genomic characterisation of an emergent SARS-CoV-2 lineage in Manaus: preliminary findings - SARS-CoV-2 coronavirus / nCoV-2019 Genomic Epidemiology. *Virological* https://virological.org/t/genomic-characterisation-of-an-emergent-sars-cov-2-lineage-in-manaus-preliminary-findings/586/2 (2021).
121. CoVariants: 20H (Beta, V2). https://covariants.org/variants/20H.Beta.V2.
122. CoVariants: 20J (Gamma, V3). https://covariants.org/variants/20J.Gamma.V3.
123. Tegally, H. *et al.* Detection of a SARS-CoV-2 variant of concern in South Africa. *Nature* **592**, 438–443 (2021).
124. Pondé, R. A. A. Physicochemical effect of the N501Y, E484K/Q, K417N/T, L452R and T478K mutations on the SARS-CoV-2 spike protein RBD and its influence on agent fitness and on attributes developed by emerging variants of concern. *Virology* **572**, 44–54 (2022).
125. Cele, S. *et al.* Escape of SARS-CoV-2 501Y.V2 from neutralization by convalescent plasma. *Nature* **593**, 142–146 (2021).
126. Souza, W. M. *et al.* Neutralisation of SARS-CoV-2 lineage P.1 by antibodies elicited through natural SARS-CoV-2 infection or vaccination with an inactivated SARS-CoV-2 vaccine: an immunological study. *Lancet Microbe* **2**, e527–e535 (2021).
127. CoVariants: 21A (Delta). https://covariants.org/variants/21A.Delta.

128. Bhattacharya, M., Chatterjee, S., Sharma, A. R., Lee, S.-S. & Chakraborty, C. Delta variant (B.1.617.2) of SARS-CoV-2: current understanding of infection, transmission, immune escape, and mutational landscape. *Folia Microbiol. (Praha)* **68**, 17–28 (2023).
129. Dhawan, M. *et al.* Delta variant (B.1.617.2) of SARS-CoV-2: Mutations, impact, challenges and possible solutions. *Hum. Vaccines Immunother.* **18**, 2068883.
130. Chavda, V. P., Bezbaruah, R., Deka, K., Nongrang, L. & Kalita, T. The Delta and Omicron Variants of SARS-CoV-2: What We Know So Far. *Vaccines* **10**, 1926 (2022).
131. This is no time to stop tracking COVID-19. *Nature* **603**, 550–550 (2022).
132. Nextstrain / ncov / gisaid / global / 6m. https://nextstrain.org/ncov/gisaid/global/6m.
133. Zahradník, J. *et al.* SARS-CoV-2 variant prediction and antiviral drug design are enabled by RBD in vitro evolution. *Nat. Microbiol.* **6**, 1188–1198 (2021).
134. Kim, S. *et al.* Binding of Human ACE2 and RBD of Omicron Enhanced by Unique Interaction Patterns Among SARS-CoV-2 Variants of Concern. *bioRxiv* 2022.01.24.477633 (2022) doi:10.1101/2022.01.24.477633.
135. Kumar, S., Karuppanan, K. & Subramaniam, G. Omicron (BA.1) and sub-variants (BA.1.1, BA.2, and BA.3) of SARS-CoV-2 spike infectivity and pathogenicity: A comparative sequence and structural-based computational assessment. *J. Med. Virol.* **94**, 4780–4791 (2022).
136. Chatterjee, S., Bhattacharya, M., Nag, S., Dhama, K. & Chakraborty, C. A Detailed Overview of SARS-CoV-2 Omicron: Its Sub-Variants, Mutations and Pathophysiology, Clinical Characteristics, Immunological Landscape, Immune Escape, and Therapies. *Viruses* **15**, 167 (2023).
137. Feng, S., O'Brien, A., Chen, D.-Y., Saeed, M. & Baker, S. C. SARS-CoV-2 nonstructural protein 6 from Alpha to Omicron: evolution of a transmembrane protein. *mBio* **14**, e0068823 (2023).
138. Abdel-Moneim, A. S. & Abdelwhab, E. M. Evidence for SARS-CoV-2 Infection of Animal Hosts. *Pathogens* **9**, 529 (2020).
139. Sun, Y., Lin, W., Dong, W. & Xu, J. Origin and evolutionary analysis of the SARS-CoV-2 Omicron variant. *J. Biosaf. Biosecurity* **4**, 33–37 (2022).
140. Li, K. *et al.* Adaptation of SARS-CoV-2 to ACE2H353K mice reveals new spike residues that drive mouse infection. *J. Virol.* **98**, e01510-23.
141. Press reports. *Charité – Universitätsmedizin Berlin* https://www.charite.de/en/service/press_reports/artikel/detail/where_did_omicron_come_from.
142. Marques, A. D. *et al.* SARS-CoV-2 evolution during prolonged infection in immunocompromised patients. *mBio* **15**, e00110-24 (2024).
143. Liu, W. *et al.* Evolution of the SARS-CoV-2 Omicron Variants: Genetic Impact on Viral Fitness. *Viruses* **16**, 184 (2024).
144. Fischer, C. *et al.* RETRACTED: Gradual emergence followed by exponential spread of the SARS-CoV-2 Omicron variant in Africa. *Science* **378**, eadd8737 (2022).
145. COVID-19 Vaccines - Paul-Ehrlich-Institut. https://www.pei.de/EN/medicinal-products/vaccines-human/covid-19/covid-19-node.html.
146. Petrova, V. N. & Russell, C. A. The evolution of seasonal influenza viruses. *Nat. Rev. Microbiol.* **16**, 47–60 (2018).
147. Suthar, M. S. *et al.* The KP.2-adapted COVID-19 vaccine improves neutralising activity against the XEC variant. *Lancet Infect. Dis.* **25**, e122–e123 (2025).
148. Elsner, R. A. & Shlomchik, M. J. Germinal Center and Extrafollicular B Cell Responses in Vaccination, Immunity, and Autoimmunity. *Immunity* **53**, 1136–1150 (2020).

149. Qi, H., Liu, B., Wang, X. & Zhang, L. The humoral response and antibodies against SARS-CoV-2 infection. *Nat. Immunol.* **23**, 1008–1020 (2022).
150. Akkaya, M., Kwak, K. & Pierce, S. K. B cell memory: building two walls of protection against pathogens. *Nat. Rev. Immunol.* **20**, 229–238 (2020).
151. Long, Q.-X. *et al.* Antibody responses to SARS-CoV-2 in patients with COVID-19. *Nat. Med.* **26**, 845–848 (2020).
152. Abebe, E. C. & Dejenie, T. A. Protective roles and protective mechanisms of neutralizing antibodies against SARS-CoV-2 infection and their potential clinical implications. *Front. Immunol.* **14**, 1055457 (2023).
153. Chen, Y. *et al.* Broadly neutralizing antibodies to SARS-CoV-2 and other human coronaviruses. *Nat. Rev. Immunol.* **23**, 189–199 (2023).
154. Filippatos, C. *et al.* Convalescent Plasma Therapy for COVID-19: A Systematic Review and Meta-Analysis on Randomized Controlled Trials. *Viruses* **15**, 765 (2023).
155. Focosi, D. *et al.* Monoclonal antibody therapies against SARS-CoV-2. *Lancet Infect. Dis.* **22**, e311–e326 (2022).
156. Cox, M. *et al.* SARS-CoV-2 variant evasion of monoclonal antibodies based on in vitro studies. *Nat. Rev. Microbiol.* **21**, 112–124 (2023).
157. Tao, K., Tzou, P. L., Kosakovsky Pond, S. L., Ioannidis, J. P. A. & Shafer, R. W. Susceptibility of SARS-CoV-2 Omicron Variants to Therapeutic Monoclonal Antibodies: Systematic Review and Meta-analysis. *Microbiol. Spectr.* **10**, e0092622 (2022).
158. Zhang, A. *et al.* Beyond neutralization: Fc-dependent antibody effector functions in SARS-CoV-2 infection. *Nat. Rev. Immunol.* **23**, 381–396 (2023).
159. Lu, L. L., Suscovich, T. J., Fortune, S. M. & Alter, G. Beyond binding: antibody effector functions in infectious diseases. *Nat. Rev. Immunol.* **18**, 46–61 (2018).
160. Vanderven, H. A. & Kent, S. J. Fc-mediated functions and the treatment of severe respiratory viral infections with passive immunotherapy – a balancing act. *Front. Immunol.* **14**, (2023).
161. Maltseva, M., Keeshan, A., Cooper, C. & Langlois, M.-A. Immune imprinting: The persisting influence of the first antigenic encounter with rapidly evolving viruses. *Hum. Vaccines Immunother.* **20**, 2384192 (2024).
162. Vatti, A. *et al.* Original antigenic sin: A comprehensive review. *J. Autoimmun.* **83**, 12–21 (2017).
163. Weber, T. *et al.* Enhanced SARS-CoV-2 humoral immunity following breakthrough infection builds upon the preexisting memory B cell pool. *Sci. Immunol.* **8**, eadk5845 (2023).
164. Ding, X. *et al.* Original antigenic sin: A potential double-edged effect for vaccine improvement. *Biomed. Pharmacother.* **178**, 117187 (2024).
165. Henry, C., Palm, A.-K. E., Krammer, F. & Wilson, P. C. From Original Antigenic Sin to the Universal Influenza Virus Vaccine. *Trends Immunol.* **39**, 70–79 (2018).
166. Gong, X. *et al.* Repeated Omicron infection dampens immune imprinting from previous vaccination and induces broad neutralizing antibodies against Omicron sub-variants. *J. Infect.* **89**, 106208 (2024).
167. Kotaki, R. *et al.* Repeated Omicron exposures redirect SARS-CoV-2–specific memory B cell evolution toward the latest variants. *Sci. Transl. Med.* **16**, eadp9927 (2024).
168. Graham, C. *et al.* The effect of Omicron breakthrough infection and extended BNT162b2 booster dosing on neutralization breadth against SARS-CoV-2 variants of concern. *PLOS Pathog.* **18**, e1010882 (2022).

169. COVID-19 vaccine doses administered by manufacturer. *Our World in Data* https://ourworldindata.org/grapher/covid-vaccine-doses-by-manufacturer?country=USA~OWID_EU27.
170. Bellino, S. COVID-19 vaccines approved in the European Union: current evidence and perspectives. *Expert Rev. Vaccines* 1–5 doi:10.1080/14760584.2021.1962304.
171. Beladiya, J. *et al.* Safety and efficacy of COVID-19 vaccines: A systematic review and meta-analysis of controlled and randomized clinical trials. *Rev. Med. Virol.* **34**, e2507 (2024).
172. Chakraborty, C., Bhattacharya, M. & Dhama, K. SARS-CoV-2 Vaccines, Vaccine Development Technologies, and Significant Efforts in Vaccine Development during the Pandemic: The Lessons Learned Might Help to Fight against the Next Pandemic. *Vaccines* **11**, 682 (2023).
173. Deming, M. E. *et al.* Vaccine efficacy of NVX-CoV2373 against SARS-CoV-2 infection in adolescents in the USA: an ancillary study to a phase 3, observer-blinded, randomised, placebo-controlled trial. *Lancet Microbe* **6**, (2025).
174. Sanofi and GSK to seek regulatory authorization for COVID-19 vaccine | GSK. https://www.gsk.com/en-gb/media/press-releases/sanofi-and-gsk-to-seek-regulatory-authorization-for-covid-19-vaccine/ (2022).
175. Lazarus, R. *et al.* Safety and immunogenicity of the inactivated whole-virus adjuvanted COVID-19 vaccine VLA2001: A randomized, dose escalation, double-blind phase 1/2 clinical trial in healthy adults. *J. Infect.* **85**, 306–317 (2022).
176. Jin, L., Li, Z., Zhang, X., Li, J. & Zhu, F. CoronaVac: A review of efficacy, safety, and immunogenicity of the inactivated vaccine against SARS-CoV-2. *Hum. Vaccines Immunother.* **18**, 2096970 (2022).
177. Song, S., Madewell, Z. J., Liu, M., Longini, I. M. & Yang, Y. Effectiveness of SARS-CoV-2 vaccines against Omicron infection and severe events: a systematic review and meta-analysis of test-negative design studies. *Front. Public Health* **11**, 1195908 (2023).
178. He, X., Su, J., Ma, Y., Zhang, W. & Tang, S. A comprehensive analysis of the efficacy and effectiveness of COVID-19 vaccines. *Front. Immunol.* **13**, 945930 (2022).
179. Goldblatt, D., Alter, G., Crotty, S. & Plotkin, S. A. Correlates of protection against SARS-CoV-2 infection and COVID-19 disease. *Immunol. Rev.* 10.1111/imr.13091 (2022) doi:10.1111/imr.13091.
180. Khoury, D. S. *et al.* Neutralizing antibody levels are highly predictive of immune protection from symptomatic SARS-CoV-2 infection. *Nat. Med.* **27**, 1205–1211 (2021).
181. Sun, K. *et al.* SARS-CoV-2 correlates of protection from infection against variants of concern. *Nat. Med.* **30**, 2805–2812 (2024).
182. Benkeser, D. *et al.* Comparing antibody assays as correlates of protection against COVID-19 in the COVE mRNA-1273 vaccine efficacy trial. *Sci. Transl. Med.* **15**, eade9078 (2023).
183. Bertoletti, A., Le Bert, N. & Tan, A. T. SARS-CoV-2-specific T cells in the changing landscape of the COVID-19 pandemic. *Immunity* **55**, 1764–1778 (2022).
184. Swadling, L. *et al.* Pre-existing polymerase-specific T cells expand in abortive seronegative SARS-CoV-2. *Nature* **601**, 110–117 (2022).
185. McMahan, K. *et al.* Mucosal boosting enhances vaccine protection against SARS-CoV-2 in macaques. *Nature* **626**, 385–391 (2024).
186. Rudolph, J. E., Zhong, Y., Duggal, P., Mehta, S. H. & Lau, B. Defining representativeness of study samples in medical and population health research. *BMJ Med.* **2**, e000399 (2023).
187. Olsen, J. Random sampling - is it worth it? *Paediatr. Perinat. Epidemiol.* **27**, 27–28 (2013).
188. Nohr, E. A. & Olsen, J. Commentary: Epidemiologists have debated representativeness for more than 40 years—has the time come to move on? *Int. J. Epidemiol.* **42**, 1016–1017 (2013).

189. Szklo, M. Population-based Cohort Studies. *Epidemiol. Rev.* **20**, 81–90 (1998).
190. Tyrer, S. & Heyman, B. Sampling in epidemiological research: issues, hazards and pitfalls. *BJPsych Bull.* **40**, 57–60 (2016).
191. Neyman, J. On the Two Different Aspects of the Representative Method: The Method of Stratified Sampling and the Method of Purposive Selection. *J. R. Stat. Soc.* **97**, 558–625 (1934).
192. Elwood, J. M. Commentary: On representativeness. *Int. J. Epidemiol.* **42**, 1014–1015 (2013).
193. Rosenberg, A. R., Skapek, S. X. & Hawkins, D. S. The Inconvenience of Convenience Cohorts: Rhabdomyosarcoma and the PAX-FOXO1 Biomarker. *Cancer Epidemiol. Biomark. Prev. Publ. Am. Assoc. Cancer Res. Cosponsored Am. Soc. Prev. Oncol.* **21**, 1012–1018 (2012).
194. Convenience Sample - an overview | ScienceDirect Topics. https://www.sciencedirect.com/topics/mathematics/convenience-sample.
195. D'Ambrosio, A., Garlasco, J., Quattrocolo, F., Vicentini, C. & Zotti, C. M. Data quality assessment and subsampling strategies to correct distributional bias in prevalence studies. *BMC Med. Res. Methodol.* **21**, 90 (2021).
196. Doubal, F. N. *et al.* Big data and data repurposing - using existing data to answer new questions in vascular dementia research. *BMC Neurol.* **17**, 72 (2017).
197. Naing, N. N. Easy Way to Learn Standardization : Direct and Indirect Methods. *Malays. J. Med. Sci. MJMS* **7**, 10–15 (2000).
198. Nicholls, A. The standardised mortality ratio and how to calculate it. *Students 4 Best Evidence* https://s4be.cochrane.org/blog/2020/08/26/the-standardised-mortality-ratio-and-how-to-calculate-it/ (2020).
199. Schoenbach, V. J. Standardization of rates and ratios.
200. Understanding the fundamentals of epidemiology: an evolving text; Table of contents. https://www.epidemiolog.net/evolving/TableOfContents.htm.
201. Wagner, R. *et al.* Estimates and Determinants of SARS-Cov-2 Seroprevalence and Infection Fatality Ratio Using Latent Class Analysis: The Population-Based Tirschenreuth Study in the Hardest-Hit German County in Spring 2020. *Viruses* **13**, 1118 (2021).
202. Huitfeldt, A., Swanson, S. A., Stensrud, M. J. & Suzuki, E. Effect heterogeneity and variable selection for standardizing causal effects to a target population. *Eur. J. Epidemiol.* **34**, 1119–1129 (2019).
203. Corman, V. M. *et al.* Comparison of seven commercial SARS-CoV-2 rapid point-of-care antigen tests: a single-centre laboratory evaluation study. *Lancet Microbe* **2**, e311–e319 (2021).
204. How Good are COVID-19 (SARS-CoV-2) Diagnostic PCR Tests? *College of American Pathologists* https://www.cap.org/member-resources/articles/how-good-are-covid-19-sars-cov-2-diagnostic-pcr-tests.
205. Kostoulas, P., Eusebi, P. & Hartnack, S. Diagnostic Accuracy Estimates for COVID-19 Real-Time Polymerase Chain Reaction and Lateral Flow Immunoassay Tests With Bayesian Latent-Class Models. *Am. J. Epidemiol.* **190**, 1689–1695 (2021).
206. Martínez-Barnetche, J. *et al.* Comparable diagnostic accuracy of SARS-CoV-2 Spike RBD and N-specific IgG tests to determine pre-vaccination nation-wide baseline seroprevalence in Mexico. *Sci. Rep.* **12**, 18014 (2022).
207. Elecsys® Anti-SARS-CoV-2 Antikörper Test | roche.de. https://www.roche.de/diagnostik/produkte-loesungen/tests-parameter/elecsys-anti-sars-cov-2.
208. Tan, C. W. *et al.* A SARS-CoV-2 surrogate virus neutralization test based on antibody-mediated blockage of ACE2-spike protein-protein interaction. *Nat. Biotechnol.* **38**, 1073–1078 (2020).

209. Schmidt, F. *et al.* Measuring SARS-CoV-2 neutralizing antibody activity using pseudotyped and chimeric viruses. *J. Exp. Med.* **217**, e20201181 (2020).
210. Syed, A. M. *et al.* Rapid assessment of SARS-CoV-2–evolved variants using virus-like particles. *Science* **374**, 1626–1632 (2021).
211. Horbach, I. S. *et al.* Plaque Reduction Neutralization Test (PRNT) Accuracy in Evaluating Humoral Immune Response to SARS-CoV-2. *Dis. Basel Switz.* **12**, 29 (2024).
212. Salazar, E. *et al.* Convalescent plasma anti–SARS-CoV-2 spike protein ectodomain and receptor-binding domain IgG correlate with virus neutralization. *J. Clin. Invest.* **130**, 6728–6738 (2020).
213. Mayr, L. M., Su, B. & Moog, C. Non-Neutralizing Antibodies Directed against HIV and Their Functions. *Front. Immunol.* **8**, 1590 (2017).
214. Santini, A., Man, A. & Voidăzan, S. Accuracy of Diagnostic Tests. *J. Crit. Care Med.* **7**, 241–248 (2021).
215. Monaghan, T. F. *et al.* Foundational Statistical Principles in Medical Research: Sensitivity, Specificity, Positive Predictive Value, and Negative Predictive Value. *Medicina (Mex.)* **57**, 503 (2021).
216. Trevethan, R. Sensitivity, Specificity, and Predictive Values: Foundations, Pliabilities, and Pitfalls in Research and Practice. *Front. Public Health* **5**, (2017).
217. Skittrall, J. P. *et al.* Specificity and positive predictive value of SARS-CoV-2 nucleic acid amplification testing in a low-prevalence setting. *Clin. Microbiol. Infect. Off. Publ. Eur. Soc. Clin. Microbiol. Infect. Dis.* **27**, 469.e9-469.e15 (2021).
218. Braunstein, G. D., Schwartz, L., Hymel, P. & Fielding, J. False Positive Results With SARS-CoV-2 RT-PCR Tests and How to Evaluate a RT-PCR-Positive Test for the Possibility of a False Positive Result. *J. Occup. Environ. Med.* **63**, e159–e162 (2021).
219. Sinha, P., Calfee, C. S. & Delucchi, K. L. Practitioner's Guide to Latent Class Analysis: Methodological Considerations and Common Pitfalls. *Crit. Care Med.* **49**, e63 (2021).
220. Liu, K.-T., Han, Y.-J., Wu, G.-H., Huang, K.-Y. A. & Huang, P.-N. Overview of Neutralization Assays and International Standard for Detecting SARS-CoV-2 Neutralizing Antibody. *Viruses* **14**, 1560 (2022).
221. Zhen, H. *et al.* Performance evaluation of four kits for the detection of neutralizing antibody against SARS-CoV-2 in human serum. *J. Clin. Virol. Plus* **4**, 100192 (2024).
222. Zhu, F. *et al.* WHO international standard for SARS-CoV-2 antibodies to determine markers of protection. *Lancet Microbe* **3**, e81–e82 (2022).
223. Smith, D. J. *et al.* Mapping the Antigenic and Genetic Evolution of Influenza Virus. *Science* **305**, 371–376 (2004).
224. Lapedes, A. & Farber, R. The geometry of shape space: application to influenza. *J. Theor. Biol.* **212**, 57–69 (2001).
225. Smith, D. J., Forrest, S., Hightower, R. R. & Perelson, A. S. Deriving shape space parameters from immunological data. *J. Theor. Biol.* **189**, 141–150 (1997).
226. An introduction to antigenic cartography. https://acorg.github.io/Racmacs/articles/intro-to-antigenic-cartography.html.
227. Liu, D. C. & Nocedal, J. On the limited memory BFGS method for large scale optimization. *Math. Program.* **45**, 503–528 (1989).
228. acorg/ablandscapes. Antigenic Cartography (2024).
229. Fonville, J. M. *et al.* Antibody landscapes after influenza virus infection or vaccination. *Science* **346**, 996–1000 (2014).
230. Harrell Jr, F. E. Regression Modeling Strategies. https://hbiostat.org/rmsc/ (2025).

231. Science, O.-O. D. Comparing Five Different Smooths — Which One Rules Them All? *Medium* https://odsc.medium.com/comparing-five-different-smooths-which-one-rules-them-all-5fa1578fb09a (2018).
232. Einav, T., Creanga, A., Andrews, S. F., McDermott, A. B. & Kanekiyo, M. Harnessing low dimensionality to visualize the antibody–virus landscape for influenza. *Nat. Comput. Sci.* **3**, 164–173 (2023).
233. Mühlemann, B. *et al.* Antigenic cartography using variant-specific hamster sera reveals substantial antigenic variation among Omicron subvariants. *Proc. Natl. Acad. Sci. U. S. A.* **121**, e2310917121.
234. Sarker, I. H. Machine Learning: Algorithms, Real-World Applications and Research Directions. *SN Comput. Sci.* **2**, 160 (2021).
235. Neijzen, D. & Lunter, G. Unsupervised learning for medical data: A review of probabilistic factorization methods. *Stat. Med.* **42**, 5541–5554 (2023).
236. Bouman, R., Bukhsh, Z. & Heskes, T. Unsupervised Anomaly Detection Algorithms on Real-world Data: How Many Do We Need? *J. Mach. Learn. Res.* **25**, 1–34 (2024).
237. Du, K.-L., Swamy, M. N. S., Wang, Z.-Q. & Mow, W. H. Matrix Factorization Techniques in Machine Learning, Signal Processing, and Statistics. *Mathematics* **11**, 2674 (2023).
238. Jiang, T., Gradus, J. L. & Rosellini, A. J. Supervised machine learning: A brief primer. *Behav. Ther.* **51**, 675–687 (2020).
239. Rashidi, H. H., Albahra, S., Robertson, S., Tran, N. K. & Hu, B. Common statistical concepts in the supervised Machine Learning arena. *Front. Oncol.* **13**, 1130229 (2023).
240. Wallisch, C. *et al.* Review of guidance papers on regression modeling in statistical series of medical journals. *PLOS ONE* **17**, e0262918 (2022).
241. Perraillon, M. C. Week 14: Choosing models. https://clas.ucdenver.edu/marcelo-perraillon/sites/default/files/attached-files/week_14_selection_v08_0.pdf (2019).
242. Allison, P. D. Measures of Fit for Logistic Regression. https://support.sas.com/resources/papers/proceedings14/1485-2014.pdf.
243. Liu, X. Comparison of different machine learning models: Linear model, forest and SVM. *Appl. Comput. Eng.* **51**, 225–230 (2024).
244. Linear vs. Non-linear Classification: Analyzing Differences Using the Kernel Trick. *GeeksforGeeks* https://www.geeksforgeeks.org/machine-learning/linear-vs-non-linear-classification-analyzing-differences-using-the-kernel-trick/ (11:26:29+00:00).
245. Sachinsoni. Mastering Random Forests: Unraveling the Magic of Ensemble Learning. *Medium* https://medium.com/@sachinsoni600517/mastering-random-forests-unraveling-the-magic-of-ensemble-learning-e80472723cee (2023).
246. A Comprehensive Review On Ensemble Modeling: Techniques, Benefits and Application. *Debutinfotech* https://www.debutinfotech.com/blog/ensemble-modeling.
247. Xu, Y. & Goodacre, R. On Splitting Training and Validation Set: A Comparative Study of Cross-Validation, Bootstrap and Systematic Sampling for Estimating the Generalization Performance of Supervised Learning. *J. Anal. Test.* **2**, 249–262 (2018).
248. Wilimitis, D. & Walsh, C. G. Practical Considerations and Applied Examples of Cross-Validation for Model Development and Evaluation in Health Care: Tutorial. *JMIR AI* **2**, e49023 (2023).
249. Tibshirani, R. Regression Shrinkage and Selection Via the Lasso. *J. R. Stat. Soc. Ser. B Methodol.* **58**, 267–288 (1996).
250. Hoerl, R. W. Ridge Regression: A Historical Context. *Technometrics* **62**, 420–425 (2020).

251. A Gentle Introduction to Early Stopping to Avoid Overtraining Neural Networks - MachineLearningMastery.com. https://machinelearningmastery.com/early-stopping-to-avoid-overtraining-neural-network-models/.
252. Standish, R. K. Why Occam'S Razor. *Found. Phys. Lett.* **17**, 255–266 (2004).
253. Jones, T. C. *et al.* An analysis of SARS-CoV-2 viral load by patient age. 2020.06.08.20125484 Preprint at https://doi.org/10.1101/2020.06.08.20125484 (2020).
254. Ludvigsson, J. F. Children are unlikely to be the main drivers of the COVID-19 pandemic – A systematic review. *Acta Paediatr.* **109**, 1525–1530 (2020).
255. Gudbjartsson, D. F. *et al.* Early Spread of SARS-Cov-2 in the Icelandic Population. 2020.03.26.20044446 Preprint at https://doi.org/10.1101/2020.03.26.20044446 (2020).
256. Munro, A. P. S. & Faust, S. N. Children are not COVID-19 super spreaders: time to go back to school. (2020) doi:10.1136/archdischild-2020-319474.
257. Davies, P. *et al.* Intensive care admissions of children with paediatric inflammatory multisystem syndrome temporally associated with SARS-CoV-2 (PIMS-TS) in the UK: a multicentre observational study. *Lancet Child Adolesc. Health* **4**, 669–677 (2020).
258. Rothan, H. A. & Byrareddy, S. N. The potential threat of multisystem inflammatory syndrome in children during the COVID-19 pandemic. *Pediatr. Allergy Immunol.* **32**, 17–22 (2021).
259. Brandstetter, S. *et al.* Symptoms and immunoglobulin development in hospital staff exposed to a SARS-CoV-2 outbreak. *Pediatr. Allergy Immunol.* **31**, 841–847 (2020).
260. Peterhoff, D. *et al.* A highly specific and sensitive serological assay detects SARS-CoV-2 antibody levels in COVID-19 patients that correlate with neutralization. *Infection* **1**, 1 (2020).
261. Hippich, M. *et al.* A public health antibody screening indicates a marked increase of SARS-CoV-2 exposure rate in children during the second wave. *Med* **2**, 571–572 (2021).
262. Fill Malfertheiner, S. *et al.* Immune response to SARS-CoV-2 in health care workers following a COVID-19 outbreak: A prospective longitudinal study. *J. Clin. Virol.* **130**, 104575 (2020).
263. Kuri-Cervantes, L. *et al.* Comprehensive mapping of immune perturbations associated with severe COVID-19. *Sci. Immunol.* **5**, eabd7114 (2020).
264. Sweeney-Reed, C. M., Wolff, D., Niggel, J., Kabesch, M. & Apfelbacher, C. Pool Testing as a Strategy for Prevention of SARS-CoV-2 Outbreaks in Schools: Protocol for a Feasibility Study. *JMIR Res. Protoc.* **10**, e28673 (2021).
265. Evaluation of Roche Elecsys anti SARS CoV 2 PHE 110620. https://assets.publishing.service.gov.uk/government/uploads/system/uploads/attachment_data/file/891598/Evaluation_of_Roche_Elecsys_anti_SARS_CoV_2_PHE_200610_v8.1_FINAL.pdf.
266. Šimánek, V. *et al.* Five Commercial Immunoassays for SARS-CoV-2 Antibody Determination and Their Comparison and Correlation with the Virus Neutralization Test. *Diagnostics* **11**, 593 (2021).
267. Kontou, P. I., Braliou, G. G., Dimou, N. L., Nikolopoulos, G. & Bagos, P. G. Antibody Tests in Detecting SARS-CoV-2 Infection: A Meta-Analysis. *Diagnostics* **10**, 319 (2020).
268. Werner, M. *et al.* Evaluation of a Broad Panel of SARS-CoV-2 Serological Tests for Diagnostic Use. *J. Clin. Med.* **10**, 1580 (2021).
269. Ransohoff, D. F. & Feinstein, A. R. Problems of Spectrum and Bias in Evaluating the Efficacy of Diagnostic Tests. *N. Engl. J. Med.* **299**, 926–930 (1978).
270. Brenner, H. & Gefeller, O. Variation of sensitivity, specificity, likelihood ratios and predictive values with disease prevalence. *Stat. Med.* **16**, 981–991 (1997).
271. Goehring, C., Perrier, A. & Morabia, A. Spectrum bias: a quantitative and graphical analysis of the variability of medical diagnostic test performance. *Stat. Med.* **23**, 125–135 (2004).

272. Sui, Y., Bekele, Y. & Berzofsky, J. A. Potential SARS-CoV-2 Immune Correlates of Protection in Infection and Vaccine Immunization. *Pathogens* **10**, 138 (2021).
273. Bossuyt, P. M. *et al.* STARD 2015: an updated list of essential items for reporting diagnostic accuracy studies. (2015) doi:10.1136/bmj.h5527.
274. Kalton, G. & Flores Cervantes, I. Weighting Methods. *Httplst-Iiepiiep-Unescoorgcgi-Binwwwi32exeinepidoc1int2000019622100* **19**, (2003).
275. COVID-19 Datenhub. https://npgeo-corona-npgeo-de.hub.arcgis.com/.
276. Elecsys® Anti-SARS-CoV-2 Antikörper Test | roche.de. https://www.roche.de/diagnostik/produkte-loesungen/tests-parameter/elecsys-anti-sars-cov-2.
277. Elecsys® Anti-SARS-CoV-2 S | roche.de. https://www.roche.de/diagnostik/produkte-loesungen/tests-parameter/elecsys-anti-sars-cov-2-s.
278. Riepler, L. *et al.* Comparison of Four SARS-CoV-2 Neutralization Assays. *Vaccines* **9**, 13 (2021).
279. Elecsys Anti-SARS-CoV-2-S. https://www.roche.de/diagnostik-produkte/produktkatalog/tests-parameter/elecsys-anti-sars-cov-2-s.
280. Elecsys Anti-SARS-CoV-2. https://www.roche.de/diagnostik-produkte/produktkatalog/tests-parameter/elecsys-anti-sars-cov-2.
281. Thompson, W. D. & Walter, S. D. A reappraisal of the kappa coefficient. *J. Clin. Epidemiol.* **41**, 949–958 (1988).
282. Vollset, S. E. Confidence intervals for a binomial proportion. *Stat. Med.* **12**, 809–824 (1993).
283. Lazarsfeld, P. F. Studies in Social Psychology in World War II. Vol. IV: Measurement and Prediction. *J. Inf. Secur. Appl.* (1950).
284. van Smeden, M., Naaktgeboren, C. A., Reitsma, J. B., Moons, K. G. M. & de Groot, J. A. H. Latent class models in diagnostic studies when there is no reference standard--a systematic review. *Am. J. Epidemiol.* **179**, 423–431 (2014).
285. Lanza, S. T., Collins, L. M., Lemmon, D. R. & Schafer, J. L. PROC LCA: A SAS Procedure for Latent Class Analysis. *Struct. Equ. Model. Multidiscip. J.* **14**, 671–694 (2007).
286. Legros, V. *et al.* A longitudinal study of SARS-CoV-2-infected patients reveals a high correlation between neutralizing antibodies and COVID-19 severity. *Cell. Mol. Immunol.* **18**, 318–327 (2021).
287. Gaebler, C. *et al.* Evolution of antibody immunity to SARS-CoV-2. *Nature* **591**, 639–644 (2021).
288. Kubina, R. & Dziedzic, A. Molecular and Serological Tests for COVID-19 a Comparative Review of SARS-CoV-2 Coronavirus Laboratory and Point-of-Care Diagnostics. *Diagn. Basel Switz.* **10**, 434 (2020).
289. Dimeglio, C. *et al.* The real seroprevalence of SARS-CoV-2 in France and its consequences for virus dynamics. *Sci. Rep.* **11**, 12597 (2021).
290. Liu, S. T. H. *et al.* Convalescent plasma treatment of severe COVID-19: a propensity score-matched control study. *Nat. Med.* **26**, 1708–1713 (2020).
291. Cantoni, D. *et al.* Neutralisation Hierarchy of SARS-CoV-2 Variants of Concern Using Standardised, Quantitative Neutralisation Assays Reveals a Correlation With Disease Severity; Towards Deciphering Protective Antibody Thresholds. *Front. Immunol.* **13**, 716 (2022).
292. Castillo-Olivares, J. *et al.* Towards Internationally standardised humoral Immune Correlates of Protection from SARS-CoV-2 infection and COVID-19 disease. 2021.05.21.21257572 Preprint at https://doi.org/10.1101/2021.05.21.21257572 (2021).
293. Dörschug, A. *et al.* Comparison of Five Serological Assays for the Detection of SARS-CoV-2 Antibodies. *Diagn. Basel Switz.* **11**, 78 (2021).
294. Roche Diagnostics Elecsys Anti-SARS-CoV-2 - IFU | FDA. https://www.fda.gov/media/137605.

295. Resman Rus, K., Korva, M., Knap, N., Avšič Županc, T. & Poljak, M. Performance of the rapid high-throughput automated electrochemiluminescence immunoassay targeting total antibodies to the SARS-CoV-2 spike protein receptor binding domain in comparison to the neutralization assay. *J. Clin. Virol. Off. Publ. Pan Am. Soc. Clin. Virol.* **139**, 104820 (2021).
296. Muench, P. *et al.* Development and Validation of the Elecsys Anti-SARS-CoV-2 Immunoassay as a Highly Specific Tool for Determining Past Exposure to SARS-CoV-2. *J. Clin. Microbiol.* **58**, e01694-20 (2020).
297. Jung, K. *et al.* Performance evaluation of three automated quantitative immunoassays and their correlation with a surrogate virus neutralization test in coronavirus disease 19 patients and pre-pandemic controls. *J. Clin. Lab. Anal.* **35**, e23921 (2021).
298. Favresse, J. *et al.* Persistence of Anti-SARS-CoV-2 Antibodies Depends on the Analytical Kit: A Report for Up to 10 Months after Infection. *Microorganisms* **9**, 556 (2021).
299. Gilbert, P. B. *et al.* Immune Correlates Analysis of the mRNA-1273 COVID-19 Vaccine Efficacy Trial. 2021.08.09.21261290 Preprint at https://doi.org/10.1101/2021.08.09.21261290 (2021).
300. Giles, B., Meredith, P., Robson, S., Smith, G. & Chauhan, A. The SARS-CoV-2 B.1.1.7 variant and increased clinical severity—the jury is out. *Lancet Infect. Dis.* **21**, 1213–1214 (2021).
301. Weekly epidemiological update on COVID-19 - 11 May 2021. https://www.who.int/publications/m/item/weekly-epidemiological-update-on-covid-19---11-may-2021.
302. GISAID - hCov19 Variants. https://www.gisaid.org/hcov19-variants/.
303. Update on Omicron. https://www.who.int/news/item/28-11-2021-update-on-omicron.
304. Levin, A. T. *et al.* Assessing the age specificity of infection fatality rates for COVID-19: systematic review, meta-analysis, and public policy implications. *Eur. J. Epidemiol.* **35**, 1123–1138 (2020).
305. Tunheim, G. *et al.* Trends in seroprevalence of SARS-CoV-2 and infection fatality rate in the Norwegian population through the first year of the COVID-19 pandemic. *Influenza Other Respir. Viruses* **16**, 204–212 (2022).
306. Canto e Castro, L. *et al.* Longitudinal SARS-CoV-2 seroprevalence in Portugal and antibody maintenance 12 months after infection. *Eur. J. Immunol.* **52**, 149–160 (2022).
307. Gornyk, D. *et al.* SARS-CoV-2 seroprevalence in Germany. *Dtsch. Ärztebl. Int.* (2021) doi:10.3238/arztebl.m2021.0364.
308. Aziz, N. A. *et al.* Seroprevalence and correlates of SARS-CoV-2 neutralizing antibodies from a population-based study in Bonn, Germany. *Nat. Commun.* **12**, 1–10 (2021).
309. Radon, K. *et al.* Protocol of a population-based prospective COVID-19 cohort study Munich, Germany (KoCo19). *BMC Public Health* **20**, 1036 (2020).
310. RKI - CORONA-MONITORING lokal - Corona-Monitoring lokal. https://www.rki.de/DE/Content/Gesundheitsmonitoring/Studien/cml-studie/Factsheet_Berlin-Mitte.html.
311. Streeck, H. *et al.* Infection fatality rate of SARS-CoV2 in a super-spreading event in Germany. *Nat. Commun.* **11**, 1–12 (2020).
312. Wachtler, B. *et al.* The risk of infection with SARS-CoV-2 among healthcare workers during the pandemic. *Dtsch. Ärztebl. Int.* (2021) doi:10.3238/arztebl.m2021.0376.
313. Fischer, B., Knabbe, C. & Vollmer, T. SARS-CoV-2 IgG seroprevalence in blood donors located in three different federal states, Germany, March to June 2020. *Eurosurveillance* **25**, 2001285 (2020).

314. Theuring, S. *et al.* SARS-CoV-2 infection and transmission in school settings during the second COVID-19 wave: a cross-sectional study, Berlin, Germany, November 2020. *Eurosurveillance* **26**, 2100184 (2021).
315. Lohse, S. *et al.* German federal-state-wide seroprevalence study of 1st SARS-CoV-2 pandemic wave shows importance of long-term antibody test performance. *Commun. Med. 2022 21* **2**, 1–12 (2022).
316. Peterhoff, D. *et al.* Comparative Immunogenicity of COVID-19 Vaccines in a Population-Based Cohort Study with SARS-CoV-2-Infected and Uninfected Participants. *Vaccines* **10**, 324 (2022).
317. Brandl, M. *et al.* Mass gathering events and undetected transmission of SARS-CoV-2 in vulnerable populations leading to an outbreak with high case fatality ratio in the district of Tirschenreuth, Germany. *Epidemiol. Infect.* **148**, (2020).
318. Tirschenreuth, L. RKI-Ergebnis Tirschenreuth. (2020).
319. Kellam, P. & Barclay, W. The dynamics of humoral immune responses following SARS-CoV-2 infection and the potential for reinfection. *J. Gen. Virol.* **101**, 791–797 (2020).
320. Koch-Institut, R. *Epidemiologisches Bulletin Des Robert Koch-Instituts - Online Vorab Ausgabe 17/2020*.
321. Khalili, M. *et al.* Epidemiological Characteristics of COVID-19: A Systematic Review and Meta-Analysis. *Epidemiol. Infect.* **148**, (2020).
322. Einhauser, S. *et al.* Spectrum bias and individual strengths of SARS-CoV-2 serological tests–A population-based evaluation. *Diagnostics* **11**, 1843 (2021).
323. Sempos, C. T. & Tian, L. Adjusting Coronavirus Prevalence Estimates for Laboratory Test Kit Error. *Am. J. Epidemiol.* **190**, 109–115 (2021).
324. Healy, B., Khan, A., Metezai, H., Blyth, I. & Asad, H. The impact of false positive COVID-19 results in an area of low prevalence. *Clin. Med. J. R. Coll. Physicians Lond.* **21**, E54–E56 (2021).
325. He, Z. *et al.* Seroprevalence and humoral immune durability of anti-SARS-CoV-2 antibodies in Wuhan, China: a longitudinal, population-level, cross-sectional study. *Lancet Lond. Engl.* **397**, 1075–1084 (2021).
326. Pritsch, M. *et al.* Prevalence and Risk Factors of Infection in the Representative COVID-19 Cohort Munich. *Int. J. Environ. Res. Public. Health* **18**, 3572 (2021).
327. Neuhauser, H. *et al.* Germany's low SARS-CoV-2 seroprevalence confirms effective containment in 2020: Results of the nationwide RKI-SOEP study. *medRxiv* 2021.11.22.21266711 (2021) doi:10.1101/2021.11.22.21266711.
328. Radon, K. *et al.* From first to second wave: follow-up of the prospective COVID-19 cohort (KoCo19) in Munich (Germany). *BMC Infect. Dis.* **21**, (2021).
329. GEMEINSAM GEGEN COVID: Prospektive COVID-19 Kohorte München (KoCo19). http://www.klinikum.uni-muenchen.de/Abteilung-fuer-Infektions-und-Tropenmedizin/de/COVID-19/KoCo19/index.html.
330. Experience. https://experience.arcgis.com/experience/478220a4c454480e823b17327b2bf1d4.
331. Fenwick, C. *et al.* Changes in SARS-CoV-2 Spike versus Nucleoprotein Antibody Responses Impact the Estimates of Infections in Population-Based Seroprevalence Studies. *J. Virol.* **95**, (2021).
332. Davies, N. G. *et al.* Increased mortality in community-tested cases of SARS-CoV-2 lineage B.1.1.7. *Nature* (2021).
333. Variation in the COVID-19 infection–fatality ratio by age, time, and geography during the pre-vaccine era: a systematic analysis. *The Lancet* (2022) doi:10.1016/S0140-6736(21)02867-1.
334. COVID-19 vaccination dashboard. https://impfdashboard.de/en/.

335. Peters, A., Rospleszcz, S., Greiser, K. H., Dallavalle, M. & Berger, K. The Impact of the COVID-19 Pandemic on Self-Reported Health. *Dtsch. Arzteblatt Int.* **117**, 861–867 (2020).
336. Mullard, A. Pfizer's COVID-19 vaccine secures first full FDA approval. *Nat. Rev. Drug Discov.* **20**, 728 (2021).
337. Aldridge, R. W. *et al.* Waning of SARS-CoV-2 antibodies targeting the Spike protein in individuals post second dose of ChAdOx1 and BNT162b2 COVID-19 vaccines and risk of breakthrough infections: analysis of the Virus Watch community cohort. *medRxiv* 2021.11.05.21265968 (2021) doi:10.1101/2021.11.05.21265968.
338. Richards, N. E. *et al.* Comparison of SARS-CoV-2 Antibody Response by Age among Recipients of the BNT162b2 vs the mRNA-1273 Vaccine. *JAMA Netw. Open* **4**, e2124331–e2124331 (2021).
339. Hillus, D. *et al.* Safety, reactogenicity, and immunogenicity of homologous and heterologous prime-boost immunisation with ChAdOx1 nCoV-19 and BNT162b2: a prospective cohort study. *Lancet Respir. Med.* **9**, 1255–1265 (2021).
340. Schmidt, T. *et al.* Immunogenicity and reactogenicity of heterologous ChAdOx1 nCoV-19/mRNA vaccination. *Nat. Med.* **27**, 1530–1535 (2021).
341. Liu, X. *et al.* Safety and immunogenicity of heterologous versus homologous prime-boost schedules with an adenoviral vectored and mRNA COVID-19 vaccine (Com-COV): a single-blind, randomised, non-inferiority trial. *The Lancet* **398**, 856–869 (2021).
342. Tenbusch, M. *et al.* Heterologous prime–boost vaccination with ChAdOx1 nCoV-19 and BNT162b2. *Lancet Infect. Dis.* **21**, 1212–1213 (2021).
343. Einhauser, S. *et al.* Time Trend in SARS-CoV-2 Seropositivity, Surveillance Detection- and Infection Fatality Ratio until Spring 2021 in the Tirschenreuth County—Results from a Population-Based Longitudinal Study in Germany. *Viruses 2022 Vol 14 Page 1168* **14**, 1168 (2022).
344. Lapuente, D. *et al.* Protective mucosal immunity against SARS-CoV-2 after heterologous systemic prime-mucosal boost immunization. *Nat. Commun.* **12**, (2021).
345. Dispinseri, S. *et al.* Neutralizing antibody responses to SARS-CoV-2 in symptomatic COVID-19 is persistent and critical for survival. *Nat. Commun.* **12**, (2021).
346. Herrmann, A. *et al.* Cloning of a passage-free SARS-CoV-2 genome and mutagenesis using red recombination. *Int. J. Mol. Sci.* **22**, (2021).
347. Wood, S. N. *Generalized Additive Models: An Introduction with R (2nd Edition).* (Chapman and Hall/CRC., 2017).
348. R Core Team. R: A language and environment for statistical computing. R Foundation for Statistical Computing (2021).
349. Glück, V. *et al.* Immunity after COVID-19 and vaccination: follow-up study over 1 year among medical personnel. *Infection* **1**, 3 (2021).
350. Wilhelm, A. *et al.* Reduced Neutralization of SARS-CoV-2 Omicron Variant by Vaccine Sera and Monoclonal Antibodies. *medRxiv* 2021.12.07.21267432 (2021) doi:10.1101/2021.12.07.21267432.
351. Wratil, P. R. *et al.* Three exposures to the spike protein of SARS-CoV-2 by either infection or vaccination elicit superior neutralizing immunity to all variants of concern. *Nat. Med.* 1–1 (2022) doi:10.1038/s41591-022-01715-4.
352. Uk Health Security Agency. *COVID-19 Vaccine Surveillance Report - Week 4*. (2022).
353. Bozio, C. H. *et al.* Laboratory-Confirmed COVID-19 Among Adults Hospitalized with COVID-19–Like Illness with Infection-Induced or mRNA Vaccine-Induced SARS-CoV-2 Immunity — Nine States, January–September 2021. *MMWR Morb. Mortal. Wkly. Rep.* **70**, 1539–1544 (2021).

354. Young-Xu, Y., Smith, J. & Korves, C. SARS-Cov-2 Infection versus Vaccine-Induced Immunity among Veterans. *medRxiv* 2021.09.27.21264194 (2021) doi:10.1101/2021.09.27.21264194.
355. Gazit, S. *et al.* Title page Comparing SARS-CoV-2 natural immunity to vaccine-induced immunity: reinfections versus breakthrough infections. *medRxiv* 2021.08.24.21262415 (2021) doi:10.1101/2021.08.24.21262415.
356. Grant, R. *et al.* Impact of SARS-CoV-2 Delta variant on incubation, transmission settings and vaccine effectiveness: Results from a nationwide case-control study in France. *Lancet Reg. Health - Eur.* 100278 (2021) doi:10.1016/j.lanepe.2021.100278.
357. Wang, Z. *et al.* Naturally enhanced neutralizing breadth against SARS-CoV-2 one year after infection. *Nature* **595**, 426–431 (2021).
358. Goel, R. R. *et al.* Distinct antibody and memory B cell responses in SARSCoV-2 naïve and recovered individuals following mRNA vaccination. *Sci. Immunol.* **6**, 1–19 (2021).
359. Krammer, F. *et al.* Antibody Responses in Seropositive Persons after a Single Dose of SARS-CoV-2 mRNA Vaccine. *N. Engl. J. Med.* **384**, 1372–1374 (2021).
360. Muecksch, F. *et al.* Affinity maturation of SARS-CoV-2 neutralizing antibodies confers potency, breadth, and resilience to viral escape mutations. *Immunity* **54**, 1853-1868.e7 (2021).
361. Bar-On, Y. M. *et al.* Protection of BNT162b2 Vaccine Booster against Covid-19 in Israel. *N. Engl. J. Med.* **385**, 1393–1400 (2021).
362. Hacisuleyman, E. *et al.* Vaccine Breakthrough Infections with SARS-CoV-2 Variants. *N. Engl. J. Med.* **384**, 2212–2218 (2021).
363. Vivaldi, G. *et al.* Risk factors for SARS-CoV-2 infection after primary vaccination with ChAdOx1 nCoV-19 or BNT162b2 and after booster vaccination with BNT162b2 or mRNA-1273: A population-based cohort study (COVIDENCE UK). *Lancet Reg. Health - Eur.* **22**, (2022).
364. Lee, C. M. *et al.* Breakthrough COVID-19 Infection During the Delta Variant Dominant Period: Individualized Care Based on Vaccination Status Is Needed. *J. Korean Med. Sci.* **37**, (2022).
365. Feikin, D. R. *et al.* Duration of effectiveness of vaccines against SARS-CoV-2 infection and COVID-19 disease: results of a systematic review and meta-regression. *Lancet Lond. Engl.* **399**, 924–944 (2022).
366. Goldberg, Y. *et al.* Waning Immunity after the BNT162b2 Vaccine in Israel. *N. Engl. J. Med.* **385**, e85 (2021).
367. Menegale, F. *et al.* Evaluation of Waning of SARS-CoV-2 Vaccine–Induced Immunity: A Systematic Review and Meta-analysis. *JAMA Netw. Open* **6**, e2310650–e2310650 (2023).
368. Yamamoto, S. *et al.* Durability and determinants of anti-SARS-CoV-2 spike antibodies following the second and third doses of mRNA COVID-19 vaccine. *Clin. Microbiol. Infect. Off. Publ. Eur. Soc. Clin. Microbiol. Infect. Dis.* **29**, 1201.e1-1201.e5 (2023).
369. Stein, C. *et al.* Past SARS-CoV-2 infection protection against re-infection: a systematic review and meta-analysis. *The Lancet* **401**, 833–842 (2023).
370. Zhou, Z., Barrett, J. & He, X. Immune Imprinting and Implications for COVID-19. *Vaccines* **11**, 875 (2023).
371. Hoehl, S. & Ciesek, S. Recalling ancestral SARS-CoV-2 variants: is it an original sin with benefits? *Lancet Infect. Dis.* **23**, 272–273 (2023).
372. Aguilar-Bretones, M., Fouchier, R. A. M., Koopmans, M. P. G. & van Nierop, G. P. Impact of antigenic evolution and original antigenic sin on SARS-CoV-2 immunity. *J. Clin. Invest.* **133**, (2023).
373. Pillai, S. SARS-CoV-2 vaccination washes away original antigenic sin. *Trends Immunol.* **43**, 271–273 (2022).
374. Krause, P. R. *et al.* SARS-CoV-2 Variants and Vaccines. *N. Engl. J. Med.* **385**, 179–186 (2021).

375. Asamoah-Boaheng, M. *et al.* The Relationship Between Anti-Spike SARS-CoV-2 Antibody Levels and Risk of Breakthrough COVID-19 Among Fully Vaccinated Adults. *J. Infect. Dis.* **227**, 339–343 (2023).
376. Nixon, D. F., Schwartz, R. E. & Ndhlovu, L. C. Booster vaccines for COVID-19 vaccine breakthrough cases? *Lancet Lond. Engl.* **399**, 1224 (2022).
377. Prelog, M. *et al.* Clinical and immunological benefits of full primary COVID-19 vaccination in individuals with SARS-CoV-2 breakthrough infections: A prospective cohort study in non-hospitalized adults. *J. Clin. Virol.* **170**, 105622 (2024).
378. Sampson, A. T. *et al.* Coronavirus Pseudotypes for All Circulating Human Coronaviruses for Quantification of Cross-Neutralizing Antibody Responses. *Viruses* **13**, (2021).
379. Montefiori, D. C. *et al.* Magnitude and breadth of the neutralizing antibody response in the RV144 and Vax003 HIV-1 vaccine efficacy trials. *J. Infect. Dis.* **206**, 431–441 (2012).
380. Huang, Y., Gilbert, P. B., Montefiori, D. C. & Self, S. G. Simultaneous Evaluation of the Magnitude and Breadth of a Left and Right Censored Multivariate Response, with Application to HIV Vaccine Development. *Stat. Biopharm. Res.* **1**, 81 (2009).
381. Gilbert, P. *et al.* Magnitude and breadth of a nonprotective neutralizing antibody response in an efficacy trial of a candidate HIV-1 gp120 vaccine. *J. Infect. Dis.* **202**, 595–605 (2010).
382. Wilks, S. H. *et al.* Mapping SARS-CoV-2 antigenic relationships and serological responses. *Science* **382**, (2023).
383. Rössler, A. *et al.* BA.2 and BA.5 omicron differ immunologically from both BA.1 omicron and pre-omicron variants. *Nat. Commun. 2022 131* **13**, 1–9 (2022).
384. Wang, W. *et al.* Antigenic cartography of well-characterized human sera shows SARS-CoV-2 neutralization differences based on infection and vaccination history. *Cell Host Microbe* **30**, 1745-1758.e7 (2022).
385. Wilks, S. Racmacs: Antigenic Cartography Macros. (2023).
386. Wilks, S. ablandscapes: An R package for making antibody landscapes. (2023).
387. Walls, A. C. *et al.* SARS-CoV-2 breakthrough infections elicit potent, broad, and durable neutralizing antibody responses. *Cell* **185**, 872 (2022).
388. Lechmere, T. *et al.* Broad Neutralization of SARS-CoV-2 Variants, Including Omicron, following Breakthrough Infection with Delta in COVID-19-Vaccinated Individuals. *mBio* **13**, (2022).
389. Liu, H. *et al.* Simultaneous measurement of multiple variant-specific SARS-CoV-2 neutralizing antibodies with a multiplexed flow cytometric assay. *Front. Immunol.* **13**, 1039163 (2022).
390. Bates, T. A. *et al.* An extended interval between vaccination and infection enhances hybrid immunity against SARS-CoV-2 variants. *JCI Insight* **8**, (2023).
391. Kaplonek, P. *et al.* Hybrid immunity expands the functional humoral footprint of both mRNA and vector-based SARS-CoV-2 vaccines. *Cell Rep. Med.* **4**, (2023).
392. Gerhards, C. *et al.* Heterologous Vector-mRNA Based SARS-CoV-2 Vaccination Strategy Appears Superior to a Homologous Vector-Based Vaccination Scheme in German Healthcare Workers Regarding Humoral SARS-CoV-2 Response Indicating a High Boosting Effect by mRNA Vaccines. *Vaccines* **11**, 701 (2023).
393. Barda, N. *et al.* Effectiveness of a third dose of the BNT162b2 mRNA COVID-19 vaccine for preventing severe outcomes in Israel: an observational study. *The Lancet* **398**, 2093–2100 (2021).
394. Moreira, E. D. *et al.* Safety and Efficacy of a Third Dose of BNT162b2 Covid-19 Vaccine. *N. Engl. J. Med.* **386**, 1910–1921 (2022).
395. Levine-Tiefenbrun, M. *et al.* Viral loads of Delta-variant SARS-CoV-2 breakthrough infections after vaccination and booster with BNT162b2. *Nat. Med. 2021 2712* **27**, 2108–2110 (2021).

396. Pradenas, E. *et al.* Impact of hybrid immunity booster vaccination and Omicron breakthrough infection on SARS-CoV-2 VOCs cross-neutralization. *iScience* **26**, 106457 (2023).
397. Smith, D. J. *et al.* Mapping the antigenic and genetic evolution of influenza virus. *Science* **305**, 371–376 (2004).
398. Wang, Q. *et al.* Alarming antibody evasion properties of rising SARS-CoV-2 BQ and XBB subvariants. *Cell* **186**, 279-286.e8 (2023).
399. Wilks, S. H. *et al.* Mapping SARS-CoV-2 antigenic relationships and serological responses. *bioRxiv* (2023) doi:10.1101/2022.01.28.477987.
400. Mykytyn, A. Z. *et al.* Antigenic cartography of SARS-CoV-2 reveals that Omicron BA.1 and BA.2 are antigenically distinct. *Sci. Immunol.* **7**, (2022).
401. Carreño, J. M., Singh, G., Simon, V. & Krammer, F. Bivalent COVID-19 booster vaccines and the absence of BA.5-specific antibodies. *Lancet Microbe* **4**, e569 (2023).
402. Weber, T. *et al.* Enhanced SARS-CoV-2 humoral immunity following breakthrough infection builds upon the preexisting memory B cell pool. *Sci. Immunol.* **8**, (2023).
403. Yisimayi, A. *et al.* Repeated Omicron exposures override ancestral SARS-CoV-2 immune imprinting. *Nat. 2023 6257993* **625**, 148–156 (2023).
404. Kaku, Y. *et al.* Virological characteristics of the SARS-CoV-2 JN.1 variant. *Lancet Infect. Dis.* **24**, e82 (2024).
405. Malik, M. M. A Hierarchy of Limitations in Machine Learning. Preprint at https://doi.org/10.48550/arXiv.2002.05193 (2020).
406. Riester, E. *et al.* Performance evaluation of the Roche Elecsys Anti-SARS-CoV-2 S immunoassay. *J. Virol. Methods* **297**, 114271 (2021).
407. Cruz-Cardenas, J. A. *et al.* A pseudovirus-based platform to measure neutralizing antibodies in Mexico using SARS-CoV-2 as proof-of-concept. *Sci. Rep.* **12**, 17966 (2022).
408. Manu, A. A. *et al.* Development and utility of a SARS-CoV-2 pseudovirus assay for compound screening and antibody neutralization assays. *Heliyon* **10**, (2024).
409. Huang, Y. *et al.* Calibration of two validated SARS-CoV-2 pseudovirus neutralization assays for COVID-19 vaccine evaluation. *Sci. Rep.* **11**, 23921 (2021).
410. Aguilar, R. *et al.* RBD-Based ELISA and Luminex Predict Anti-SARS-CoV-2 Surrogate-Neutralizing Activity in Two Longitudinal Cohorts of German and Spanish Health Care Workers. *Microbiol. Spectr.* **11**, e03165-22.
411. Tan, C. W. *et al.* A SARS-CoV-2 surrogate virus neutralization test based on antibody-mediated blockage of ACE2–spike protein–protein interaction. *Nat. Biotechnol.* **38**, 1073–1078 (2020).
412. Dapporto, F. *et al.* Antibody Avidity and Neutralizing Response against SARS-CoV-2 Omicron Variant after Infection or Vaccination. *J. Immunol. Res.* **2022**, 4813199 (2022).
413. Astakhova, E. A. *et al.* Antibody Avidity Maturation Following Booster Vaccination with an Intranasal Adenovirus Salnavac Vaccine. *Vaccines* **12**, 1362 (2024).
414. Tortorici, M. A. *et al.* Persistent immune imprinting occurs after vaccination with the COVID-19 XBB.1.5 mRNA booster in humans. *Immunity* **57**, 904-911.e4 (2024).
415. Dépéry, L. *et al.* Anti-SARS-CoV-2 serology based on ancestral RBD antigens does not correlate with the presence of neutralizing antibodies against Omicron variants. *Microbiol. Spectr.* **13**, e01568-24.
416. Pidal, P. *et al.* Reduced neutralization against Delta, Gamma, Mu, and Omicron BA.1 variants of SARS-CoV-2 from previous non-Omicron infection. *Med. Microbiol. Immunol. (Berl.)* **212**, 25–34 (2023).

417. Dejnirattisai, W. *et al.* Reduced neutralisation of SARS-CoV-2 omicron B.1.1.529 variant by post-immunisation serum. *The Lancet* **399**, 234–236 (2022).
418. D'Apice, L. *et al.* Comparative analysis of the neutralizing activity against SARS-CoV-2 Wuhan-Hu-1 strain and variants of concern: Performance evaluation of a pseudovirus-based neutralization assay. *Front. Immunol.* **13**, 981693 (2022).
419. Cantoni, D., Mayora-Neto, M. & Temperton, N. The role of pseudotype neutralization assays in understanding SARS CoV-2. *Oxf. Open Immunol.* **2**, iqab005 (2021).
420. Le Gleut, R. *et al.* The representative COVID-19 cohort Munich (KoCo19): from the beginning of the pandemic to the Delta virus variant. *BMC Infect. Dis.* **23**, 466 (2023).
421. Knabl, L. *et al.* High SARS-CoV-2 seroprevalence in children and adults in the Austrian ski resort of Ischgl. *Commun. Med.* **1**, 4 (2021).
422. Neuhauser, H. *et al.* Nationally representative results on SARS-CoV-2 seroprevalence and testing in Germany at the end of 2020. *Sci. Rep.* **12**, 19492 (2022).
423. Warszawski, J. *et al.* Prevalence of SARS-Cov-2 antibodies and living conditions: the French national random population-based EPICOV cohort. *BMC Infect. Dis.* **22**, 41 (2022).
424. Stringhini, S. *et al.* Seroprevalence of anti-SARS-CoV-2 IgG antibodies in Geneva, Switzerland (SEROCoV-POP): a population-based study. *Lancet Lond. Engl.* **396**, 313–319 (2020).
425. WHO Director-General's opening remarks at the media briefing on COVID-19 - 3 March 2020. https://www.who.int/director-general/speeches/detail/who-director-general-s-opening-remarks-at-the-media-briefing-on-covid-19---3-march-2020.
426. Ioannidis, J. P. A. Infection fatality rate of COVID-19 inferred from seroprevalence data. *Bull. World Health Organ.* **99**, 19-33F (2021).
427. Riedmann, U. *et al.* COVID-19 case fatality rate and infection fatality rate from 2020 to 2023: Nationwide analysis in Austria. *J. Infect. Public Health* **18**, 102698 (2025).
428. Saucier, A. *et al.* Generalizability of anti–SARS-CoV-2 seroprevalence estimates to the Montréal pediatric population: a comparison between 2 weighting methods. *Am. J. Epidemiol.* **194**, 1112–1121 (2024).
429. Harvey, W. T. *et al.* SARS-CoV-2 variants, spike mutations and immune escape. *Nat. Rev. Microbiol.* **19**, 409–424 (2021).
430. Former vaccination recommendations of the <abbr title="Standing Committee on Vaccination">STIKO</abbr>. https://www.rki.de/EN/Topics/Infectious-diseases/Immunisation/STIKO/STIKO-recommendations/archive_tab.html.
431. SARS-CoV-2 coronavirus: Current rules on isolation and quarantine.
432. Brierley, L. Lessons from the influx of preprints during the early COVID-19 pandemic. *Lancet Planet. Health* **5**, e115–e117 (2021).
433. Watson, C. Rise of the preprint: how rapid data sharing during COVID-19 has changed science forever. *Nat. Med.* **28**, 2–5 (2022).
434. Schons, M. *et al.* The German National Pandemic Cohort Network (NAPKON): rationale, study design and baseline characteristics. *Eur. J. Epidemiol.* **37**, 849–870 (2022).
435. Kunzler, A. M. *et al.* Informing pandemic management in Germany with trustworthy living evidence syntheses and guideline development: lessons learned from the COVID-19 evidence ecosystem. *J. Clin. Epidemiol.* **173**, 111456 (2024).
436. ORCHESTRA - EU Horizon 2020 cohort to tackle COVID-19 internationally. *ORCHESTRA Cohort* https://orchestra-cohort.eu/.
437. Census COVID-19 Data Hub Redirect. https://covid19.census.gov/.

438. COVID-19 Open Data — Google Health. https://health.google.com/covid-19/open-data/raw-data.
439. COVID-19 Data Hub. https://covid19datahub.io/.
440. Stivas, D. & and Cole, A. The importance of trust and transparency in managing the COVID-19 pandemic. Evidence from sixteen EU member states. *J. Contemp. Eur. Stud.* **0**, 1–18 (2023).
441. COVID-19_Lessons_Learned_Summary. https://www.leibniz-gemeinschaft.de/fileadmin/user_upload/Bilder_und_Downloads/%C3%9Cber_uns/Strategie-_und_Wissenschaftspolitik/COVID-19_Lessons_Learned_Summary.pdf.
442. Dan, J. M. *et al.* Immunological memory to SARS-CoV-2 assessed for up to 8 months after infection. *Science* **371**, eabf4063 (2021).
443. Stamatatos, L. *et al.* mRNA vaccination boosts cross-variant neutralizing antibodies elicited by SARS-CoV-2 infection. *Science* **372**, 1413–1418 (2021).
444. Lasrado, N. & Barouch, D. H. SARS-CoV-2 Hybrid Immunity: The Best of Both Worlds. *J. Infect. Dis.* **228**, 1311–1313 (2023).
445. Berlin, D. A., Gulick, R. M. & Martinez, F. J. Severe Covid-19. *N. Engl. J. Med.* **383**, 2451–2460 (2020).
446. Desai, A. D., Lavelle, M., Boursiquot, B. C. & Wan, E. Y. Long-term complications of COVID-19. *Am. J. Physiol. - Cell Physiol.* **322**, C1–C11 (2022).
447. Barros-Martins, J. *et al.* Immune responses against SARS-CoV-2 variants after heterologous and homologous ChAdOx1 nCoV-19/BNT162b2 vaccination. *Nat. Med.* **27**, 1525–1529 (2021).
448. Milne, G. *et al.* Does infection with or vaccination against SARS-CoV-2 lead to lasting immunity? *Lancet Respir. Med.* **9**, 1450–1466 (2021).
449. Zhou, G. *et al.* Effectiveness of COVID-19 vaccines against SARS-CoV-2 infection and severe outcomes in adults: a systematic review and meta-analysis of European studies published up to 22 January 2024. *Eur. Respir. Rev. Off. J. Eur. Respir. Soc.* **34**, 240222 (2025).
450. Wahl, I. & Wardemann, H. Sterilizing immunity: Understanding COVID-19. *Immunity* **55**, 2231–2235 (2022).
451. Wei, J. *et al.* Protection against SARS-CoV-2 Omicron BA.4/5 variant following booster vaccination or breakthrough infection in the UK. *Nat. Commun.* **14**, 2799 (2023).
452. Russell, M. W. & Mestecky, J. Mucosal immunity: The missing link in comprehending SARS-CoV-2 infection and transmission. *Front. Immunol.* **13**, 957107 (2022).
453. Mitsi, E. *et al.* Respiratory mucosal immune memory to SARS-CoV-2 after infection and vaccination. *Nat. Commun.* **14**, 6815 (2023).
454. Puhach, O. *et al.* SARS-CoV-2 convalescence and hybrid immunity elicits mucosal immune responses. *eBioMedicine* **98**, (2023).
455. Mao, T. *et al.* Unadjuvanted intranasal spike vaccine elicits protective mucosal immunity against sarbecoviruses. *Science* **378**, eabo2523 (2022).
456. Agbayani, G. *et al.* Intranasal administration of unadjuvanted SARS-CoV-2 spike antigen boosts antigen-specific immune responses induced by parenteral protein subunit vaccine prime in mice and hamsters. *Eur. J. Immunol.* **54**, e2350620 (2024).
457. Dhama, K. *et al.* COVID-19 intranasal vaccines: current progress, advantages, prospects, and challenges. *Hum. Vaccines Immunother.* **18**, 2045853.
458. Planas, D. *et al.* Considerable escape of SARS-CoV-2 Omicron to antibody neutralization. *Nature* **602**, 671–675 (2022).
459. de Gier, B. *et al.* Effects of COVID-19 vaccination and previous infection on Omicron SARS-CoV-2 infection and relation with serology. *Nat. Commun.* **14**, 4793 (2023).

460. Cele, S. *et al.* Escape of SARS-CoV-2 501Y.V2 from neutralization by convalescent plasma. *Nature* **593**, 142–146 (2021).
461. Burki, T. COVID vaccine booster doses for omicron variants. *Lancet Respir. Med.* **10**, 936 (2022).
462. Koutsakos, M. & Ellebedy, A. H. Immunological imprinting: Understanding COVID-19. *Immunity* **56**, 909–913 (2023).
463. Chow, I. C. L. & Wong, S.-S. Immunological imprinting and risks of influenza B virus infection. *Nat. Immunol.* **25**, 1319–1321 (2024).
464. Reynolds, C. J. *et al.* Immune boosting by B.1.1.529 (Omicron) depends on previous SARS-CoV-2 exposure. *Science* **377**, eabq1841 (2022).
465. Chemaitelly, H. *et al.* Duration of mRNA vaccine protection against SARS-CoV-2 Omicron BA.1 and BA.2 subvariants in Qatar. *Nat. Commun.* **13**, 3082 (2022).
466. Park, S. *et al.* An ancestral SARS-CoV-2 vaccine induces anti-Omicron variants antibodies by hypermutation. *Nat. Commun.* **15**, 3368 (2024).
467. Nickle, D. C. *et al.* Consensus and ancestral state HIV vaccines. *Science* **299**, 1515–1518; author reply 1515-1518 (2003).
468. Ducatez, M. F. *et al.* Feasibility of reconstructed ancestral H5N1 influenza viruses for cross-clade protective vaccine development. *Proc. Natl. Acad. Sci.* **108**, 349–354 (2011).
469. Khoury, D. S. *et al.* Predicting the efficacy of variant-modified COVID-19 vaccine boosters. *Nat. Med. 2023 293* **29**, 574–578 (2023).
470. Peterhoff, D. & Wagner, R. Guiding the long way to broad HIV neutralization. *Curr. Opin. HIV AIDS* **12**, 257–264 (2017).
471. Caniels, T. G. *et al.* Germline-targeting HIV vaccination induces neutralizing antibodies to the CD4 binding site. *Sci. Immunol.* **9**, eadk9550 (2024).
472. Amanat, F. & Krammer, F. SARS-CoV-2 Vaccines: Status Report. *Immunity* **52**, 583–589 (2020).
473. Trinh, N. T. *et al.* Effectiveness of COVID-19 vaccines to prevent long COVID: data from Norway. *Lancet Respir. Med.* **12**, e33–e34 (2024).
474. Park, H. J. *et al.* Comparing frequency of booster vaccination to prevent severe COVID-19 by risk group in the United States. *Nat. Commun.* **15**, 1883 (2024).
475. The protective effect of COVID-19 vaccines on developing multisystem inflammatory syndrome in children (MIS-C): a systematic literature review and meta-analysis | springermedizin.de. https://www.springermedicine.com/link?doi=10.1186/s12969-023-00848-1.
476. Cankat, S., Demael, M. U. & Swadling, L. In search of a pan-coronavirus vaccine: next-generation vaccine design and immune mechanisms. *Cell. Mol. Immunol.* **21**, 103–118 (2024).
477. Huang, C. Q., Vishwanath, S., Carnell, G. W., Chan, A. C. Y. & Heeney, J. L. Immune imprinting and next-generation coronavirus vaccines. *Nat. Microbiol.* **8**, 1971–1985 (2023).
478. Greenhalgh, T., Sivan, M., Perlowski, A. & Nikolich, J. Ž. Long COVID: a clinical update. *The Lancet* **404**, 707–724 (2024).

11 Danksagung

Als aller erstes möchte ich mich herzlich bei meinem Doktorvater, Prof. Dr. Ralf Wagner, bedanken. Du hast mich während der gemeinsamen Zeit in deiner Arbeitsgruppe immer unterstützt, gepusht, gefördert und dir, trotz eines Teils übervollen Terminkalenders immer Zeit für mich genommen, was ich sehr schätze. Auch unser gemeinsames Brainstorming, sei es über aktuelle Daten, Paper in Arbeit, neue kreative Ideen und Methoden oder einfach übers Bergsteigen und Reisen fand ich immer sehr bereichernd.

Ein weiterer großer Dank geht an meine Mentoren, Prof. Dr. Gernot Längst und Prof. Dr. Klaus Überla. Ihr habt mich über die Jahre hinweg immer wieder mit wertvollem Input in gemeinsamen Projekten, Publikationen und Mentoren Treffen begleitet und unterstützt.

Mein besonderer Dank geht auch an alle Studienteilnehmer*innen der TiKoCo-, CoVaKo-, Cokiba-Studien und aller anderen Studien an denen ich mitwirken durfte. Ohne euch wäre diese Arbeit nicht möglich gewesen. In diesem Zusammenhang danke ich auch den vielen Kooperationspartnern in diesen Projekten und Studien. Insbesondere Prof. Dr. Michael Kabesch, Dr. Christof Geldmacher, Prof. John Heeney, Prof. Nigel Temperton, Prof. Dr. Martina Prelog, Prof. Dr. Antie Bäumner, Prof. Dr. Joachim Wegener, Dr. George Carnell, Dr. David Peterhoff, Dr. Claudia Asam, Dr. Philip Steininger, Dr. Felix Günther, Dr. Diego Cantoni, Dr. Stephanie Beileke, Simon Wiegrebe, Anne-Kathrin Mildner/Grimm, Simon Streif, Kilian Höcherl und Christina Reiner, die mich alle tatkräftig bei Publikationen unterstützt haben und mit denen ich sehr gerne zusammen gearbeitet habe. Besonders hervorheben möchte ich Prof. Dr. Olaf Gefeller und Prof. Dr. Iris Heid. Durch euer geduldiges Lehren und eure kritischen Fragen habt ihr meine Begeisterung für Statistik und Datenwissenschaften geweckt. Außerdem möchte ich mich bei Dr. Janine Kimpel, Dr. Markus Hoffmann und Prof. Dr. Stefan Pöhlmann für die unkomplizierte Unterstützung mit Reagenzien, Protokollen und ihrem angehäuften Wissen bedanken.

Ein herzliches Dankeschön geht auch an alle Mitglieder der AG Wagner: Dr. Benedikt Asbach und Dr. Martina Pfranger, ihr wart immer meine erste Anlaufstelle bei Fragen und Problemen im Labor und dabei immer nett und kompetent. Auch Dr. Patrick Neckermann möchte ich besonders danken. Du hast mich seit meiner Masterarbeit immer belgeitet, erst als Betreuer, dann als Kollege und als Freund, mit dem ich immer gerne gemeinsam geforscht, gequatscht und Zeit verbracht habe. Gleiches gilt für meine Masterstudent*innen Valentin und Toni, ich hatte viel Spaß dabei, eure Masterarbeiten zu betreuen und gemeinsam neue spannende Themen zu erforschen. Umso mehr freut es mich, euch heute als Kollegen in der Arbeitsgruppe wiederzufinden. Ein aufrichtiges Danke geht natürlich auch an die vielen anderen Student*innen, die ich in meiner Zeit hier betreuen durfte, auch wenn ich euch hier nicht alle namentlich nennen kann. Ihr habt mir viel geholfen und ich hoffe, dass ich euch im Umkehrschluss auch in eurer akademischen Karriere helfen konnte.

Nicht vergessen möchte ich alle anderen Kollegen während meiner Zeit hier, Michi, Jasmin, Franz, Manu, Christina, Alex, Domi, Flo, Meldra, Meli und Anja. Während einer Doktorarbeit verbringt man bekanntlich viel Zeit im Labor, eure nette und entspannte Art war dabei einer der Gründe, warum ich mich hier immer wohl gefühlt habe.

Ein besonderer Dank gilt auch Tom und Richie, meinen ehemaligen Betreuern, durch die ich überhaupt erst zur AG Wagner gekommen bin. Euer Humor und eure Kompetenz haben einen bleibenden Eindruck hinterlassen und waren ein Grund dafür, dass ich geblieben bin.

Abschließend möchte ich mich bei meiner Familie, insbesondere bei meinen Eltern/Stiefeltern, Alois und Marianne, Eveline und Peter bedanken, die mich, obwohl es manchmal holprig war, immer auf meinem Weg unterstützt haben. Ohne euch wäre ich heute sicher nicht hier.

Zu guter Letzt: Liebe Louise, danke, dass es dich gibt.